

Properties of Nucleosyl Amino Acid- Modified Oligonucleotides

Dissertation

Zur Erlangung des Grades des Doktors
der Naturwissenschaften der
Naturwissenschaftlich-Technischen Fakultät
der Universität des Saarlandes

von

Melissa Wojtyniak

Diplom-Pharmazeutin/Apothekerin

Saarbrücken
2021

Tag des Kolloquiums:	11. Juni 2021
Dekan:	Prof. Dr. Jörn Eric Walter
Berichterstatter:	Prof. Dr. Christian Ducho Prof. Dr. Alexandra K. Kiemer
Vorsitz:	Prof. Dr. Andriy Luzhetskyy
Akademischer Mitarbeiter:	Dr. Dominik Selzer

Die Inhalte der vorliegenden Arbeit wurden an der Universität des Saarlandes an der Naturwissenschaftlich-Technischen Fakultät in der Fachrichtung Pharmazie im Zeitraum von November 2015 bis Februar 2020 angefertigt.

Erstgutachter: Prof. Christian Ducho

Zweitgutachter: Prof. Alexandra K. Kiemer

Meiner Familie

"Yesterday is history, tomorrow is a mystery, but today is a gift

– that is why we call it present ."

- Master Ogway -

Abstract

Antisense technology has the potential to evolve into a powerful biomedical tool. By utilizing the unique hybridization behavior of antisense oligonucleotides (ON) the antisense approach facilitates a specific intervention in cellular processes that would be barely feasible by using conventional drugs. However, the tremendous potential that comes with the antisense strategy is paired with the insufficient pharmacokinetic profile of native DNA ONs. Thus, an overall low stability *in vivo* as well as limited cellular uptake due to the extremely polar DNA structure, represent two of the main obstacles. Consequently, alterations of the native DNA structure are required to obtain applicable, drug-like substances. The reported work focuses on the synthesis and evaluation of modified ONs carrying the nucleosyl amino acid (NAA)-modification, a peptide-like internucleoside structure featuring a free amino group, within their backbone. Part A of this thesis concentrates on the biological stability of partially zwitterionic NAA-modified ONs in the presence of 3'→5'- and 5'→3'-exonucleases as well as human plasma and whole cell lysate. In part B, the hybridization properties of cationic, fully NAA-modified ONs in presence of matched and mismatched counterstrands were analyzed and validated. Finally, part C focuses on the synthesis and evaluation of a chimeric NAA/LNA-gapmer structure with the aim to obtain a selective, high-affinity precursor of an antisense ON.

Zusammenfassung in deutscher Sprache

Die Antisense-Technologie hat das Potenzial, sich zu einem leistungsfähigen biomedizinischen Werkzeug zu entwickeln. Durch die Nutzung des einzigartigen Hybridisierungsverhaltens von Antisense-Oligonucleotiden (ON) ermöglicht sie einen gezielten Eingriff in zelluläre Prozesse, der mit herkömmlichen Methoden kaum durchführbar wäre. Das enorme Potenzial, das mit dem Antisense-Ansatz einhergeht, ist jedoch an das unzureichende pharmakokinetische Profil nativer DNA-ON geknüpft. Hierbei stellen eine insgesamt geringe *in-vivo*-Stabilität sowie eine erschwerte zelluläre Aufnahme aufgrund der polaren DNA-Struktur zwei der Hauptprobleme dar. Folglich sind Veränderungen der nativen DNA-Struktur erforderlich, um applizierbare Substanzen zu erhalten. Daher konzentriert sich die folgende Arbeit auf die Synthese und Evaluierung modifizierter ON, die in ihrem Rückgrat die Nucleosylaminosäure-(NAA)-Modifikation, eine peptidähnliche Internucleosid-Struktur mit einer freien Aminogruppe, tragen. Teil A dieser Arbeit befasst sich mit der biologischen Stabilität von teilweise zwitterionischen NAA-modifizierten ON in Gegenwart von 3'→5'- und 5'→3'-Exonukleasen sowie humanem Plasma und Zelllysat. In Teil B wurden die Hybridisierungseigenschaften von kationischen, vollständig NAA-modifizierten ON analysiert und validiert. Zuletzt befasst sich Teil C mit der Synthese und Untersuchung einer chimären NAA/LNA-Gapmer-Struktur mit dem Ziel, eine selektive, hochaffine Vorstufe eines Antisense-ON zu erhalten.

Papers Included in This Thesis

Oligonucleotide Analogues with Cationic Backbone Linkages

Melissa Meng and Christian Ducho

Beilstein J. Org. Chem. **2018**, *14*, 1293-1308, DOI: 10.3762/bjoc.14.111.

(Review included in the introduction)

A. Enhanced Stability of DNA Oligonucleotides with Partially Zwitterionic Backbone Structures in Biological Media

Melissa Meng, Boris Schmidtgall and Christian Ducho

Molecules **2018**, *23*, 2941-2952, DOI: 10.3390/molecules23112941.

B. Oligonucleotides with Cationic Backbone and Their Hybridization with DNA: Interplay of Base Pairing and Electrostatic Attraction

Boris Schmidtgall, Arne Kuepper, Melissa Meng, Tom N. Grossmann and Christian Ducho

Chem. Eur. J. **2018**, *24*, 1544-1553, DOI: 10.1002/chem.201704338.

C. Towards Zwitterionic Oligonucleotides with Improved Properties: the NAA/LNA-Gapmer Approach

Melissa Wojtyniak, Boris Schmidtgall, Philine Kirsch and Christian Ducho

ChemBioChem. **2020**, *21*, 3234-3243, DOI: 10.1002/cbic.202000450.

Contribution Report

The author wishes to clarify her contribution to the manuscripts included in this thesis.

Review (included in the introduction): Oligonucleotide Analogues with Cationic Backbone Linkages

The author participated equally with her co-author in the preparation, editing and review of the manuscript.

Manuscript A: Enhanced Stability of DNA Oligonucleotides with Partially Zwitterionic Backbone Structures in Biological Media

The author planned, carried out, analyzed and validated the work described in this publication. She prepared, implemented and performed the SVP and BSP exonuclease assays as well as the human plasma and whole cell lysate assays. Furthermore, she prepared the cell culture of the U937 cells and the corresponding lysate. Lastly, she conceived and wrote the manuscript.

Manuscript B: Oligonucleotides with Cationic Backbone and Their Hybridization with DNA: Interplay of Base Pairing and Electrostatic Attraction

The author was involved in the design, execution and analysis of the UV-Vis-monitored melting temperature experiments and the CD-spectroscopic analyses of the fully NAA-modified oligomers. She prepared the corresponding figures and was involved in the writing process of the manuscript.

Manuscript C: Towards Zwitterionic Oligonucleotides with Improved Properties: the NAA/LNA-Gapmer Approach

The author planned, carried out, analyzed and validated most of the experimental work described in this publication. She re-synthesized the dimeric CxT-building block and prepared the NAA/LNA-gapmer as well as the DNA/LNA control gapmer. She prepared and performed the UV-Vis-monitored melting studies, the CD spectroscopy, the biological stability assays and the ³²P-labelled RNase H assay. Finally, she conceived and wrote the manuscript.

Further Papers Not Included in This Thesis

A. An Oligonucleotide Probe Incorporating the Chromophore of Green Fluorescent Protein Is Useful for the Detection of HER-2 mRNA Breast Cancer Marker

Abed Saady, Verena Böttner, [Melissa Meng](#), Eli Varon, Yaron Shav-Tal, Christian Ducho and Bilha Fischer

Eur. J. Med. Chem. **2019**, *173*, 99-106, DOI: 10.1016/j.ejmech.2019.04.013.

B. Synthesis of 2'-Deoxyuridine Modified with a 3,5-Difluoro-4-Methoxybenzylidene Imidazolinone Derivative for Incorporation into Oligonucleotide Probes for Detection of HER2 Breast Cancer Marker

Abed Saady, Noam Y Steinman, [Melissa Wojtyniak](#), Christian Ducho and Bilha Fischer

Curr. Protoc. Nucleic Acid Chem. **2020**, *80*, e104, DOI: 10.1002/cpnc.104.

C. Specific, Sensitive, and Quantitative Detection of HER-2 mRNA Breast Cancer Marker by Fluorescent Light-Up Hybridization Probes

Abed Saady, [Melissa Wojtyniak](#), Eli Varon, Verena Böttner, Noa Kinor, Yaron Shav-Tal, Christian Ducho and Bilha Fischer

Bioconjug Chem. **2020**, *31*, 1188-1198, DOI: 10.1021/acs.bioconjchem.0c00130.

Danksagung

Die vorliegende Arbeit trägt meinen Namen als Autor, wäre jedoch ohne die tatkräftige Unterstützung einer Vielzahl von besonderen Menschen so niemals entstanden.

An erster Stelle möchte ich mich bei meinem Doktorvater Professor Christian Ducho bedanken. Du hast mir die Möglichkeit gegeben an einem wunderbar vielseitigen Forschungsprojekt zu arbeiten, das mir weitreichende Einblicke in die unterschiedlichsten Themen eröffnet hat. Bei aufkommenden Fragen warst du stets motiviert passende Lösungen zu finden – wobei du mir aber auch die Chance gelassen hast meine eigenen Vorstellungen und Ideen zu verfolgen. Auch für die vielen Gelegenheiten an fachspezifischen Konferenzen aktiv teilzunehmen und die Oligo-Community kennenlernen zu können, möchte ich mich aufrichtig bedanken. Ebenfalls gilt mein großer Dank Frau Professorin Alexandra K. Kiemer, die sich bereit erklärt hat die Rolle meiner Zweitgutachterin zu übernehmen und mich über Ihren Arbeitskreis vor allem bei der Durchführung der FACS-Analysen maßgeblich unterstützt hat.

Darüber hinaus möchte ich mich bei Herrn Dr. Frank Hannemann für die Unterstützung bei der Aufnahme diverser CD-Spektren bedanken, bei Frau Dr. Jessica Hoppstädter für ihre große Hilfe bei allen FACS-Studien sowie bei Frau Dr. Brigitta Loretz und ihrem Team für ihre Bereitschaft mich mit ihrem Know-how im Bereich Konfokalmikroskopie zu unterstützen. Weiterhin gilt mein Dank Herrn Dr. Arne Küpper für die angenehme Zusammenarbeit während der Analyse unserer kationischen Oligos. Ein Dankeschön geht ebenso an meinen Vertiefungspraktikanten Kevin Bauer für das Nachziehen meines dringend benötigten T-Bausteins.

Weiterhin kann ein Projekt noch so gut und interessant sein – wenn die Kollegen nicht stimmen macht auch die spannendste Thematik keinen Spaß. Deshalb an dieser Stelle ein riesiges Dankeschön an all meine fabelhaften Kollegen aus dem AK Ducho. Vorneweg möchte ich mich bei meinen "Mädels" Dr. Verena Böttner (Schlager-, Kuchen- und Oligo-Queen), Reem Fathalla ("Habibi" und Bad-Cop in EAB), Dr. Giuliana Niro (Bolognese-Meisterin und Chemie-Lexikon) und Stefanie Weck (Pöbelbeauftragte und Sonnenschein) bedanken, die für mich nicht nur Kollegen, sondern auch wunderbare Freunde geworden sind. Ihr habt den AK zu einem Ort gemacht, an den ich auch nach den katastrophalsten

Tagen nochmal zurückkommen wollte! Ein spezielles Dankeschön geht auch an meinen Büro-Nachbarn Sven Lauterbach für seine unverwüstliche gute Laune und seine stetige Hilfsbereitschaft – sowohl im Labor als auch an der Boulderwand! Selbstverständlich möchte ich mich auch bei all den anderen für die wundervolle Zeit im Labor, auf AK Ausflügen, beim Boßeln, den Betriebsausflügen und den vielseitigen anderen Events bedanken. Ich vermisse euch jetzt schon!

Ohne Frage wäre ich heute auch nicht an diesem Punkt ohne die liebevolle und nie endende Unterstützung meiner ganzen Familie. Hier möchte ich besonders meinen Eltern, Christine Kloß und Matthias Meng sowie Harald Kloß und Birgit Meng-Wuttke danken. Ihr habt mir auch in turbulenten Zeiten immer Mut gemacht und mich unterstützt, wo ihr nur konntet – auch wenn ihr mit machen meine Laborberichte nicht viel anfangen konntet. Ebenfalls danken möchte ich meinen wunderbaren Freunden und hier ganz besonders Samira Meng und Quirin Werthner für all die zahlreichen schönen Momente und die dringend benötigte Entspannung nach Laborschluss. Zuletzt gilt mein Dank meinem wundervollen Mann Jan-Georg. Du hast mich durch jede noch so komplizierte Lage begleitet, mir unglaublich viel Zuversicht und Vertrauen in mich selbst gegeben und dafür gesorgt, dass ich auch in belastenden Situationen (wie morgens um halb zwei am DNA-Synthi) nicht die Nerven verloren habe.

Ich danke euch allen von ganzem Herzen!

Abbreviations and Symbols

A	adenine
ASO	antisense oligonucleotide
B	nucleobase
BMT	benzylmercaptotetrazole
BNA	bridged nucleic acid
BSP	bovine spleen phosphodiesterase
C	cytosine
°C	degree Celsius
CD	circular dichroism
CH ₂ Cl ₂	dichloromethane
°C/mod	degree Celsius per modification
CPG	controlled pore glass
CPP	cell-penetrating peptide
Cy5	cyanine 5
Δ	delta, difference
d	doublet
DAPI	4',6-diamidino-2-phenylindole
dd	doublet of doublet
DMTr	4,4'-dimethoxytrityl
DNA	deoxyribonucleic acid
DNG	deoxyribonucleic guanidines
DNmt	S-methylthiourea modification
ds	double stranded
FACS	fluorescence-activated cell sorting
FCS	fetal calf serum
FDA	Food and Drug Administration
G	guanine
hp	human plasma

HRMS	high resolution mass spectrometry
LNA	locked nucleic acid
MeCN	acetonitrile
MMI	methylene(methylimino)
MMTr	4-monomethoxytrityl
mod	modification
MOE	2'- <i>O</i> -methoxyethyl
MP	methylphosphonate
mRNA	messenger RNA
NAA	nucleosyl amino acid
NMR	nuclear magnetic resonance spectrometry
ON	oligonucleotide
PAGE	polyacrylamide gel electrophoresis
PCR	polymerase chain reaction
PFA	paraformaldehyde
PMO	phosphoramidate-linked morpholino modification
PNA	peptide nucleic acid
PS	phosphorothioate
q	quartet
RISC	RNA-induced-silencing complex
RNA	ribonucleic acid
RNAi	RNA interference
RNase H	ribonuclease H
rSNA	dimethylene sulfone-modified RNA
s	singlet
SELEX	systematic evolution of ligands by exponential enrichment
SPPS	solid-phase peptide synthesis
siRNA	small interfering RNA
ss	single stranded
SVP	snake venom phosphodiesterase

t	triplet
T	thymine
TCA	trichloroacetic acid
TFO	triplex-forming oligonucleotide
T _m	melting temperature
WCL	whole cell lysate
x	NAA modification

Comments on the citation style:

References are given as superscripted numbers inside square brackets^[number] and refer to the numbers inside square brackets [number] listed in Chapter 5 'References'. If a reference refers to the informational content of a whole sentence, it is placed immediately after the punctuation finishing the sentence. If one sentence contains more than one information, the reference is placed immediately posterior to the information it refers to.

Content

Abstract	I
Zusammenfassung in deutscher Sprache	II
Papers Included in This Thesis	III
Contribution Report	IV
Further Papers Not Included in This Thesis	V
Danksagung	VI
Abbreviations and Symbols	VIII
Content	XI
1. Introduction	1
1.1 Oligonucleotides as Biomedical Agents	1
1.2 Chemical Modification of the Oligonucleotide Structure	7
1.2.1 Modification of the Nucleobase	9
1.2.2 Modification of the (2'-Deoxy)Ribose	13
1.2.3 Modification of the Internucleoside Linkage	18
1.2.3.1 Anionic Backbone Linkages	18
1.2.3.2 Neutral Backbone Linkages	20
1.2.3.3 Cationic Backbone Linkages	24
1.2.4 Chimeric Oligonucleotides: The Gapmer Approach	41
2. Objectives	43
3. Results	47
A. Enhanced Stability of DNA Oligonucleotides with Partially Zwitterionic Backbone Structures in Biological Media	47
B. Oligonucleotides with Cationic Backbone and Their Hybridization with DNA: Interplay of Base Pairing and Electrostatic Attraction	59
C. Towards Zwitterionic Oligonucleotides with Improved Properties: the NAA/LNA-Gapmer Approach	71
4. Final Discussion	83
4.1 Evaluation of the Biological Stability of Partially Zwitterionic NAA-Modified Oligomers (Manuscript A)	84
4.2 Analysis of the Hybridization Properties of Cationic Fully NAA-Modified Oligomers (Manuscript B)	86
4.3 Synthesis and Evaluation of an NAA/LNA-Gapmer Structure (Manuscript C)	88

4.4 Conclusion and Outlook.....	90
5. References.....	91
6. Appendix	108
6.1 Studies on the Cellular Uptake of the Partially Zwitterionic NAA/LNA-Gapmer	108
6.1.1 Synthesis of the Fluorophore-Labeled NAA/LNA- and DNA/LNA-Gapmers.....	110
6.1.2 Evaluation of the Fluorophore-Labeled NAA/LNA- and DNA/LNA-Gapmers....	113
6.1.2.1 Fluorescence-Activated Cell Sorting (FACS) Analysis.....	113
6.1.3.2 Confocal Microscopy.....	114
6.1.3 Experimental Section	117
6.1.3.1 Synthesis of Cy5-labeled Gapmers A and B.....	117
6.1.3.2 Purification of Gapmers A and B	118
6.1.3.3 Fluorescence-Activated Cell Sorting (FACS) Analysis.....	118
6.1.3.4 Confocal Microscopy.....	119
6.2 Supporting Information	121
6.2.1 Manuscript B: Oligonucleotides with Cationic Backbone and Their Hybridization with DNA: Interplay of Base Pairing and Electrostatic Attraction	121
6.2.2 Manuscript C: Towards Zwitterionic Oligonucleotides with Improved Properties: the NAA/LNA-Gapmer Approach	156
6.3 Syntheses Appending to Manuscript C.....	189
6.3.1 Synthesis of 2-Iodoxybenzoic Acid 4.....	189
6.3.2 Synthesis of <i>tert</i> -Butyl Ester Phosphonate 6.....	190
6.3.3 Synthesis of the T-Building Block	193
7. Curriculum Vitae	203

1. Introduction

1.1 Oligonucleotides as Biomedical Agents

Deoxyribonucleic acid (DNA) is anchored in our heads as the blueprint of life. Localized in the nucleus of eukaryotic cells and the cytoplasm of some prokaryotes, it carries the genetic directives for protein expression and thus functionality, evolution and reproduction of every living organism. Its unique double-helical structure was first fully resolved by *Watson* and *Crick* in 1953, describing the sugar-phosphate chain of both single strands as outer backbones of the duplex and the canonical nucleobases – thymine (T), cytosine (C), guanine (G) and adenine (A) – as central parts linking the two strands together *via* hydrogen bonding.^[1] This fundamental discovery triggered a cascade of research focusing on the properties, biological functions and origin of DNA and has thrown light on numerous processes this biopolymer is involved in. But apart from this existential point of view, DNA also possesses tremendous potential as biomedical agent. Conventional treatment of most diseases requires highly selective compounds that combine excellent target recognition and affinity with low side effect rates and minimal off-target binding. To meet these requirements, traditional small-molecule drugs have to undergo intensive optimization processes, necessitating individual changes and modifications regarding their molecular structure, to fit the desired applications. Such procedures, however, are not generally transferable and therefore time consuming and difficult in their implementation. Furthermore, low-molecular-weight drugs mostly interact with protein pockets, leaving numerous intracellular pathways and regulatory cascades, which employ potential targets lacking these binding grooves, untouched. One possible way to overcome these issues is the use of short single stranded nucleic acids, so called oligonucleotides (ONs). Due to their unique structure and the associated binding behavior, ONs offer desirable properties in terms of target recognition, target selectivity and target affinity. Hence, the usage of ONs as templates for therapeutic agents has raised hope to enable a rationalized drug design.

More than four decades ago, *Zamecnik* and *Stephenson* laid the foundation for the therapeutic use of ONs. They demonstrated that the presence of a short, single stranded DNA, complementary to 13 nucleotides encoding for the 35S subunit of *Rous sarcoma virus*, inhibits viral replication and translation of viral mRNA.^[2,3] Since then, the improvement of

the pharmacokinetic profile and the development of different target strategies for ONs have been in focus of intensive research. Hereby, the interaction partners of biomedically applicable ONs, can generally be divided into three main classes: (i) the interaction with DNA (as in the antigene approach), (ii) the targeting of RNA (i.e. through the antisense mechanism or the RNA interference (RNAi) mechanism) and (iii) the interactions with proteins as well as the modulation of their cellular effects. An overview of the different strategies, their respective targets as well as some examples of therapeutic ONs following these targeting strategies are depicted in *Figure 1.1*.

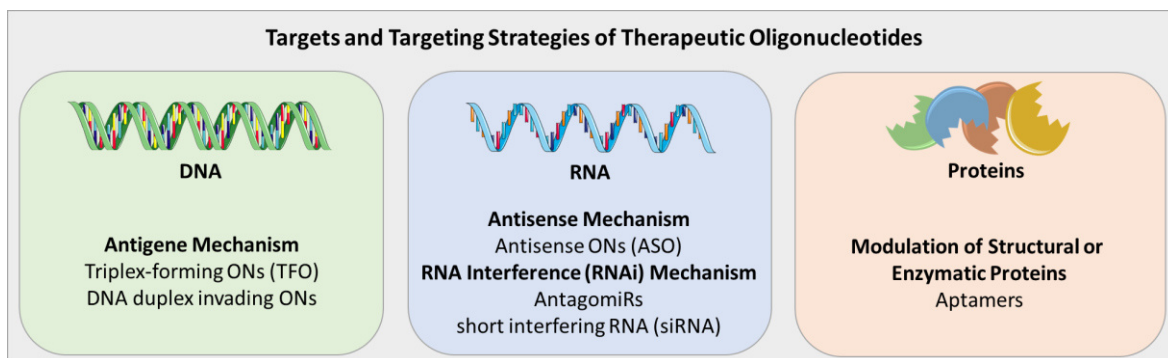


Figure 1.1. Schematic representation of different targeting strategies and their corresponding cellular targets for oligonucleotides as biomedical agents (DNA and RNA templates were taken from <https://smart.servier.com>, CC BY 3.0).

The various strategies displayed in *Figure 1.1* have their own perks and benefits, but also suffer from distinct disadvantages. In the following, a brief overview will be provided.

Aiming at the inhibition of gene expression at the transcriptional level, the antigene strategy directly targets chromosomal double-stranded DNA (dsDNA) located in the nucleus of the cell.^[4] This tactic has mainly been pursued *via* two different mechanisms: the formation of triplex structures through triplex-forming oligonucleotides (TFOs)^[5,6] or the invasion of the DNA duplex by strand displacement^[7]. Crucial for the first of the two approaches were discoveries made by *Hoogsteen*. In 1963, he observed hydrogen bond-mediated interactions between two nucleosides, which differed from the previously known 'regular' Watson-Crick base pairing principle.^[8] Later on, these interactions should be known as Hoogsteen hydrogen bonds. Further investigations on this new binding mode resulted in the discovery of DNA triplexes, in which a third strand was shown to be associated to a helical DNA duplex *via* the aforementioned Hoogsteen hydrogen bonds. Finally, these interactions laid the foundation for the usage of TFOs as antigene agents.^[9] Upon interaction with dsDNA, TFOs form stable triplehelical clusters that cannot be

recognized by RNA polymerases. As consequence, the steric shielding of the transcriptional site results in decelerated mRNA synthesis and thus a blockage of transcription. In contrast to TFOs, strand-invading ONs do not form triplexes, but squeeze in between an existing DNA duplex to interact with either one or both strands through Watson-Crick, or a mixture of Watson-Crick and Hoogsteen base pairing.^[7,10] However, the result remains, like for the TFO strategy, a hampered transcriptional mRNA synthesis. Yet, these approaches are highly demanding concerning both the structural design of the antigene ONs as well as the delivery of the antigene agent into the nucleus. Hence, several strategies to improve the antigene approach are currently still under investigation.^[11]

While the antigene approach focuses on chromosomal dsDNA, the antisense strategy targets cytosolic RNA and is based on the interference with translation and thus protein synthesis. Thereby, this method includes either a steric block of ribosomal translation through formation of a mRNA-ON duplex or the activation of the DNA/RNA hybrid-recognizing enzyme ribonuclease H (RNase H), which ultimately results in RNA cleavage. Following the name of the approach, ONs used in this strategy are called antisense oligonucleotides (ASOs). Regarding both modes of action, the steric blockade has been described first, in fact already by *Zamecnik* and *Stephenson*, and remains one of the most investigated mechanisms of the antisense approach.^[12] Central for its function is the formation of a stable hybrid duplex between the ASO and the mRNA sequence encoding for the targeted protein. As a result of successful duplex formation, movement of the ribosome along the mRNA is blocked and the elongation of the translated amino acid chain is interrupted. Consequently, the translational arrest induces a downregulation of the target protein's abundance. To obtain such an outcome, the applied ASO has to show a certain stability in its cellular surroundings as well as a sufficient affinity towards the target sequence, to prevent early dissociation. Following this tactic, approximately 130 ASOs have found their way into clinical trials^[13] and some even received approval by the FDA. A thereby well-studied example is the fully backbone-modified ASO fomivirsen, which was the first approved ON drug for clinical usage.^[14] In contrast to the steric block of translation, which requires sufficient stability and target affinity, induction of the enzymatic cleavage of RNA is slightly more challenging. Since the ASO not only has to interact with its target, but also needs to be structurally suitable for enzymatic recognition, the ON sequence and the incorporated modifications have to be carefully chosen.^[15] The enzyme which can be

utilized for the ASO-controlled cleavage of RNA is the ribonuclease RNase H.^[16] RNase H, belongs to a family of unspecific endonucleases, which cleave the RNA component in DNA-RNA hybrid duplexes to afford free single stranded DNA.^[17] Thereby, sufficient activation of the RNase H-mediated degradation of RNA requires the counterstrand ON to at least include five or more neighboring DNA nucleotides.^[18] Since RNase H is involved in the regulation of numerous vital cellular processes, like DNA replication and repair^[19], it occurs in high abundance and hence represents an attractive tool for antisense applications. Another approach to modulate mRNA translation is based on the RNA interference (RNAi) mechanism. The RNAi pathway occurs in most eukaryotes and represents an endogenous process for the regulation of gene expression and protein synthesis through purposed cleavage of mRNA.^[20] By this means, mRNA degradation is induced through two classes of short double stranded RNA (dsRNA): the micro RNAs (miRNA)^[21,22] and the small interfering RNAs (siRNA)^[23]. Both short dsRNA species consist of a guide strand that takes a key role in the RNAi mechanism, and a passenger strand. Although length and appearance of both species are rather similar, miRNAs represent endogenous non-coding RNAs that are involved in the regulation of gene expression^[24], whereas siRNAs are derived from long, exogenous dsRNA^[25]. Furthermore, miRNAs have been shown to address multiple targets, where siRNA was reported to be highly specific for only one mRNA sequence.^[26] However, both short dsRNA species are capable of inducing mRNA degradation through activation of the RNA-induced silencing complex (RISC).^[27,28] The RISC itself represents a multiprotein complex incorporating, among others, an endonuclease named argonaute, which can bind to the guide strand of the short dsRNA species (miRNA or siRNA), while the passenger strand is ejected.^[29,30] The resulting complex between the remaining guide strand, and the argonaute furnishes the mature and active RISC. *Via* the recognition mechanism of the guide strand, complementary mRNA can now be bound to the RISC and is subsequently degraded through the endonuclease activity of argonaute.^[30,31] Thus, this endogenous regulatory mechanism offers a unique platform for controlled gene-silencing by the usage of artificial ONs. As shown in *Figure 1.1*, this can include, among others, the usage of altered and improved siRNA^[32] or the application of chemically modified, single stranded RNA analogues complementary to miRNA, so called antagomiRs^[33]. Thereby, modified siRNA utilizes the RNAi mechanism to selectively degrade mRNA and induce the controlled downregulation of defined target proteins.^[34] AntagomiRs on the other hand, bind to their

complementary miRNA target and block mRNA binding to the mature RISC, thus inhibiting mRNA cleavage.^[35] Moreover, the initiation of direct miRNA degradation in presence of antagomiRs has been uncovered as a further mode of action.^[33,36] In any case, silencing of the miRNA activity was reported to result in the upregulation of distinct miRNA target proteins, what again has been shown as beneficial for the treatment of numerous human diseases.^[37] However, as for many other nucleic acid based agents, difficulties concerning intracellular delivery as well as defective stability *in vivo* remain in the focus of ongoing research.^[38,39]

The third targeting strategy for therapeutic ONs does not involve the interaction with nucleic acids but the binding of proteins. Consequently, molecular recognition is not facilitated through base pairing of complementary strands. Instead, the ON adapts a distinct, three-dimensional shape that interacts with its targets in a way closely related to the binding mode of antibodies. Oligomers that are capable to exert this role of a 'nucleic acid antibody' are called aptamers (from Latin *aptus* (fit) and Greek *meros* (part)).^[40,41] Compared to 'traditional antibodies', aptamers are single stranded ONs that possess a rather flexible structure and a relatively small size. The selection process to identify fitting aptamers is known as systematic evolution of ligands by exponential enrichment (SELEX).^[42] During SELEX, the desired target is presented to a large library of random, single stranded ONs with primers attached to their 5'- and 3'-ends. After incubation, non-bound ONs are separated from the ON-target complexes and the bound ONs are amplified through polymerase chain reaction (PCR). A variable round of binding, separating and amplifying steps follows, leaving only the most suitable aptamers, which can again be modified and improved. Compared with antibodies, aptamers possess several advantages: they are more stable towards temperature fluctuations, are synthetically accessible and generally last longer before losing activity. Furthermore, latest studies verified not only the interaction between aptamers and proteins, but also lipoglycans^[43], carbohydrates^[44] and many further metabolites^[45].

Although all the described approaches appear to be promising, they are all facing the same problem. The application of ONs *in vivo* is strongly hampered due to their limited stability and poor pharmacokinetic profile. Thus, chemical modifications of the ON structure are

required. Some of the most prominent ON modifications that are employed to resolve these hurdles will be discussed in the following sections.

1.2 Chemical Modification of the Oligonucleotide Structure

As ONs can be employed for numerous biological and clinical applications, the number of known modifications accessible in literature is comprehensive and continuously rising. Thus, the improvement of nuclease stability, the increase of cellular uptake, the enhancement of target affinity and selectivity or the modulation of steric and spatial arrangements of ONs are just some few examples of how a structural alteration can influence the properties of a nucleic acid. In general, ONs offer various sites for modifications. A brief overview is given in *Figure 1.2*.

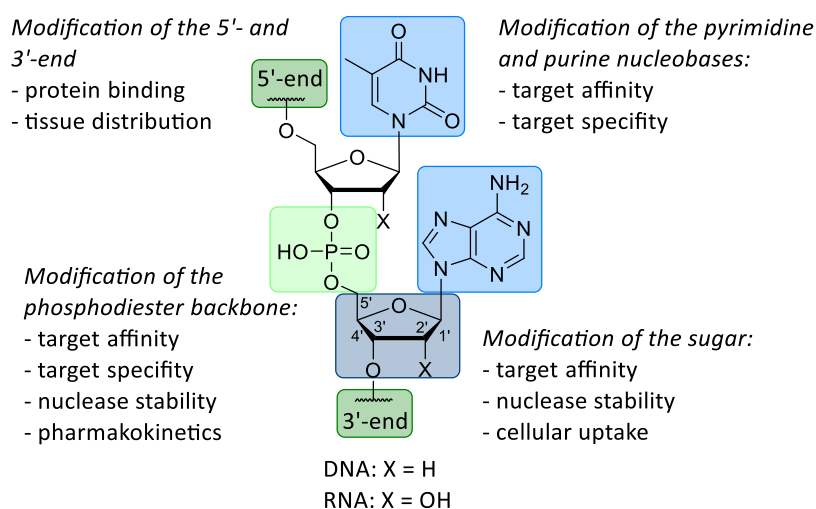


Figure 1.2. Overview of possible sites for ON modifications and their desired impact on the ON properties.

The most well studied site and also the one with the richest selection of different modifications is the ON backbone structure. Since the biological instability of native nucleic acids is largely connected to the lability of the phosphodiester linker against endogenous nucleases, chemical alteration of this position was the obvious choice. Apart of stabilizing effects, several backbone modifications have been developed to enhance the affinity and specificity for complementary strands, thereby improving the overall efficiency of the ON. Furthermore, ONs represent highly polar substances, which makes them prone to fast renal excretion. Consequently, selected backbone modifications were designed to modulate the affinity to plasma and cellular proteins, hence improving bioavailability and the pharmacokinetic profile. The second position that has come into focus was the (2'-deoxy)ribose sugar. Modification of this site has proven to exert tremendous effects on target affinity. Due to pre-organization and chemical fixation of the relatively flexible five-

membered ring, the entropic penalty upon duplex formation was found to be drastically reduced. This insight has been utilized to design rigidified sugar modifications to improve target affinity and to stabilize the resulting duplexes. Additionally, alterations at the 2'-position have been used to increase lipophilicity and nuclease stability. Modifications of the nucleobases have primarily been introduced to support Watson-Crick base pairing between the complementary bases and improve π - π -interactions. Lastly, conjugation of several biomolecules, carriers or lipids to the 3'- or 5'-end have been investigated. These modifications have mostly been employed to enhance cellular uptake and ensure delivery of the ON to distinct organs or molecular targets.

Since this work has focused on the attempt to validate and improve an artificial ON based on the antisense approach, the following chapters will concentrate on selected modifications serving this purpose.

1.2.1 Modification of the Nucleobase

As central connectors of the DNA duplex, a well-balanced affinity between the nucleobases is vital for duplex stability and the recognition of matching counterstrands. The two driving forces that steer the base pairing process are hydrogen bonds between the complementary A-T and G-C base pairs as well as π - π interactions resulting from stacking of the aromatic purine and pyrimidine heterocycles. Since these two interactions are influenced by the amount of hydrogen donors/acceptors on the one hand and the size of the aromatic system on the other, alteration of these variables might lead to modified building blocks with improved properties. Thus, it has been envisioned by many to manipulate the substitution pattern or even the overall structure of the canonical bases to enhance affinity towards antisense targets or furnish TFOs. As described in chapter 1.1, TFOs can be employed to form a DNA triplex structure by incorporation of a third strand within the major groove of a regular DNA duplex.^[46] Triplex formation was thereby shown to be mediated by interactions between the TFO and exposed bases of the helical duplex *via* Hoogsteen or reverse-Hoogsteen hydrogen bonds, thus forming parallel or anti-parallel base triplets. This interaction could be proven by *Moser* and *Dervan* to happen in a sequence specific manner and in addition, could even lead to controlled cleavage of the double helical DNA.^[5] As a result, TFOs have been used to interfere with gene expression by either sterically blocking the initiation of transcription^[47] or preventing the passage of DNA polymerase and hence, DNA replication^[48]. However, several issues still leave room for improvement like pH restrictions for triplex formation or varying binding affinities.

As mentioned above, modification of the nucleobases might enhance the binding affinity and thus duplex stability. Yet, just the opposite effect could occur due to distortion of the helical structure, which would entail an overall destabilization. To gain further insights into this system, slight changes concerning the nucleobase substitution pattern, extensions of the ring systems and even the creation of completely artificial bases have been explored.

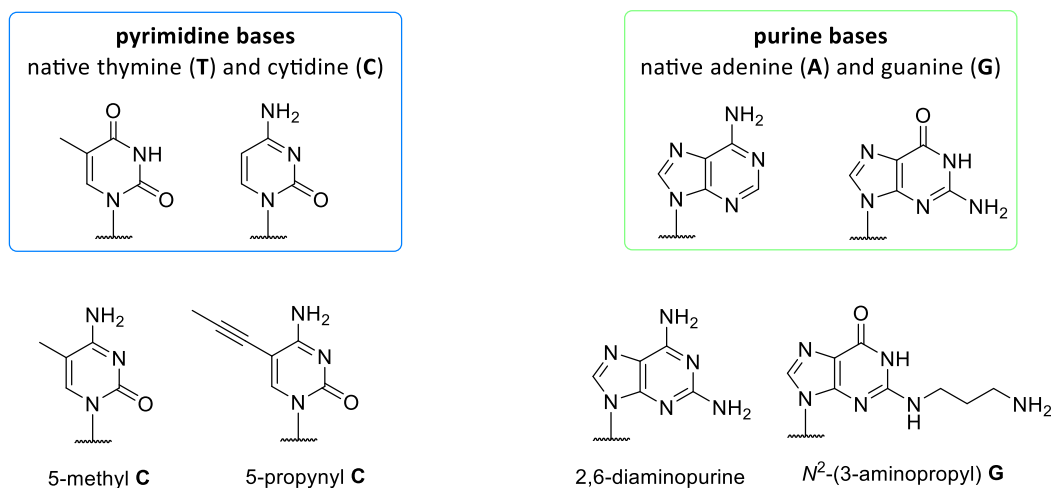


Figure 1.3. Examples for nucleobase modifications with altered substitution pattern.

Regarding the introduction of new substituents, numerous modifications have been reported, with the 5-position of the pyrimidine bases (C and T) being one of the most well studied sites.^[49] Thereby, a prominent example is the insertion of a methyl group in the 5-position of cytosine (5-methyl C, *Figure 1.3*), leading to an enhanced affinity towards RNA antisense targets.^[11] This effect could be traced back to a stabilization of the DNA/RNA hybrid duplex due to stacking of the lipophilic methyl group between the nucleobases in the major groove of the helix. Interestingly, 5-methyl cytosine also plays a role in nature, where it has been found to control gene expression through formation of extremely stable DNA duplexes.^[49] Another example for the insertion of a lipophilic residue to a pyrimidine base is 5-propynyl cytosine (5-propynyl C, *Figure 1.3*).^[50,51] Like the 5-methyl substituent, this unsaturated moiety reinforces duplex stability due to a positive influence of the triple bond on base stacking. Furthermore, 5-propynyl C-modified ONs have been shown to exert improved stability against nuclease mediated degradation.^[52] Apart from the pyrimidines, the purine-derived nucleobases have also been subject to changes in the substitution pattern. 2,6-diaminopurine (*Figure 1.3*) carries an additional amino group in the 2-position, leading to an extra H-donor for interactions with thymine. As a result the 2,6-diaminopurine-T base pair displays attractions similar to the G-C pair, which contribute to duplex stability and increased thermal melting temperatures.^[53] A further concept to enhance duplex stability is the linkage of basic groups to the purine system as in case of N^2 -(3-aminopropyl)-guanine (N^2 -(3-aminopropyl) G, *Figure 1.3*). Due to the positive charge of the free primary amine, this modified base has been shown to strongly interact with the anionic phosphodiester backbone, thus furnishing potent ionic interactions.^[54]

An alternative approach to modulate the properties of the canonical bases lies within the enlargement of the aromatic ring system. *Figure 1.4 A* depicts congeners of T (dxT) and A (dxA), respectively, whose systems are expanded by a benzene ring. Both bases were first described by *Kool* and co-workers, who reported a duplex-stabilizing effect for the case that the dx-bases are placed in just one of the two strands ($T_m = +3.4$ to $+5$ °C/mod).^[55] In this case, the distances between the two DNA strands was increased compared to the native Watson-Crick duplex, yet still a helical system was formed. Positioning of the bulkier bases in both strands however, led to a drop in thermal stability caused by significant distortion of the helical topology.^[55]

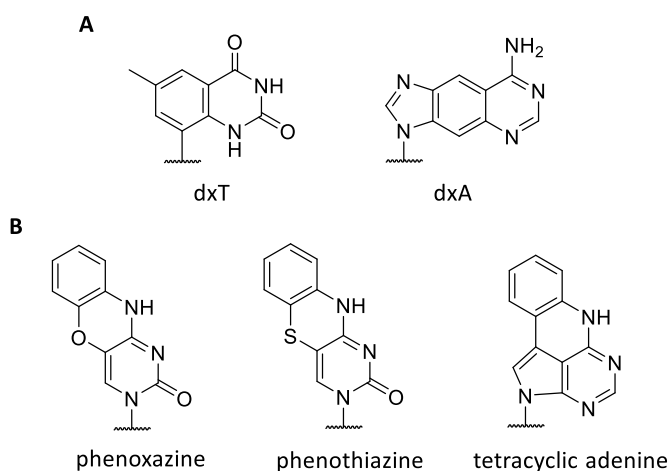


Figure 1.4. Modified nucleobases with expanded ring systems. **A:** extended T (dxT) and A (dxT) nucleobases by *Kool* et al. **B:** tri- and tetracyclic bases derived from cytidine and adenine.

Phenoxazines and phenothiazines (*Figure 1.4 B*) represent two examples of tricyclic artificial nucleobases that have been designed as cytidine analogues by *Lin* et al.^[56] Mismatch experiments confirmed a selective binding to guanine in an RNA counterstrand, as well as an increase in thermal duplex stability upon incorporation of both bases, respectively. The stabilizing effect was even more pronounced when the tricyclic bases were placed in adjacent positions (solely positioned: $T_m \approx +2$ °C, clustered: $T_m \approx +5$ °C). This phenomenon could be explained through enhanced base stacking of the neighboring tricyclic systems. Similar observations were made by *Buhr* et al. when investigating a tetracyclic adenine analogue (*Figure 1.4 B*).^[57] Also, the A congener bound selectively to its Watson-Crick partner T, yet several adjacent tetracyclic bases were necessary to increase duplex stability.

In a third approach to examine the possibilities arising from modified nucleobases, *Inouye et al.* created a pyrimidine-only nucleobase system by substituting all four canonical bases with unnatural pyrimidine-alkynyl analogues (*Figure 1.5*).^[58]

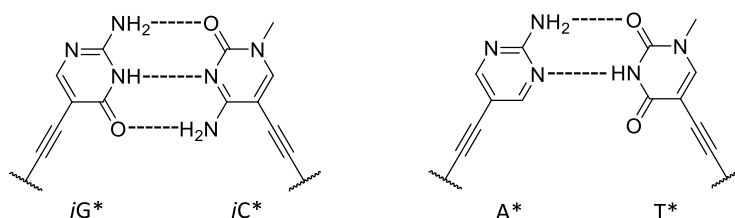


Figure 1.5. Artificial all-pyrimidine nucleobases.

They described the formation of a right-handed helix between an *iG*/iC**-rich, artificial DNA strand and a native complementary DNA. Duplex formation was thereby claimed to happen in a sequence-specific manner with anti-parallel orientation. In addition, T_m values were found to be close to a corresponding native DNA/DNA duplex. Interestingly, complementary strands composed solely of *A** and *T**, respectively, were reported to only form triplexes. Similar efforts have been made by *Switzer et al.* who reported an all-purine base system (not shown).^[59] By replacing adenine, cytosine and thymidine with diaminopurine, *iso*-guanine and 7-deazaxanthine, *Switzer* and co-workers obtained artificial duplexes with similar stability compared to native DNA/DNA congeners. However, they also reported about self-association of a variety of sequences, which might occur when working with purine-rich systems.^[59]

1.2.2 Modification of the (2'-Deoxy)Ribose

The (2'deoxy)ribose displays an attractive site for the implementation of chemical modifications, since it is, in contrast to the aforementioned nucleobases, independent of the oligonucleotide sequence. Furthermore, changes on the furanose ring, which serves as linkage between the canonical nucleobases and the phosphodiester backbone, play a central role in the modulation of properties of nucleic acids. One of the most prominent examples underlining this statement is the comparison between DNA and RNA. The two biopolymers (nearly) consist of the same building blocks, yet show significant differences concerning their biophysical and biochemical properties, along with their role in cellular processes. Responsible for these considerable differences is the substitution pattern of the 2'-position of the ribose unit (H = DNA, OH = RNA). In RNA, the electron withdrawing effect of the 2'-hydroxy moiety steers the conformationally flexible five-membered ring into the *C3'-endo* form, whereas the 2'-hydrogen of DNA directs the ring towards the *C2'-endo* confirmation (*Figure 1.6*).^[60–62] This conformational equilibrium has a far-reaching impact on the overall structure of DNA and RNA, thus leading to differences in duplex stability and the spatial arrangement. While RNA-RNA duplexes appear in a right-handed A form, DNA-DNA duplexes of the same sequence take on a right-handed B form.^[63] As a consequence, RNA-RNA duplexes show higher stability than comparable DNA-DNA duplexes, with RNA-DNA hybrids being of intermediate stability. This principle has found great interest regarding the search for modifications to improve the affinity of ASOs towards RNA, as well as their overall pharmacokinetic profile.

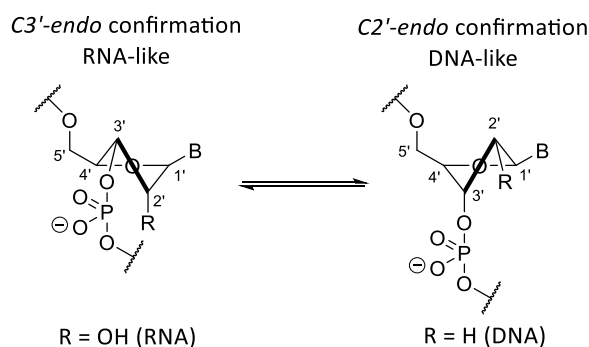


Figure 1.6. Equilibrium of the *C3'-endo* conformation (RNA-like) and the *C2'-endo* confirmation (DNA-like).

B = nucleobases.

One of the first modifications introduced to the ribose unit has been inspired by a naturally occurring congener of RNA: the 2'-*O*-methyl moiety (2'-*O*-Me RNA, *Figure 1.7*). The

seemingly minor change in the sugar structure has been proven to exert several beneficial effects. Thus, ONs carrying the 2'-*O*-Me modification were shown to possess improved nuclease stability and enhanced binding affinity towards complementary RNA.^[64,65] In addition, the immune response triggered through the application of ONs was observed to be reduced due to the presence of the 2'-*O*-Me residue.^[66] As a consequence, the 2'-*O*-Me modification has become one of the most widely employed alterations in antisense technology and even found its way to advanced clinical trials.^[67]

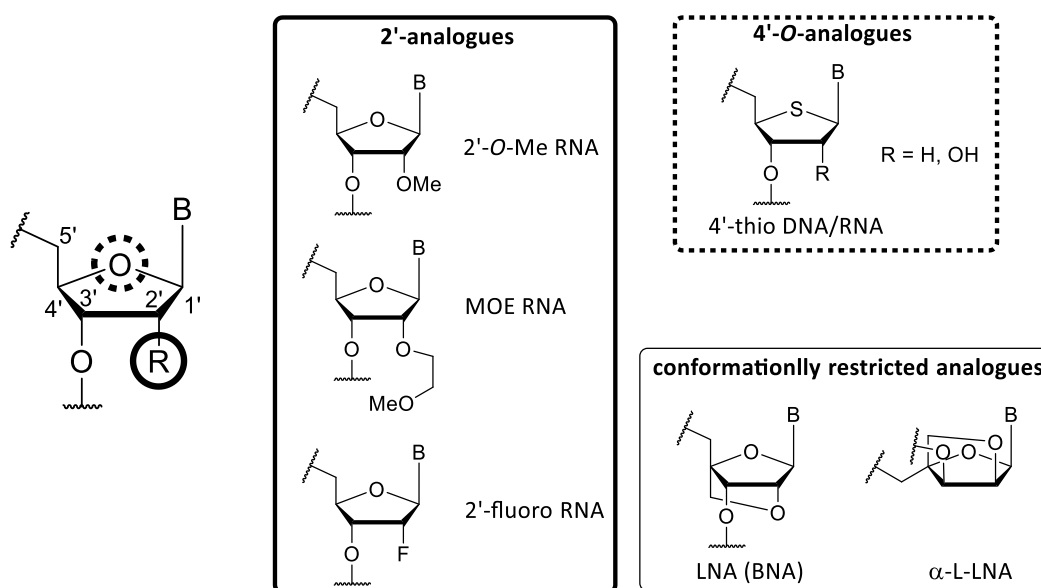


Figure 1.7. Overview of selected modifications of the ribose sugar unit. B = nucleobase.

Following the example of the 2'-*O*-Me modification, 2'-*O*-methoxyethyl RNA (MOE RNA, *Figure 1.7*) was developed as a further variant of 2'-altered ONs. This analogue revealed an even more pronounced rise in nuclease resistance compared to its predecessor, combined with an increased thermal stability.^[68] An explanation for this phenomenon was found to be the ethyl linker of MOE, which positions the ethylene glycol oxygen in close proximity to the 2'-hydroxyl group, thus creating a gauche orientation of the two oxygen atoms. Consequently, the structure becomes more rigid, which contributes to the fixation of the sugar ring in the *C3'*-*endo* conformation and, finally, to enhanced binding affinity and biological stability.^[68] These favorable properties have led to a recent approval of an ASO incorporating the MOE modification, mipomersen, by the U.S. Food and Drug Administration (FDA).^[69,70] Another congener of 2'-modified RNA is 2'-fluoro RNA (*Figure 1.7*).^[71,72] The fluorine atom replacing the 2'-hydroxyl function of RNA possesses a strong electronegative potential. As a result of the pronounced electron withdrawing

effect, the equilibrium depicted in *Figure 1.6* is shifted towards the *C3'-endo* confirmation, again promoting hybridization with RNA and nuclease stability.^[73] Moreover, the relatively small size of the fluorine atom makes it structurally inert, since no spatial deformation of the helical structure is required to accommodate the modification.^[74]

An exchange of the 4'-oxygen atom represents yet another approach towards the modification of the (2'-deoxy)ribose unit. One of the most prominent examples is the introduction of sulfur instead of oxygen at the 4'-position, resulting in 4'-thio congeners of DNA and RNA (4'-thio DNA/RNA, *Figure 1.7*).^[75] *Imbach* et al. demonstrated that 4'-thio RNA recognizes complementary RNA strands and forms stable helical duplexes with an A-type structure.^[76] Additionally, they observed an improved sturdiness towards nuclease-mediated degradation, rendering 4'-thio RNAs as RNA analogues with advanced properties. In case of 4'-thio DNA, a stabilizing effect to the attack of endo- but not 3'-exonucleases was reported by *Walker* et al., as well as a moderate increase in DNA-binding affinity.^[77] A second example for this type of alterations are the 4'-selenoligonucleotides (not shown). Their synthesis and characteristics were first described by *Damha* et al., who reported about DNA congeners that, despite their B-form-like conformation, revealed enhanced affinity towards RNA but not DNA.^[78]

There are numerous modifications designed to alter the nucleic acid ribose structure and only a few can be mentioned within the scope of this work. However, there is one exemplar which has in particular been in focus of intensive investigations, and also has been of great importance for this thesis. This modification is known under two different names, locked nucleic acid (LNA) or 2',4'-methyleneoxy bridged nucleic acid (BNA), and has been established at the same time yet independently by *Wengel* and *Imanishi*.^[79–81] Both groups intended to lock the ribose in its beneficial *C3'-endo* conformation by inserting a methylene bridge between the 2'- and the 4'-position, thus creating a structurally inflexible sugar (LNA (BNA), *Figure 1.7*).^[79–81] Incorporation of LNA in an ASO results in a drastic increase of binding affinity towards both DNA and RNA ($T_m \approx + 5 \text{ }^\circ\text{C}/\text{mod}$ for DNA, $T_m \approx + 8 \text{ }^\circ\text{C}/\text{mod}$ for RNA), while mismatch sensitivity is still retained.^[80,82] This combination, however, was unique at the time LNA was established. Since such excessive increases in thermal stability were usually obtained by usage of minor-groove binders or the addition of intercalating agents, loss of specificity was a well-known side-effect.^[83] One explanation for the

advantageous properties of the LNA modification lies within the conformational preorganization of the sugar moiety. Through locking of the ribose into the favorable North conformation, no significant conformational changes have to occur upon hybridization, thus reducing the entropic penalty and ultimately boosting the strength of duplex binding. Likewise, structural studies on LNA-LNA duplexes revealed a more 'coiled' structure of the modified helix, containing ~ 14 base pairs per helical turn. These are four more compared to the native DNA B-form duplex and three additional base pairs compared to the A-form RNA duplex.^[84] Consequently, base stacking was suggested to be improved when using LNA ONs. A further plus for LNAs is connected to their simplicity. In total, only one methylene unit has been added to the structure of a native RNA nucleoside. This adjustment does not require any additional protection groups or adjustment of reagents applied in automated DNA synthesis. Thus, suitable LNA building blocks can be readily applied in the well-established phosphoramidite coupling chemistry, making it an easily accessible modification.^[85]

As a result, LNA has found its way into several different applications. When introduced to ASOs, the LNA modification causes effective gene silencing *via* mRNA binding, paired with an increased effectiveness compared to differently modified congeners.^[85–87] In addition, usage of LNA in the flanks of a chimeric ON can decrease the minimally required size of an ASO by several bases, allowing the application of 'truncated ASO'.^[88,89] This innovation has already affected some strategies for gene-silencing by the RNA interference mechanism.^[90] As described in section 1.1, the RNAi mechanism requires a double-stranded small interfering RNA (siRNA) to trigger the RISC complex and initialize mRNA degradation. One concern circles around the passenger strand, which is released from the guide strand upon Argonaut binding and is hence at risk to interact with off-targets.^[90] Through bisection of the passenger strand into two short LNA-modified RNA snippets, off-target binding could be significantly reduced. Beyond alteration of gene activity by the antisense mechanism, LNA has also been implemented in the antigene approach. Through either strand invasion of chromosomal dsDNA by Watson-Crick base pairing or the formation of triplex structures via Hoogsteen base pairing, regulation of gene expression could be observed.^[91,92] Due to the success of LNA, numerous LNA-based nucleoside modifications have followed. An example, which is of particular interest, is α -L-LNA, one of the eight LNA stereoisomers (*Figure 1.7*). A nonamer of an α -L-LNA:RNA hybrid,

incorporating three modified bases, was described by *Petersen* et al. to adapt a spatial arrangement somewhere in between an A- and B-form.^[93] Nonetheless, the melting temperature of the hybrid was increased by 17 °C in comparison to the native duplex, although no N-type conformation was verified for the α -L-LNA sugar. In addition, α -L-LNA, in contrast to LNA, was claimed to trigger RNase H-mediated cleavage of a complementary RNA strand.^[94] However, since the experimental setup in this study is lacking some vital control experiments, the outcome remains rather questionable.

Nevertheless, even though LNA appears to be a promising tool to achieve highly potent antisense and antigene agents, there are still certain limitations concerning its use that must be taken into account. For example, the high binding affinity exerted by LNA is accompanied by the tendency to form hairpin structures or homoduplexes of notable stability, particularly if LNA-LNA base pairs can be formed.^[95] Thus, the abundance and position of the LNA-modification has to be carefully adjusted. Additionally, a strong hepatotoxic potential related to the presence of LNA has been reported by *Swayze* and co-workers.^[86] The toxicity was detectable for several different sequences, with and without the presence of a complementary counterstrand. Further evidence for the described hepatotoxicity was published by *Dieckmann* et al. who observed that high-affinity ASOs tend to randomly bind off-targets, thus resulting in severe side effects.^[96]

Overall, application of the LNA-modification to the ASO approach provides manifold possibilities. However, its usage has to be carefully planned.

1.2.3 Modification of the Internucleoside Linkage

The phosphodiester linkage, as present in DNA and RNA, is unique in its structure and function. In the process of transcription, as well as during the replication of DNA, the phosphodiester linkages are formed through the enzymatic conversion of highly energetic triphosphates, resulting in a polar, polyanionic chain. The durability of the emerging internucleoside bridge is a compromise between an adequate stability for the safe storage of genetic information and sufficient lability to be cleaved, repaired or recycled if needed. In 1987, *Westheimer* wrote about the 'importance of being ionized' and the necessity of the anionic charge pattern for nucleic acids to prevent their diffusion over cellular membranes.^[97] Roughly 15 years later, *Benner* and *Hutter* reported about the need of the permanently negatively charged backbone for the overall function of DNA and RNA.^[98] Accordingly, the charge repulsion between the phosphate groups (i) prevents self-aggregation of single stranded nucleic acids so that they can serve as templates, (ii) provides just the right distance between the backbones of two complementary strands to facilitate base recognition and duplex formation and (iii) displays the necessary scaffold for DNA replication and mutation. In summary, the polyanionic, highly polar and fairly stable nucleic acid backbone structure is the perfect match for its function as a genetic biopolymer. On the other hand, these properties that are favorable for biological processes are incompatible with the prerequisites for drug-like agents.^[99] Due to their pronounced polarity, ONs are not resorbed well and get excreted rapidly. Furthermore, the negative charge hampers cellular uptake as well as tissue distribution. Even if ONs were resorbed, degradation by endogenous nucleases would cleave the phosphodiester backbone of the ON agent before it could exert any effect. Thus, it is the task for medicinal chemists to create a modified backbone structure that provides a fitting pharmacokinetic profile while preserving the unique recognition properties and target affinity of native nucleic acids.

1.2.3.1 Anionic Backbone Linkages

One of the earliest backbone modifications maintaining the anionic charge were the phosphorothioates (PS) (*Figure 1.8*) first described by *Eckstein*.^[100] They can be obtained through a rather minor modification in which a sulfur replaces one of the non-bridging oxygen atoms of the phosphate linkage. However, this one-atom exchange has been shown to have a far-reaching impact on the general ON characteristics. Unlike the native DNA

backbone, PS linkages are stable towards nuclease-mediated degradation^[101,102] and show an improved stability in biological media. Furthermore, the sulfur atom is well tolerated by RNase H, which still recognizes hybrid duplexes of PS ONs and RNA.^[103,104] Also, the PS modification has been reported to exert a beneficial effect on pharmacokinetics. Due to enhanced binding to plasma proteins, renal excretion was shown to drop significantly.^[103] On the other hand, cellular uptake was shown to be improved, resulting from an increased interaction with cell surface proteins.^[105] Still, these desirable effects have also been proven to have a down side, since PS ONs also strongly bind to immune receptors, thus triggering pro-inflammatory reactions.^[106] Also, the introduction of the sulfur atom furnishes a chiral center at the phosphorus, thus leading to R_p and S_p isomers.^[102] Both isomers show differing physicochemical properties. The presence of the R_p isomer contributes to higher thermal stability, but it is slightly more labile in terms of nuclease stability.^[107] For this reason, several possibilities for the synthesis of stereochemically pure PS ONs have been explored.^[108–110] However, biological evaluation of *all*- R_p -ONs and *all*- S_p -ONs in cell and animal models could allocate no significant benefit of the pure isomers over a stereorandom PS ON.^[111] Nonetheless, the PS modification represents one of the most widely used backbone modifications and has, with the FDA approval of the *all*-PS-modified ASO fomivirsen, already made its way into the clinic.

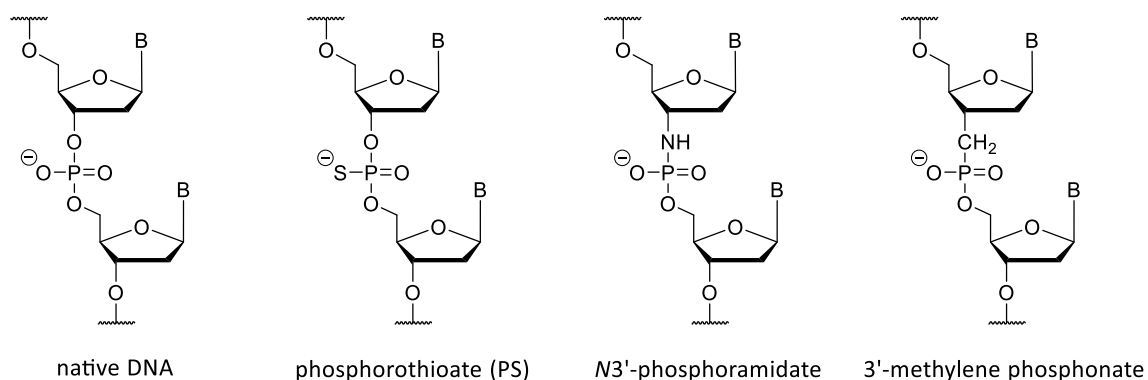


Figure 1.8. Overview of selected anionic backbone modifications in comparison with native DNA.

B = nucleobase.

Further examples for anionic backbone linkages are the $N3'$ -phosphoramidates^[112] and the $3'$ -methylene phosphonates^[113]. *Wilson* and his group described^[114] the synthesis and properties of the $N3'$ -phosphoramidates. In thermal dissociation studies they observed an enhanced affinity of uniformly $N3'$ -phosphoramidate modified ONs towards DNA, RNA and other $N3'$ -phosphoramidate containing ONs. In general, an increase of about 2.2-2.6 °C/mod

could be achieved. Furthermore, the phosphoramidate linkage steers the backbone into an RNA-like A-form and, additionally, shows physicochemical properties closely related to RNA congeners. Yet, for ONs carrying the *N3'*-modification, no activation of RNase H could be observed.^[114] 3'-Methylene phosphonates by An et al. were reported to possess enhanced stability towards nucleases as well as good affinity for their RNA targets.

1.2.3.2 Neutral Backbone Linkages

An alternative approach to alter the properties of native nucleic acids is the introduction of uncharged internucleoside connectors. Replacement of the anionic phosphodiester by neutral groups was thereby hoped to enhance cellular uptake due to a generally more lipophilic structure. Also, an improved binding affinity to complementary strands was desired, since neutral linkages would cancel out the electrostatic repulsion that is normally present between the two negatively charged ON backbones. One of the earliest described uncharged backbone modifications were the methylphosphonates (MP), in which one of the non-linking oxygens is replaced with a methyl group (*Figure 1.9*).^[115] Similar to their congeners, the phosphorothioates, insertion of the MP-modification resulted in a mixture of diastereomers.^[116] The thus obtained ONs showed an increased stability towards nuclease-mediated degradation, yet are relatively sensitive regarding decomposition under basic conditions, which are necessary in standard protocols for DNA synthesis. Additionally, their affinity towards complementary RNA was described to be less pronounced than for unmodified ONs. Also, poor solubility in water and the incapability to activate RNase H add up to the list of unwanted characteristics.

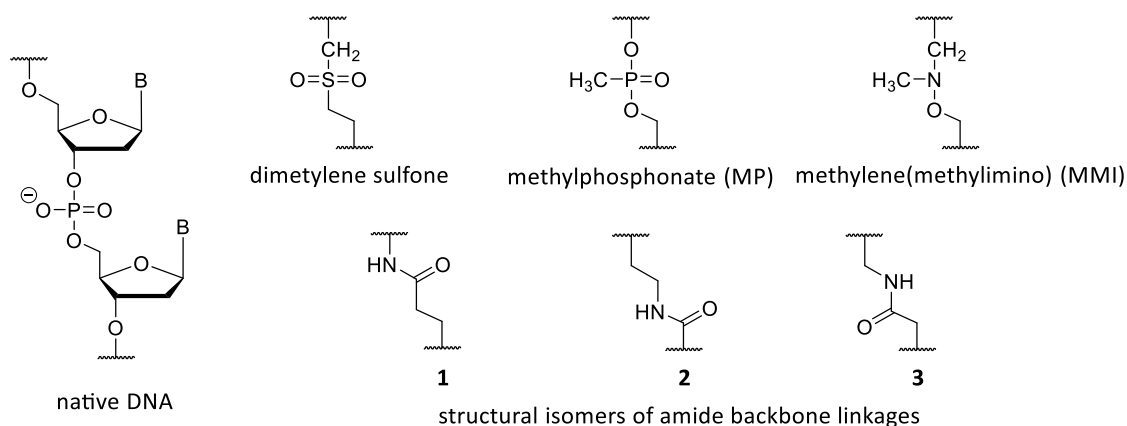


Figure 1.9. Overview of selected neutral backbone modifications in comparison with native DNA.

B = nucleobase.

Although, *Reynolds* et al. accomplished the synthesis of *all-R_p*-modified MP ONs, which furnished duplexes with higher stability compared to the diastereomeric mixture, their overall unfavorable profile left the methylphosphonates as a less frequently used option.^[117] Another variant to obtain neutrally charged backbone structures has been explored by *Schneider* and *Benner*, who worked on sulfur-linked ONs and created building blocks for the assembly of sulfide-, sulfoxide- and sulfone-linked congeners of DNA (*Figure 1.9*).^[118] This approach was further investigated by *Richert* and *Benner* who focused on the synthesis and properties of fully dimethylene sulfone-modified RNA (rSNA).^[119] Although rSNA was proven to suffer from an immense loss in binding affinity towards both DNA and RNA ($\Delta T_m \approx -15$ °C/mod), it also provided valuable insights into the role and significance of the anionic backbone structure for duplex formation. This information, as mentioned above, has also been subject of a review by *Benner* and *Hutter* in 2002.^[98] Yet a different approach, i.e. to create a neutral, achiral internucleoside bridge without the usage of sulfur or phosphorus, was applied by *Sanghvi* et al. The resulting modification is known as the methylene(methylimino) (MMI) backbone linkage (*Figure 1.9*).^[120] Synthesis of fully alternating ONs through dimeric phosphoramidate building blocks incorporating the MMI-modification was described to produce highly biologically as well as chemically stable oligomers. Furthermore, excellent target recognition, good water solubility and retained base-pairing fidelity were reported. Still, hybrid duplexes with RNA were no substrates for RNase H.

The successful exchange of the phosphodiester with several structural isomers of an amide linkage was presented by *De Mesmaeker* and co-workers (*Figure 1.9*, structures **1-3**).^[121-123] As for the MMIs, the synthesis of partially modified amide ONs was feasible through usage of dimeric phosphoramidite building blocks in standard automated DNA synthesis. While partial substitution of the native backbone structure with **1** and **2** resulted in slightly destabilized duplexes with RNA and DNA, the insertion of **3** furnished a modestly improved affinity to RNA ($\Delta T_m \approx +0.5$ °C/mod) but not DNA.^[121] An explanation could be the general rigidity of the amide structure, which preorganizes the sugar in a *C3'-endo* conformation and is therefore more likely to form A-type helices. Additionally, improved biological stability against nuclease-mediated cleavage could be observed. Moreover, *Rozners* et al. studied the effects of the amide modification on siRNA performance.^[124] Interestingly, amides were shown to be well tolerated by both the passenger and the guide strand when

placed in the center of the sequence, and they even improved the silencing effect when located close to the 5'-end of the passenger RNA.

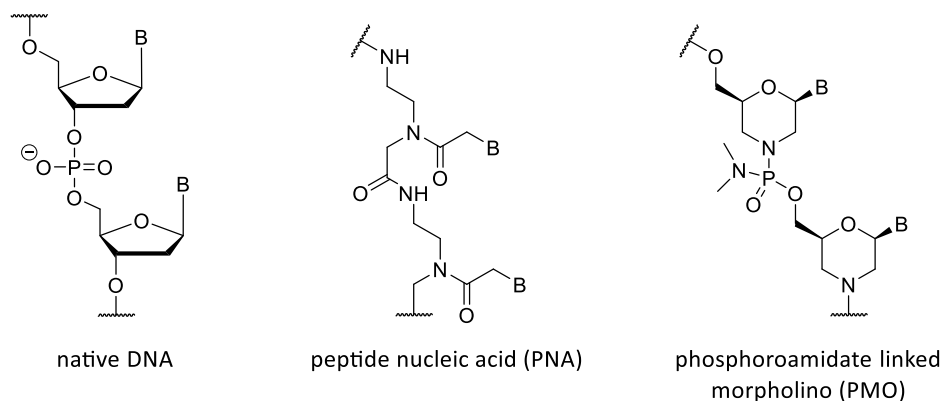


Figure 1.10. Neutral backbone modifications replacing the whole phosphate-sugar backbone, in comparison to native DNA. B = nucleobases.

In contrast to the aforementioned backbone alterations, some versions also exist in which the whole sugar-phosphate chain has been replaced. In *Figure 1.10*, two of the most prominent congeners of this approach – the peptide nucleic acids (PNA) and the phosphoramidate-linked morpholino (PMO) structure – are depicted. Both variants belong to the uncharged backbone linkages and exert considerable effects when incorporated in a nucleic acid oligomer. The PNAs have been first described by *Nielsen* and co-workers, who synthesized a thymine-substituted oligomer with a fully replaced polyamide backbone.^[125] The *N*-(2-aminoethyl)glycine units, to which the nucleobases are attached, were inspired by the polypeptide chains of proteins. The obtained artificial structure not only displayed satisfying sequence-selective binding to a dA₁₀-mer, but was also capable of displacing an unmodified dT₁₀-mer out of an DNA-DNA duplex with the dA-target strand. Subsequent melting temperature experiments revealed a drastic increase in duplex stability of the PNA-DNA hybrid in comparison to the native DNA duplex ($\Delta T_m \approx + 6,3 \text{ }^\circ\text{C/mod.}$). Only two years later, *Nielsen* et al. published some further insights about PNAs containing all four canonical DNA bases and reported about their capability to recognize mixed counterstrands according to Watson-Crick base-pairing rules, while also exerting high stability towards nuclease-mediated degradation.^[126] Structural analysis of PNA-DNA and PNA-RNA duplexes additionally disclosed the exceptional flexibility of the PNA strands, which allows easy adaption of A- as well as B-type conformations.^[127,128] Moreover, PNAs were shown

to form highly stable triplexes with dsDNA through strand evasion, thus marking them as potential antigene agents.^[129] These results, together with the facile access to PNA ONs *via* solid phase peptide synthesis, triggered a rapidly rising interest in the artificial structural peptide/nucleic acid fusion. Over time they found application in various different strategies, like the antisense approach^[130,131], in splice modulation studies^[132] and in antigene technology^[133,134]. Yet, PNAs come with three crucial disadvantages. They only show poor water solubility, are incapable of crossing cellular membranes and possess a tendency to form self-aggregates. The resolution of these drawbacks is still subject to intensive research.^[135–137] PMOs are a class of nucleic acid analogues in which the phosphodiester linkage is substituted with a phosphorodiamidate backbone and the ribose sugar is replaced with a morpholino unit. Fully PMO-modified oligomers were described to bind complementary RNA in a more stable way than the corresponding DNA sequence. Although PMO ONs, like PNAs, are neutral DNA analogues, they were reported to show good water solubility, paired with an increased stability in biological media.^[138] Also, studies comparing PMO ONs with phosphorothioates of the same sequence unveiled superior antisense efficacy of the morpholino oligomers in both cell-free and cellular systems.^[139] However, PMO-modified ONs are neither a substrate for RNase H nor do they show enhanced cellular uptake. As a result, they only displayed poor to modest activity in *in vivo* studies and are still in need of further improvement.^[140]

1.2.3.3 Cationic Backbone Linkages

Review: Oligonucleotide analogues with cationic backbone linkages

Melissa Meng and Christian Ducho*

The contributions of each author to the review " Oligonucleotide analogues with cationic backbone linkages" are listed below:

Both authors: Were jointly responsible for the writing, editing and review of the manuscript.

All articles published in the Beilstein Journal of Organic Chemistry are licensed under the terms of the Creative Commons Attribution License (<http://creativecommons.org/licenses/by/2.0> or <http://creativecommons.org/licenses/by/4.0>), which permits unrestricted use, distribution, and reproduction in any medium, provided the original work is properly cited.

Beilstein J. Org. Chem. **2018**, *14*, 1293–1308.

DOI:10.3762/bjoc.14.111



Oligonucleotide analogues with cationic backbone linkages

Melissa Meng and Christian Ducho*

Review

Open Access

Address:
Department of Pharmacy, Pharmaceutical and Medicinal Chemistry,
Saarland University, Campus C2 3, 66123 Saarbrücken, Germany

Email:
Christian Ducho* - christian.ducho@uni-saarland.de

* Corresponding author

Keywords:
backbone modifications; cations; DNA; oligonucleotides; zwitterions

Beilstein J. Org. Chem. **2018**, *14*, 1293–1308.
doi:10.3762/bjoc.14.111

Received: 05 January 2018

Accepted: 26 April 2018

Published: 04 June 2018

This article is part of the Thematic Series "Nucleic acid chemistry II".

Guest Editor: H.-A. Wagenknecht

© 2018 Meng and Ducho; licensee Beilstein-Institut.
License and terms: see end of document.

Abstract

Their unique ability to selectively bind specific nucleic acid sequences makes oligonucleotides promising bioactive agents. However, modifications of the nucleic acid structure are an essential prerequisite for their application in vivo or even in cellulo. The oligoanionic backbone structure of oligonucleotides mainly hampers their ability to penetrate biological barriers such as cellular membranes. Hence, particular attention has been given to structural modifications of oligonucleotides which reduce their overall number of negative charges. One such approach is the site-specific replacement of the negatively charged phosphate diester linkage with alternative structural motifs which are positively charged at physiological pH, thus resulting in zwitterionic or even oligocationic backbone structures. This review provides a general overview of this concept and summarizes research on four according artificial backbone linkages: aminoalkylated phosphoramidates (and related systems), guanidinium groups, *S*-methylthiourea motifs, and nucleosyl amino acid (NAA)-derived modifications. The synthesis and properties of the corresponding oligonucleotide analogues are described.

Introduction

Oligonucleotides have the unique ability to bind endogenous nucleic acids in a selective and sequence-specific manner. They can therefore modulate biological functions via different mechanisms [1]. Single-stranded oligonucleotides (ONs) can act in cellulo mainly via two different pathways (Figure 1). In the antigene pathway [2], the ON enters the nucleus and binds to double-stranded DNA to form a triple helix. The triple helix is not a substrate for the transcription machinery, and hence, RNA biosynthesis (and therefore protein formation) is blocked. In the

antisense pathway [3], the ON binds to single-stranded mRNA in the cytoplasm, thus furnishing a duplex structure (usually a DNA–RNA heteroduplex) which cannot undergo ribosomal protein biosynthesis. Alternatively, the DNA–RNA heteroduplex can be a substrate for RNase H-mediated degradation of the mRNA strand. This way, catalytic amounts of the ON can mediate the efficient cleavage of mRNA encoding a specific protein, which leads to effective (though reversible) and selective downregulation of the protein's activity. A third option for

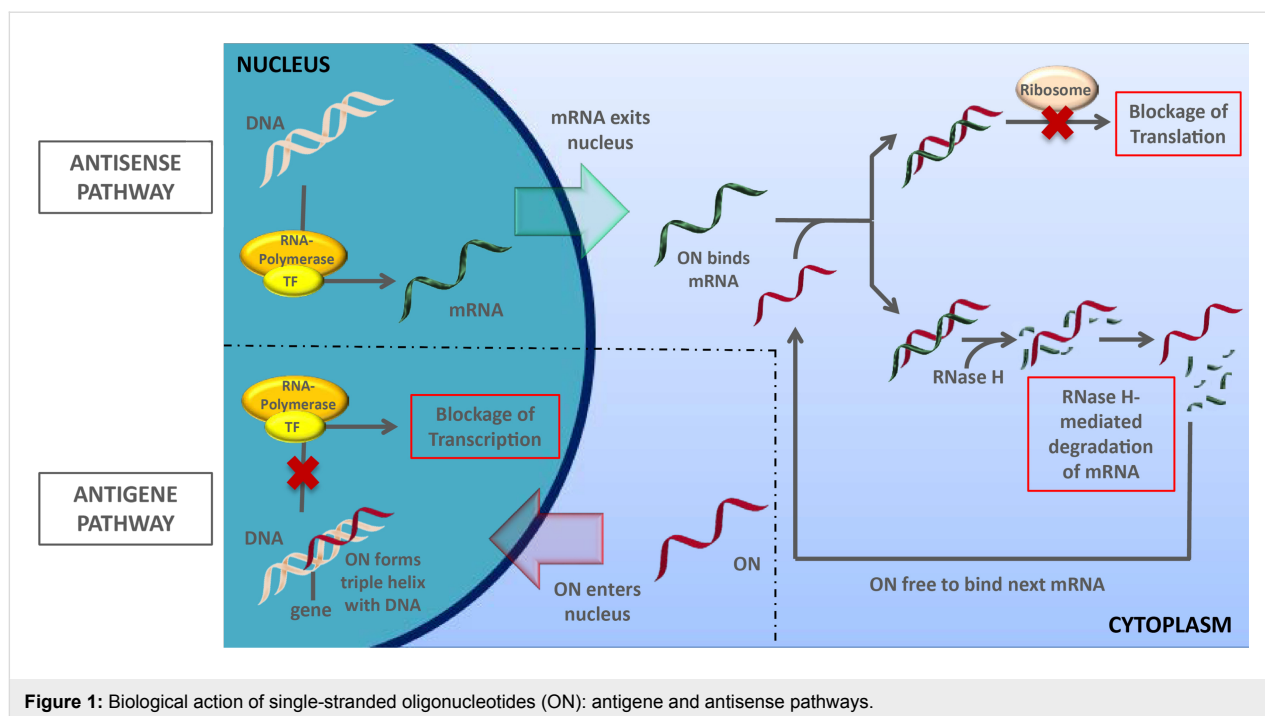


Figure 1: Biological action of single-stranded oligonucleotides (ON): antisense and antisense pathways.

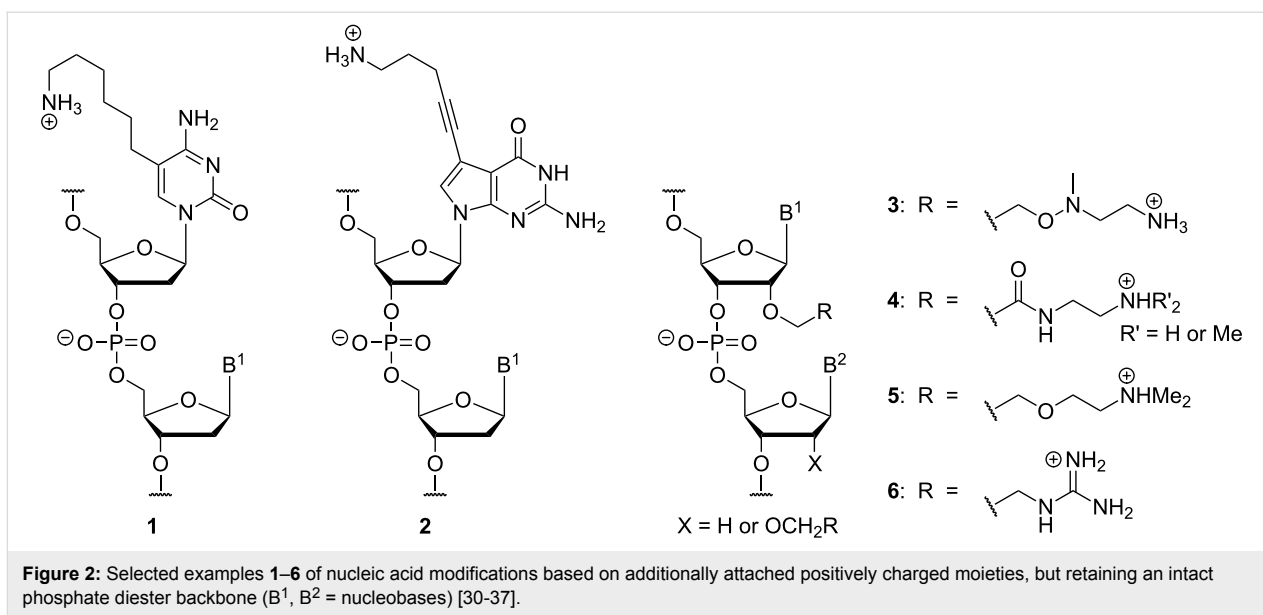
the biological action of oligonucleotide structures is the triggering of the RNA interference mechanism by double-stranded 'small interfering' RNA (siRNA, mechanism not shown) [4]. Alternatively, single-stranded oligonucleotides (anti-miRNA oligonucleotides, 'AMOs', 'antimiRs') can inhibit endogenous microRNA-mediated RNA interference by blocking the RNA strand in the involved protein–RNA complex (RISC) [5].

The capability of ONs to exert the aforementioned biological mechanisms via sequence-specific molecular recognition makes them highly attractive candidates for drug development. However, their pharmacokinetic properties are problematic and represent a significant hurdle for their therapeutic application. First, the high polarity of ONs, mainly caused by their oligoanionic phosphate diester backbone, severely hampers the penetration of biological barriers such as cellular membranes, thus leading to low cellular uptake. Second, unmodified ON structures are good substrates for nuclease-mediated degradation. Consequently, it is of vital importance to chemically modify ON structures in order to make them suitable drug candidates or chemical probes, e.g., for diagnostic purposes [6,7].

The relevance of the polyanionic phosphate diester-linked backbone to the overall function of nucleic acids has been discussed by Westheimer [8], Benner [9,10], and others. In spite of these considerations, many artificial internucleotide linkages were investigated in order to reduce the overall negative charge of the backbone and to enhance nuclease stability. One apparent approach to achieve these goals is the introduction of non-native

electroneutral backbone linkages, with the nucleic acid mimic 'peptide nucleic acid' (PNA) [11–13] representing a striking example. Although the achiral PNA backbone is pronouncedly different from native nucleic acid structures, PNAs are capable of sequence-specific hybridization to native nucleic acids. However, their moderate water solubility and peptide-like folding properties [9] are hurdles for their biological application. As an alternative strategy, the (deoxy)ribose part of the backbone has been retained and only some of the internucleotide phosphate diesters have been selectively replaced by electroneutral motifs. Such artificial neutral linkages include, among others, sulfone [14], amide [15–22], triazole [23–27], phosphoramidate [28] and phosphate triester [29] moieties.

Using a different approach, positive charges have been introduced into nucleic acid structures. Positively charged moieties were either employed (i) as additional charged structural motifs compensating for the negative charges in the backbone linkages or (ii) as replacements of the native negatively charged phosphate diester linkages. The first option has found considerable attention, with positively charged moieties attached to nucleobases or the ribose sugar. Some selected examples 1–6 of resulting nucleic acid structures are provided in Figure 2 [30–37]. Oligonucleotides of this type are at least partially zwitterionic, but overall densely charged. With respect to the aspired improvement of cellular uptake, fully cationic oligonucleotide analogues might also be attractive candidate structures, as indicated by the advantageous properties of cationic cell-penetrating peptides (CPPs) [38]. However, the design of



modifications of type 1–6 precludes the preparation of fully cationic oligonucleotide analogues.

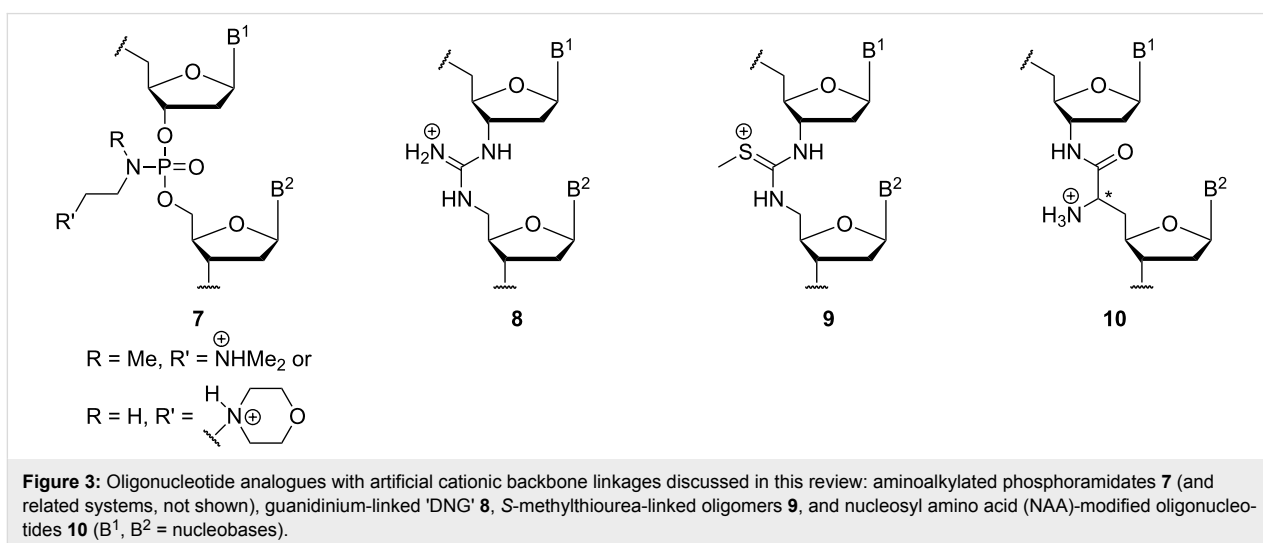
This review focusses on the second aforementioned option to employ cationic motifs in oligonucleotide structures, i.e., as replacements of the native phosphate diester linkages [39]. In principle, this approach enables the preparation of partially or fully zwitterionic as well as cationic backbones. This strategy has been studied less frequently, with research on four artificial cationic linkages summarized in this review: aminoalkylated phosphoramidates (and related systems), guanidinium groups, *S*-methylthiourea motifs, and nucleosyl amino acid (NAA)-derived modifications. The synthesis and properties of the corresponding oligonucleotide analogues of types 7–10 (Figure 3) with cationic backbone linkages are described.

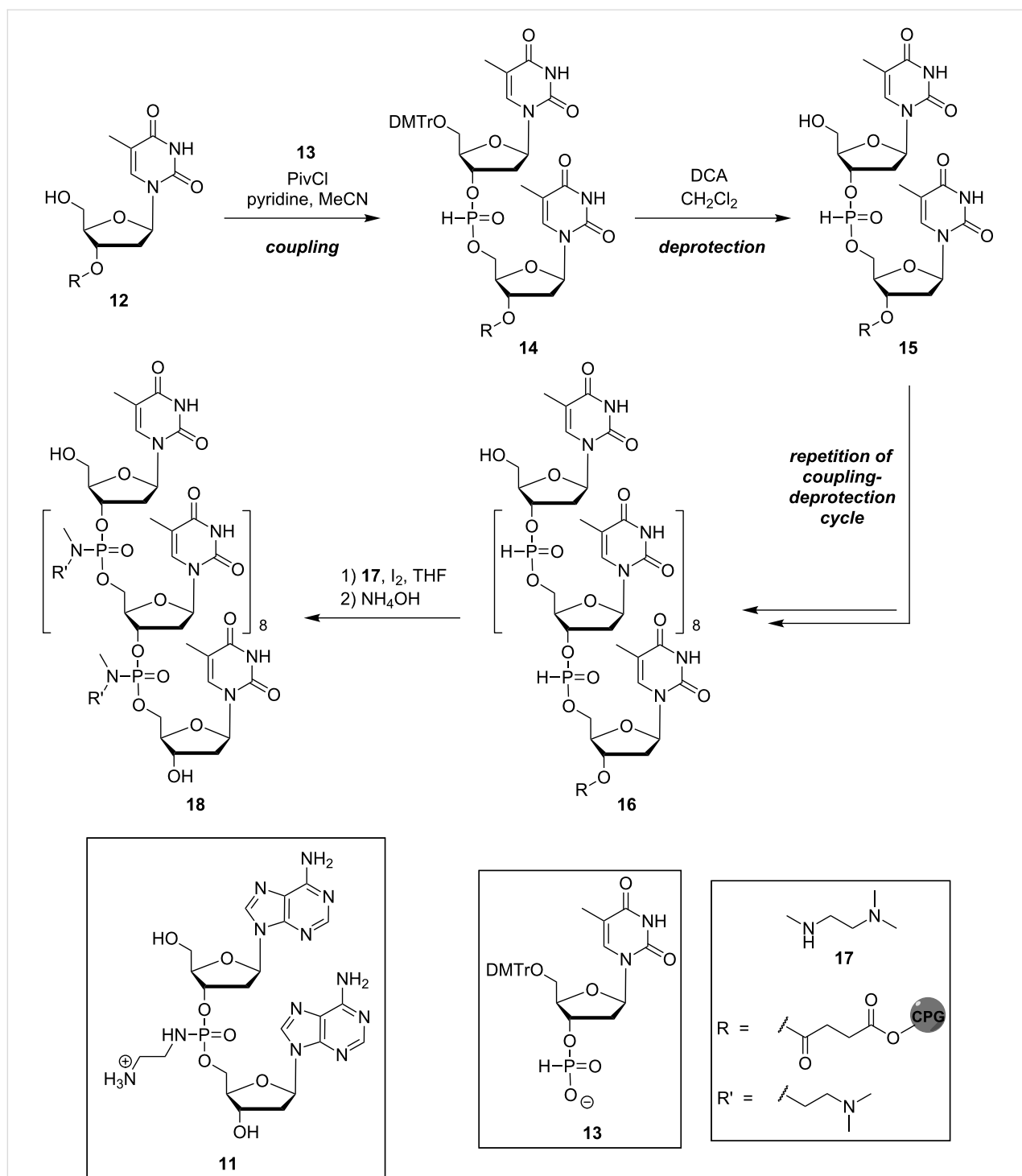
Review

Aminoalkyl phosphoramidate linkages and related systems

Pioneering work in the field has been reported by Letsinger and co-workers. In 1986, they introduced a deoxyadenosyl dinucleotide linked by an aminoethyl phosphoramidate moiety which is positively charged under acidic and neutral conditions [40]. Based on these results, they subsequently reported the synthesis of short, cationic DNA oligonucleotides with phosphoramidate linkages of type 7, which were *N*-alkylated with substituents containing basic structural motifs [41].

The synthesis of the modified deoxyadenosyl dinucleotide **11** was achieved using solution-phase chemistry (reactions not shown, for structure of **11** see Scheme 1) [40]. Subsequently,





Scheme 1: Structure of Letsinger's modified deoxyadenosyl dinucleotide **11** and synthesis of cationic oligonucleotide analogue **18** containing aminoalkyl phosphoramidate linkages. CPG = controlled pore glass (solid support).

the preparation of corresponding oligonucleotide analogues was performed on solid support using H-phosphonate chemistry (Scheme 1). Thus, solid phase-linked thymidine **12** was coupled with 5'-dimethoxytrityl-(DMTr)-protected thymidine 3'-H-phosphonate **13** to give dimeric H-phosphonate **14**, which was then

acidically DMTr-deprotected to furnish **15**. After the desired number of such coupling-deprotection cycles, the phosphite-linked oligo-thymidine **16** was transformed in an oxidative amidation reaction [42] in the presence of iodine and *N,N,N'*-trimethylethylenediamine (**17**) to yield, after basic cleavage

from the solid support, the envisioned aminoalkyl phosphoramidate-linked oligonucleotide **18**.

To study the hybridization properties of such cationic oligonucleotide analogues with native DNA and RNA, Letsinger and co-workers performed UV-monitored thermal denaturation experiments [40,41]. In the case of the modified deoxyadenosyl dimer **11**, hybridization with native RNA-T_{Poly} as well as with DNA-T_{Poly} strands was evident and the complex formed more stable than comparable complexes involving the native d(ApA) DNA reference. An increase of the measured T_m of ≈ 10 °C for complexes of the aminoethyl phosphoramidate-linked dinucleoside **11** with RNA and ≈ 25 °C for the according hybridization with DNA was observed [40]. In addition, the cationic dimer **11** was shown to bind more tightly to native RNA and DNA strands in the presence of magnesium chloride [40].

For the cationic T-oligomer **18**, Letsinger and co-workers reported a strongly reduced absorbance of a mixture of **18** with DNA-A_{Poly} in thermal melting studies, as compared to the non-hybridized, single-stranded oligonucleotides [41]. This indicated a successful complex formation with ordered base stacking of the positively charged oligonucleotide analogue and its native DNA counterstrand. When exposed to high ionic strength (1.0 M NaCl), the complex was shown to undergo a significant decrease in stability. This effect of high salt concentrations was inverse to the corresponding effect for native anionic DNA duplexes and obviously resulted from electrostatic shielding mediated by the salt ions, thus weakening the attraction of the oppositely charged backbones [41].

In order to elucidate the stability of aminoethyl phosphoramidate-linked oligonucleotides to nuclease-catalysed degradation, Letsinger and co-workers described the incubation of such oligomers, the deoxyadenosyl dimer **11** and DNA-T_{Poly} (as a reference) with snake venom phosphodiesterase and spleen phosphodiesterase, respectively [40,41]. In these assays, neither the modified dimer **11** nor oligonucleotides of type **7** (such as **18**) showed any degradation by either enzyme, while native DNA reference strands were rapidly cleaved.

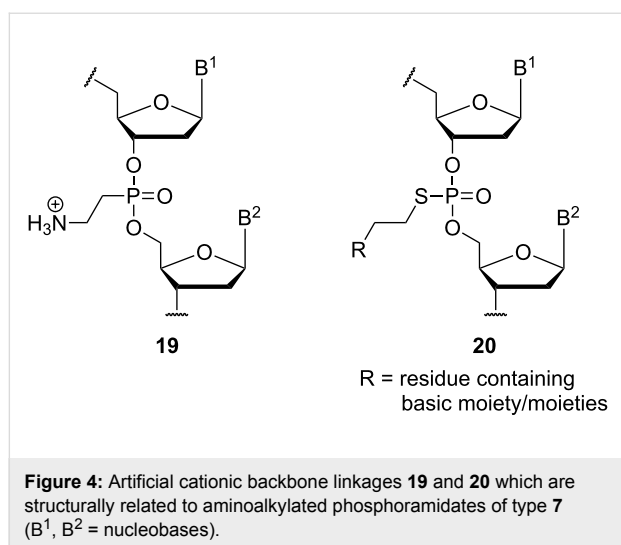
Other groups have subsequently employed Letsinger's aminoalkyl phosphoramidate linkage (or variations thereof) in biochemical and biological studies on the properties of corresponding oligonucleotides. Weeks and co-workers have demonstrated that a triplex-forming antigene oligonucleotide modified with a variant of Letsinger's linkages can efficiently inhibit the expression of plasmid DNA injected into *Xenopus* oocytes [43]. The presence of the cationic backbone modification and a sufficiently long mismatch-free target DNA sequence were essential

for this gene-silencing effect, thus indicating the relevance of enhanced nuclease stability and sequence-specific DNA binding. However, the gene-silencing effect could only be achieved if the modified oligonucleotide and the plasmid DNA were either mixed prior to cellular injection or if the oligonucleotide was injected first, pointing out a likely competition of the cationic antigene oligonucleotide with cellular histones for DNA binding [43].

Vasseur, Debart and co-workers have combined a variant of Letsinger's linkages with an α -configuration at the anomeric centers of antisense oligonucleotides [44,45]. They have found that such zwitterionic to fully cationic α -oligonucleotides bound to single-stranded DNA and RNA targets with high affinity, with duplex stabilization being proportional to the number of cationic modifications. It was also reported that these oligonucleotides showed retained base pairing fidelity, i.e., the T_m value was significantly reduced in the presence of a base mismatch. This specificity in binding suggested that such oligonucleotides should be promising sterically blocking antisense agents as their RNA targets were not digested by RNase H. This anticipated bioactivity was confirmed in whole cell assays without the presence of transfection agents, suggesting that the altered charge pattern of the oligonucleotide backbone enabled its cellular self-delivery [44]. The same authors then also studied similar oligonucleotides with guanidinium groups as cationic moieties, which were obtained by postsynthetic guanidinylation of the congeners with amino-functionalized phosphoramidate linkages (reaction not shown) [46]. The presence of the guanidinium units furnished high hybridization affinities, in particular with single-stranded RNA targets, and also in triplex formation with double-stranded DNA, though the amino-functionalized analogues gave similar triplex stabilities. A fully cationic and fluorescently labelled guanidynylated oligonucleotide was subjected to comparative cellular uptake studies. Relative to its fluorescently labelled anionic phosphorothioate congener, it showed vastly enhanced cellular uptake. Fluorescence microscopy revealed a cytoplasmic localization of the oligonucleotide without accumulation in the nuclei. This indicated an endocytotic uptake mechanism with (at least partial) retention of the material in the endocytotic vesicles. No unspecific cytotoxic effect of the guanidynylated oligonucleotide was observed.

Other types of oligonucleotides with aminoalkyl moieties as part of artificial internucleotide linkages have also been reported. With respect to their structural similarity to Letsinger's aminoalkyl phosphoramidate linkages, these variants are categorized as 'related systems' in this review. Fathi et al. have established the aminoethylphosphonate linkage **19** (i.e., a phosphonate analogue of amidate **7**) [47], and Rahman, Obika and

co-workers have described cationic phosphorothioates of type **20** [48] (Figure 4).



The preparation of phosphonate linkage **19** was achieved in diastereomerically pure form, i.e., with defined configuration at the stereogenic phosphorus atom [47]. Corresponding R_p -configured zwitterionic oligonucleotides formed duplexes with complementary DNA or RNA that were more stable than their respective native counterparts. The modified oligonucleotides showed pronounced nuclease and serum stability as well as significantly enhanced cellular uptake relative to their native congeners. As for the aforementioned phosphoramidates, fluorescence microscopy indicated a cytoplasmic localization of the tested zwitterionic oligonucleotide without significant accumulation in the nuclei, thus pointing to endocytotic uptake with retention of the compound in endocytotic vesicles (vide supra).

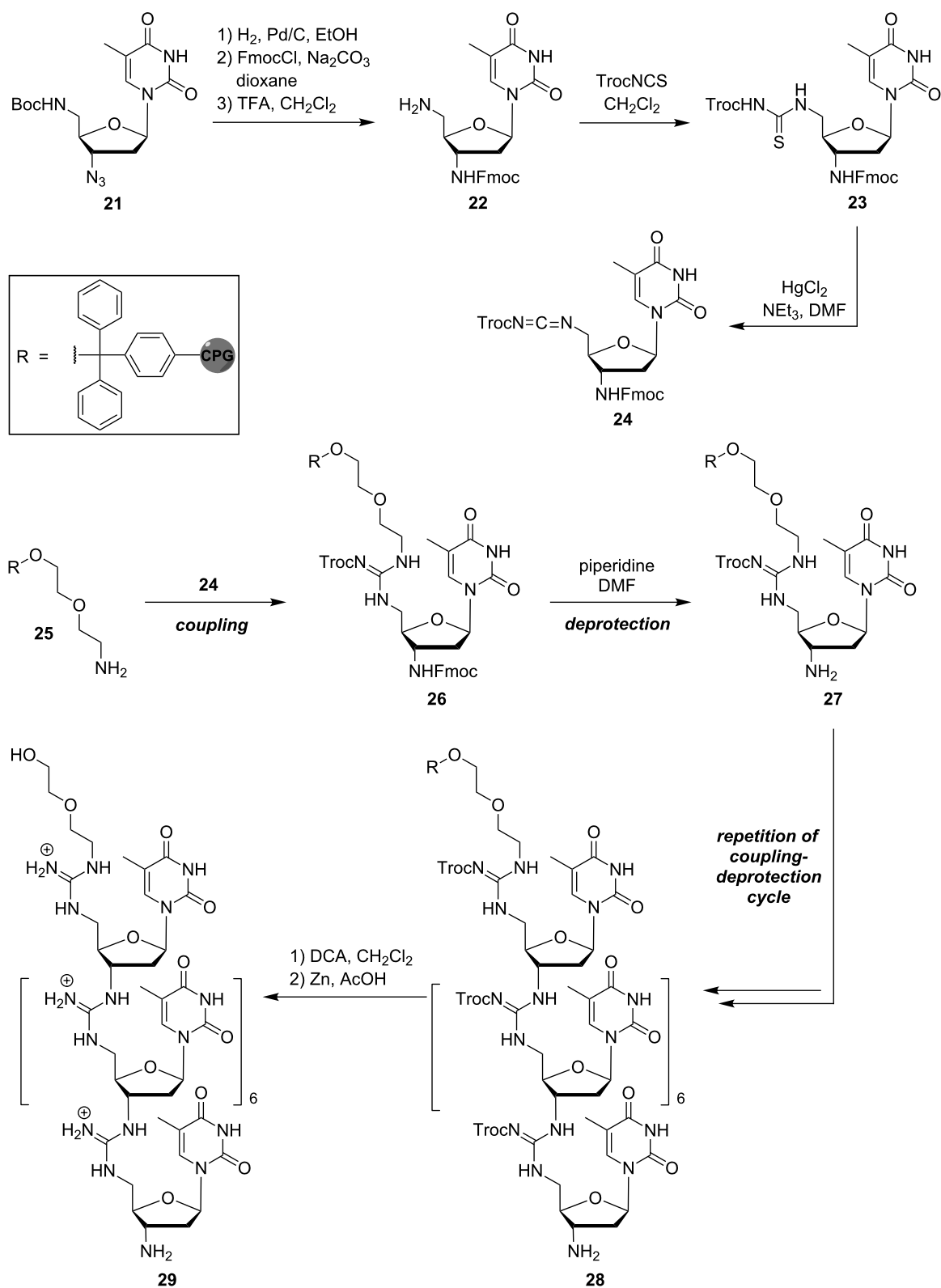
Cationically functionalized phosphorothioates of type **20** were also prepared as diastereomerically pure compounds with defined configuration at the stereogenic phosphorothioate unit [48]. A series of different residues (R in Figure 4) bearing one or two basic amino functionalities was introduced. The resulting 12-mer oligonucleotides with one cationic internucleotide linkage (all other linkages were phosphates) were tested for their ability to form duplexes with single-stranded DNA or RNA as well as triplexes with double-stranded DNA. The aminoalkylated R_p -phosphorothioates showed an increased stability of DNA duplexes while the S_p -isomers gave destabilized duplexes. Both the cationically functionalized R_p - and S_p -oligonucleotides displayed decreased affinity towards RNA, while triplex formation was enhanced for all tested R_p congeners. The aminoalkylation generally provided an increased nuclease stability, which was more pronounced for the R_p isomers.

Deoxyribonucleic guanidines (DNG) with guanidinium linkages

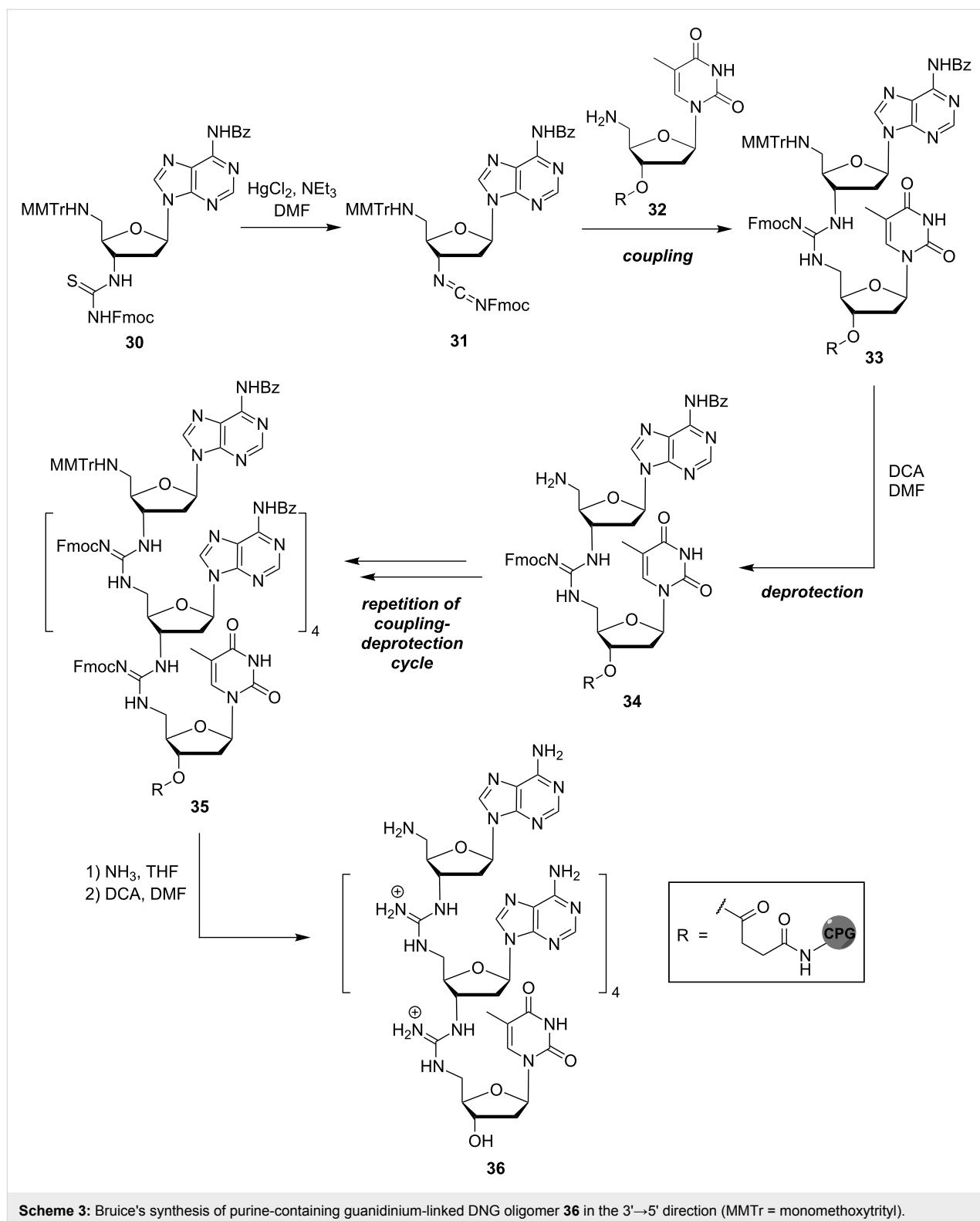
In their design of cationic oligonucleotide analogues, Bruice et al. did not just attach a cationic moiety to the modified phosphate diester backbone, but they completely replaced it with a guanidinium linkage to give 'deoxyribonucleic guanidines (DNG)' of type **8** [49]. The guanidinium group was selected owing to its maintenance of a positive charge over a broad pH range and its ability to form both intermolecular electrostatic interactions and hydrogen bonds [50]. Letsinger's aminoalkyl phosphoramidate modification was stereogenic at the phosphorus atom, thus leading to complex mixtures of diastereomeric oligomers (with the exception of the aforementioned related systems, vide supra) as the stereoselective synthesis of stereogenic phosphate derivatives is challenging. Therefore, achiral artificial linkages such as guanidinium groups may be considered advantageous from a stereochemical perspective.

For the first synthesis of a pentameric thymidynyl DNG in 1996, Bruice and co-workers used an iterative solution-phase protocol (reactions not shown) [51]. This method was associated with some limitations, such as its moderate yields and the need for purification after each synthetic step. Subsequently, two different approaches for the solid phase-supported synthesis of DNG oligomers were introduced. They enabled chain elongation either in the 5'→3' [52] or 3'→5' [53] direction, respectively. Starting from protected 3',5'-dideoxy-5'-amino-3'-azidothymidine **21**, the 5'→3' route was based on the synthesis of the diamino intermediate **22** and thiourea monomer **23**, which was then converted into a reactive carbodiimide **24** and coupled to a terminal amino group of the solid phase **25** (Scheme 2). This coupling furnished solid phase-attached intermediate **26**, which was Fmoc-deprotected to the amine **27**. Iterative repetition of this coupling-deprotection cycle gave oligomer **28**, which was then acidically cleaved from the solid support and reductively Troc-deprotected to afford octameric thymidynyl DNG **29**.

Based on this method, the solid phase-supported synthesis operating in the 3'→5' direction was later developed. As described by Bruice and co-workers, it was compatible with the cleavage conditions used in the solid phase-supported synthesis of native DNA and also allowed the introduction not only of pyrimidine, but also of purine bases into the oligonucleotide analogue [53]. The method was based on the activation of the 5'-monomethoxytrityl (MMTr)-protected 3'-thiourea monomer **30** to the corresponding carbodiimide **31** (Scheme 3). Using long-chain alkylamine controlled pore glass (CPG) loaded with 5'-amino-5'-deoxythymidine (**32**) as solid phase, the reaction cycle started with the guanidine-forming coupling of **31** and **32** to give **33**, followed by acidic cleavage of the MMTr protecting group to yield the free 5'-amine **34**. Subsequent iterative coupling-depro-



Scheme 2: Bruce's synthesis of guanidinium-linked DNG oligomer **29** in the 5'→3' direction (Troc = 2,2,2-trichloroethoxy carbonyl).



tection cycles resulted in the formation of the guanidinium-linked oligomer **35**. After basic guanidine and purine deprotection and concomitant cleavage from the solid support, final acidic deprotection furnished A₅T oligonucleotide analogue **36**.

In addition to these protocols, the solid phase-supported syntheses of DNG-DNA chimeras with partially zwitterionic backbone structures [54,55] as well as of further mixed DNG sequences [56,57] have been described (reactions not shown). It is

also noteworthy that Bruice and co-workers succeeded in the preparation of corresponding guanidine-linked RNA analogues [58,59], though this is not within the main scope of this review.

Bruice et al. reported that oligonucleotide analogues containing the cationic DNG-modification bind to DNA with retention of base-pairing fidelity, furnishing thermally highly stable complexes with native complementary DNA and RNA counterstrands [51,60–64]. The increase in melting temperature for the DNG-DNA complex was reported to be around 15–25 °C per bp under nearly physiological conditions, dependent on the surrounding ionic strength. As shown by Job plot analysis, an oligo-thymidyl DNG forms triple-stranded complexes in a 2:1 mixture with its native DNA counterstrand, i.e., the resulting triplex contains two DNG oligo-thymidylate analogues and one oligo-adenylate DNA strand [64]. The same binding stoichiometry was observed for an oligo-deoxyadenosyl DNG in complex with a native oligo-thymidylate DNA [53]. Overall, the obtained results suggest that adenosine- and thymidine-derived DNG oligomers support the formation of triplex structures, but that the DNG-DNA ratio within the complex is determined by the respective nucleobases. Remarkably, neither cytidinyl nor 7-deazaguanyl DNG oligomers furnish triplexes, but bind their complementary DNA counterstrand in a 1:1 ratio [65,66]. Furthermore, it was shown that an increase in ionic strength shields the oppositely charged backbones, thus destabilizing both DNG-DNA duplexes and triple-stranded DNG-DNA complexes, respectively. The triple-stranded DNG-DNA complex was less affected than its duplex congener though [51,60,61].

Regarding base-pairing fidelity, Bruice and co-workers have reported significantly reduced stabilities of DNG-DNA duplexes and triplexes, respectively, upon the insertion of base mismatches in the DNA counterstrand. Analyzing a 2:1 complex formed from two octameric thymidyl DNG strands and one native DNA A₈-mer, they concluded that base mismatches at either end of the DNA counterstrand sequence do not hamper hybridization as strongly as a single base mismatch in the center of the DNA strand. Two base mismatches in the center of the DNA counterstrand led to a complete loss of hybridization [64].

In addition to these thermal denaturation experiments, Bruice et al. also reported circular dichroism (CD) spectroscopic studies to obtain further information on the solution structures of DNG strands and their complexes with DNA. The corresponding analysis of the aforementioned triplex (DNG-T₈)₂/DNA-A₈ indicated a usual B-DNA-derived triple helix structure, while the comparison of single-stranded DNG-T₈ with native DNA-T₈ furnished two very different CD spectra [64].

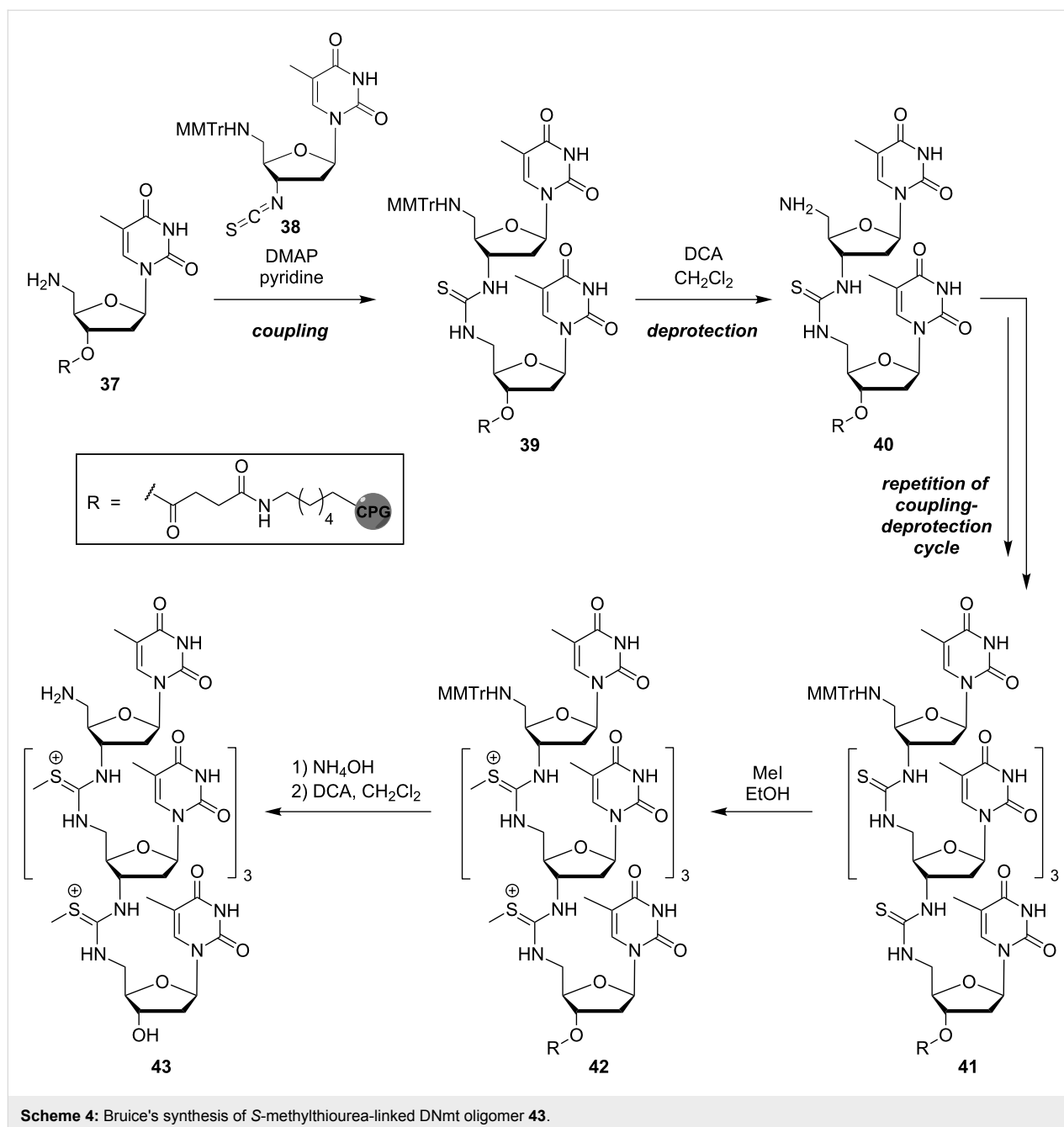
S-Methylthiourea linkages

In addition to their work on DNG oligonucleotide analogues, Bruice et al. also reported the positively charged *S*-methylthiourea backbone modification as an artificial internucleotide linkage [67–69]. For oligomers containing this replacement of the backbone phosphate diesters, the term 'DNmts' was coined. Just like the guanidinium linkage in DNGs, the *S*-methylthiourea modification is not stereogenic and stable towards nuclease-mediated cleavage. Furthermore, it retains its positive charge independent of pH conditions.

Bruice and co-workers initially reported a solution-phase synthesis that enabled the formation of pentameric thymidyl DNmt in the 3'→5' direction (reactions not shown) [68]. They then introduced an automated solid phase-supported synthesis which was compatible with standard techniques of DNA synthesis (Scheme 4) [69]. A derivative of 5'-amino-5'-deoxythymidine attached to CPG (**37**) served as the solid phase. The construction of the oligomer, achieved in 3'→5' direction, was based on the coupling of 3'-isothiocyanate **38** with the 5'-amino group of **37** to give **39** and, after acidic MMTr cleavage, **40**. Iterative repetition of this coupling-deprotection cycle afforded thiourea-linked oligonucleotide analogue **41**. Subsequent reaction of the thiourea internucleotide linkages with methyl iodide furnished the protected *S*-methylthiourea-linked oligomer **42** and finally, after cleavage from the solid support and acidic deprotection, the envisioned DNmt oligomer **43**.

As for the pentameric DNG congener (vide supra), the DNmt-T₅ oligonucleotide analogue was shown to bind more tightly to complementary DNA than DNA itself [68]. Under nearly physiological conditions with respect to pH and ionic strength, the *T_m* value for the DNmt-T₅/DNA-A_{Poly} complex was reported to be above 80 °C whereas a comparable DNA–DNA duplex was only stable up to 13 °C. DNmt-T₅ complexes with native RNA-A_{Poly} showed an even higher thermal stability. Job plot analysis revealed the formation of triple-stranded complexes between the DNmt pentamer and DNA-A_{Poly} or RNA-A_{Poly}, respectively [68,70]. Similar to the results obtained for DNG-T₅ (vide supra), a triplex with 2:1 stoichiometry (DNmt:DNA and DNmt:RNA, respectively) was confirmed.

Remarkably, Bruice et al. identified two different hyperchromic shifts for the DNmt-T₅/DNA-A_{Poly} complex, but not for comparable DNmt-RNA aggregates when these mixtures were exposed to higher ionic strength, denoting the thermal denaturation of the (DNmt-T₅)₂/DNA-A_{Poly} triplex and, subsequently, the DNmt-DNA duplex. However, the corresponding melting temperatures were significantly lower than *T_m* values measured in aqueous solutions with physiological ionic



strength. This indicates a pronounced destabilization of the DNmt-DNA complex with increasing ionic strength [70]. Comparable DNmt-RNA complexes were less destabilized under identical conditions.

Bruice and co-workers also performed further thermal denaturation studies to elucidate base-pairing fidelity of the pentameric thymidynyl DNmt. No increase in hyperchromicity was observed for combinations of DNmt-T₅ with either DNA-G_{Poly}, DNA-C_{Poly} or DNA-T_{Poly}, over a temperature range from 5 to 93 °C, thus ruling out complex formation with these fully

mismatched native DNA counterstrands. Furthermore, a pronounced drop in thermal stability of DNmt-DNA complexes containing 50% T-C mismatches and also for congeners containing 20% T-C mismatches was described [71].

In CD spectroscopic studies performed on the thymidynyl DNmt pentamer, Bruice et al. further confirmed the base-pairing specificity of oligonucleotides containing the artificial S-methylthiourea backbone linkage [70,71]. CD spectra of DNmt-T₅ in complex with five different DNA oligonucleotides containing an increasing number of C mismatches showed significant

changes dependent on the mismatch content. While the combination of DNmt-T₅ with DNA-A₂₀ resulted in a CD difference spectrum with distinct amplitude, the addition of DNA oligonucleotides with an increasing number of C mismatches led to continuous slackening of signals in the difference spectra, until those were almost flat for DNA oligonucleotides containing 50% C mismatches. Hence, this indicates that the ability of the DNmt pentamer to associate with a native DNA oligomer is dependent on Watson–Crick base pairing and is severely hampered by an increasing amount of base-pairing mismatches.

Nucleosyl amino acid (NAA)-derived linkages

Both Letsinger's and Bruce's approaches for the introduction of positive charges into artificial backbone linkages have characteristic conformational features. Letsinger's aminoalkyl phosphoramidate modification and related systems involve a pronounced conformational flexibility of the moieties carrying the positively charged groups. Hence, it cannot be ruled out that interactions with the phosphate groups occur which would be less likely if the positively charged units were more rigidly fixed to the backbone. In contrast, both Bruce's DNG and DNmt oligonucleotide analogues are characterized by conformationally rigid internucleotide linkages. Apparently, an alternative strategy providing a positively charged backbone linkage with 'intermediate' conformational flexibility is missing.

These considerations have stimulated our design of a new artificial internucleotide linkage named 'nucleosyl amino acid (NAA)-modification' (Figure 5) [72–74]. In principle, the NAA-modification is inspired by 'high-carbon' nucleoside structures (i.e., nucleosides having more than five carbon atoms in the sugar unit) found in naturally occurring nucleoside antibiotics [75–77]. In muraymycin- and caprazamycin-type nucleoside antibiotics, among others, such 'high-carbon' nucleosides are uridine-derived amino acid structures ('glycyluridine', GlyU) [78–80], which are aminoribosylated at the 5'-hydroxy group. As part of our ongoing research program on muraymycin nucleoside antibiotics (e.g., muraymycin A1 (**44**)) and their analogues [81–88], we have reported the synthesis of simplified (i.e., 5'-defunctionalized) GlyU derivatives of type **45** (Figure 5) [86–88]. The formal amalgamation of this 'nucleosyl amino acid (NAA)' structure **45** with previously reported amide internucleotide linkages of types **46** and **47** [15–22] furnished the structure of an 'NAA-modified oligonucleotide' **48** (Figure 5). The 6'-amino group of the NAA-modification is positively charged at physiological pH values, thus providing a (partially) zwitterionic backbone structure if some phosphate diester units are replaced with the NAA-modification. In the NAA-modification, several rotatable bonds are combined with the rigid amide group, and it is therefore expected to represent an example of the aforementioned positively charged backbone linkage with 'intermediate' conformational flexibility (vide supra).

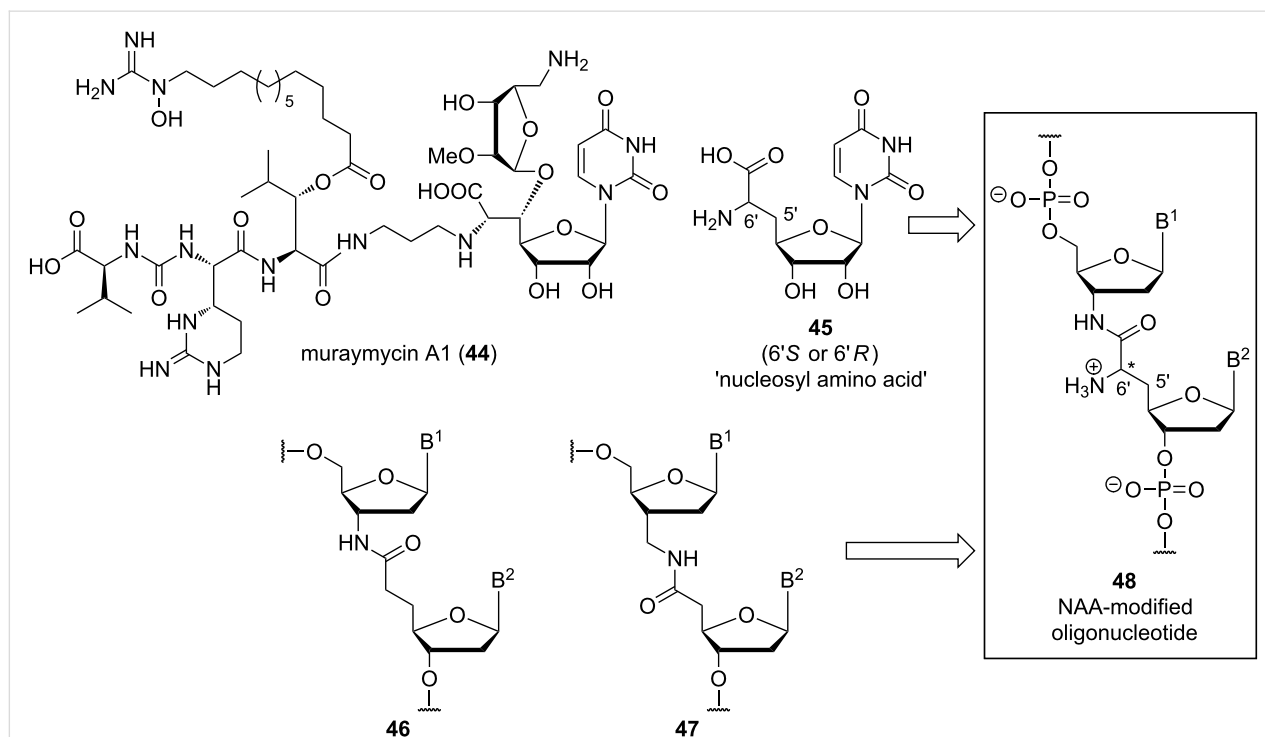


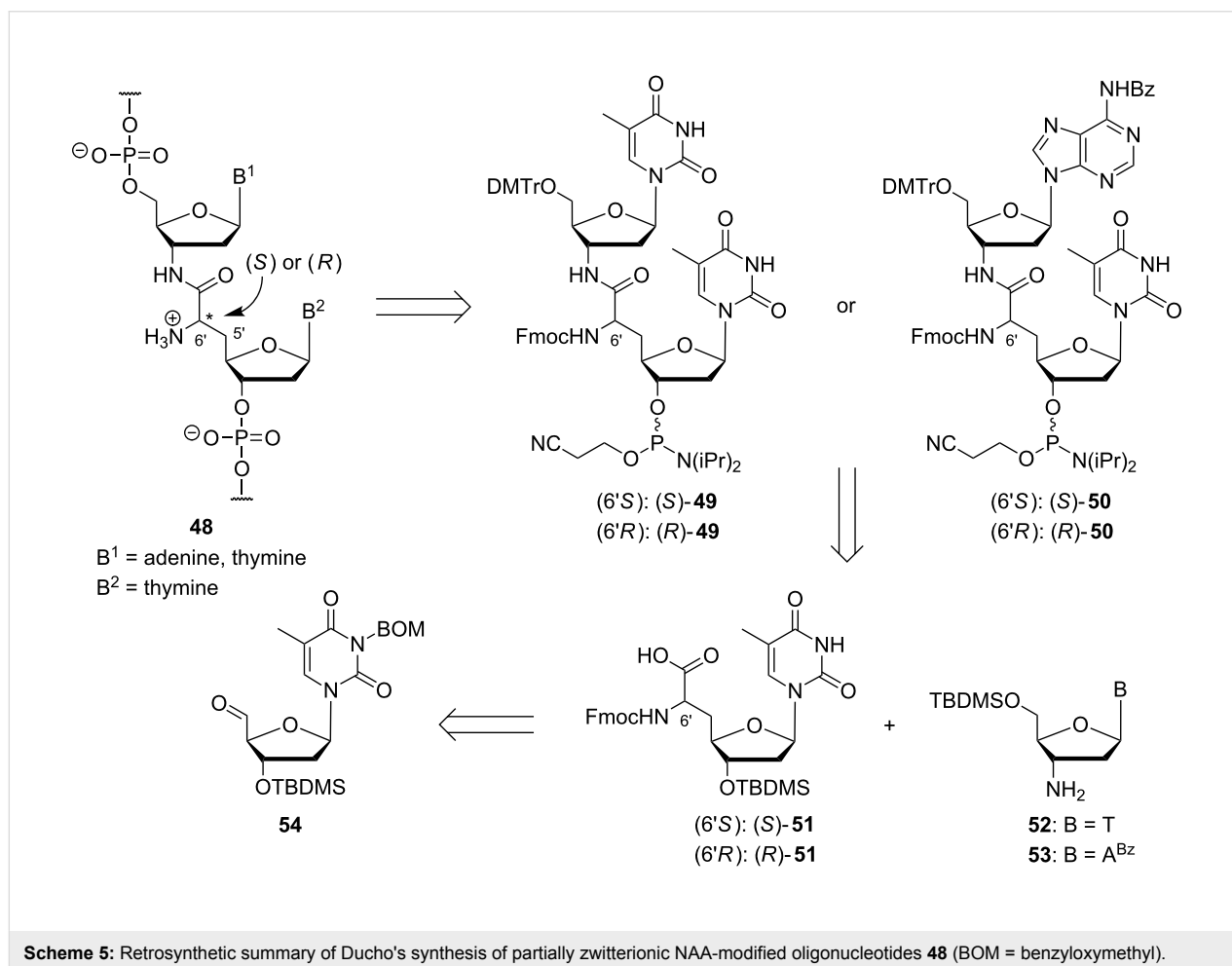
Figure 5: Structure of the natural product muraymycin A1 (**44**) and design concept of nucleosyl amino acid (NAA)-modified (partially) zwitterionic oligonucleotides of type **48** formally derived from structures **45–47** (B¹, B² = nucleobases).

We have reported that partially zwitterionic NAA-modified DNA oligonucleotides can be obtained by standard solid phase-supported automated DNA synthesis if 'dimeric' phosphoramidite building blocks **49** and **50** are employed (Scheme 5) [72,73]. For the synthesis of 'dimeric' phosphoramidites **49** and **50**, protected thymidinyl amino acids (*S*)-**51** or (*R*)-**51** were coupled with protected 3'-amino-3'-deoxythymidine **52** or protected 3'-amino-2',3'-dideoxyadenosine **53** [73,89], respectively. Thymidinyl amino acids **51** were obtained from 3'-*O*-silylated thymidine-5'-aldehyde **54** via a previously established route using Wittig–Horner olefination and catalytic asymmetric hydrogenation as key steps (reactions not shown) [86,87,90–92].

Using 'dimeric' building blocks (*S*)-**49**, (*R*)-**49**, (*S*)-**50**, and (*R*)-**50** (Scheme 5), automated DNA synthesis under standard conditions enabled the preparation of partially zwitterionic NAA-modified oligonucleotides with defined configuration at the 6'-position, i.e., with control over the spatial orientation of the positive charge [72,73]. Thus, the NAA-modification was placed in T–T ('TxT', with x representing the NAA-linkage) and A–T segments ('AxT') of the oligonucleotide sequence, respec-

tively. Further variation of the 3'-aminonucleoside component (**52** and **53** in Scheme 5) should potentially also allow the introduction of the NAA-modification at C–T and G–T sites within a given sequence.

So far, 24 different oligonucleotides with one to four TxT NAA-modifications at various positions [72] as well as two oligonucleotides with two AxT NAA-modifications [73] have been reported. The properties of the TxT-containing congeners have been studied in detail [72]. Thermal denaturation experiments showed that the TxT NAA-modified DNA oligonucleotides formed duplexes with complementary native DNA or RNA counterstrands, but with moderate destabilization relative to unmodified native duplexes, in particular for DNA–RNA hybrids. The fidelity of base pairing was studied using native DNA counterstrands containing a single base mismatch. Furthermore, structures of the duplexes were investigated by CD spectroscopy. The following properties of TxT NAA-modified DNA oligonucleotides were reported [72]: (i) they formed reasonably stable duplexes with complementary counterstrands, in particular with native DNA; (ii) the influence of the spatial

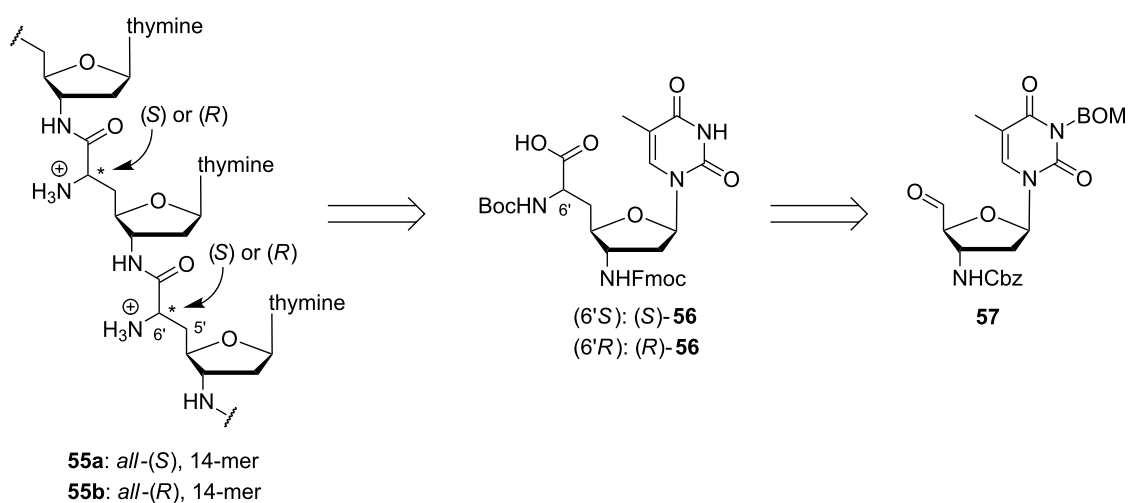


orientation of the positive charge, i.e., of the configuration at the 6'-position, was moderate, with a tendency that (6'*R*)-configured linkages furnished slightly more stable duplexes; (iii) the modified oligonucleotides showed no impairment of mismatch discrimination, i.e., single base mismatches led to a significant drop in duplex stability; (iv) the formed duplexes were devoid of significant structural distortion, i.e., their CD spectra indicated B-type helices for DNA–DNA duplexes and A-type helices for DNA–RNA duplexes. Overall, these results demonstrated that typical chemical properties of nucleic acids are retained in partially zwitterionic NAA-modified DNA oligonucleotides. However, corresponding studies on NAA-modified DNA oligonucleotides with a fully zwitterionic backbone have not been conducted yet.

With respect to the aforementioned favourable properties of zwitterionic NAA-modified oligonucleotides, the obvious aim was to synthesize fully cationic oligomers, i.e., oligonucleotide analogues with the cationic NAA-modification as their sole internucleotide linkage. The phosphoramidite-based synthetic strategy depicted in Scheme 5 was not suitable to reach this goal as it furnishes phosphate diester linkages at least at every second position within a given sequence. Therefore, a different synthetic route was developed (Scheme 6) [74]. The envisioned fully cationic thymidine-derived oligomers **55a** (*all*-(*S*)-configured at the 6'-positions) and **55b** (*all*-(*R*)-configured at the 6'-positions) were assembled by manual Fmoc-based solid phase-supported peptide synthesis using the monomeric 3'-amino-nucleosyl amino acids (*S*)-**56** and (*R*)-**56**, respectively, as building blocks. The synthesis of thymidinyl amino acids **56** was again started from a corresponding 5'-aldehyde **57** using Wittig–Horner olefination and catalytic asymmetric hydrogenation as key steps (reactions not shown) [74].

The properties of fully cationic oligonucleotide analogues **55a** and **55b** were studied in detail [74]. Thermal denaturation experiments demonstrated a strong hybridization of both thymidinyl oligomers with native complementary A₁₄ DNA, with *T_m* values being 9 and 17 °C higher, respectively, than the *T_m* value of an unmodified T₁₄–A₁₄ DNA reference duplex. As anticipated based on Letsinger's and Bruce' work (vide supra), the *T_m* value of the **55**–DNA complex decreased with increasing ionic strength. Studies on base-pairing fidelity gave the remarkable result that both **55a** and **55b** were largely insensitive to the presence of a single base mismatch in the counter-strand, thus indicating that electrostatic attraction overruled Watson–Crick base-pairing specificity in these cases. CD spectroscopy indicated that both **55a** and **55b** formed double-helical duplex structures with complementary DNA, apparently with slight distortions in case of the **55b**–DNA duplex.

The hampered base-pairing fidelity of **55a** and **55b** raised the question if the hybridization of these oligocations with oligoanionic DNA was dependent on Watson–Crick base-pairing at all or if it was mainly mediated by electrostatic attraction. Thermal denaturation studies of mixtures of **55a** or **55b**, respectively, with a fully mismatched DNA counterstrand (G₆TTG₆) showed a pronounced hyperchromicity upon heating in both cases, but also indicated that no transition between two defined states occurred [74]. It was derived from these results that **55a** and **55b** probably formed less defined, unspecific aggregates with the fully mismatched counterstrand, which then disassembled at elevated temperatures. This hypothesis was further supported by CD-spectroscopic studies. The overall conclusion was that the formation of defined double-helical duplex structures of **55a** and **55b** with DNA was mainly steered by Watson–Crick base-



Scheme 6: Retrosynthetic summary of Ducho's and Grossmann's synthesis of fully cationic NAA-modified oligonucleotides **55a** and **55b**.

pairing, but that unspecific electrostatic attraction also contributed to the hybridization of the strands.

Conclusion

In summary, this review provides an overview of four different approaches to introduce cationic backbone linkages as replacements of the phosphate diester units into oligonucleotide structures: i) aminoalkylated phosphoramidates and related systems; ii) guanidinium groups; iii) *S*-methylthiourea motifs and iv) nucleosyl amino acid (NAA)-derived modifications. All of these artificial internucleotide linkages are accessible by means of chemical synthesis, which is either based on the application of H-phosphonate (for i) or phosphoramidite-based (for iv) DNA synthesis, or on a massively modified version of DNA synthesis (for ii and iii), or on solid phase-supported peptide synthesis (for iv).

Studies on the properties of resulting oligomers are not fully conclusive yet. Some data, for instance on base-pairing fidelity, are missing for Letsinger's originally reported aminoalkylated phosphoramidates, while subsequently reported variants thereof and related systems have been studied in more detail. Thus, both retained base-pairing fidelity and improved cellular uptake have been reported for some oligonucleotides with structural similarity to Letsinger's first-generation aminoalkylated phosphoramidates. Bruce's guanidinium- and *S*-methylthiourea-linked systems have a pronounced tendency to form triple-helical structures with native nucleic acids, which makes a direct comparison with the other approaches difficult. Bruce's data suggest retained base-pairing fidelity for fully cationic oligomers, which is in remarkable contrast to our results obtained for NAA-modified oligonucleotides. The latter showed excellent base-pairing fidelity in the case of partially zwitterionic backbones, but insensitivity to single base mismatches for the hybridization of fully cationic oligomers with native DNA. Recently reported results on such fully cationic NAA oligomers [74] indicate that in addition to Watson–Crick base-pairing, unspecific electrostatic attraction also plays a role in the hybridization process. Overall, one must state that the interplay of the structural and conformational properties of cationic internucleotide linkages and the physicochemical behaviour of corresponding oligomers in their binding to anionic nucleic acids is only scarcely understood and will require further research efforts.

Studies on the biological properties of (partially) zwitterionic and cationic oligonucleotide analogues in cellular systems, in particular with respect to their cellular uptake, are currently only available for some aminoalkylated phosphoramidate-linked oligonucleotides and a related phosphonate analogue. The anticipated vast improvement of cellular uptake due to the

presence of the cationic internucleotide linkages was proven for these systems, even though they displayed hampered endosomal release. On the other hand, our results on NAA-derived cationic oligomers suggest that, as a paradigm for the design of cationic oligonucleotide analogues for biological applications, one should potentially be cautious with respect to the number of positive charges in the backbone: base-pairing fidelity might be hampered, dependent on the structure of the artificial internucleotide linkage. It will therefore also be of significant relevance to further investigate the influence of the charge pattern in the backbone on the oligonucleotides' cellular uptake. The stage is set to perform such studies, which will further advance the development of cationically linked oligonucleotide analogues for potential applications as drug candidates, diagnostic agents or chemical tool compounds.

Acknowledgements

We thank the Deutsche Forschungsgemeinschaft (DFG, grant DU 1095/2-1) and the Fonds der Chemischen Industrie (FCI, Sachkostenzuschuss) for financial support of our research on NAA-modified oligonucleotides.

ORCID® iDs

Christian Ducho - <https://orcid.org/0000-0002-0629-9993>

References

- Sharma, V. K.; Rungta, P.; Prasad, A. K. *RSC Adv.* **2014**, *4*, 16618–16631. doi:10.1039/c3ra47841f
- Xodo, L. E.; Cogoi, S.; Rapozzi, V. *Curr. Pharm. Des.* **2004**, *10*, 805–819. doi:10.2174/1381612043452983
- Wagner, R. W. *Nature* **1994**, *372*, 333–335. doi:10.1038/372333a0
- Mello, C. C. *Angew. Chem.* **2007**, *119*, 7114–7124. doi:10.1002/ange.200701713
Angew. Chem., Int. Ed. **2007**, *46*, 6985–6994. doi:10.1002/anie.200701713
- Lennox, K. A.; Behlke, M. A. *Gene Ther.* **2011**, *18*, 1111–1120. doi:10.1038/gt.2011.100
- Cobb, A. J. A. *Org. Biomol. Chem.* **2007**, *5*, 3260–3275. doi:10.1039/b709797m
- Deleavey, G. F.; Damha, M. J. *Chem. Biol.* **2012**, *19*, 937–954. doi:10.1016/j.chembiol.2012.07.011
- Westheimer, F. H. *Science* **1987**, *235*, 1173–1178. doi:10.1126/science.2434996
- Benner, S. A.; Hutter, D. *Bioorg. Chem.* **2002**, *30*, 62–80. doi:10.1006/bioo.2001.1232
- Benner, S. A. *Acc. Chem. Res.* **2004**, *37*, 784–797. doi:10.1021/ar040004z
- Nielsen, P. E.; Egholm, M.; Berg, R. H.; Buchardt, O. *Science* **1991**, *254*, 1497–1500. doi:10.1126/science.1962210
- Zhilina, Z. V.; Ziemba, A. J.; Ebbinghaus, S. W. *Curr. Top. Med. Chem.* **2005**, *5*, 1119–1131. doi:10.2174/156802605774370892
- Karkare, S.; Bhatnagar, D. *Appl. Microbiol. Biotechnol.* **2006**, *71*, 575–586. doi:10.1007/s00253-006-0434-2
- Huang, Z.; Benner, S. A. *J. Org. Chem.* **2002**, *67*, 3996–4013. doi:10.1021/jo0003910

15. Lebreton, J.; De Mesmaeker, A.; Waldner, A.; Fritsch, V.; Wolf, R. M.; Freier, S. M. *Tetrahedron Lett.* **1993**, *34*, 6383–6386. doi:10.1016/0040-4039(93)85051-W
16. De Mesmaeker, A.; Lebreton, J.; Waldner, A.; Fritsch, V.; Wolf, R. M.; Freier, S. M. *Synlett* **1993**, 733–736. doi:10.1055/s-1993-22588
17. De Mesmaeker, A.; Waldner, A.; Lebreton, J.; Hoffmann, P.; Fritsch, V.; Wolf, R. M.; Freier, S. M. *Angew. Chem.* **1994**, *106*, 237–240. doi:10.1002/ange.19941060230
Angew. Chem., Int. Ed. **1994**, *33*, 226–229. doi:10.1002/anie.199402261
18. Lebreton, J.; Waldner, A.; Fritsch, V.; Wolf, R. M.; De Mesmaeker, A. *Tetrahedron Lett.* **1994**, *35*, 5225–5228. doi:10.1016/S0040-4039(00)77069-9
19. Rozners, E.; Katkevica, D.; Bizdena, E.; Strömberg, R. *J. Am. Chem. Soc.* **2003**, *125*, 12125–12136. doi:10.1021/ja0360900
20. Selvam, C.; Thomas, S.; Abbott, J.; Kennedy, S. D.; Rozners, E. *Angew. Chem.* **2011**, *123*, 2116–2118. doi:10.1002/ange.201007012
Angew. Chem., Int. Ed. **2011**, *50*, 2068–2070. doi:10.1002/anie.201007012
21. Tanui, P.; Kennedy, S. D.; Lunstad, B. D.; Haas, A.; Leake, D.; Rozners, E. *Org. Biomol. Chem.* **2014**, *12*, 1207–1210. doi:10.1039/C3OB42532K
22. Mutisya, D.; Selvam, C.; Lunstad, B. D.; Pallan, P. S.; Haas, A.; Leake, D.; Egli, M.; Rozners, E. *Nucleic Acids Res.* **2014**, *42*, 6542–6551. doi:10.1093/nar/gku235
23. El-Sagheer, A. H.; Brown, T. J. *Am. Chem. Soc.* **2009**, *131*, 3958–3964. doi:10.1021/ja8065896
24. El-Sagheer, A. H.; Sanzone, A. P.; Gao, R.; Tavassoli, A.; Brown, T. *Proc. Natl. Acad. Sci. U. S. A.* **2011**, *108*, 11338–11343. doi:10.1073/pnas.1101519108
25. Sanzone, A. P.; El-Sagheer, A. H.; Brown, T.; Tavassoli, A. *Nucleic Acids Res.* **2012**, *40*, 10567–10575. doi:10.1093/nar/gks756
26. Birts, C. N.; Sanzone, A. P.; El-Sagheer, A. H.; Blaydes, J. P.; Brown, T.; Tavassoli, A. *Angew. Chem.* **2014**, *126*, 2394–2397. doi:10.1002/ange.201308691
Angew. Chem., Int. Ed. **2014**, *53*, 2362–2365. doi:10.1002/anie.201308691
27. Kukwikila, M.; Gale, N.; El-Sagheer, A. H.; Brown, T.; Tavassoli, A. *Nat. Chem.* **2017**, *9*, 1089–1098. doi:10.1038/nchem.2850
28. Ozaki, H.; Kitamura, M.; Yamana, K.; Murakami, A.; Shimidzu, T. *Bull. Chem. Soc. Jpn.* **1990**, *63*, 1929–1936. doi:10.1246/bcsj.63.1929
29. Moody, H. M.; van Genderen, M. H. P.; Koole, L. H.; Kocken, H. J. M.; Meijer, E. M.; Buck, H. M. *Nucleic Acids Res.* **1989**, *17*, 4769–4782. doi:10.1093/nar/17.12.4769
30. Strauss, J. K.; Roberts, C.; Nelson, M. G.; Switzer, C.; Maher, L. J., III. *Proc. Natl. Acad. Sci. U. S. A.* **1996**, *93*, 9515–9520. doi:10.1073/pnas.93.18.9515
31. Ramzaeva, N.; Mittelbach, C.; Seela, F. *Helv. Chim. Acta* **1997**, *80*, 1809–1822. doi:10.1002/hlca.19970800605
32. Rosemeyer, H.; Ramzaeva, N.; Becker, E.-M.; Feiling, E.; Seela, F. *Bioconjugate Chem.* **2002**, *13*, 1274–1285. doi:10.1021/bc020024q
33. Prakash, T. P.; Kawasaki, A. M.; Lesnik, E. A.; Sioufi, N.; Manoharan, M. *Tetrahedron* **2003**, *59*, 7413–7422. doi:10.1016/S0040-4020(03)01104-9
34. Prakash, T. P.; Kawasaki, A. M.; Lesnik, E. A.; Owens, S. R.; Manoharan, M. *Org. Lett.* **2003**, *5*, 403–406. doi:10.1021/ol027131k
35. Prhavc, M.; Prakash, T. P.; Minasov, G.; Cook, P. D.; Egli, M.; Manoharan, M. *Org. Lett.* **2003**, *5*, 2017–2020. doi:10.1021/ol0340991
36. Prakash, T. P.; Püschl, A.; Lesnik, E.; Mohan, V.; Tereshko, V.; Egli, M.; Manoharan, M. *Org. Lett.* **2004**, *6*, 1971–1974. doi:10.1021/ol049470e
37. Milton, S.; Honcharenko, D.; Rocha, C. S. J.; Moreno, P. M. D.; Smith, C. I. E.; Strömberg, R. *Chem. Commun.* **2015**, *51*, 4044–4047. doi:10.1039/C4CC08837A
38. Brock, R. *Bioconjugate Chem.* **2014**, *25*, 863–868. doi:10.1021/bc500017t
39. Jain, M. L.; Bruice, P. Y.; Szabó, I. E.; Bruice, T. C. *Chem. Rev.* **2012**, *112*, 1284–1309. doi:10.1021/cr1004265
40. Letsinger, R. L.; Bach, S. A.; Eadie, J. S. *Nucleic Acids Res.* **1986**, *14*, 3487–3499. doi:10.1093/nar/14.8.3487
41. Letsinger, R. L.; Singman, C. N.; Histan, G.; Salunkhe, M. *J. Am. Chem. Soc.* **1988**, *110*, 4470–4471. doi:10.1021/ja00221a089
42. Froehler, B. C. *Tetrahedron Lett.* **1986**, *27*, 5575–5578. doi:10.1016/S0040-4039(00)85269-7
43. Bailey, C. P.; Weeks, D. L.; Dagle, J. M. *Nucleic Acids Res.* **1998**, *26*, 4860–4867. doi:10.1093/nar/26.21.4860
44. Michel, T.; Martinand-Mari, C.; Debart, F.; Lebleu, B.; Robbins, I.; Vasseur, J.-J. *Nucleic Acids Res.* **2003**, *31*, 5282–5290. doi:10.1093/nar/gkg733
45. Deglane, G.; Abes, S.; Michel, T.; Laurent, A.; Naval, M.; Martinand-Mari, C.; Prevot, P.; Vives, E.; Robbins, I.; Barvik, I., Jr.; Lebleu, B.; Debart, F.; Vasseur, J.-J. *Collect. Symp. Ser.* **2005**, *7*, 143–147. doi:10.1135/css200507143
46. Deglane, G.; Abes, S.; Michel, T.; Prévot, P.; Vives, E.; Debart, F.; Barvik, I.; Lebleu, B.; Vasseur, J.-J. *ChemBioChem* **2006**, *7*, 684–692. doi:10.1002/cbic.200500433
47. Fathi, R.; Huang, Q.; Coppola, G.; Delaney, W.; Teasdale, R.; Krieg, A. M.; Cook, A. F. *Nucleic Acids Res.* **1994**, *22*, 5416–5424. doi:10.1093/nar/22.24.5416
48. Rahman, S. M. A.; Baba, T.; Kodama, T.; Islam, M. A.; Obika, S. *Bioorg. Med. Chem.* **2012**, *20*, 4098–4102. doi:10.1016/j.bmc.2012.05.009
49. Dempcy, R. O.; Almarsson, O.; Bruice, T. C. *Proc. Natl. Acad. Sci. U. S. A.* **1994**, *91*, 7864–7868. doi:10.1073/pnas.91.17.7864
50. Perreault, D. M.; Cabell, L. A.; Anslyn, E. V. *Bioorg. Med. Chem.* **1997**, *5*, 1209–1220. doi:10.1016/S0968-0896(97)00051-5
51. Blaskó, A.; Dempcy, R. O.; Minyat, E. E.; Bruice, T. C. *J. Am. Chem. Soc.* **1996**, *118*, 7892–7899. doi:10.1021/ja961308m
52. Linkletter, B. A.; Bruice, T. C. *Bioorg. Med. Chem. Lett.* **1998**, *8*, 1285–1290. doi:10.1016/S0960-894X(98)00228-5
53. Linkletter, B. A.; Szabo, I. E.; Bruice, T. C. *Nucleic Acids Res.* **2001**, *29*, 2370–2376. doi:10.1093/nar/29.11.2370
54. Barawkar, D. A.; Bruice, T. C. *Proc. Natl. Acad. Sci. U. S. A.* **1998**, *95*, 11047–11052. doi:10.1073/pnas.95.19.11047
55. Challa, H.; Bruice, T. C. *Bioorg. Med. Chem. Lett.* **2001**, *11*, 2423–2427. doi:10.1016/S0960-894X(01)00455-3
56. Reddy, P. M.; Bruice, T. C. *Bioorg. Med. Chem. Lett.* **2003**, *13*, 1281–1285. doi:10.1016/S0960-894X(03)00119-7
57. Challa, H.; Bruice, T. C. *Bioorg. Med. Chem.* **2004**, *12*, 1475–1481. doi:10.1016/j.bmc.2003.12.043
58. Dempcy, R. O.; Luo, J.; Bruice, T. C. *Proc. Natl. Acad. Sci. U. S. A.* **1996**, *93*, 4326–4330. doi:10.1073/pnas.93.9.4326
59. Kojima, N.; Szabo, I. E.; Bruice, T. C. *Tetrahedron* **2002**, *58*, 867–879. doi:10.1016/S0040-4020(01)01185-1
60. Dempcy, R. O.; Browne, K. A.; Bruice, T. C. *J. Am. Chem. Soc.* **1995**, *117*, 6140–6141. doi:10.1021/ja00127a035

61. Dempcy, R. O.; Browne, K. A.; Bruice, T. C. *Proc. Natl. Acad. Sci. U. S. A.* **1995**, *92*, 6097–6101. doi:10.1073/pnas.92.13.6097
62. Browne, K. A.; Dempcy, R. O.; Bruice, T. C. *Proc. Natl. Acad. Sci. U. S. A.* **1995**, *92*, 7051–7055. doi:10.1073/pnas.92.15.7051
63. Blaskó, A.; Minyat, E. E.; Dempcy, R. O.; Bruice, T. C. *Biochemistry* **1997**, *36*, 7821–7831. doi:10.1021/bi970064v
64. Linkletter, B. A.; Szabo, I. E.; Bruice, T. C. *J. Am. Chem. Soc.* **1999**, *121*, 3888–3896. doi:10.1021/ja984212w
65. Szabo, I. E.; Bruice, T. C. *Bioorg. Med. Chem.* **2004**, *12*, 4233–4244. doi:10.1016/j.bmc.2004.05.010
66. Jain, M. L.; Bruice, T. C. *Bioorg. Med. Chem.* **2006**, *14*, 7333–7346. doi:10.1016/j.bmc.2006.05.074
67. Arya, D. P.; Bruice, T. C. *J. Am. Chem. Soc.* **1998**, *120*, 6619–6620. doi:10.1021/ja980629q
68. Arya, D. P.; Bruice, T. C. *J. Am. Chem. Soc.* **1998**, *120*, 12419–12427. doi:10.1021/ja9829416
69. Arya, D. P.; Bruice, T. C. *Bioorg. Med. Chem. Lett.* **2000**, *10*, 691–693. doi:10.1016/S0960-894X(00)00085-8
70. Arya, D. P.; Bruice, T. C. *Proc. Natl. Acad. Sci. U. S. A.* **1999**, *96*, 4384–4389. doi:10.1073/pnas.96.8.4384
71. Arya, D. P.; Bruice, T. C. *J. Am. Chem. Soc.* **1999**, *121*, 10680–10684. doi:10.1021/ja992871i
72. Schmidtgall, B.; Spork, A. P.; Wachowius, F.; Höbartner, C.; Ducho, C. *Chem. Commun.* **2014**, *50*, 13742–13745. doi:10.1039/C4CC06371F
73. Schmidtgall, B.; Höbartner, C.; Ducho, C. *Beilstein J. Org. Chem.* **2015**, *11*, 50–60. doi:10.3762/bjoc.11.8
74. Schmidtgall, B.; Kuepper, A.; Meng, M.; Grossmann, T. N.; Ducho, C. *Chem. – Eur. J.* **2018**, *24*, 1544–1553. doi:10.1002/chem.201704338
75. Kimura, K.-i.; Bugg, T. D. H. *Nat. Prod. Rep.* **2003**, *20*, 252–273. doi:10.1039/b202149h
76. Winn, M.; Goss, R. J. M.; Kimura, K.-i.; Bugg, T. D. H. *Nat. Prod. Rep.* **2010**, *27*, 279–304. doi:10.1039/B816215H
77. Ichikawa, S.; Yamaguchi, M.; Matsuda, A. *Curr. Med. Chem.* **2015**, *22*, 3951–3979. doi:10.2174/0929867322666150818103502
78. Chi, X.; Pahari, P.; Nonaka, K.; Van Lanen, S. G. *J. Am. Chem. Soc.* **2011**, *133*, 14452–14459. doi:10.1021/ja206304k
79. Barnard-Britson, S.; Chi, X.; Nonaka, K.; Spork, A. P.; Tibrewal, N.; Goswami, A.; Pahari, P.; Ducho, C.; Rohr, J.; Van Lanen, S. G. *J. Am. Chem. Soc.* **2012**, *134*, 18514–18517. doi:10.1021/ja308185q
80. Funabashi, M.; Baba, S.; Takatsu, T.; Kizuka, M.; Ohata, Y.; Tanaka, M.; Nonaka, K.; Spork, A. P.; Ducho, C.; Chen, W.-C. L.; Van Lanen, S. G. *Angew. Chem.* **2013**, *125*, 11821–11825. doi:10.1002/ange.201305546
Angew. Chem., Int. Ed. **2013**, *52*, 11607–11611. doi:10.1002/anie.201305546
81. McDonald, L. A.; Barbieri, L. R.; Carter, G. T.; Lenoy, E.; Lotvin, J.; Petersen, P. J.; Siegel, M. M.; Singh, G.; Williamson, R. T. *J. Am. Chem. Soc.* **2002**, *124*, 10260–10261. doi:10.1021/ja017748h
82. Wiegmann, D.; Koppermann, S.; Wirth, M.; Niro, G.; Leyerer, K.; Ducho, C. *Beilstein J. Org. Chem.* **2016**, *12*, 769–795. doi:10.3762/bjoc.12.77
83. Spork, A. P.; Koppermann, S.; Ducho, C. *Synlett* **2009**, 2503–2507. doi:10.1055/s-0029-1217742
84. Spork, A. P.; Koppermann, S.; Dittrich, B.; Herbst-Irmer, R.; Ducho, C. *Tetrahedron: Asymmetry* **2010**, *21*, 763–766. doi:10.1016/j.tetasy.2010.03.037
85. Spork, A. P.; Ducho, C. *Synlett* **2013**, *24*, 343–346. doi:10.1055/s-0032-1318117
86. Spork, A. P.; Ducho, C. *Org. Biomol. Chem.* **2010**, *8*, 2323–2326. doi:10.1039/c003092a
87. Spork, A. P.; Wiegmann, D.; Granitzka, M.; Stalke, D.; Ducho, C. *J. Org. Chem.* **2011**, *76*, 10083–10098. doi:10.1021/jo201935w
88. Spork, A. P.; Büschleb, M.; Ries, O.; Wiegmann, D.; Boettcher, S.; Mihalyi, A.; Bugg, T. D. H.; Ducho, C. *Chem. – Eur. J.* **2014**, *20*, 15292–15297. doi:10.1002/chem.201404775
89. Eisenhuth, R.; Richert, C. *J. Org. Chem.* **2008**, *74*, 26–37. doi:10.1021/jo8018889
90. Vineyard, B. D.; Knowles, W. S.; Sabacky, M. J.; Bachman, G. L.; Wienkauff, D. J. *J. Am. Chem. Soc.* **1977**, *99*, 5946–5952. doi:10.1021/ja00460a018
91. Schmidt, U.; Lieberknecht, A.; Schanbacher, U.; Beuttler, T.; Wild, J. *Angew. Chem.* **1982**, *94*, 797–798. doi:10.1002/ange.19820941027
Angew. Chem., Int. Ed. Engl. **1982**, *21*, 776–777. doi:10.1002/anie.198207761
92. Ducho, C.; Hamed, R. B.; Batchelar, E. T.; Sorensen, J. L.; Odell, B.; Schofield, C. J. *Org. Biomol. Chem.* **2009**, *7*, 2770–2779. doi:10.1039/b903312b

License and Terms

This is an Open Access article under the terms of the Creative Commons Attribution License (<http://creativecommons.org/licenses/by/4.0>), which permits unrestricted use, distribution, and reproduction in any medium, provided the original work is properly cited.

The license is subject to the *Beilstein Journal of Organic Chemistry* terms and conditions: (<https://www.beilstein-journals.org/bjoc>)

The definitive version of this article is the electronic one which can be found at: [doi:10.3762/bjoc.14.111](https://doi.org/10.3762/bjoc.14.111)

1.2.4 Chimeric Oligonucleotides: The Gapmer Approach

As discussed in the preceding sections, there are numerous different modifications available that allow tuning and alteration of ON properties. Yet, only a handful have proceeded to be truly useful and applicable for therapeutic purposes. Also, even these few examples remain connected to adverse drug events due to unwanted side effects. As a prime example for this phenomenon, the LNA modification by *Wengel et al.* can be named. Incorporation of LNA into an ON sequence was shown to be accompanied by an unmatched boost in target affinity and biological stability.^[141] But, together with these improvements, loss of RNase H activation as well as an enhanced predisposition for off-target binding^[96] was also confirmed. Hence, it would be of major value for antisense applications to find a way of optimizing ON properties while keeping unwanted side effects to a minimum. One strategy that pursuits this goal is the gapmer approach. Through merging of several modifications with each other, or with native DNA, an accumulation of beneficial characteristics is aspired. Thus, in this strategy, the ON sequence is subdivided into several segments as depicted in *Figure 1.11*. The module positioned in the middle of the sequence - the gap region - is envisioned to maintain base-pairing fidelity and facilitate activation of RNase H-mediated RNA degradation. Therefore, it is mostly composed of unmodified DNA or artificial nucleosides that still facilitate RNase H activation (like phosphorothioates^[104]). On the other side, the flank regions located at the 5'- and 3'-end contain modified nucleosides to prevent rapid biological cleavage and to increase the affinity for duplex formation.^[11]

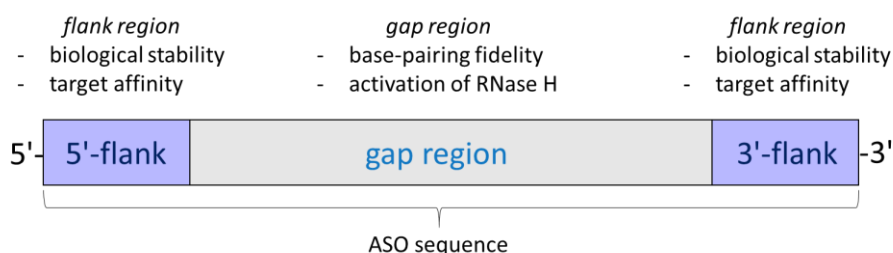


Figure 1.11. Principle structure of a gapmer ON.

Following this principle, a considerable number of different ASO gapmers have been developed and are currently under investigation in different clinical trials, ranging from phase I to phase III studies.^[142] Thereby, gapmers using flanks made of MOE- or LNA-modified nucleosides occur with striking frequency. However, although the overall

pharmacokinetic profile of these gapmer drugs has been demonstrated to be somewhat improved compared to modified sequences consisting of only one type of alteration, the full potential of this approach has not been uncovered yet. Nonetheless, the gapmer approach remains a valuable tool for the adaptation and variation of ON characteristics and thus has also found application in the following work.

2. Objectives

The focus of this work was set on the properties of ONs carrying the nucleosyl amino acid (NAA) modification - a cationic, amide-derived backbone linkage developed by the *Ducho* group.^[143,144] This included: (i) the evaluation of the biological stability of partially zwitterionic NAA-modified ONs in the presence of different biological media, (ii) the examination of the hybridization behavior of completely NAA-modified and thus fully cationic oligomers with both DNA and RNA and finally (iii) the synthesis and evaluation of an ON gapmer structure consisting of a zwitterionic NAA-modified gap and two fully LNA-modified flanks. A brief overview of the three objectives is given in *Figure 2.1*.

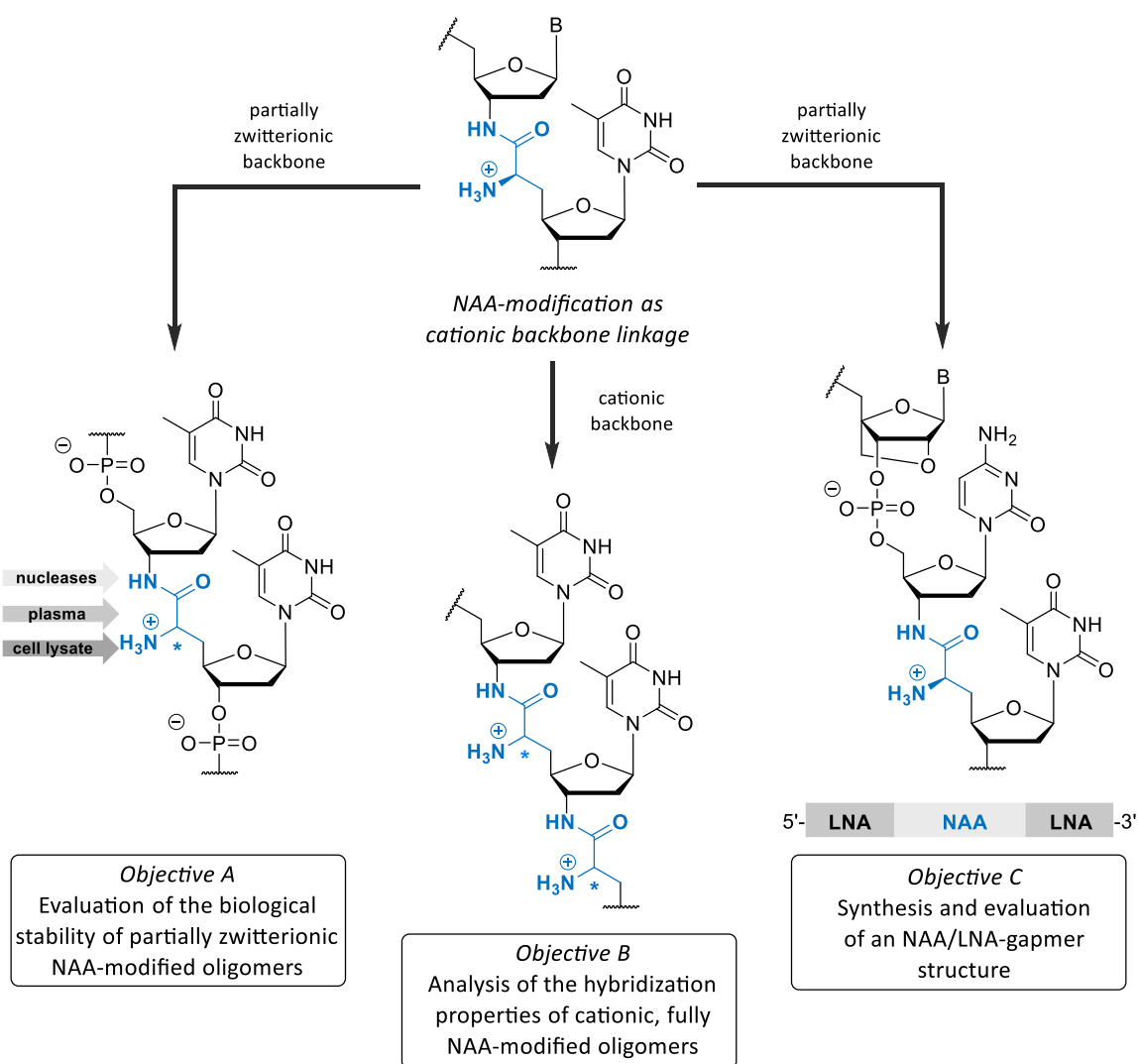


Figure 2.1. Graphical summary of the aims defined for this doctoral thesis. B = nucleobases.

Through these investigations it was envisioned to elucidate the overall potential of the NAA-modification as a tool for the design of ONs with improved biological and biophysical properties.

The planning of the three parts of this work was based on preceding studies by *Schmidtgall* et al.^[143,144] and *Kirsch*^[145]. Experiments done by *Schmidtgall* et al. showed that partially zwitterionic NAA-modified ONs are capable to form helical duplexes with complementary DNA and RNA.^[143] However, the introduction of up to four NAA linkages into an ON sequence was also observed to induce a destabilization of the resulting ON-DNA or ON-RNA duplex structures. Thereby, helical duplexes with DNA were less destabilized (-0.5 to -2 °C/mod), while duplexes with complementary RNA were observed to be more sensitive towards the presence of the NAA-modification, resulting in a more pronounced drop in thermal stability (-2 to -4 °C/mod). Moreover, melting experiments revealed a difference in duplex stability for duplexes containing either the (6'S)-NAA- or the (6'R)-NAA-modification, with the (6'R)-isomer being slightly less destabilizing (~ 1 °C/mod). Nevertheless, the NAA-modified ONs were also proven to display excellent base-pairing fidelity, which was decisive for the further investigation of their biological properties during the first part of this work. As depicted in *Figure 2.1*, the first objective was focused on the *in vitro* stability of the zwitterionic systems synthesized by *Schmidtgall* et al.^[143] Therefore, a set of different biological assays was designed, established and applied to validate whether the NAA-modification is capable to slow down or even prevent ON cleavage. As a starting point, it was aspired to analyze the impact of 3'→5'- and 5'→3'-exonucleases on the partially zwitterionic sequences. Particular attention was paid on the influence of the position and configuration of the NAA-linkages. As follow-up, the influence of more complex biological media - human plasma and whole cell lysate of a lymphoma cell line – on the stability of such ONs was examined.

Subsequent to the investigations on the partially zwitterionic NAA-ONs, the second part of this work was concerned with the synthesis and evaluation of fully NAA-modified oligomers. Thereby, it should be elucidated how such completely cationic ON sequences behave in the presence of complementary as well as mismatched counterstrands. Here, focus was set on the impact of the positive charge on duplex formation, binding affinity and base-pairing fidelity. Additionally, the influence of the fully cationic backbone structure

on the topology of both the single-stranded and hybridized forms of the cationic NAA ONs was studied.

Finally, in the third part it was envisioned to create an advanced partially zwitterionic NAA-containing oligomer with improved binding affinity towards RNA. Hence, the synthesis of a gapmer system including two LNA-flanks with high affinity for RNA^[82] and a zwitterionic gap containing NAA using automated DNA synthesis was planned. The synthesis of the therefore required dimeric phosphoramidite building block was based on previous work by *Schmidtgall et al.*^[143,144] and *Kirsch*^[145], who established the synthetic routes towards three dimeric NAA-building blocks (TxT, AxT and CxT, x = NAA modification) suitable for automated DNA synthesis (*Figure 2.2*).

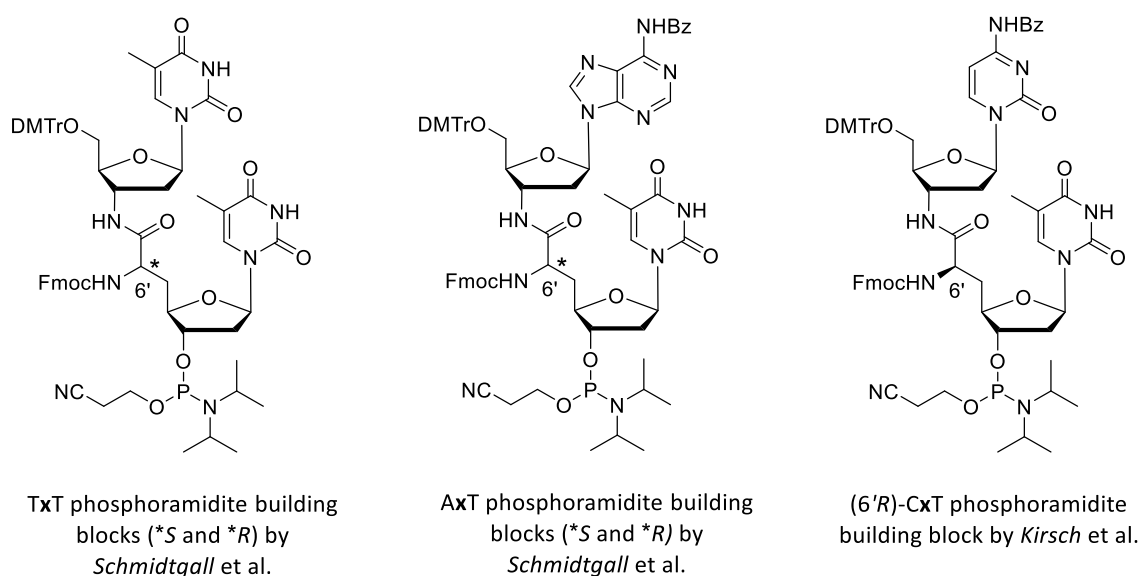


Figure 2.2. Preliminary work performed by *Schmidtgall* and *Kirsch et al.* Shown are the TxT (*S and *R), AxT (*S and *R) and (6'R)-CxT phosphoramidite building blocks suitable for automated DNA synthesis.

From these building blocks the CxT-dimer was chosen for gapmer synthesis, since it is synthetically easier accessible than its AxT-congener and allows the design of sequences with a reasonable G-C content. Furthermore, with regard to the findings of *Schmidtgall et al.*^[143], preparation of the (6'R)-isomer was aspired, as it has a higher potential to exert a less destabilizing effect on the gapmer-RNA hybrid duplex. On the basis of the synthetic route described by *Kirsch*^[145] the (6'R)-CxT phosphoramidite was synthesized starting from thymidine and 2'-deoxycytidine. Then, the dimeric building block was subjected to automated DNA synthesis together with commercially available LNA phosphoramidites. Subsequently, the resulting gapmer structure was examined regarding its hybridization

properties, its biological stability and its capability to activate the RNA-degrading enzyme RNase H. As control, a DNA/LNA-gapmer structure was used that incorporated unmodified DNA in the gap region and thus possessed no partially zwitterionic backbone segment.

The three projects, their corresponding experimental work and the respective results are summarized in the following publications (Manuscripts **A**, **B** and **C**).

3. Results

A. Enhanced Stability of DNA Oligonucleotides with Partially Zwitterionic Backbone Structures in Biological Media

Manuscript A

The contributions of each author to Manuscript A "Enhanced Stability of DNA Oligonucleotides with Partially Zwitterionic Backbone Structure in Biological Media" are listed below:

Melissa Wojtyniak (née Meng): She planned, carried out, analyzed and validated the work described in this publication. She prepared, implemented and performed the SVP and BSP exonuclease assays as well as the human plasma and whole cell lysate assays. Furthermore, she prepared the cell culture of the U937 cells and the corresponding lysate. Lastly, she conceived and wrote the manuscript.

Boris Schmidtgal: He synthesized the NAA-containing oligonucleotides.

Christian Ducho: He was responsible for the project design, supervision and administration and reviewed and edited the manuscript.

This article is an open access article distributed under the terms and conditions of the Creative Commons Attribution (CC BY) license (<http://creativecommons.org/licenses/by/4.0/>).

© 2018 by the authors. Licensee MDPI, Basel, Switzerland.

M. Meng, B. Schmidtgal and C. Ducho, *Molecules* **2018**, *23*, 2941-2952.

DOI:10.3390/molecules23112941

Article

Enhanced Stability of DNA Oligonucleotides with Partially Zwitterionic Backbone Structures in Biological Media †

Melissa Meng ¹, Boris Schmidtgal ^{1,2} and Christian Ducho ^{1,2,*} 

¹ Saarland University, Department of Pharmacy, Pharmaceutical and Medicinal Chemistry, Campus C2 3, 66123 Saarbrücken, Germany; melissa.meng@uni-saarland.de (M.M.); boris.schmidtgal@gmail.com (B.S.)

² University of Paderborn, Department of Chemistry, Warburger Str. 100, 33098 Paderborn, Germany

* Correspondence: christian.ducho@uni-saarland.de; Tel.: +49-(0)681-302-70343

† In memory of Professor Joachim Engels (1944–2018).

Received: 29 October 2018; Accepted: 8 November 2018; Published: 10 November 2018



Abstract: Deficient stability towards nuclease-mediated degradation is one of the most relevant tasks in the development of oligonucleotide-derived biomedical agents. This hurdle can be overcome through modifications to the native oligonucleotide backbone structure, with the goal of simultaneously retaining the unique hybridization properties of nucleic acids. The nucleosyl amino acid (NAA)-modification is a recently introduced artificial cationic backbone linkage. Partially zwitterionic NAA-modified oligonucleotides had previously shown hybridization with DNA strands with retained base-pairing fidelity. In this study, we report the significantly enhanced stability of NAA-modified oligonucleotides towards 3'- and 5'-exonuclease-mediated degradation as well as in complex biological media such as human plasma and whole cell lysate. This demonstrates the potential versatility of the NAA-motif as a backbone modification for the development of biomedically active oligonucleotide analogues.

Keywords: DNA; oligonucleotides; backbone modifications; nucleases; biological media

1. Introduction

As they efficiently modulate biological processes, oligonucleotides hold immense potential to serve as scaffolds for novel pharmaceutical agents. Due to their sequence-specific hybridization to DNA duplexes or single-stranded mRNA, single-stranded exogenous oligonucleotides can display antigene or antisense activity, respectively. In contrast, exogenous double-stranded RNA (siRNA) can regulate gene expression via the RNA interference mechanism [1]. However, the high polarity of native nucleic acid structures is a major disadvantage with these approaches. The oligoanionic phosphate diester-linked backbone significantly hampers cellular uptake and accounts for an overall poor pharmacokinetic profile. Furthermore, the phosphate-sugar backbone is prone to nuclease-mediated cleavage, thus further preventing applications *in vivo*.

As a consequence, numerous chemical modifications to the nucleic acid backbone have been studied with the aim of altering its polarity and sensitivity to enzymatic degradation [2,3]. The structural variety of such synthetic artificial linkages ranges from minor alterations to a complete replacement of the native internucleotide connection. In this context, phosphorothioates are one of the earliest and most well-established backbone variations [4]. This rather minor modification prevents nuclease-mediated cleavage while preserving the overall architecture of the native DNA structure. While phosphorothioates conserve the native negative charge pattern of the backbone, several artificial nucleic acid mimics contain electroneutral internucleotide linkages, thus aiming for

enhanced lipophilicity and, therefore, for improved penetration of cellular membranes. For instance, non-natural electroneutral modifications such as triazoles [5–9], amides [10–15], phosphate triesters [16] and sulfones [17] have been developed. Another electroneutral congener that displays only a remote resemblance to the native DNA backbone is the amide-based peptide nucleic acid (PNA) [18,19]. PNA exhibits high fidelity in sequence-specific hybridization with native nucleic acid strands. However, fully electroneutral oligonucleotide analogues tend to form aggregates and suffer from low water solubility, thus hampering their potential biomedical application.

An alternative approach to modifying the oligoanionic architecture of nucleic acid strands is the introduction of positive charges into the oligomer, which enables a partial ‘masking’ of its anionic motifs and may lead to zwitterionic nucleic acid analogues. In many such approaches, the oligoanionic phosphate diester backbone was retained, while the positively charged moieties were attached either to the nucleobase or the 2'-hydroxy group (in RNA) [20–23]. The resultant oligonucleotide analogues display a zwitterionic character but also densely charged structures, as the positively charged moiety is just an additional feature.

One approach to overcoming such limitations is the introduction of positively charged units as a site-specific replacement of the native phosphate diester internucleotide linkages. This may furnish partially or fully zwitterionic or even fully cationic oligonucleotide analogues, dependent on the number of artificial cationic linkages in a sequence. The altered properties of an accordingly modified nucleic acid strand might potentially be advantageous for biomedical applications with respect to nuclease stability and cellular uptake. Remarkably, this strategy has received only limited attention so far [24,25]. Undertaking pioneering work in this field, Letsinger and co-workers have introduced the conformationally flexible alkylphosphoramidate linkage [26], which later found use in several related systems [25]. Bruce and co-workers have developed conformationally rigid cationic linkages, i.e., guanidine [27–29] and *S*-methylthiourea units [30,31].

We have introduced a novel cationic internucleotide linkage with intermediate conformational flexibility named the ‘nucleosyl amino acid (NAA)-modification’. This artificial backbone motif was proposed to be conformationally advantageous relative to Letsinger’s and Bruce’s systems [32]. Therefore, it was initially employed to prepare partially zwitterionic oligonucleotides of type 1 (Figure 1) [32,33]. In a recent study, we have also reported fully cationic oligonucleotide analogues with backbones solely comprising NAA internucleotide linkages [34]. The NAA-modification was originally inspired by the ‘high-carbon’ nucleoside core structure of muraymycin nucleoside antibiotics and structurally simplified analogues thereof [32,35–38]. Thus, the stereochemical configuration in the 6'-position determines the spatial orientation of the positive charge (Figure 1).

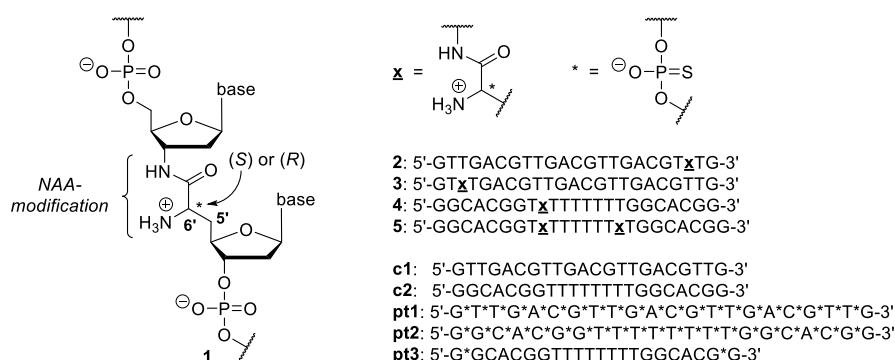


Figure 1. Principle structure 1 of an NAA-modified DNA oligonucleotide with a partially zwitterionic backbone; NAA-modified DNA oligonucleotides 2–5 investigated in this study with unmodified controls **c1** and **c2** as well as phosphorothioate-modified controls **pt1–pt3** (the linkages not highlighted are phosphate diesters; all sequences are 2'-deoxy).

In the context of partially zwitterionic NAA-modified oligonucleotides of type 1, we have synthesized a series of such oligonucleotides and studied their hybridization with DNA and RNA

counterstrands, both with full base complementarity and containing single-base mismatches [32]. The most important results for partially zwitterionic NAA-modified DNA oligonucleotides were as follows: (i) they hybridized with complementary unmodified DNA and RNA counterstrands to form duplexes; (ii) these duplexes were moderately destabilized (with DNA) and fairly significantly destabilized (with RNA), relative to the corresponding native duplexes; (iii) the spatial orientation of the positive charge ($6'S/6'R$) only had a minor influence on duplex stability, with a tendency for the ($6'R$)-configuration to furnish slightly more stable duplexes with native DNA or RNA counterstrands; (iv) base-pairing fidelity was retained, i.e., a single-base mismatch in the counterstrand led to significant destabilization of the duplex; (v) for the DNA-DNA duplexes, no significant distortion of the helical structure was found using CD spectroscopy [32]. Hence, it was concluded that fundamental chemical characteristics of nucleic acids are retained in NAA-modified DNA oligonucleotides. This qualifies the NAA-modification as an attractive addition to the existing 'toolbox' of nucleic acid backbone modifications. Remarkably, the recently reported fully cationic NAA-derived oligonucleotide analogues showed impaired base-pairing fidelity [34], thus indicating that the NAA-modification might only be suitable for (partially) zwitterionic backbone structures.

In order to further establish the NAA-modification as a versatile structural alteration of the nucleic acid backbone, detailed information on its properties in biological media are required. This particularly concerns the stability of NAA-modified oligonucleotides towards nuclease-mediated degradation. Up to this point, only very limited insights into the potential overall stabilization of the oligonucleotide backbone due to the presence of cationic linkages have been available. As previously reported by Bruice, 'chimeric' zwitterionic oligonucleotides with an artificial cationic linkage at the 3'-end (either with a guanidinium [28] or *S*-methylthiourea [31] moiety), were completely stable towards degradation by 3'→5'-exonucleases. However, the influence of 5'→3'-nucleases on such partially zwitterionic structures has not been studied yet. Furthermore, no investigations regarding the influence of some positive charges in the oligonucleotide backbone on its stability in more complex biological media (plasma, cell lysates) are available.

Hence, in this work, we report on the *in vitro* stability of some selected zwitterionic NAA-modified DNA oligonucleotides in nuclease-containing buffer as well as in complex biological media such as human plasma and cell lysates. Most likely, the NAA-modification itself will not be prone to enzymatic cleavage. It needs to be elucidated, however, whether this artificial backbone motif simply serves as a 'stopper' in nuclease-mediated degradation of the backbone or if it might exert a general stabilizing effect. In this context, the term 'general stabilizing effect' means that the sequence may be degraded until the NAA-modification is reached, but that the overall half-life of the oligonucleotide is increased relative to an unmodified native congener.

For the according studies, we have selected a set of four previously reported NAA-modified DNA oligonucleotides 2–5 (Figure 1) [32]. In sequences 2 and 3, the NAA-modification is placed in close proximity to the 5'- and 3'-ends, respectively, with one adjacent phosphate diester linkage at the terminus. In oligonucleotides 4 and 5, one or two NAA-modifications are placed in an oligo-T internal segment of the sequence. With respect to their slightly superior hybridization properties, oligomers with ($6'R$)-configuration in the NAA unit were chosen, except where indicated. Furthermore, oligonucleotides **c1** and **c2** served as unmodified native controls for 2/3 and 4/5, respectively. Phosphorothioate-linked oligonucleotides **pt1**–**pt3** were employed as stable, non-degradable additional controls for 2/3 (**pt1**) and 4/5 (**pt2** and **pt3**), respectively (Figure 1).

2. Results

2.1. Stability of NAA-modified Oligonucleotides towards Nuclease-mediated Cleavage

First, we investigated the *in vitro* stability of 2–5 towards nuclease-mediated degradation using nuclease-containing buffer. Based on literature precedent [39–41], two exonucleases commonly employed to test the stability of DNA oligonucleotides were chosen: the 3'→5' exonuclease snake

venom phosphodiesterase (SVP) from *Crotalus adamanteus* and the 5'→3' exonuclease bovine spleen phosphodiesterase (BSP), respectively. Endonucleases only target duplex structures and therefore play a less significant role with respect to potential biomedical applications of single-stranded oligonucleotide analogues. Consequently, they were not included in the assay. After incubation with one of the two exonucleases, the assay mixtures were analyzed by denaturing polyacrylamide gel electrophoresis (PAGE) using urea-containing gels. Concentrations of the oligonucleotides were chosen with respect to their UV detection limits, and the amounts of enzyme (0.4 mU SVP, 30 mU BSP) were adjusted so that unmodified oligonucleotides were completely degraded within less than two hours at 37 °C.

Using these conditions, native control **c1** and phosphorothioate-modified control **pt1** were incubated with either SVP or BSP and analyzed (Figure 2). As anticipated, **c1** was degraded rapidly, whereas the fully phosphorothioate-modified oligomer **pt1** remained stable over the complete incubation period. When NAA-modified oligomer **2** (with (6'*R*)-configuration in the NAA unit) was tested with the SVP 3'→5' exonuclease, it showed excellent stability (Figure 2a). In contrast, when the same oligonucleotide was subjected to BSP 5'→3' exonuclease activity, it underwent rather rapid degradation (Figure 2b). Remarkably, this nuclease-mediated cleavage appeared to be slowed down relative to the degradation of native control **c1**. The results were inverted when NAA-modified oligomer **3** was tested under identical conditions. It showed degradation with SVP (though again, apparently not as rapid as native control **c1**, Figure 2a), but excellent stability with BSP (Figure 2b). However, for both NAA-modified oligomers **2** and **3**, cleavage of the terminal nucleotide located in immediate proximity to the NAA-modification could be verified (**2** with SVP and **3** with BSP) using a higher resolution sequencing gel (Figure 2c).

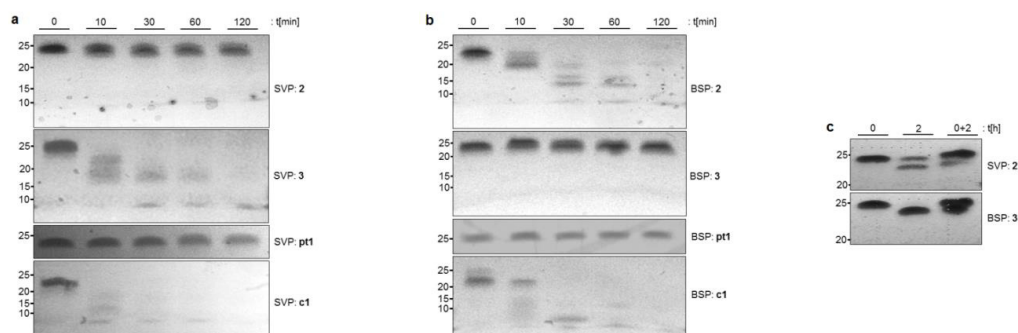


Figure 2. (a,b) Nuclease assays with NAA-modified oligonucleotides **2** and **3**, controls **c1** and **pt1** and exonucleases SVP (3'→5', a) and BSP (5'→3', b). (c) Sequencing gel analysis of the assays with oligonucleotide **2** and SVP, and **3** and BSP, respectively; left lane: assay mixture after 0 h incubation time, middle lane: assay mixture after 2 h incubation time, right lane: mixture of assay mixtures after 0 h and 2 h incubation times. In the interest of clarity, the oligonucleotide ladder indicating the lengths of the oligomers is not displayed and has been replaced with labels on the left side of the gels.

In a next step, we then studied the nuclease stability of oligonucleotide **4** with an internal NAA-modification. In this context, we also aimed to study longer incubation periods. Thus, oligomer **4** was treated with either SVP or BSP over a total time course of eight hours. In both assays, degradation of the termini, but not beyond the point of modification, was detected (Figure 3a). Another aspect of interest was the influence of the configuration of the NAA 6'-stereocenter on nuclease stability. Therefore, both the (6'*R*)- and the (6'*S*)-configured versions of **4** were incubated with SVP and BSP, respectively, over two hours (Figure 3b,c). However, no notable difference in nuclease stability was observed, indicating that the stereochemical configuration of the NAA-modification was not relevant to its effect on stabilization towards nucleases. It should be noted that the presence of the NAA-modification slowed down BSP-mediated degradation more efficiently.

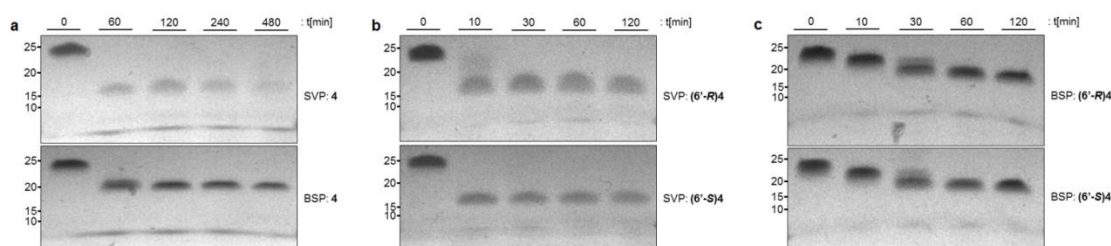


Figure 3. (a) Nuclease assays with NAA-modified oligonucleotide **4** and either SVP or BSP exonuclease over a time course of eight hours. (b,c) Nuclease assays with diastereomers of **4** differing in the configuration of the NAA 6'-stereocenter (6'/6'R) using SVP (b) or BSP (c). In the interest of clarity, the oligonucleotide ladder indicating the lengths of the oligomers is not displayed and has been replaced with labels on the left side of the gels.

2.2. Stability of NAA-modified Oligonucleotides in Complex Biological Media

The aforementioned nuclease assays are versatile but simplified model systems to elucidate the biochemical stability of NAA-modified DNA oligonucleotides. Consequently, we subsequently studied their properties *in vitro* in more complex biological media (Figure 4). First, the stabilities in human plasma were investigated using a slightly adjusted protocol (as the addition of organic solvent after incubation led to the precipitation and agglomeration of plasma components). With unmodified control oligonucleotide **c2**, the results were as expected as it underwent full cleavage. Remarkably, phosphorothioate-modified control oligonucleotide **pt2** gave no detectable bands in the ureaPAGE gel. This phenomenon might correlate with the pronounced plasma protein binding of phosphorothioates [42] and was circumvented using **pt3** as a control instead, which only had two terminal phosphorothioate modifications to mediate exonuclease stability. As anticipated, **pt3** was found to be reasonably stable over nearly the whole eight-hour time course of incubation (Figure 4a). The odd shape of the bands in the gel probably resulted from some remaining unspecific binding to plasma proteins and the slow dissociation of **pt3** from these complexes. The influence of more complex biological media on DNA analogues with partially zwitterionic backbones had not been studied before. Oligomer **5** was chosen to enable a sequential degradation from the 3'- as well as from the 5'-end. It was envisioned that further insights would be obtained into the potential general stabilizing effect of the NAA-linkage. For NAA-modified oligonucleotide **5**, some slight initial degradation in human plasma was observed, which resulted in the accumulation of a shorter fragment over the full time course (Figure 4a). Overall, the partial degradation of **5** in plasma was significantly slower than the full cleavage of unmodified control **c2**.

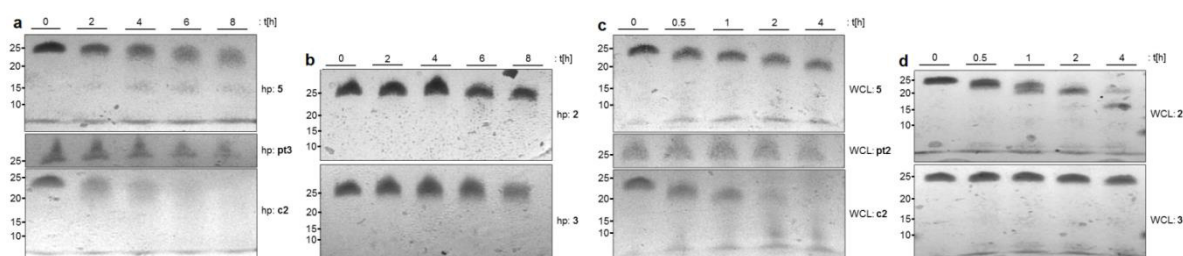


Figure 4. (a,b) Influence of human plasma (hp) on NAA-modified oligonucleotides **2**, **3** (b) and **5** (a) with controls **c2** and **pt3**. (c,d) Influence of whole cell lysate (WCL) on NAA-modified oligonucleotides **2**, **3** (d) and **5** (c) with controls **c2** and **pt2**. In the interest of clarity, the oligonucleotide ladder indicating the lengths of the oligomers is not displayed and has been replaced with labels on the left side of the gels.

We then performed additional studies on human plasma with oligomers **2** and **3**, which are modified close to the termini. Both sequences showed high stability over a course of eight hours when compared to **c2** (Figure 4b). Oligonucleotide **2** seems to undergo some initial cleavage within the first

4 h. However, the sharp bands appearing at time points 6 and 8 h, respectively, indicate no further decomposition and therefore stabilization of the sequence. For 5'-modified congener **3**, a degradation process similar to **5** was observed.

We also examined stabilities in whole cell lysate (human U937 lymphoma cell line). This assay was performed in a similar manner as the assays for nuclease stabilities (vide supra). In this case, control **pt2** gave more defined bands than in the plasma assays, and therefore, its anticipated stability in cell lysate could be proven. In contrast, native control **c2** was rapidly degraded (Figure 4c). However, incubation of NAA-modified oligomer **5** with whole cell lysate resulted in considerably slower cleavage. Remarkably, the degradation process had not even reached the modified backbone segment by the time native control **c2** was already completely decomposed (Figure 4c). Further assays were performed using oligomers **2** and **3**. Relative to control **c2**, a single NAA-linkage positioned adjacent to the 3'-end (as in **2**) slightly slowed down degradation, while the congener with the modification close to the 5'-position (i.e., **3**) showed high stability over the complete period of incubation (Figure 4d).

3. Discussion

Overall, the assays performed with SVP and BSP nucleases (Figure 2) strongly indicate that, as expected, the NAA-modification was not hydrolyzed by the nucleases. For instance, NAA-modified oligomer **3** (with the modification close to the 5'-end) showed 3'→5' degradation with SVP (though apparently not as rapid as native control **c1**, Figure 2a), but excellent stability towards 5'→3' cleavage mediated by BSP (Figure 2b). It can also be derived that the presence of the NAA-modification apparently slows down nuclease-mediated cleavage of adjacent phosphate diester linkages (**2** with SVP, **3** with BSP). However, for both NAA-modified oligomers **2** and **3**, cleavage of the terminal nucleotide located in immediate proximity to the NAA-modification could be verified (**2** with SVP, **3** with BSP, Figure 2c). This is in some contrast to the findings of Bruice, who reported no cleavage of the unmodified nucleotide at the 3'-terminus of partially zwitterionic backbones containing his modifications [28,31]. On the other hand, the intact oligonucleotide was still found alongside the degradation product after two hours incubation of oligomer **2** (Figure 2c). This further confirms that the nuclease-mediated hydrolysis of phosphate diester linkages adjacent to NAA-modified sites is decelerated relative to native backbone structures. The observation that a single NAA-modification in a distant position also furnished a slight stabilization of the oligonucleotides (**3** with SVP, **2** with BSP, Figure 2a,b) hinted towards a moderate general stabilizing effect of the cationic modification in spite of its remote position. This might be due to either: (i) a potentially reduced binding affinity to nucleases as a consequence of the zwitterionic segment of the backbone; and/or (ii) the formation of transient folded structures of the oligomer as a result of intramolecular electrostatic attraction.

For the internally modified oligomer **4**, the presence of the NAA-modification slowed down BSP-mediated degradation more efficiently relative to the (more rapid) SVP-catalyzed cleavage (Figure 3). This observation is in line with BSP being a 5'→3' exonuclease as the NAA-modification is placed closer to the 5'-end in oligomer **4**. It might also indicate though that BSP is generally more sensitive to an altered charge pattern in the oligonucleotide backbone than SVP.

When NAA-modified oligonucleotide **5** was incubated in human plasma, some slight initial degradation was observed, which resulted in the accumulation of a shorter fragment over the full time course (Figure 4a). This indicated that, most likely, no degradation beyond the position of the NAA-modification occurred. Overall, the partial degradation of **5** in plasma was significantly slower than the full cleavage of unmodified control **c2**. For the incubation of 5'-modified congener **3** in human plasma, a degradation process similar to **5** was observed, while 3'-modified oligomer **2** showed stabilization of the sequence after initial cleavage. One can therefore conclude that a single NAA-modification at the 3'-end (as in **2**) sufficiently stabilized the remaining phosphate diester backbone and that the NAA-modification overall furnishes a general stabilizing effect in human plasma.

For incubations in human cell lysate, it was observed that the degradation process of doubly NAA-modified oligonucleotide **5** had not even reached the modified backbone segment by the time native control **c2** was already completely decomposed (Figure 4c). As for the assays with exonucleases (vide supra), the NAA-linkage seems to exert a general stabilizing effect. This was further verified by the results from the according assays with oligomers **2** and **3**. Relative to control **c2**, a single NAA-linkage adjacent to the 3'-end (as in **2**) slightly slowed down degradation, while the congener with the modification close to the 5'-position (i.e., **3**) showed high stability (Figure 4d). These results also indicate that 5'-exonuclease activity appears to be significantly higher than 3'-exonuclease activity in the investigated U937 human lymphoma cell line.

4. Materials and Methods

4.1. Synthesis of NAA-Modified Oligonucleotides

The synthesis of NAA-modified oligonucleotides **2-5** was performed as reported earlier [32]. Briefly, a 'dimeric' T-T phosphoramidite building block containing the protected NAA-linkage was employed in solid phase-supported automated DNA synthesis. After cleavage from the resin and concomitant deprotection under standard conditions, the resultant NAA-modified oligonucleotides were purified using gel electrophoresis and precipitation [32,33].

4.2. Stability Assay with 3'-exonuclease

The stability of oligonucleotides against 3'-exonuclease-mediated degradation was determined using snake venom phosphodiesterase from *Crotalus adamanteus* venom (vial of ≥ 0.40 units, purified, Sigma-Aldrich, Saint Louis, MO, USA). The enzyme was dissolved in water according to the manufacturer's protocol. The oligonucleotide (1.4 nmol, 7 μ L of 200 nM stock solution in water) was mixed with glycine buffer (200 mM glycine, 15 mM MgCl₂, pH 9) to a volume of 92 μ L and then cooled to 0 °C. Snake venom phosphodiesterase (0.4 mU, 8 μ L of 0.05 mU/ μ L stock solution) was added. The resultant assay mixture was incubated at 37 °C for a total of 120 and 480 min, respectively. Samples were taken at the time points indicated in the Figures. The enzymatic reaction was quenched by mixing the sample (17.9 μ L assay mixture, corresponding to 0.25 nmol oligomer) with MeCN (17.9 μ L). The resultant mixture was dried in vacuo, dissolved in 7 μ L 0.5x TBE-running buffer (10x TBE-running buffer: 890 mM Tris, 890 mM boric acid, 20 mM EDTA, pH 8.3) and mixed with 4 μ L loading buffer (90% formamide, 10% glycerol, bromophenol blue). Analysis of the samples was performed on a ureaPAGE gel (4.75 g urea (7 M), 5.63 mL Rotiphorese™ (Carl Roth, Karlsruhe, Germany), 1.125 mL 10x TBE-running buffer, 11.25 mL water, 8.75 μ L TEMED, 62.5 μ L APS (10% in water)) run at room temperature for 2 h. Bands were detected using UV (254 nm) after placing the gel on a plastic foil-covered TLC plate (aluminum plate precoated with silica gel 60 F₂₅₄ (VWR)).

4.3. Stability Assay with 5'-exonuclease

The stability of oligonucleotides against 5'-exonuclease-mediated degradation was determined using phosphodiesterase II, bovine spleen phosphodiesterase (vial of 10 units, purified, Sigma-Aldrich). The enzyme was dissolved in water according to the manufacturer's protocol. The assay was performed as described for 3'-exonuclease (vide supra), with the following differences: the oligonucleotide (1.4 nmol, 7 μ L of 200 nM stock solution in water) was mixed with acetate buffer (100 mM ammonium acetate, 1 mM EDTA, 1 mM TWEEN 80, pH 6-7) to a volume of 97 μ L and cooled down to 0 °C. Bovine spleen phosphodiesterase (30 mU, 3 μ L of 10 mU/ μ L stock solution) was then added.

4.4. Stability Assay with Human Plasma

The stability of oligonucleotides against degradation in plasma was determined using pooled human plasma (BIOTREND Chemikalien GmbH, Cologne, Germany). The oligonucleotide (1.4 nmol, 7 μ L of 200 nM stock solution in water) was mixed with 38 μ L undiluted human plasma and cooled to

0 °C. The resultant assay mixture was incubated at 37 °C for a total of 480 min. Samples were taken at the time points indicated in the Figures. The degradation process was quenched by mixing the sample (8 µL assay mixture, corresponding to 0.25 nmol oligomer) with stopping solution (9 M urea, 15% glycerol, 1:1, 8 µL) and storing it on ice. An analysis of the resultant mixtures was performed on a ureaPAGE gel as described above.

4.5. Stability Assay with Whole Cell Lysate

The stability of oligonucleotides against degradation in whole cell lysate was determined using self-prepared lysate of the U937 cell line. U937 cells (Sigma-Aldrich) were cultured according to the manufacturer's protocol. For cell lysis, a general lysis buffer (50 mM Tris-HCl pH 7.5, 100 mM NaCl, 5% glycerol) was used. Immediately prior to lysis, 1 mM dithiothreitol (DTT) and 250 mM phenylmethylsulfonyl fluoride (PMSF) were added to the lysis buffer. Subsequently, the pellet (cell count before harvesting ~150,000,000 cells) of a freshly harvested U937 cell culture was mixed with 40 mL of general lysis buffer and ultra-sonicated (5 cycles, 15 pulses, 20%) with the cell suspension being stored on ice. Centrifugation (13 000 rpm, 30 min, 4 °C) and collecting the supernatant furnished the final whole cell lysate. The oligonucleotide (1.4 nmol, 7 µL of 200 nM stock solution in water) was mixed with 93 µL undiluted whole cell lysate. The resultant assay mixture was incubated at 37 °C for a total of 240 min. Samples were taken at the time points indicated in the Figures. The degradation process was quenched by mixing the sample (17.9 µL assay mixture, corresponding to 0.25 nmol oligomer) with MeCN (17.9 µL). The resultant mixture was dried in vacuo, dissolved in 7 µL 0.5x TBE-running buffer (vide supra for 10x TBE-running buffer) and mixed with 4 µL loading buffer (vide supra). Analysis of the samples was performed on a ureaPAGE gel as described above.

5. Conclusions

In summary, we have reported the first systematic study on the effect of an artificial cationic internucleotide linkage on the stability of corresponding partially zwitterionic oligonucleotides. We have investigated the degradation of NAA-modified zwitterionic oligonucleotides in different media, i.e., nuclease-containing buffer, human plasma, and human whole cell lysate. Overall, we have demonstrated the enhanced stability of such oligonucleotide analogues. No indication was found for a cleavage or excision of the NAA-modified site even in complex biological media (i.e., plasma and cell lysate). Most NAA-modified oligonucleotides investigated herein showed a remarkable general stabilization both in human plasma and in cell lysate, often even when the cationic NAA-modification was not in close proximity to the termini of the sequence. This might be due to a generally weakened binding of partially zwitterionic oligonucleotides to degrading enzymes such as exonucleases, most likely as a result of the altered charge pattern in the backbone. Alternatively, nuclease-mediated degradation might be slower due to the formation of transient folded structures of the zwitterionic oligomers as a result of intramolecular electrostatic attraction. As a consequence, placing only a few cationic NAA-linkages into an otherwise unmodified sequence should be sufficient to significantly enhance its stability in complex biological media. These beneficial properties complement the other favorable characteristics of NAA-modified zwitterionic oligonucleotides, such as their ability to form reasonably stable duplexes and their retained base-pairing fidelity. Overall, our results therefore confirm that the cationic NAA-linkage appears to be a potentially useful addition to the existing 'toolbox' of artificial backbone linkages for the development of oligonucleotide-based therapeutics or diagnostics.

Author Contributions: Conceptualization, Christian Ducho; Formal analysis, Melissa Meng, Boris Schmidtgall and Christian Ducho; Funding acquisition, Christian Ducho; Investigation, Melissa Meng and Boris Schmidtgall; Project administration, Christian Ducho; Supervision, Christian Ducho; Writing—original draft, Melissa Meng; Writing—review and editing, Melissa Meng, Boris Schmidtgall and Christian Ducho.

Funding: This research was funded by the Deutsche Forschungsgemeinschaft (DFG, grant DU 1095/2-1), the Fonds der Chemischen Industrie (FCI, Sachkostenzuschuss) and the Studienstiftung des deutschen Volkes (doctoral fellowship to B.S.).

Conflicts of Interest: The authors declare no conflict of interest.

References

1. Sharma, V.K.; Rungta, P.; Prasad, A.K. Nucleic acid therapeutics: basic concepts and recent developments. *RSC Adv.* **2014**, *4*, 16618–16631. [[CrossRef](#)]
2. Cobb, A.J.A. Recent highlights in modified oligonucleotide chemistry. *Org. Biomol. Chem.* **2007**, *5*, 3260–3275. [[CrossRef](#)] [[PubMed](#)]
3. Deleavey, G.F.; Damha, M.J. Designing chemically modified oligonucleotides for targeted gene silencing. *Chem. Biol.* **2012**, *19*, 937–954. [[CrossRef](#)] [[PubMed](#)]
4. Eckstein, F. Nucleoside phosphorothioates. *Ann. Rev. Biochem.* **1985**, *54*, 367–402. [[CrossRef](#)] [[PubMed](#)]
5. El-Sagheer, A.H.; Brown, T. Synthesis and Polymerase Chain Reaction Amplification of DNA Strands Containing an Unnatural Triazole Linkage. *J. Am. Chem. Soc.* **2009**, *131*, 3958–3964. [[CrossRef](#)] [[PubMed](#)]
6. El-Sagheer, A.H.; Sanzone, A.P.; Gao, R.; Tavassoli, A.; Brown, T. Biocompatible artificial DNA linker that is read through by DNA polymerases and is functional in *Escherichia coli*. *Proc. Natl. Acad. Sci. USA* **2011**, *108*, 11338–11343. [[CrossRef](#)] [[PubMed](#)]
7. Sanzone, A.P.; El-Sagheer, A.H.; Brown, T.; Tavassoli, A. Assessing the biocompatibility of click-linked DNA in *Escherichia coli*. *Nucleic Acids Res.* **2012**, *40*, 10567–10575. [[CrossRef](#)] [[PubMed](#)]
8. Birts, C.N.; Sanzone, A.P.; El-Sagheer, A.H.; Blaydes, J.P.; Brown, T.; Tavassoli, A. Transcription of Click-Linked DNA in Human Cells. *Angew. Chem. Int. Ed.* **2014**, *53*, 2362–2365. [[CrossRef](#)] [[PubMed](#)]
9. Kukwikila, M.; Gale, N.; El-Sagheer, A.H.; Brown, T.; Tavassoli, A. Assembly of a biocompatible triazole-linked gene by one-pot click-DNA ligation. *Nat. Chem.* **2017**, *9*, 1089–1098. [[CrossRef](#)] [[PubMed](#)]
10. Lebreton, J.; De Mesmaeker, A.; Waldner, A.; Fritsch, V.; Wolf, R.M.; Freier, S.M. Synthesis of thymidine dimer derivatives containing an amide linkage and their incorporation into oligodeoxyribonucleotides. *Tetrahedron Lett.* **1993**, *34*, 6383–6386. [[CrossRef](#)]
11. De Mesmaeker, A.; Waldner, A.; Lebreton, J.; Hoffmann, P.; Fritsch, V.; Wolf, R.M.; Freier, S.M. Amides as Substitute for the Phosphodiester Linkage in Antisense Oligonucleotides. *Synlett* **1993**, 733–736. [[CrossRef](#)]
12. De Mesmaeker, A.; Waldner, A.; Lebreton, J.; Hoffmann, P.; Fritsch, V.; Wolf, R.M.; Freier, S.M. Amides as a New Type of Backbone Modification in Oligonucleotides. *Angew. Chem. Int. Ed.* **1994**, *33*, 226–229. [[CrossRef](#)]
13. Selvam, C.; Thomas, S.; Abbott, J.; Kennedy, S.D.; Rozners, E. Amides as Excellent Mimics of Phosphate Linkages in RNA. *Angew. Chem. Int. Ed.* **2011**, *50*, 2068–2070. [[CrossRef](#)]
14. Tanui, P.; Kennedy, S.D.; Lunstad, B.D.; Haas, A.; Leake, D.; Rozners, E. Synthesis, biophysical studies and RNA interference activity of RNA having three consecutive amide linkages. *Org. Biomol. Chem.* **2014**, *12*, 1207–1210. [[CrossRef](#)] [[PubMed](#)]
15. Mutisya, D.; Selvam, C.; Lunstad, B.D.; Pallan, P.S.; Haas, A.; Leake, D.; Egli, M.; Rozners, E. Amides are excellent mimics of phosphate internucleoside linkages and are well tolerated in short interfering RNAs. *Nucleic Acids Res.* **2014**, *42*, 6542–6551. [[CrossRef](#)] [[PubMed](#)]
16. Moody, H.M.; van Genderen, M.H.P.; Koole, L.H.; Kocken, H.J.M.; Meijer, E.M.; Buck, H.M. Regiospecific inhibition of DNA duplication by antisense phosphate-methylated oligodeoxynucleotides. *Nucleic Acids Res.* **1989**, *17*, 4769–4782. [[CrossRef](#)] [[PubMed](#)]
17. Huang, Z.; Benner, S.A. Oligodeoxyribonucleotide Analogues with Bridging Dimethylene Sulfide, Sulfoxide, and Sulfone Groups. Toward a Second-Generation Model of Nucleic Acid Structure. *J. Org. Chem.* **2002**, *67*, 3996–4013. [[CrossRef](#)] [[PubMed](#)]
18. Nielsen, P.E.; Egholm, M.; Berg, R.H.; Buchardt, O. Sequence-selective recognition of DNA by strand displacement with a thymine-substituted polyamide. *Science* **1991**, *254*, 1497–1500. [[CrossRef](#)] [[PubMed](#)]
19. Zhilina, Z.V.; Ziemba, A.J.; Ebbinghaus, S.W. Peptide nucleic acid conjugates: synthesis, properties and applications. *Curr. Top. Med. Chem.* **2005**, *5*, 1119–1131. [[CrossRef](#)] [[PubMed](#)]
20. Strauss, J.K.; Roberts, C.; Nelson, M.G.; Switzer, C.; Maher, L.J., III. DNA bending by hexamethylene-tethered ammonium ions. *Proc. Natl. Acad. Sci. USA* **1996**, *93*, 9515–9520. [[CrossRef](#)] [[PubMed](#)]

21. Prakash, T.P.; Kawasaki, A.M.; Lesnik, E.A.; Sioufi, N.; Manoharan, M. Synthesis of 2'-O-[2-[(N,N-dialkylamino)oxy]ethyl]-modified oligonucleotides: hybridization affinity, resistance to nuclease, and protein binding characteristics. *Tetrahedron* **2003**, *59*, 7413–7422. [[CrossRef](#)]
22. Prhavc, M.; Prakash, T.P.; Minasov, G.; Cook, P.D.; Egli, M.; Manoharan, M. 2'-O-[2-[2-(N,N-Dimethylamino)ethoxy]ethyl] Modified Oligonucleotides: Symbiosis of Charge Interaction Factors and Stereoelectronic Effects. *Org. Lett.* **2003**, *5*, 2017–2020. [[CrossRef](#)] [[PubMed](#)]
23. Milton, S.; Honcharenko, D.; Rocha, C.S.J.; Moreno, P.M.D.; Smith, C.I.E.; Strömberg, R. Nuclease resistant oligonucleotides with cell penetrating properties. *Chem. Commun.* **2015**, *51*, 4044–4047. [[CrossRef](#)] [[PubMed](#)]
24. Jain, M.L.; Bruice, P.Y.; Szabo, I.E.; Bruice, T.C. Incorporation of Positively Charged Linkages into DNA and RNA Backbones: A Novel Strategy for Antigene and Antisense Agents. *Chem. Rev.* **2012**, *112*, 1284–1309. [[CrossRef](#)] [[PubMed](#)]
25. Meng, M.; Ducho, C. Oligonucleotide analogues with cationic backbone linkages. *Beilstein J. Org. Chem.* **2018**, *14*, 1293–1308. [[CrossRef](#)] [[PubMed](#)]
26. Letsinger, R.L.; Singman, C.N.; Hestand, G.; Salunkhe, M. Cationic oligonucleotides. *J. Am. Chem. Soc.* **1988**, *110*, 4470–4471. [[CrossRef](#)]
27. Blasko, A.; Dempcy, R.O.; Minyat, E.E.; Bruice, T.C. Association of Short-Strand DNA Oligomers with Guanidinium-Linked Nucleosides. A Kinetic and Thermodynamic Study. *J. Am. Chem. Soc.* **1996**, *118*, 7892–7899. [[CrossRef](#)]
28. Barawkar, D.A.; Bruice, T.C. Synthesis, biophysical properties, and nuclease resistance properties of mixed backbone oligodeoxynucleotides containing cationic internucleoside guanidinium linkages: deoxynucleic guanidine/DNA chimeras. *Proc. Natl. Acad. Sci. USA* **1998**, *95*, 11047–11052. [[CrossRef](#)] [[PubMed](#)]
29. Linkletter, B.A.; Szabo, I.E.; Bruice, T.C. Solid-Phase Synthesis of Deoxynucleic Guanidine (DNG) Oligomers and Melting Point and Circular Dichroism Analysis of Binding Fidelity of Octameric Thymidyl Oligomers with DNA Oligomers. *J. Am. Chem. Soc.* **1999**, *121*, 3888–3896. [[CrossRef](#)]
30. Arya, D.P.; Bruice, T.C. Replacement of the Negative Phosphodiester Linkages of DNA by Positive S-Methylthiourea Linkers: A Novel Approach to Putative Antisense Agents. *J. Am. Chem. Soc.* **1998**, *120*, 6619–6620. [[CrossRef](#)]
31. Challa, H.; Bruice, T.C. Incorporation of positively charged deoxynucleic S-methylthiourea linkages into oligodeoxyribonucleotides. *Bioorg. Med. Chem. Lett.* **2001**, *11*, 2423–2427. [[CrossRef](#)]
32. Schmidtgal, B.; Spork, A.P.; Wachowius, F.; Höbartner, C.; Ducho, C. Synthesis and properties of DNA oligonucleotides with a zwitterionic backbone structure. *Chem. Commun.* **2014**, *50*, 13742–13745. [[CrossRef](#)] [[PubMed](#)]
33. Schmidtgal, B.; Höbartner, C.; Ducho, C. NAA-modified DNA oligonucleotides with zwitterionic backbones: stereoselective synthesis of A–T phosphoramidite building blocks. *Beilstein J. Org. Chem.* **2015**, *11*, 50–60. [[CrossRef](#)] [[PubMed](#)]
34. Schmidtgal, B.; Kuepper, A.; Meng, M.; Grossmann, T.N.; Ducho, C. Oligonucleotides with Cationic Backbone and Their Hybridization with DNA: Interplay of Base Pairing and Electrostatic Attraction. *Chem. Eur. J.* **2018**, *24*, 1544–1553. [[CrossRef](#)] [[PubMed](#)]
35. Spork, A.P.; Ducho, C. Novel 5'-deoxy nucleosyl amino acid scaffolds for the synthesis of muraymycin analogues. *Org. Biomol. Chem.* **2010**, *8*, 2323–2326. [[CrossRef](#)] [[PubMed](#)]
36. Spork, A.P.; Wiegmann, D.; Granitzka, M.; Stalke, D.; Ducho, C. Stereoselective Synthesis of Uridine-Derived Nucleosyl Amino Acids. *J. Org. Chem.* **2011**, *76*, 10083–10098. [[CrossRef](#)] [[PubMed](#)]
37. Spork, A.P.; Büschleb, M.; Ries, O.; Wiegmann, D.; Boettcher, S.; Mihalyi, A.; Bugg, T.D.H.; Ducho, C. Lead structures for new antibacterials: stereocontrolled synthesis of a bioactive muraymycin analogue. *Chem. Eur. J.* **2014**, *20*, 15292–15297. [[CrossRef](#)] [[PubMed](#)]
38. Wiegmann, D.; Koppermann, S.; Wirth, M.; Niro, G.; Leyerer, K.; Ducho, C. Muraymycin nucleoside-peptide antibiotics: uridine-derived natural products as lead structures for the development of novel antibacterial agents. *Beilstein J. Org. Chem.* **2016**, *12*, 769–795. [[CrossRef](#)] [[PubMed](#)]
39. Williams, E.J.; Sung, S.; Laskowski, M. Action of Venom Phosphodiesterase on Deoxyribonucleic Acid. *J. Biol. Chem.* **1961**, *236*, 1130–1134. [[PubMed](#)]
40. Letsinger, R.L.; Bach, S.A.; Eadie, J.S. Effects of pendant groups at phosphorus on binding properties of d-ApA analogues. *Nucleic Acids Res.* **1986**, *14*, 3487–3499. [[CrossRef](#)] [[PubMed](#)]

41. Saneyoshi, H.; Seio, K.; Sekine, M. A General Method for the Synthesis of 2'-O-Cyanoethylated Oligoribonucleotides Having Promising Hybridization Affinity for DNA and RNA and Enhanced Nuclease Resistance. *J. Org. Chem.* **2005**, *25*, 10453–10460. [[CrossRef](#)] [[PubMed](#)]
42. Geary, R.S.; Norris, D.; Yu, R.; Bennett, C.F. Pharmacokinetics, biodistribution and cell uptake of antisense oligonucleotides. *Adv. Drug Deliv. Rev.* **2015**, *87*, 46–51. [[CrossRef](#)] [[PubMed](#)]

Sample Availability: Samples of the compounds are not available from the authors.



© 2018 by the authors. Licensee MDPI, Basel, Switzerland. This article is an open access article distributed under the terms and conditions of the Creative Commons Attribution (CC BY) license (<http://creativecommons.org/licenses/by/4.0/>).

B. Oligonucleotides with Cationic Backbone and Their Hybridization with DNA: Interplay of Base Pairing and Electrostatic Attraction

Manuscript B

The contributions of each author to Manuscript B "Oligonucleotides with Cationic Backbone and Their Hybridization with DNA: Interplay of Base Pairing and Electrostatic Attraction" are listed below:

Boris Schmidtgall: He performed the synthesis and analytical characterization of the monomeric building blocks and was involved in the writing process of the manuscript.

Arne Kuepper: He performed the synthesis and analytical characterization of the fully cationic NAA-oligonucleotides. He was involved in the design, execution and analysis of the UV-Vis-monitored melting temperature experiments and the CD-spectroscopic analyses of the fully NAA-modified oligomers. He was involved in the writing process of the manuscript.

Melissa Wojtyniak (née Meng): She was involved in the design, execution and analysis of the UV-Vis-monitored melting temperature experiments and the CD-spectroscopic analyses of the fully NAA-modified oligomers. She prepared the corresponding figures and was involved in the writing process of the manuscript.

Tom Grossmann: He was co-responsible for the project supervision and administration and reviewed and edited the manuscript.

Christian Ducho: He was responsible for the project design, supervision and administration and reviewed and edited the manuscript.

This is an open access article under the terms of the Creative Commons Attribution-NonCommercial-NoDerivs License, which permits use and distribution in any medium, provided the original work is properly cited:

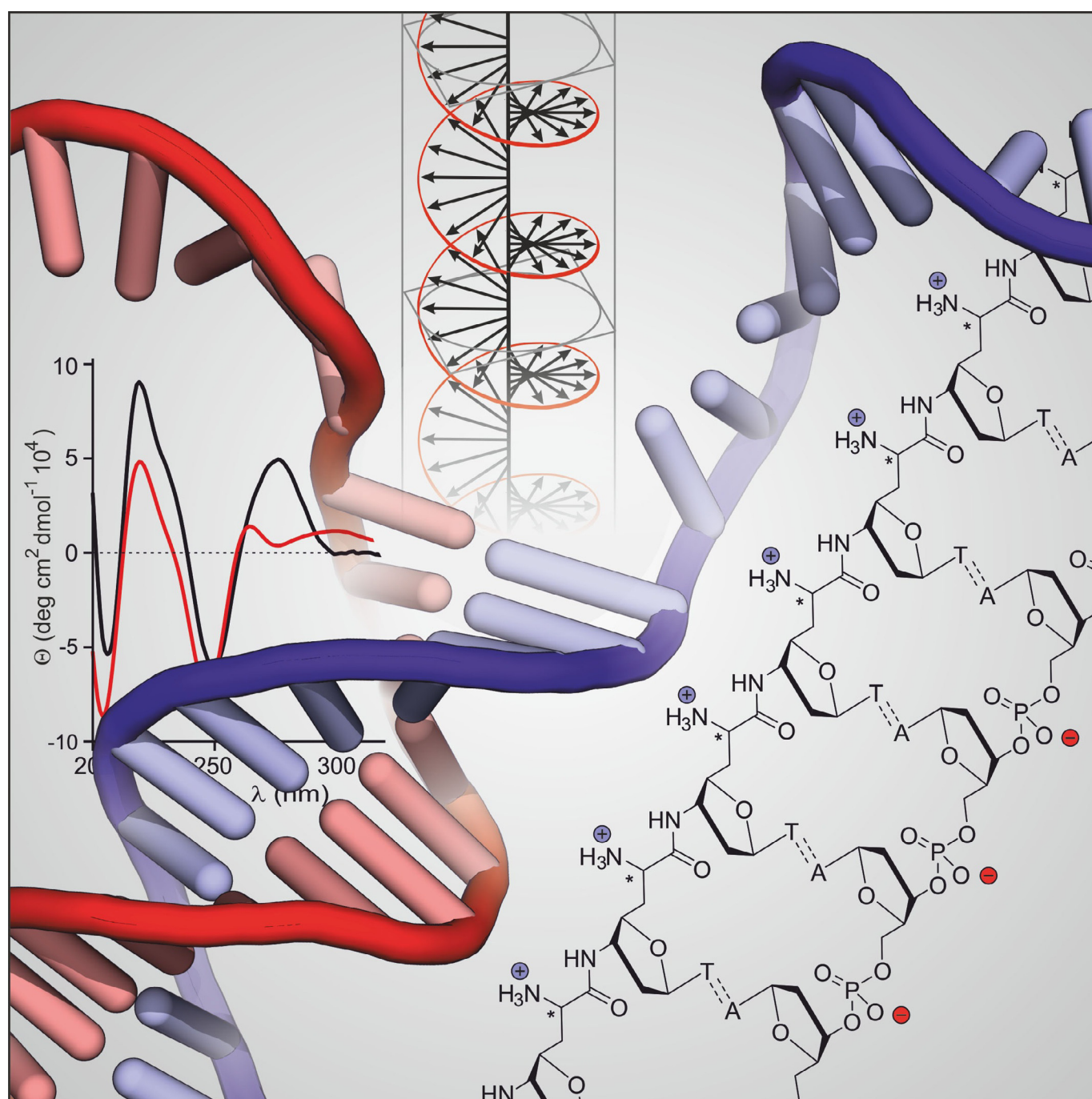
© 2017 The Authors. Published by Wiley-VCH Verlag GmbH & Co. KGaA.

B. Schmidtgal, A. Kuepper, M. Meng, T. N. Grossmann, C. Ducho, *Chem. Eur. J.* **2018**, *24*, 1544-1553. DOI: 10.1002/chem.201704338

■ Oligonucleotides | *Hot Paper* |

● Oligonucleotides with Cationic Backbone and Their Hybridization with DNA: Interplay of Base Pairing and Electrostatic Attraction

Boris Schmidtgal,^[a, b] Arne Kuepper,^[c, d] Melissa Meng,^[a] Tom N. Grossmann,^{*,[c, d, e]} and Christian Ducho^{*,[a, b]}



Abstract: Non-natural oligonucleotides represent important (bio)chemical tools and potential therapeutic agents. Backbone modifications altering hybridization properties and biostability can provide useful analogues. Here, we employ an artificial nucleosyl amino acid (NAA) motif for the synthesis of oligonucleotides containing a backbone decorated with primary amines. An oligo-T sequence of this cationic DNA analogue shows significantly increased affinity for complementary DNA. Notably, hybridization with DNA is still gov-

erned by Watson–Crick base pairing. However, single base pair mismatches are tolerated and some degree of sequence-independent interactions between the cationic NAA backbone and fully mismatched DNA are observed. These findings demonstrate that a high density of positive charges directly connected to the oligonucleotide backbone can affect Watson–Crick base pairing. This provides a paradigm for the design of therapeutic oligonucleotides with altered backbone charge patterns.

Introduction

Oligonucleotides have unique binding properties, rendering them essential molecules in living organisms and providing a platform for the modulation of biological functions through antigene, antisense, or RNA interference approaches.^[1] In natural nucleic acids (DNA and RNA), nucleotides are linked by phosphate diester moieties, thus leading to a polyanionic backbone at physiological pH.^[2] The polyanionic character contributes to the low cellular uptake of such oligonucleotides, thereby compromising in vivo applications. In addition, DNA and RNA possess low stability toward nucleases, which are ubiquitous in biological systems. These limitations have led to the development of artificial, biostable nucleic acids (e.g., phosphorothioates and “locked” nucleic acids (LNA)).^[3] In many cases, these analogues exhibit altered binding properties, providing insights into the structural contributions to duplex formation. For instance, the charge pattern of the oligonucleotide backbone can influence both hybridization and pharmacokinetic properties. Therefore, artificial electroneutral internucleotide linkages, for example, amide,^[4] sulfone,^[5] or triazole^[6] moi-

eties, have been developed. Triazole linkers have even been shown to be biocompatible, that is, triazole-modified DNA can be recognized by polymerases in cells and can therefore be employed to construct genes.^[6b–e] Peptide nucleic acid (PNA) is an example of an electroneutral nucleic acid mimic with an amide-based backbone exhibiting only limited resemblance to DNA and RNA.^[7] However, fully electroneutral nucleic acid analogues often suffer from low water solubility and a tendency to aggregate in aqueous solution. These limitations and the quest for oligonucleotides with fundamentally different properties have led to the development of positively charged nucleic acids. In most cases, positive charges were introduced through a modification of the 2'-hydroxy groups (in RNA) or nucleobases leaving the phosphate diester backbone unchanged. These strategies furnished zwitterionic structures,^[8] but resulted in densely charged oligonucleotides.

An alternative approach involves the replacement of phosphate diester units by non-natural positively charged linkers, thus providing an oligomer with a retained overall number of charges, but reversed polarity. This may be advantageous for biomedical applications, in particular with respect to cellular uptake, as indicated by the favorable properties of cationic cell-penetrating peptides (CPPs).^[9] Only a few positively charged internucleotide linkages have been reported so far:^[10] 1) Bruice's guanidine^[11] and S-methylthiourea^[12] linkages; 2) Letsinger's phosphoramidate linkages, in which amines were connected to the backbone through alkyl linkers,^[13] and 3) our recently reported NAA-modified oligonucleotides.^[14]

Bruice's rather rigid guanidine linkage and Letsinger's flexible aminoalkyl moiety provide cationic oligonucleotides with high affinity for DNA, but conformational properties that deviate significantly from native nucleic acids. This raises the question of how moderately flexible internucleoside linkages would impact the hybridization properties of cationic oligonucleotide analogues. In principle, the NAA modification (with its rigid amide bond and the adjacent 5'-C-6'-C single bond, Figure 1) could be used to assemble corresponding oligonucleotides. However, previously reported “dimeric” phosphoramidite building blocks only allow incorporation of the NAA modification adjacent to phosphate diester units, thus resulting in partially zwitterionic DNA analogues.^[14]

The favorable properties of these partially zwitterionic NAA-modified DNAs and the general interest in fully cationic oligonucleotides have inspired us to design oligomers of type 1,

[a] Dr. B. Schmidtgal, M. Meng, Prof. Dr. C. Ducho
Department of Pharmacy, Pharmaceutical and Medicinal Chemistry
Saarland University, Campus C23, 66123 Saarbrücken (Germany)
E-mail: christian.ducho@uni-saarland.de

[b] Dr. B. Schmidtgal, Prof. Dr. C. Ducho
Department of Chemistry, University of Paderborn
Warburger Strasse 100, 33098 Paderborn (Germany)

[c] A. Kuepper, Prof. Dr. T. N. Grossmann
Chemical Genomics Centre (CGC) of the Max Planck Society
Otto-Hahn-Str. 15, 44227 Dortmund (Germany)

[d] A. Kuepper, Prof. Dr. T. N. Grossmann
Faculty of Chemistry and Chemical Biology
TU Dortmund University, Otto-Hahn-Strasse 6, 44227 Dortmund (Germany)

[e] Prof. Dr. T. N. Grossmann
Department of Chemistry & Pharmaceutical Sciences
VU University Amsterdam, De Boelelaan 1083, 1081 HV
Amsterdam (The Netherlands)
E-mail: t.n.grossmann@vu.nl

Supporting information and the ORCID identification numbers for the authors of this article can be found under:
<https://doi.org/10.1002/chem.201704338>.

© 2017 The Authors. Published by Wiley-VCH Verlag GmbH & Co. KGaA. This is an open access article under the terms of Creative Commons Attribution NonCommercial-NoDerivs License, which permits use and distribution in any medium, provided the original work is properly cited, the use is non-commercial and no modifications or adaptations are made.

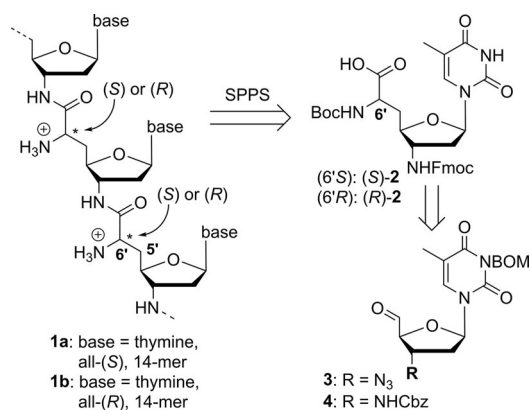


Figure 1. NAA-derived fully cationic oligonucleotides **1a** and **1b** including their retrosynthesis. SPPS: solid-phase peptide synthesis; BOM = benzyloxymethyl.

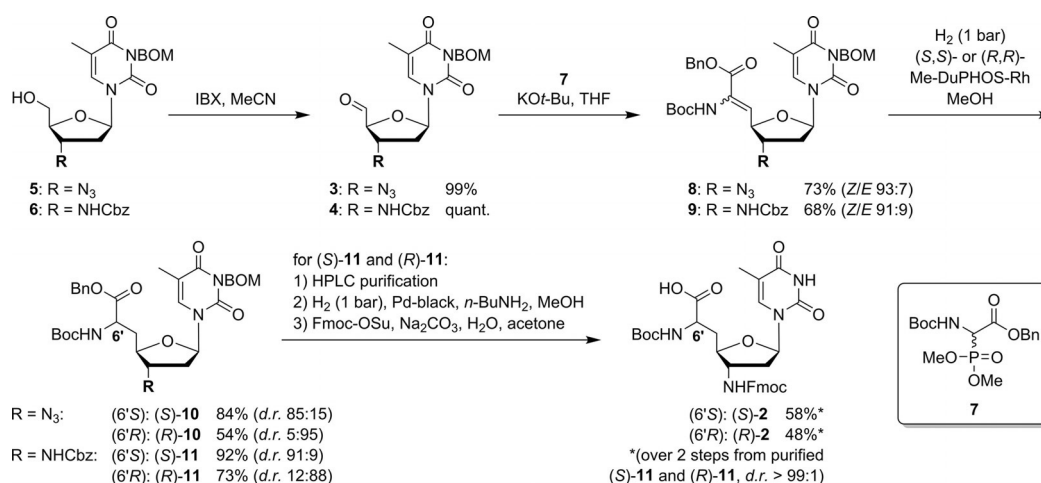
which are completely assembled from NAA internucleoside linkages (Figure 1). The availability of such cationic oligonucleotide analogues provides the basis for answering some of the questions highlighted above. In particular, it would allow an assessment of the influence of the fully cationic backbone on duplex stability and sequence specificity of hybridization with native DNA.

Results and Discussion

For the synthesis of nucleoside-derived δ -peptide-like oligomers **1**, we envisioned connecting monomeric units of type **2** through amide formation in analogy to solid-phase peptide synthesis (SPPS, Figure 1). Building block **2** should be obtained either from the 3'-azido-substituted nucleoside-5'-aldehyde **3**, or via its protected 3'-amino analogue **4**. We decided to focus on cationic oligomers with thymine as nucleobase, aiming to prepare both the all-(*S*)- and the all-(*R*)-configured oligomers (with respect to the stereochemical configuration at the 6'-position). For subsequent hybridization experiments and biophys-

ical characterizations, we designed 14-mer oligomers **1a** and **1b** (Figure 1).

The synthesis of building blocks (*S*)-**2** and (*R*)-**2** started from 3-*N*-benzyloxymethyl-(BOM)-protected 3'-azido-3'-deoxy-thymidine **5** and its 3'-*N*-Cbz-protected 3'-amino congener **6**, respectively, to compare the routes via azide **3** and protected amine **4** (Scheme 1; see Supporting Information for synthesis of **5** and **6**). Aldehydes **3** and **4** were obtained by IBX oxidation of **5** and **6** in quantitative yields. On the basis of our previously reported syntheses of nucleosyl amino acids,^[15] we applied a sequence of Wittig–Horner olefination and asymmetric hydrogenation to introduce the amino acid motif. Wittig–Horner transformations of aldehydes **3** and **4** with phosphonate **7** (see Supporting Information) furnished didehydro amino acids **8** and **9** in yields of 73% and 68%, respectively, with high stereoselectivities toward the desired *Z*-isomers (93:7 and 91:9, respectively). However, the concomitantly formed *E*-isomers could not be fully removed, and thus, asymmetric hydrogenations were performed with the *Z/E*-mixtures. Hydrogenation of **8** and **9** in the presence of chiral Rh^I catalysts (*S,S*)- and (*R,R*)-Me-DuPHOS-Rh^[16] afforded the nucleosyl amino acid products **10** and **11** in yields of 54–92%, with the major isomer (6'*S* or 6'*R*) depending on the employed catalyst [(*S,S*)-catalyst for (6'*S*), (*R,R*)-catalyst for (6'*R*); for stereochemical assignments see Experimental Section]. In contrast to our previous syntheses of nucleosyl amino acids,^[15] the hydrogenation products were not obtained in diastereomerically pure form, but with diastereomeric ratios ranging from 85:15 to 95:5. HPLC purification of (*S*)-**11** and (*R*)-**11** gave the pure 6'-epimers (d.r. > 99:1), to be followed by the efficient concomitant hydrogenolytic removal of Cbz, Bn, and BOM groups. As this hydrogenation step proceeded less satisfactorily for the 3'-azido congeners, the synthesis of the target structures through the 3'-*N*-Cbz-amino route (using aldehyde **4**) was superior overall. Subsequent 3'-*N*-Fmoc protection furnished diastereomerically pure building blocks (*S*)-**2** and (*R*)-**2** in yields of 58% and 48%, respectively, over the last two steps (Scheme 1). Fmoc-based SPPS employing either (*S*)-**4** or (*R*)-**4**, followed by final acidic cleavage and



Scheme 1. Synthesis of building blocks (*S*)-**2** and (*R*)-**2** for the preparation of cationic target oligomers **1a** and **1b**.

deprotection (reactions not shown), gave the two 14-mer diastereomers **1a** and **1b**, respectively.

For investigation of the hybridization properties with DNA, fully cationic 6'-all-(5)-14-mer **1a** was incubated with complementary 14-mer DNA (A_{14}). The influence of ion strength on duplex formation was investigated by varying the concentration of NaCl (50–125 mM, all in phosphate buffer, pH 7.4). Under all conditions, duplex formation was observed, as indicated by hyperchromicity upon heating, leading to the typical sigmoidal (though slightly broadened) melting curves (Figure S2, Supporting Information) allowing the determination of melting temperatures (T_m) (Table 1, entries 1 to 4, and Figure S2). As expected,^[13] we observed a decrease in T_m with increasing NaCl concentration, which can be ascribed to salt-mediated shielding of the backbone in **1a** (positive charges) and in DNA (negative charges). We then decided to use 100 mM NaCl, as this represents a commonly applied concentration. As a reference, the native DNA–DNA duplex (T_{14} - A_{14}) was used. At 100 mM NaCl, the duplexes of both cationic analogues (**1a** and **1b**) with fully complementary DNA (A_{14}) were more stable than the corresponding DNA–DNA duplex, as indicated by the differences in melting temperatures (ΔT_m 9°C and 17°C, respectively; Table 1, entry 3; melting curves shown in Figure 2, solid lines). The cationic 14-mers **1a** and **1b** con-

tained 13 non-native internucleoside linkages (“modifications”, mod.), so these results were equivalent to $\Delta T_m/\text{mod.}$ values of +0.7°C (**1a**) and +1.3°C (**1b**), respectively.

Subsequently, we studied the base-specificity of duplex formation of **1a** and **1b** with partially mismatched DNA strands. Upon introduction of a single base mismatch (C, G, or T instead of A in the middle of the DNA sequence), sigmoidal UV melting curves with **1a** and **1b** were observed, indicating duplex formation (Figures S3 and S4, Supporting Information). Remarkably, both cationic oligomers **1a** and **1b** showed nearly retained duplex stability upon incorporation of this single mismatch (Table 1, entries 5–7 vs. entry 3). In contrast, the corresponding DNA–DNA duplexes encountered the expected destabilization of approximately 13°C. This led to ΔT_m values (difference from the corresponding single mismatched native DNA duplex) of up to around 30°C. In the case of T-C and T-G mismatches, isomer **1a** furnished slightly more stable duplexes with the single-mismatched DNA than with the fully complementary A_{14} strand. For the same base mismatches, the **1b**-DNA duplexes were slightly destabilized relative to the fully complementary analogues (Table 1, entries 5 and 6 vs. entry 3). Overall, the (6'R)-configured NAA linkage (**1b**) furnished more stable duplexes than the (6'S)-configured congener in the case of the fully matched sequence and of the T-T mismatch (Table 1, entries 3 and 7, **1b** vs. **1a**). Remarkably, **1b** shows some preference for fully complementary DNA, resulting in T_m values that are 0.3–4.1°C lower with the single mismatched counterstrands.

These results indicate that oligonucleotide analogues **1a** and **1b** were relatively insensitive to single base mismatches in the DNA counterstrand. Hence, we aimed to probe whether Watson–Crick base pairing contributes to duplex formation, or if hybridization merely results from electrostatic attraction of the two backbones (oligocation **1a,b** with oligoanionic DNA). Therefore, melting curves were recorded for equimolar mixtures of thymidine-derived oligomers **1a** or **1b** with a fully mismatched 14-mer DNA ($G_6\text{T}T\text{G}_6$, Figure 2, Table 1, entry 8). The resultant curves indicate no specific melting process, that is, no defined transition between an aggregated and a non-aggregated state was observed (Figure 2B, C, dashed lines). However, **1a** in particular and also **1b** to some extent showed considerable hyperchromicity with $G_6\text{T}T\text{G}_6$ upon heating (up to

Table 1. T_m values (in °C \pm SD)^[a] of cationic oligonucleotide analogues **1a** and **1b** (as well as the T_{14} DNA reference) with native DNA strands.

DNA ^[b]	NaCl [mM]	T_{14} ref. T_m	1a (6'S) T_m	ΔT_m ^[c]	1b (6'R) T_m	ΔT_m ^[d]
1 A_{14}	50	n.d. ^[e]	53.6 \pm 0.9	–	n.d.	–
2 A_{14}	75	n.d.	51.1 \pm 0.6	–	n.d.	–
3 A_{14}	100	36.4 \pm 0.6	45.1 \pm 0.9	+9	53.8 \pm 0.4	+17
4 A_{14}	125	n.d.	43.1 \pm 0.4	–	n.d.	–
5 $A_7\text{CA}_6$	100	23.8 \pm 0.3	49.8 \pm 0.3	+26	49.7 \pm 0.5	+26
6 $A_7\text{GA}_6$	100	23.7 \pm 0.2	50.0 \pm 0.3	+26	50.3 \pm 1.4	+27
7 $A_7\text{TA}_6$	100	23.1 \pm 1.5	45.9 \pm 0.0	+23	53.5 \pm 0.3	+30
8 $G_6\text{T}T\text{G}_6$	100	– ^[f]	– ^[f]	– ^[f]	– ^[f]	– ^[f]

[a] In aqueous 10 mM NaH_2PO_4 (pH 7.4) and NaCl. [b] Base mismatches underlined and in bold. [c] $T_m(\mathbf{1a}\text{-DNA}) - T_m(\text{DNA-DNA})$; $T_m(\text{DNA-DNA})$: T_m value of the corresponding native DNA–DNA duplex. [d] $T_m(\mathbf{1b}\text{-DNA}) - T_m(\text{DNA-DNA})$. [e] n.d. = not determined. [f] No sigmoidal melting curve was observed.

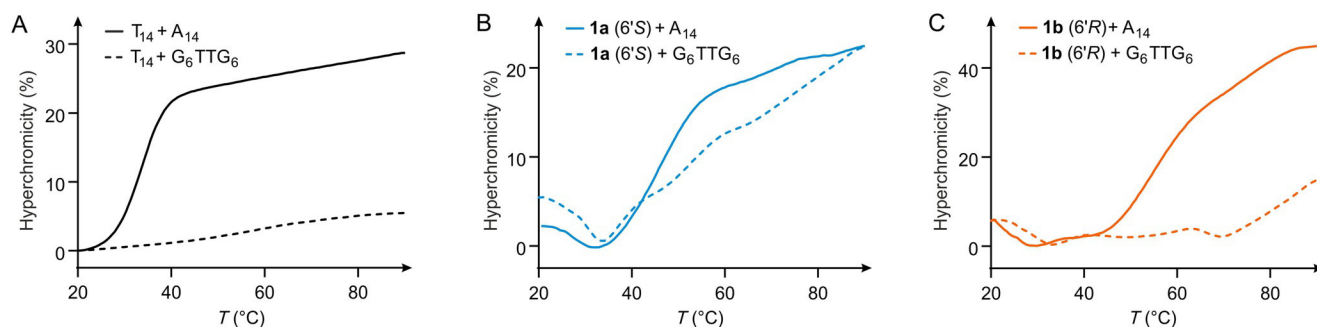


Figure 2. Melting curves (average of triplicates) for A) native DNA oligonucleotide T_{14} , B) cationic oligonucleotide analogue **1a** (6'S), and C) cationic oligonucleotide analogue **1b** (6'R) with native complementary DNA (A_{14} , solid lines), as well as with native fully mismatched DNA ($G_6\text{T}T\text{G}_6$, dashed lines).

$\approx 25\%$ for **1a**+G₆TTG₆ and $\approx 15\%$ for **1b**+G₆TTG₆, whereas the DNA–DNA reference T₁₄+G₆TTG₆ only displays a moderate hyperchromicity of up to $\approx 5\%$, steadily rising over the temperature range 20–90 °C (Figure 2A, dashed line). In contrast, the hyperchromicity of the mixture **1a**+G₆TTG₆ starts to increase at around 35 °C, but this is less pronounced for **1b**+G₆TTG₆, setting in at approximately 70 °C. A possible explanation for this behavior is a charge-mediated unspecific formation of aggregates at lower temperatures for both **1a** and **1b** with fully mismatched DNA. Elevated temperatures can then be expected to induce the disassembly of these structures. An additional indication of the presence of charge-mediated unspecific interactions are the less defined transitions in the melting curves of **1a** and **1b** with the fully matched A₁₄ DNA counterstrand (Figure 2B, C, solid lines). These duplexes appear to undergo complex temperature-induced transitions, with several changes in UV absorbance in addition to the main transition (that is, melting of the duplex). In comparison, the native DNA–DNA (T₁₄-A₁₄) reference duplex (Figure 2A, solid line) shows a sharp transition.

To obtain insights into the structural properties of cationic oligomers **1a** and **1b** and the resultant duplexes, we performed circular dichroism (CD) spectroscopy. Initially, the single-stranded oligonucleotides were investigated (Figure 3A), including the corresponding native DNA (T₁₄, black) and complementary native DNA (A₁₄, grey). A comparison of their CD spectra reveals differences between all oligomeric thymidine analogues (T₁₄, **1a** and **1b**). Notably, the spectra of native T₁₄ (black) and cationic **1a** (blue) are more similar in comparison to **1b** (orange), which differs particularly at lower wavelengths. This indicates substantial structural differences between both cationic oligomers in their single-stranded form (note that **1a** and **1b** are diastereomers).

Subsequently, duplexes of both cationic oligomers (**1a** and **1b**) and of native DNA (T₁₄) with complementary DNA (A₁₄) were investigated (Figure 3B). The CD spectrum of the **1a**-A₁₄ duplex (blue) shows resemblance to the CD signals of the native T₁₄-A₁₄ DNA–DNA duplex^[17] (black, Figure 3B). On the

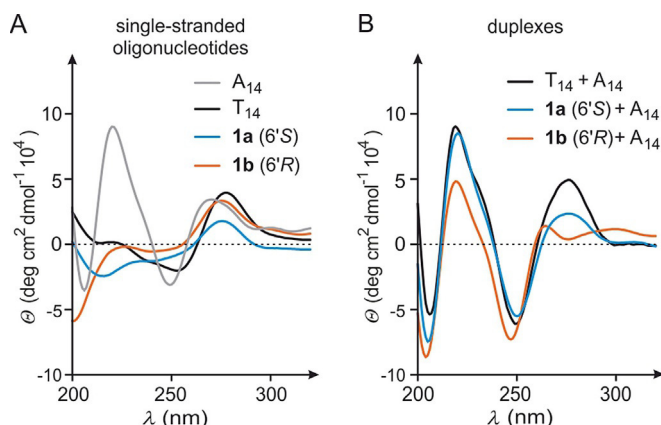


Figure 3. A) CD spectra of single-stranded cationic oligonucleotides **1a** (6'S), **1b** (6'R), and of native single-stranded DNA oligonucleotides T₁₄ and A₁₄. B) CD spectra of the aggregates **1a** (6'S)-A₁₄ and **1b** (6'R)-A₁₄ and of the native DNA–DNA reference duplex (T₁₄-A₁₄).

other hand, differences are observed for the **1b**-A₁₄ duplex (orange, Figure 3B): although the pattern of signals for $\lambda < 260$ nm is rather similar to that of the native duplex, it significantly differs for $\lambda > 260$ nm. Instead of a single maximum at approximately 275 nm, **1b**-A₁₄ exhibits two maxima at around 260 nm and 300 nm, respectively. Overall, the similarities in the CD spectra suggest that binding of both isomers **1a** and **1b** to complementary DNA probably furnished duplexes with mainly DNA-like helical topologies. However, **1b** (which, remarkably, formed the most stable duplex with A₁₄) displayed the most pronounced deviations both in its single-stranded form and in its complex with complementary native DNA A₁₄.

We then studied the CD spectra of equimolar mixtures of oligomers **1a** or **1b** with fully mismatched 14-mer DNA (G₆TTG₆, Figure 4). For the (6'S)-configured oligomer **1a**, the CD spectrum of the mixture with mismatched DNA (Figure 4A,

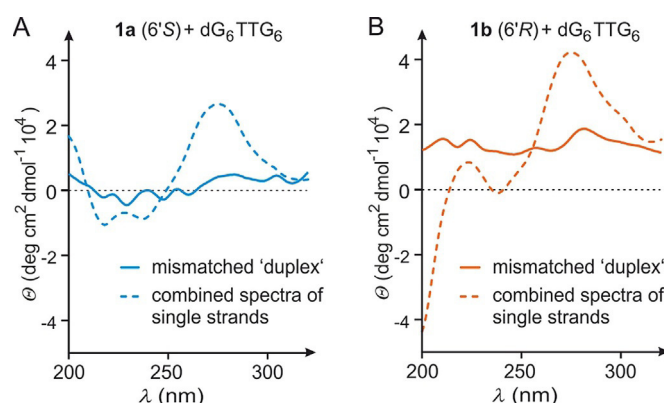


Figure 4. A) CD spectrum of the mixture of oligomer **1a** (6'S) with fully mismatched native DNA (G₆TTG₆, solid line) and calculated superposition of the CD spectra of both single strands (dashed line). B) CD spectrum of the mixture of oligomer **1b** (6'R) with fully mismatched native DNA (G₆TTG₆, solid line) and calculated superposition of the CD spectra of both single strands (dashed line).

solid line) does not show any signal pattern indicative of a helical duplex structure (as compared with that of the corresponding matched duplex, Figure 3B). To assess the possibility of nonspecific interactions between both single strands in this mixture, we determined the CD spectrum of G₆TTG₆ alone (Figure S5, Supporting Information) and added it to the spectrum of single-stranded **1a**. This combined spectrum (Figure 4A, dashed line) differs significantly from the experimentally obtained spectrum of the mixture. This suggests Watson–Crick-independent nonspecific interactions between **1a** and fully mismatched G₆TTG₆ at ambient temperature, and is in line with the aforementioned melting behavior (Figure 2). Similar results were obtained for the mixture of (6'R)-configured oligomer **1b** with fully mismatched DNA (Figure 4B).

Conclusion

We report the synthesis of a novel amide-linked cationic oligonucleotide analogue based on NAA internucleoside linkages. Two cationic oligomers (**1a** and **1b**, 6'-epimers) were synthe-

sized and investigated by UV melting studies and CD spectroscopy. Both oligomers form very stable, presumably helical, duplexes with native complementary DNA strands. The high duplex stability (compared with the native DNA–DNA duplex) resembles that of some previously reported cationic oligomers, in particular Bruice's guanidine-linked oligonucleotides.^[11] Notably, hybridization of **1a** and **1b** with DNA was insensitive to single base mismatches, thus indicating robustness of hybridization toward limited local perturbations within the duplex. However, duplex formation was not detected in the case of a fully mismatched DNA counterstrand, demonstrating Watson–Crick base pairing to be a requirement for hybridization and the occurrence of a defined topology. The most likely explanation for our observations is that electrostatic attraction can compensate for single base mismatches, but is not sufficient to foster the formation of a defined structure in the absence of Watson–Crick base pairing. In the latter case, sequence-unspecific charge-mediated aggregation phenomena occur. This behavior is in sharp contrast to the pronounced mismatch sensitivity of partially zwitterionic oligonucleotides containing up to four NAA linkages.^[14a]

Interestingly, both isomers differ moderately in their DNA-binding affinity as well as selectivity, and on the basis of their CD spectra, also in their structural topology. Apparently, the (6'*R*)-configuration in **1b** is slightly more beneficial for hybridization. Notably, an analogous behavior had also been observed for previously reported partially zwitterionic NAA-modified oligonucleotides.^[14a] Both isomers **1a** and **1b** appear to adopt different structures in their single-stranded form. Furthermore, the CD spectrum of duplex **1b**-A₁₄ reveals a maximum at approximately 300 nm, which is unusual for fully helical oligonucleotide duplexes.

Overall, our findings will contribute to the future design of oligonucleotides for potential biomedical applications. The favorable properties of cationic cell-penetrating peptides (CPPs)^[9] indicate that the introduction of positive charges into the oligonucleotide backbone might be beneficial for their therapeutic or diagnostic use, in particular with respect to cellular uptake. However, as demonstrated in this work, fully cationic (in contrast to partially zwitterionic) oligonucleotides can suffer from impaired base pairing fidelity and unspecific aggregation in the absence of Watson–Crick base pairing. In our future work, we will therefore study how the ratio of negatively and positively charged linkages impacts base-pairing fidelity. In addition, more detailed structural studies will be performed, with the long-term goal of obtaining a thorough understanding of the interplay of conformation, base pairing, and electrostatic attraction in duplexes of (partially) cationic and anionic oligonucleotide strands.

Experimental Section

General methods

The syntheses of starting materials **5** and **6** and of phosphonate **7** are described in the Supporting Information. All other chemicals were purchased from standard suppliers. Reactions involving

oxygen- and/or moisture-sensitive reagents were performed under an atmosphere of argon using anhydrous solvents. Anhydrous solvents were obtained in the following manner: THF was dried over sodium/benzophenone and distilled, CH₂Cl₂ was dried over CaH₂ and distilled, MeOH was dried over activated molecular sieves (3 Å) and degassed, MeCN was dried over P₂O₅ and distilled, pyridine was dried over CaH₂ and distilled, toluene was dried over sodium/benzophenone and distilled. The thus-obtained solvents were stored over molecular sieves (4 Å; in case of MeOH and MeCN, 3 Å). All other solvents were of technical quality and distilled prior to use, and deionized water was used throughout. Column chromatography was performed on silica gel 60 (0.040–0.063 mm, 230–400 mesh ASTM, VWR) under flash conditions unless otherwise indicated. TLC was performed on aluminum plates precoated with silica gel 60 F₂₅₄ (VWR). Visualization of the spots was achieved using UV light (254 nm) and/or staining under heating (H₂SO₄ staining solution: 4 g vanillin, 25 mL conc. H₂SO₄, 80 mL AcOH, and 680 mL MeOH; KMnO₄ staining solution: 1 g KMnO₄, 6 g K₂CO₃, and 1.5 mL NaOH (1.25 M) solution, all dissolved in 100 mL H₂O; ninhydrin staining solution: 0.3 g ninhydrin, 3 mL AcOH, and 100 mL 1-butanol). Analytical chiral HPLC was performed on a Jasco system equipped with a pu 2080 Plus pump, an AS 2055 Plus autosampler, an MD 2010 Plus multiwavelength detector, and an IB Chiralpak™ column (0.8×27.5 cm) purchased from Diacel. Method: isocratic eluent 70:30 *n*-hexane-EtOAc; flow 0.8 mL min⁻¹; injection volume 10 μL (*c* ≈ 4 mg mL⁻¹ in EtOAc). Preparative chiral HPLC was performed on a Jasco system equipped with a pu 2080 Plus pump, an MD 2010 Plus multiwavelength detector, and an IB Chiralpak™ column (1.5×28 cm) purchased from Diacel. Method: isocratic eluent 73:27 *n*-hexane-EtOAc; flow 5 mL min⁻¹; injection volume 100 μL (*c* ≈ 100 mg mL⁻¹ in EtOAc). 300 MHz- and 500 MHz-¹H, 75 MHz- and 126 MHz-¹³C, and 121 MHz-³¹P NMR spectra were recorded on Varian MERCURY 300, UNITY 300, INOVA 500, and INOVA 600 spectrometers. All ¹³C NMR spectra were H-decoupled. All spectra were recorded at room temperature unless indicated otherwise, and were referenced internally to solvent reference frequencies. For calibration of ³¹P NMR signals, 85% phosphoric acid was used as an external standard. Chemical shifts (δ) are quoted in ppm and coupling constants (*J*) are reported in Hz. Signals were assigned by using H,H-COSY, HSQC, and HMBC spectra obtained on the spectrometers detailed above. Mass spectra of small molecules were measured on a Finnigan LCQ ion-trap mass spectrometer or on a Bruker microTOF spectrometer. For ESI measurements in the negative mode, solutions of the compounds in pure MeOH were used, whereas for measurements in the positive mode, solutions in MeOH containing 0.1% formic acid were employed. High-resolution spectra were measured on a Bruker 7 Tesla Fourier transform ion cyclotron resonance (FTICR) mass spectrometer. Melting points (m.p.) were measured on a Büchi instrument and were not corrected. Optical rotations were recorded on a PerkinElmer polarimeter 241 with a Na source using a 10 cm cell. Solutions of the compounds (\approx 10 mg) in CHCl₃ or pyridine (1 mL) were used, and concentrations are given in g/100 mL. Infrared (IR) spectroscopy was performed on a PerkinElmer Vektor 22 spectrometer with solids measured as KBr pills or on a Jasco FT/IR-4100 spectrometer equipped with an integrated ATR unit (GladiATR™, PIKE Technologies). Wavenumbers (ν) are quoted in cm⁻¹. UV spectroscopy of small molecules was performed on a PerkinElmer Lambda 2 spectrometer. Measurements were performed with solutions of approximately 0.1 mg of the compound in 10 mL MeCN and in the range 190–500 nm. Wavelengths of maximum absorption (λ_{max}) are reported in nm with the corresponding logarithmic molar extinction coefficient (log ϵ) given in parentheses (ϵ in dm³ mol⁻¹ cm⁻¹).

Syntheses and characterization data

6'-N-Boc-3'-N-Fmoc-amino-3'-deoxy-(S)-thymidinyl amino acid (S)-2: Pd-black (1.28 g, 12.0 mmol) and *n*-butylamine (1.80 g, 2.43 mL, 24.2 mmol) were added to a solution of diastereomerically pure NAA (S)-11 (vide infra, 900 mg, 1.21 mmol) in MeOH (28 mL). The resultant suspension was stirred for 24 h under a hydrogen atmosphere (1 bar). It was then filtered and the filter cake was washed with MeOH (3 × 10 mL). The combined filtrates were evaporated and the residue was coevaporated with pyridine (3 × 4 mL). The solid thus obtained was used for the subsequent Fmoc protection without further purification.

Na₂CO₃ (115 mg, 1.09 mmol) and Fmoc-OSu (368 mg, 1.09 mmol) were added to a solution of the obtained product (435 mg, 1.09 mmol) in a mixture of acetone and water (1:1, 3 mL). The reaction mixture was stirred for 1 h at RT. It was then acidified to pH 2 with 2 M HCl and partitioned between a mixture of CH₂Cl₂ (15 mL) and brine (15 mL). The aqueous layer was extracted with CH₂Cl₂ (3 × 10 mL). The combined organics were dried over Na₂SO₄, filtered, and evaporated. The resultant crude product was purified by column chromatography (9:1 CH₂Cl₂-MeOH, 0.5% AcOH). The obtained product was coevaporated with toluene (3 × 5 mL) to give (S)-2 as a fine white powder (393 mg, 58% over two steps from (S)-11). M.p. decomposition > 110 °C; TLC: R_f = 0.26 (9:1 CH₂Cl₂-MeOH); [α]_D²⁰ = +39.7 (c = 1.2, CHCl₃); ¹H NMR (500 MHz, CD₃OD): δ = 1.44 (s, 9H, C(CH₃)₃), 1.93 (s, 3H, 7-H), 2.06–2.16 (m, 1H, 5'-H_a), 2.21–2.39 (m, 3H, 2'-H_a, 2'-H_b, 5'-H_b), 3.89–3.97 (m, 1H, 4'-H), 4.05–4.14 (m, 1H, 3'-H), 4.18–4.27 (m, 2H, Fmoc-CH₂), 4.32–4.48 (m, 3H, 9'-H, 6'-H, 6'-NH), 6.08–6.15 (m, 1H, 1'-H), 7.31 (dd, J = 7.3, 7.3 Hz, 2H, 2''-H, 7''-H), 7.34 (dd, J = 7.3, 7.3 Hz, 2H, 3''-H, 6''-H), 7.53 (brs, 1H, 6-H), 7.65 (d, J = 7.3 Hz, 2H, 4''-H, 5''-H), 7.79 ppm (d, J = 7.3 Hz, 2H, 1''-H, 8''-H); ¹³C NMR (126 MHz, CD₃OD): δ = 11.1 (C-7), 27.3 (C(CH₃)₃), 35.3 (C-5'), 36.8 (C-2'), 46.8 (Fmoc-CH₂), 51.3 (C-6'), 54.2 (C-3'), 66.4 (C-9''), 79.2 (C(CH₃)₃), 81.0 (C-4'), 84.4 (C-1'), 110.5 (C-5), 119.5 (C-1'', C-8''), 124.7, 124.8 (C-4'', C-5''), 126.8, 127.4 (C-2'', C-7''), 127.8, 128.5 (C-3'', C-6''), 136.4 (C-6), 141.3 (C-8''a, C-9''a), 143.9 (C-4''a, C-4''b), 150.8 (C-2), 156.3 (Boc-C=O), 156.3 (Fmoc-C=O), 165.0 (C-4), 174.4 ppm (COOH); IR (ATR): $\tilde{\nu}$ = 1680, 1519, 1447, 1250, 1161, 1050, 1022, 759, 736 cm⁻¹; UV (MeCN): λ_{max} (log ϵ) = 206 (4.95), 264 nm (4.65); HRMS (ESI) calcd for C₃₂H₃₆N₄NaO₉: 643.2374; found: 643.2368 [M+Na]⁺.

6'-N-Boc-3'-N-Fmoc-amino-3'-deoxy-(R)-thymidinyl amino acid (R)-2: The synthesis of (6'R)-configured NAA (R)-2 was performed according to the procedure for the synthesis of (6'S)-configured NAA (S)-2 with diastereomerically pure NAA (R)-11 (vide infra, 370 mg, 0.498 mmol), Pd-black (528 mg, 4.98 mmol), *n*-butylamine (731 mg, 1.00 mL, 10.0 mmol), MeOH (12 mL), Na₂CO₃ (53 mg, 0.50 mmol), Fmoc-OSu (169 mg, 0.502 mmol), and acetone/water (1:1, 1.4 mL). The crude product was purified by column chromatography (9:1 CH₂Cl₂-MeOH, 0.5% AcOH). The obtained product was coevaporated with toluene (3 × 5 mL) to give (R)-2 as a fine white powder (150 mg, 48% over two steps from (R)-11). M.p. decomposition > 110 °C; TLC: R_f = 0.26 (9:1 CH₂Cl₂-MeOH); [α]_D²⁰ = +23.5 (c 1.1, CHCl₃); ¹H NMR (500 MHz, CD₃OD): δ = 1.44 (s, 9H, C(CH₃)₃), 1.93 (s, 3H, 7-H), 2.03–2.14 (m, 1H, 5'-H_a), 2.14–2.24 (m, 1H, 5'-H_b), 2.24–2.32 (m, 1H, 2'-H_a), 2.32–2.42 (m, 1H, 2'-H_b), 3.84–3.91 (m, 1H, 4'-H), 4.03–4.11 (m, 1H, 3'-H), 4.19–4.26 (m, 2H, Fmoc-CH₂), 4.26–4.35 (m, 1H, 6'-H), 4.38–4.48 (m, 2H, 9'-H, 6'-NH), 6.14–6.21 (m, 1H, 1'-H), 7.33 (dd, J = 7.3, 7.3 Hz, 2H, 2''-H, 7''-H), 7.40 (dd, J = 7.3, 7.3 Hz, 2H, 3''-H, 6''-H), 7.50 (brs, 1H, 6-H), 7.66 (d, J = 7.3 Hz, 2H, 4''-H, 5''-H), 7.80 ppm (d, J = 7.3 Hz, 2H, 1''-H, 8''-H); ¹³C NMR (126 MHz, CD₃OD): δ = 11.0 (C-7), 27.3 (C(CH₃)₃), 35.4 (C-5'), 36.5 (C-2'), 46.8 (Fmoc-CH₂), 51.3 (C-6'), 54.4 (C-3'), 66.3 (C-9''), 79.2 (C(CH₃)₃), 80.6 (C-4'), 84.7 (C-1'), 110.6 (C-5), 119.5 (C-1'', C-8''),

124.7, 124.9 (C-4'', C-5''), 126.8, 127.4 (C-2'', C-7''), 127.8, 128.5 (C-3'', C-6''), 136.4 (C-6), 141.3 (C-8''a, C-9''a), 143.9 (C-4''a, C-4''b), 150.8 (C-2), 156.7 (Boc-C=O), 157.0 (Fmoc-C=O), 164.9 (C-4), 174.8 ppm (COOH); IR (ATR): $\tilde{\nu}$ = 1685, 1519, 1447, 1255, 1161, 1070, 1050, 1022, 759, 736 cm⁻¹; UV (MeCN): λ_{max} (log ϵ) = 206 (4.58), 264 nm (4.25); HRMS (ESI) calcd for C₃₂H₃₆N₄NaO₉: 643.2374; found: 643.2373 [M+Na]⁺.

3-N-BOM-3'-azido-3'-deoxythymidine-5'-aldehyde 3: IBX (3.15 g, 11.2 mmol) was added to a solution of 3-N-BOM-3'-azido-3'-deoxythymidine 5 (1.74 g, 4.49 mmol) in MeCN (43 mL), and the reaction mixture was stirred for 45 min under reflux. It was then cooled to RT and filtered. The filter cake was washed with EtOAc (3 × 20 mL), and the combined filtrates were evaporated under reduced pressure. The resultant residue was kept under high vacuum to remove remaining volatiles to give 3 as a colorless foam (1.72 g, 99%). With respect to its limited stability, 3 was only characterized by NMR spectroscopy and then used directly in the next reaction. ¹H NMR (500 MHz, CDCl₃): δ = 1.94 (d, J = 1.2 Hz, 3H, 7-H), 2.35–2.45 (m, 1H, 2'-H_a), 2.43 (ddd, J = 14.1, 6.7, 4.0 Hz, 1H, 2'-H_b), 4.42 (d, J = 3.4 Hz, 1H, 4'-H), 4.60 (ddd, J = 7.0, 3.5, 3.4 Hz, 1H, 3'-H), 4.68 (s, 2H, 2''-H), 5.46 (s, 2H, 1''-H), 6.00 (dd, J = 6.7, 6.6 Hz, 1H, 1'-H), 7.23–7.35 ppm (m, 6H, 6-H, aryl-H); ¹³C NMR (126 MHz, CDCl₃): δ = 13.1 (C-7), 36.6 (C-2'), 61.7 (C-3'), 70.6 (C-2''), 72.4 (C-1''), 88.6 (C-1'), 90.4 (C-4'), 110.7 (C-5), 127.6 (C-6''), 127.7 (C-4'', C-8''), 128.3 (C-5'', C-7''), 135.3 (C-6), 137.9 (C-3''), 150.7 (C-2), 163.2 (C-4), 198.3 ppm (C-5').

3-N-BOM-3'-N-Cbz-amino-3'-deoxythymidine-5'-aldehyde 4: IBX (2.07 g, 7.38 mmol) was added to a solution of 3-N-BOM-3'-N-Cbz-amino-3'-deoxythymidine 6 (1.46 g, 2.95 mmol) in MeCN (28 mL), and the reaction mixture was stirred for 45 min under reflux. It was then cooled to RT and filtered. The filter cake was washed with EtOAc (3 × 15 mL), and the combined filtrates were evaporated under reduced pressure. The resultant residue was kept under high vacuum to remove remaining volatiles to give 4 as a colorless foam (1.45 g, quant.). With respect to its limited stability, 4 was only characterized by NMR spectroscopy and then used directly in the next reaction. ¹H NMR (500 MHz, CDCl₃): δ = 1.96 (s, 3H, H-7), 2.06–2.16 (m, 1H, 2'-H_a), 2.38–2.47 (m, 1H, 2'-H_b), 4.40 (m, 1H, 3'-H), 4.53–4.59 (m, 1H, 4'-H), 4.65 (s, 2H, 1''-H), 5.04–5.14 (m, 2H, 1'''-H), 5.45 (s, 2H, 2''-H), 5.81–5.89 (m, 1H, 3'-NH), 6.25–6.35 (m, 1H, 1'-H), 7.20–7.39 (m, 10H, aryl-H), 7.64 (s, 1H, 6-H), 9.71 ppm (s, 1H, 5'-H); ¹³C NMR (126 MHz, CDCl₃): δ = 13.3 (C-7), 36.5 (C-2'), 52.0 (C-3'), 67.3 (C-1''), 70.6 (C-1''), 72.3 (C-2''), 87.7 (C-1'), 88.5 (C-4'), 110.9 (C-5), 127.7, 127.7, 128.2, 128.3, 128.3, 128.7 (aryl-C), 134.7 (C-6), 135.7, 135.8 (C-3'', C-2'''), 137.9 (Cbz-C=O), 151.0 (C-2), 163.3 (C-4), 198.0 ppm (C-5'); HRMS (ESI) calcd for C₂₆H₂₆N₃O₇: 492.1776; found: 492.1780 [M-H]⁻.

(Z)-6'-N-Boc-3-N-BOM-3'-azido-5',6'-didehydro-3'-deoxythymidinyl amino acid benzyl ester 8: A solution of phosphonate 7 (1.67 g, 4.49 mmol) in THF (34 mL) was added to a precooled (-78 °C) solution of KOtBu (504 mg, 4.49 mmol) in THF (43 mL) at -78 °C. The resultant solution was stirred for 5 min at -78 °C. Subsequently, a solution of aldehyde 3 (1.45 g, 2.95 mmol) in THF (18 mL) was added. The reaction mixture was stirred for 16 h and was allowed to warm slowly to RT during this time period. The resultant suspension was cooled to 0 °C and MeOH (5 mL) was added, after which the solution was diluted with EtOAc (200 mL). It was then washed with water (1 × 100 mL) and brine (1 × 100 mL), dried over Na₂SO₄, filtered, and evaporated under reduced pressure. The resultant crude product was purified by column chromatography (3:2 *iso*-hexanes-EtOAc) to give 8 as a colorless foam (2.06 g, 73%, diastereomeric mixture *Z/E* 93:7). As described before,^[14,15a,b,16c] the stereochemical assignment (*Z/E*) was based on the

empirical rules for NMR data established by Mazurkiewicz et al.^[18]
Z-8: TLC: $R_f=0.62$ (2:3 *iso*-hexanes-EtOAc); ¹H NMR (500 MHz, CDCl₃): $\delta=1.48$ (s, 9H, C(CH₃)₃), 1.83 (d, $J=1.2$ Hz, 3H, 7-H), 2.24 (ddd, $J=13.9, 7.4, 6.6$ Hz, 1H, 2'-H₃), 2.49 (ddd, $J=13.9, 5.9, 2.9$ Hz, 1H, 2'-H_b), 4.35 (ddd, $J=6.0, 3.0, 3.0$ Hz, 1H, 3'-H), 4.69 (s, 2H, 2''-H), 4.86 (dd, $J=8.4, 2.8$ Hz, 1H, 6'-H), 5.22 (d, $J=12.2$ Hz, 2H, 1'''-H₃), 5.27 (d, $J=12.2$ Hz, 2H, 1'''-H_b), 5.46 (d, $J=9.7$ Hz, 1H, 1''-H₃), 5.48 (d, $J=9.7$ Hz, 1H, 1''-H_b), 6.07 (dd, $J=7.4, 6.0$ Hz, 1H, 1'-H), 6.31 (d, $J=8.4$ Hz, 1H, 5'-H), 6.60 (s, 1H, 6'-NH), 7.09 (q, $J=1.2$ Hz, 1H, 6-H), 7.22–7.26 (m, 1H, aryl-H), 7.28–7.33 (m, 2H, aryl-H), 7.34–7.39 ppm (m, 7H, aryl-H); ¹³C NMR (126 MHz, CDCl₃): $\delta=13.2$ (C-7), 28.1 (C(CH₃)₃), 37.4 (C-2'), 65.0 (C-3'), 68.1 (C-1'''), 70.6 (C-1''), 72.3 (C-2''), 81.9 (C-6'), 87.7 (C-1'), 110.4 (C-5), 125.3 (C-5'), 127.6, 128.3, 128.5, 128.7, 128.7, 134.0 (aryl-C), 134.9 (C-6), 138.4 (aryl-C), 150.7 (C-2), 153.1 (Boc-C=O), 163.2 (C-4), 163.9 ppm (ester-C=O); IR (KBr): $\tilde{\nu}=2101, 1708, 1652, 1242, 1151, 1065, 1027, 769, 736, 693$ cm⁻¹; UV (MeCN): λ_{\max} (log ϵ)=206 (4.56), 261 nm (4.17); HRMS (ESI) calcd for C₃₂H₃₆N₆NaO₈: 655.2492; found: 655.2487 [M+Na]⁺.

(Z)-6'-N-Boc-3-N-BOM-3'-N-Cbz-amino-5',6'-didehydro-3'-deoxy-thymidiny amino acid benzyl ester 9: A solution of phosphonate **7** (1.21 g, 3.25 mmol) in THF (25 mL) was added to a precooled (−78 °C) solution of K₂CO₃ (330 mg, 2.95 mmol) in THF (28 mL) at −78 °C. The resultant solution was stirred for 5 min at −78 °C. Subsequently, a solution of aldehyde **4** (1.45 g, 2.95 mmol) in THF (12 mL) was added. The reaction mixture was stirred for 16 h and was allowed to warm slowly to RT during this time period. The resultant suspension was cooled to 0 °C and MeOH (3 mL) was added, after which the solution was diluted with EtOAc (150 mL). It was then washed with water (1×80 mL) and brine (1×80 mL), dried over Na₂SO₄, filtered, and evaporated under reduced pressure. The resultant crude product was purified by column chromatography (3:2 *iso*-hexanes-EtOAc) to give **9** as a colorless foam (1.48 g, 68%, diastereomeric mixture *Z/E* 91:9). As described before,^[14,15a,b,16c] the stereochemical assignment (*Z/E*) was based on the empirical rules for NMR data established by Mazurkiewicz et al.^[18]
Z-9: TLC: $R_f=0.31$ (1:1 *iso*-hexanes-EtOAc); ¹H NMR (500 MHz, CDCl₃, 50 °C): $\delta=1.46$ (s, 9H, C(CH₃)₃), 1.88 (d, $J=1.1$ Hz, 3H, 7-H), 2.40 (ddd, $J=13.9, 7.0, 7.0$ Hz, 1H, 2'-H₃), 2.44 (ddd, $J=13.9, 8.0, 6.2$ Hz, 1H, 2'-H_b), 4.06–4.13 (m, 1H, 3'-H), 4.69 (s, 2H, 1''-H), 4.79 (dd, $J=8.4, 6.4$ Hz, 1H, 4'-H), 5.11 (d, $J=12.7$ Hz, 1H, 1'''-H₃), 5.13 (d, $J=12.7$ Hz, 1H, 1'''-H_b), 5.23 (d, $J=12.6$ Hz, 1H, 1''-H₃), 5.26 (d, $J=12.6$ Hz, 1H, 1''-H_b), 5.47 (d, $J=9.7$ Hz, 1H, 2''-H₃), 5.49 (d, $J=9.7$ Hz, 1H, 2''-H_b), 5.95–6.01 (m, 1H, 3'-NH), 6.20 (dd, $J=6.2, 6.2$ Hz, 1H, 1'-H), 6.31 (d, $J=8.4$ Hz, 1H, 5'-H), 6.85 (s, 1H, 6'-NH), 7.09 (s, 1H, 6-H), 7.21–7.40 ppm (m, 15H, aryl-H); ¹³C NMR (126 MHz, CDCl₃, 50 °C): $\delta=13.1$ (C-7), 28.1 (C(CH₃)₃), 38.7 (C-2'), 55.9 (C-3'), 67.0 (C-1'''), 68.0 (C-1''), 70.7 (C-1'''), 72.3 (C-2''), 79.4 (C-4'), 81.8 (C(CH₃)₃), 85.8 (C-1'), 125.5 (C-5'), 127.5, 127.6, 128.0, 128.1, 128.2, 128.5, 128.5, 128.6 (aryl-C), 128.6 (C-6), 133.5 (C-6), 135.1, 136.3, 138.1 (C-3'', C-2''', C-2''), 150.9 (C-2), 153.4 (Boc-C=O), 156.3 (Cbz-C=O), 163.1 (C-4), 164.0 ppm (ester-C=O); IR (ATR): $\tilde{\nu}=1704, 1648, 1452, 1250, 1151, 1065, 1027, 774, 736, 698$ cm⁻¹; UV (MeCN): λ_{\max} (log ϵ)=206 (4.53), 260 nm (4.03); HRMS (ESI) calcd for C₄₀H₄₄N₄NaO₁₀: 763.2955; found: 763.2953 [M+Na]⁺.

6'-N-Boc-3-N-BOM-3'-azido-3'-deoxy-(S)-thymidiny amino acid benzyl ester (S)-10: The reaction was performed under strict exclusion of oxygen. Nitrogen was bubbled through a solution of olefin **8** (*Z/E* 93:7, 950 mg, 1.50 mmol) in MeOH (50 mL) for 15 min. Subsequently, the catalyst (*S,S*)-Me-DuPHOS-Rh (19 mg, 32 μ mol) was added and the reaction was stirred for three days at RT under a hydrogen atmosphere (1 bar). A further portion of the catalyst (19 mg, 32 μ mol) was added and the reaction was stirred further under a hydrogen atmosphere (1 bar) at RT for four days. Silica

(approx. 1/3 of the solvent volume) was added to the solution and the solvent was removed under reduced pressure. The resultant crude product was purified by column chromatography (3:2 *iso*-hexanes-EtOAc) to give (*S*)-**10** as a colorless foam (800 mg, 84%, diastereomeric mixture 6'*S*/6'*R* 85:15). As described before,^[14,15a,b] the stereochemical assignment (6'*S*/6'*R*) was based on the catalyst-controlled nature of the reaction and on an X-ray crystal structure of a nucleosyl amino acid derivative.^[15b] (*S*)-**10**: TLC $R_f=0.62$ (1:1 *iso*-hexanes-EtOAc); ¹H NMR (300 MHz, C₆D₆, 70 °C): $\delta=1.39$ (s, 9H, C(CH₃)₃), 1.68 (ddd, $J=13.8, 8.0, 6.0$ Hz, 1H, 2'-H₃), 1.76–1.84 (m, 2H, 2'-H_b, 5'-H₃), 1.88 (d, $J=1.1$ Hz, 3H, 7-H), 2.01 (ddd, $J=14.4, 6.6, 4.0$ Hz, 1H, 5'-H_b), 3.28 (ddd, $J=7.4, 6.0, 6.0$ Hz, 1H, 3'-H), 3.64 (ddd, $J=8.7, 6.2, 4.0$ Hz, 1H, 4'-H), 4.50–4.58 (m, 1H, 6'-H), 4.70 (s, 2H, 2''-H), 4.90 (d, $J=12.3$ Hz, 1H, 1'''-H₃), 4.93 (d, $J=12.3$ Hz, 1H, 1'''-H_b), 5.11 (d, $J=7.4$ Hz, 1H, 6'-NH), 5.51 (s, 2H, 1''-H), 5.68 (dd, $J=6.0, 6.0$ Hz, 1H, 1'-H), 6.75 (brs, 1H, 6-H), 7.00–7.13 (m, 8H, aryl-H), 7.31–7.34 ppm (m, 2H, aryl-H); ¹³C NMR (126 MHz, C₆D₆, 70 °C): $\delta=12.6$ (C-7), 28.0 (C(CH₃)₃), 35.6 (C-5'), 36.4 (C-2'), 51.1 (C-6'), 62.8 (C-3'), 66.8 (C-1'''), 70.6 (C-1''), 72.2 (C-2''), 79.6 (C(CH₃)₃), 80.1 (C-4'), 85.9 (C-1'), 110.1 (C-5), 133.7 (C-6), 127.1, 127.9, 127.9, 128.0, 128.2, 128.3 (aryl-C), 135.4 (C-3''), 138.7 (C-2'''), 150.4 (Boc-C=O), 154.9 (C-2), 162.5 (C-4), 171.1 ppm (ester-C=O); IR (KBr): $\tilde{\nu}=2101, 1704, 1652, 1452, 1250, 1156, 1070, 774, 736, 698$ cm⁻¹; UV (MeCN): λ_{\max} (log ϵ)=206 (4.65), 266 nm (4.19); HRMS (ESI) calcd for C₃₂H₃₇N₆O₈: 633.2678; found: 633.2675 [M-H]⁻.

6'-N-Boc-3-N-BOM-3'-azido-3'-deoxy-(R)-thymidiny amino acid benzyl ester (R)-10: The synthesis of (*R*)-**10** was performed according to the procedure for the synthesis of (*S*)-**10** with olefin **8** (*Z/E* 93:7, 950 mg, 1.50 mmol), (*R,R*)-Me-DuPHOS-Rh (38 mg, 64 μ mol), MeOH (50 mL), and a reaction time of 14 days to give (*R*)-**10** as a colorless foam (541 mg, 54%, diastereomeric mixture 6'*R*/6'*S* 95:5). As described before,^[14,15a,b] the stereochemical assignment (6'*S*/6'*R*) was based on the catalyst-controlled nature of the reaction and on an X-ray crystal structure of a nucleosyl amino acid derivative.^[15b] (*R*)-**10**: TLC: $R_f=0.62$ (1:1 *iso*-hexanes-EtOAc); ¹H NMR (300 MHz, C₆D₆, 70 °C): $\delta=1.39$ (s, 9H, C(CH₃)₃), 1.72–1.85 (m, 3H, 2'-H₃, 2'-H_b, 5'-H₃), 1.78 (d, $J=1.2$ Hz, 3H, 7-H), 1.86–1.95 (m, 1H, 5'-H_b), 3.27–3.34 (m, 1H, 3'-H), 3.61 (ddd, $J=9.4, 6.4, 3.2$ Hz, 1H, 4'-H), 4.50–4.58 (m, 1H, 6'-H), 4.70 (s, 2H, 2''-H), 4.89 (d, $J=12.3$ Hz, 1H, 1'''-H₃), 5.00 (d, $J=12.3$ Hz, 1H, 1'''-H_b), 5.01–5.06 (m, 1H, 6'-NH), 5.44 (dd, $J=6.8, 5.4$ Hz, 1H, 1'-H), 5.45 (d, $J=9.3$ Hz, 2H, 1''-H₃), 5.50 (d, $J=9.3$ Hz, 2H, 1''-H_b), 6.44–6.47 (m, 1H, 6-H), 7.02–7.16 (m, 8H, aryl-H), 7.31–7.34 ppm (m, 2H, aryl-H); ¹³C NMR (126 MHz, C₆D₆, 70 °C): $\delta=12.7$ (C-7), 28.0 (C(CH₃)₃), 35.5 (C-5'), 36.4 (C-2'), 51.8 (C-6'), 63.1 (C-3'), 66.8 (C-1'''), 70.6 (C-1''), 72.2 (C-2''), 79.5 (C(CH₃)₃), 80.5 (C-4'), 86.8 (C-1'), 109.8 (C-5), 127.2, 127.3, 127.7, 128.0, 128.1, 128.3 (aryl-C), 133.9 (C-6), 135.6 (C-3''), 138.7 (C-2'''), 150.3 (Boc-C=O), 155.1 (C-2), 162.4 (C-4), 171.3 ppm (ester-C=O); IR (ATR): $\tilde{\nu}=2101, 1704, 1652, 1455, 1270, 1250, 1156, 1075, 736, 698$ cm⁻¹; UV (MeCN): λ_{\max} (log ϵ)=267 nm (3.99); HRMS (ESI) calcd for C₃₂H₃₇N₆O₈: 633.2678; found: 633.2679 [M-H]⁻.

6'-N-Boc-3-N-BOM-3'-N-Cbz-amino-3'-deoxy-(S)-thymidiny amino acid benzyl ester (S)-11: The reaction was performed under strict exclusion of oxygen. Nitrogen was bubbled through a solution of olefin **9** (*Z/E* 91:9, 1.00 g, 1.35 mmol) in MeOH (49 mL) for 15 min. Subsequently, the catalyst (*S,S*)-Me-DuPHOS-Rh (16 mg, 27 μ mol) was added and the reaction was stirred for four days at RT under a hydrogen atmosphere (1 bar). Silica (approx. 1/3 of the solvent volume) was added to the solution and the solvent was removed under reduced pressure. The resultant crude product was purified by column chromatography (3:2 *iso*-hexanes-EtOAc) to give (*S*)-**11** as a colorless foam (918 mg, 92%, diastereomeric mixture 6'*S*/6'*R* 91:9). The diastereomers were separated by preparative chiral

HPLC to give the pure (6'*S*)-diastereomer (S)-11 (900 mg from 1.00 g of diastereomeric mixture, obtained from several reactions). As described before,^[14,15a,b] the stereochemical assignment (6'*S*/6'*R*) was based on the catalyst-controlled nature of the reaction and on an X-ray crystal structure of a nucleosyl amino acid derivative.^[15b] (S)-11: M.p. 69 °C; TLC: R_f = 0.31 (3:2 *iso*-hexanes-EtOAc); HPLC (analytical): t_R = 30.5 min; HPLC (preparative): t_R = 32.0 min; $[\alpha]_D^{20}$ = +34.4 (c 1.1, CHCl₃); ¹H NMR (500 MHz, C₆D₆, 50 °C): δ = 1.39 (s, 9H, C(CH₃)₃), 1.68 (ddd, J = 13.9, 6.9, 6.9 Hz, 1H, 2'-H_a), 1.74 (ddd, J = 13.9, 8.4, 5.9 Hz, 1H, 2'-H_b), 1.88 (s, 3H, 7-H), 1.95 (ddd, J = 14.4, 7.3, 7.2 Hz, 1H, 5'-H_a), 2.17–2.26 (m, 1H, 5'-H_b), 3.59 (ddd, J = 7.3, 4.2, 4.2 Hz, 1H, 4'-H), 3.83–3.94 (m, 1H, 3'-H), 4.63–4.75 (m, 1H, 6'-H), 4.71 (s, 2H, 1''-H), 4.91 (d, J = 12.5 Hz, 1H, 1'''-H_a), 4.95 (d, J = 12.5 Hz, 1H, 1'''-H_b), 5.01 (d, J = 12.3 Hz, 1H, 1''-H), 5.06 (d, J = 12.3 Hz, 1H, Bn-CH₂), 5.41–5.49 (m, 1H, 6'-NH), 5.51 (s, 2H, 2''-H), 5.97 (dd, J = 5.9, 5.9 Hz, 1H, 1'-H), 6.93 (brs, 1H, 6-H), 6.99–7.19 (m, 11H, aryl-H), 7.23–7.27 (m, 2H, aryl-H), 7.33–7.37 ppm (m, 2H, aryl-H); ¹³C NMR (126 MHz, C₆D₆, 50 °C): δ = 12.8 (C-7), 28.0 (C(CH₃)₃), 35.6 (C-5'), 37.3 (C-2'), 51.2 (C-6'), 54.1 (C-3'), 66.8 (C-1'''), 70.6 (C-1''), 72.1 (C-2''), 79.5 (C(CH₃)₃), 80.8 (C-4'), 84.7 (C-1'), 110.3 (C-5), 127.2, 127.5, 127.7, 127.9, 128.0, 128.1, 128.1, 128.3, 128.4 (aryl-C), 133.4 (C-6), 135.6, 136.7, 138.7 (C-3'', C-2''', C-2'''), 150.7 (C-2), 155.2 (Boc-C=O), 155.7 (Cbz-C=O), 162.7 (C-4), 171.5 ppm (ester-C=O); IR (ATR): $\tilde{\nu}$ = 1709, 1647, 1528, 1270, 1237, 1212, 1161, 1022, 736, 693 cm⁻¹; UV (MeCN): λ_{max} (log ϵ) = 206 (4.66), 261 nm (4.27); HRMS (ESI) calcd for C₄₀H₄₅N₄O₁₀: 741.3141; found: 741.3144 [M-H]⁻.

6'-N-Boc-3-N-BOM-3'-N-Cbz-amino-3'-deoxy-(R)-thymidinyl amino acid benzyl ester (R)-11: The synthesis of (R)-11 was performed according to the procedure for the synthesis of (S)-11 with olefin **9** (*Z/E* 91:9, 300 mg, 0.405 mmol), (R,R)-Me-DuPHOS-Rh (10 mg, 16 μ mol), MeOH (15 mL), and a reaction time of 14 days to give (R)-11 as a colorless foam (220 mg, 73%, diastereomeric mixture 6'*R*/6'*S* 88:12). The diastereomers were separated by preparative chiral HPLC to give the pure (6'*R*)-diastereomer (R)-11 (370 mg from 430 mg of diastereomeric mixture, obtained from several reactions). As described before,^[14,15a,b] the stereochemical assignment (6'*S*/6'*R*) was based on the catalyst-controlled nature of the reaction and on an X-ray crystal structure of a nucleosyl amino acid derivative.^[15b] (R)-11: M.p. 64 °C; TLC: R_f = 0.31 (3:2 *iso*-hexanes-EtOAc); HPLC (analytical): t_R = 37.5 min; HPLC (preparative): t_R = 39.0 min; $[\alpha]_D^{20}$ = +39.1 (c 0.87, CHCl₃); ¹H NMR (500 MHz, C₆D₆, 50 °C): δ = 1.38 (s, 9H, C(CH₃)₃), 1.60–1.69 (m, 1H, 2'-H_a), 1.70–1.80 (m, 1H, 2'-H_b), 1.76 (s, 3H, 7-H), 1.88–2.00 (m, 1H, 5'-H_a), 2.00–2.09 (m, 1H, 5'-H_b), 3.52–3.59 (m, 1H, 4'-H), 3.77–3.87 (m, 1H, 3'-H), 4.60–4.70 (m, 1H, 6'-H), 4.71 (s, 2H, 1''-H), 4.89 (d, J = 12.2 Hz, 1H, 1'''-H_a), 4.97–5.04 (m, 1H, 1'''-H_b), 5.01 (d, J = 12.5 Hz, 1H, 1''-H_a), 5.06 (d, J = 12.5 Hz, 1H, 1''-H_b), 5.19–5.29 (m, 1H, 6'-NH), 5.48 (d, J = 9.5 Hz, 1H, 2''-H_a), 5.51 (d, J = 9.5 Hz, 1H, 2''-H_b), 5.75–5.85 (m, 1H, 1'-H), 6.93 (brs, 1H, 6-H), 7.00–7.19 (m, 11H, aryl-H), 7.23–7.27 (m, 2H, aryl-H), 7.33–7.37 ppm (m, 2H, aryl-H); ¹³C NMR (126 MHz, C₆D₆, 50 °C): δ = 12.9 (C-7), 28.0 (C(CH₃)₃), 35.7 (C-5'), 37.3 (C-2'), 52.0 (C-6'), 54.5 (C-3'), 66.7 (C-1'''), 70.6 (C-1''), 72.1 (C-2''), 79.5 (C(CH₃)₃), 80.9 (C-4'), 85.3 (C-1'), 110.1 (C-5), 127.3, 127.5, 127.7, 127.9, 128.1, 128.1, 128.2, 128.4, 128.4 (aryl-C), 133.2 (C-6), 135.8, 136.6, 138.7 (C-3'', C-2''', C-2'''), 150.6 (C-2), 155.4 (Boc-C=O), 155.6 (Cbz-C=O), 162.6 (C-4), 171.8 ppm (ester-C=O); IR (ATR): $\tilde{\nu}$ = 1700, 1642, 1452, 1255, 1156, 1075, 1022, 736, 698 cm⁻¹; UV (MeCN): λ_{max} (log ϵ) = 204 (4.60), 266 nm (3.94); HRMS (ESI) calcd for C₄₀H₄₅N₄O₁₀: 741.3141; found: 741.3139 [M-H]⁻.

Synthesis of oligonucleotide analogues **1a** and **1b**

The synthesis of fully cationic oligonucleotide analogues was performed manually on NovaSyn®TGR resin (Merck KGaA) according

to standard Fmoc-based solid-phase peptide synthesis (SPPS).^[19] The building blocks were coupled using three equivalents of Fmoc-protected building blocks relative to the initial Fmoc loading of the resin. The building blocks were mixed with three equivalents of benzotriazol-1-yl-oxy-tris-pyrrolidino-phosphonium hexafluorophosphate (PyBOP) and six equivalents of *N,N*-diisopropylethylamine (DIPEA) in *N*-methyl-2-pyrrolidone (NMP), and twice incubated with the resin for 1 h. Fmoc deprotection was performed with 25% piperidine in NMP for 15 min. After each double-coupling step, unreacted amines were blocked with NMP/DIPEA/acetic anhydride (10:1:1; capping solution) for 10 min. For the final *N*-terminal modification, the fully cationic oligonucleotide analogues were deprotected as mentioned above, and reacted twice for 10 min with capping solution for acetylation. The fully cationic oligonucleotide analogues were finally cleaved from the resin applying TFA/water/1,2-ethanedithiol/triisopropylsilane (94:2.5:2.5:1) for 4 h, and precipitated with Et₂O at -20 °C. After this final cleavage, crude products were dissolved in water/MeCN (7:3) and purified by RP-HPLC using a Nucleodur C18 reverse-phase column (10 × 125 mm, 110 Å, particle size 5 μ m, Macherey-Nagel; solvent A: water + 0.1% TFA, solvent B: MeCN + 0.1% TFA; flow rate: 6 mL min⁻¹). The thus-obtained pure product fractions were combined, frozen in liquid nitrogen, and lyophilized with a Heto PowerDry™ LL1500 freeze-drying system (Thermo Scientific). Analytical data of oligonucleotide analogues **1a** and **1b** are given in Table S1 and Figure S1 (Supporting Information).

Melting temperature experiments

Melting temperatures (T_m values) were determined in phosphate buffer at pH 7.4 (10 mM NaH₂PO₄) with varying NaCl concentrations (50 mM, 75 mM, 100 mM, 125 mM). The final oligonucleotide duplex concentration was 1 μ M. Prior to the measurement, the samples were heated to 90 °C for 2 min and subsequently cooled to 20 °C. Afterwards, the changes in absorption at λ = 260 nm were detected with a CARY-100 Bio UV/Vis Spectrophotometer (Varian), applying a temperature increase from 20 °C to 90 °C and a temperature decrease from 90 °C to 20 °C four times each with a heating rate of 1.0 °C min⁻¹, respectively, and a data interval of 0.5 °C (bandwidth: 1.0 nm). The T_m values correspond to the maximum of the first derivation of the melting curves and are the average of at least three measurements.

CD spectroscopy

CD spectra were recorded with a J-715 CD spectrometer (Jasco) and a quartz cuvette (path length: 0.1 cm; Hellma). The samples were dissolved in a buffer composed of 10 mM NaH₂PO₄ and 100 mM NaCl (pH 7.4) to a final concentration of 20 μ M. Five CD spectra between wavelengths of λ = 190 and 320 nm were recorded in continuous scanning mode at 20 °C and averaged (sensitivity: 10 mdeg, resolution: 1.0 nm, response: 1.0 s, bandwidth: 1.0 nm, scanning speed: 50 nm min⁻¹). Background correction was performed prior to data evaluation and the CD spectra were smoothed by applying an FFT filter. CD data are presented as the mean residual ellipticity (Θ) in degrees cm² dmol⁻¹.

Acknowledgements

We thank the group of Prof. Roland Winter (TU Dortmund) for access to their CD spectrometer and the Deutsche Forschungsgemeinschaft (DFG, grant DU 1095/2-1, Emmy Noether program GR 3592/2-1) as well as the Fonds der Chemischen Indus-

trie (FCI, Sachkostenzuschuss) for financial support. B.S. is grateful for a doctoral fellowship of the Studienstiftung des deutschen Volkes. This work was supported by AstraZeneca, Bayer CropScience, Bayer HealthCare, Boehringer Ingelheim, Merck KGaA, and the Max Planck Society.

Conflict of interest

The authors declare no conflict of interest.

Keywords: backbone modifications · DNA · oligonucleotides · peptides · stereoselective synthesis

- [1] V. K. Sharma, P. Rungta, A. K. Prasad, *RSC Adv.* **2014**, *4*, 16618–16631.
- [2] F. H. Westheimer, *Science* **1987**, *235*, 1173–1178.
- [3] a) A. J. A. Cobb, *Org. Biomol. Chem.* **2007**, *5*, 3260–3275; b) G. F. Deleavy, M. J. Damha, *Chem. Biol.* **2012**, *19*, 937–954.
- [4] a) J. Lebreton, A. De Mesmaeker, A. Waldner, V. Fritsch, R. M. Wolf, S. M. Freier, *Tetrahedron Lett.* **1993**, *34*, 6383–6386; b) A. De Mesmaeker, A. Waldner, J. Lebreton, P. Hoffmann, V. Fritsch, R. M. Wolf, S. M. Freier, *Synlett* **1993**, 733–736; c) A. De Mesmaeker, A. Waldner, J. Lebreton, P. Hoffmann, V. Fritsch, R. M. Wolf, S. M. Freier, *Angew. Chem. Int. Ed. Engl.* **1994**, *33*, 226–229; *Angew. Chem.* **1994**, *106*, 237–240; d) C. Selvam, S. Thomas, J. Abbott, S. D. Kennedy, E. Rozners, *Angew. Chem. Int. Ed.* **2011**, *50*, 2068–2070; *Angew. Chem.* **2011**, *123*, 2116–2118; e) P. Tanui, S. D. Kennedy, B. D. Lunstad, A. Haas, D. Leake, E. Rozners, *Org. Biomol. Chem.* **2014**, *12*, 1207–1210; f) D. Mutisya, C. Selvam, B. D. Lunstad, P. S. Pallan, A. Haas, D. Leake, M. Egli, E. Rozners, *Nucleic Acids Res.* **2014**, *42*, 6542–6551.
- [5] Z. Huang, S. A. Benner, *J. Org. Chem.* **2002**, *67*, 3996–4013.
- [6] a) A. H. El-Sagheer, T. Brown, *J. Am. Chem. Soc.* **2009**, *131*, 3958–3964; b) A. H. El-Sagheer, A. P. Sanzone, R. Gao, A. Tavassoli, T. Brown, *Proc. Natl. Acad. Sci. USA* **2011**, *108*, 11338–11343; c) A. P. Sanzone, A. H. El-Sagheer, T. Brown, A. Tavassoli, *Nucleic Acids Res.* **2012**, *40*, 10567–10575; d) C. N. Birts, A. P. Sanzone, A. H. El-Sagheer, J. P. Blaydes, T. Brown, A. Tavassoli, *Angew. Chem. Int. Ed.* **2014**, *53*, 2362–2365; *Angew. Chem.* **2014**, *126*, 2394–2397; e) M. Kukwikila, N. Gale, A. H. El-Sagheer, T. Brown, A. Tavassoli, *Nat. Chem.* **2017**, *9*, 1089–1098.
- [7] a) P. E. Nielsen, M. Egholm, R. H. Berg, O. Buchardt, *Science* **1991**, *254*, 1497–1500; b) Z. V. Zhilina, A. J. Ziemba, S. W. Ebbinghaus, *Curr. Top. Med. Chem.* **2005**, *5*, 1119–1131.
- [8] a) J. K. Strauss, C. Roberts, M. G. Nelson, C. Switzer, L. J. Maher III, *Proc. Natl. Acad. Sci. USA* **1996**, *93*, 9515–9520; b) T. P. Prakash, A. M. Kawasaki, E. A. Lesnik, N. Sioufi, M. Manoharan, *Tetrahedron* **2003**, *59*, 7413–7422; c) M. Prhavic, T. P. Prakash, G. Minasov, P. D. Cook, M. Egli, M. Manoharan, *Org. Lett.* **2003**, *5*, 2017–2020; d) S. Milton, D. Honcharenko, C. S. J. Rocha, P. M. D. Moreno, C. I. E. Smith, R. Strömberg, *Chem. Commun.* **2015**, *51*, 4044–4047.
- [9] R. Brock, *Bioconjugate Chem.* **2014**, *25*, 863–868.
- [10] M. L. Jain, P. Y. Bruice, I. E. Szabo, T. C. Bruice, *Chem. Rev.* **2012**, *112*, 1284–1309.
- [11] a) A. Blaskó, R. O. Dempcy, E. E. Minyat, T. C. Bruice, *J. Am. Chem. Soc.* **1996**, *118*, 7892–7899; b) D. A. Barawkar, T. C. Bruice, *Proc. Natl. Acad. Sci. USA* **1998**, *95*, 11047–11052; c) B. A. Linkletter, I. E. Szabo, T. C. Bruice, *J. Am. Chem. Soc.* **1999**, *121*, 3888–3896; d) H. Challa, T. C. Bruice, *Bioorg. Med. Chem. Lett.* **2001**, *11*, 2423–2427.
- [12] D. P. Arya, T. C. Bruice, *J. Am. Chem. Soc.* **1998**, *120*, 6619–6620.
- [13] R. L. Letsinger, C. N. Singman, G. Hstand, M. Salunkhe, *J. Am. Chem. Soc.* **1988**, *110*, 4470–4471.
- [14] a) B. Schmidtgal, A. P. Spork, F. Wachowius, C. Höbartner, C. Ducho, *Chem. Commun.* **2014**, *50*, 13742–13745; b) B. Schmidtgal, C. Höbartner, C. Ducho, *Beilstein J. Org. Chem.* **2015**, *11*, 50–60.
- [15] a) A. P. Spork, C. Ducho, *Org. Biomol. Chem.* **2010**, *8*, 2323–2326; b) A. P. Spork, D. Wiegmann, M. Granitzka, D. Stalke, C. Ducho, *J. Org. Chem.* **2011**, *76*, 10083–10098; c) A. P. Spork, M. Büschleb, O. Ries, D. Wiegmann, S. Boettcher, A. Mihalyi, T. D. H. Bugg, C. Ducho, *Chem. Eur. J.* **2014**, *20*, 15292–15297; d) D. Wiegmann, S. Koppermann, M. Wirth, G. Niro, K. Leyerer, C. Ducho, *Beilstein J. Org. Chem.* **2016**, *12*, 769–795.
- [16] a) M. J. Burk, *J. Am. Chem. Soc.* **1991**, *113*, 8518–8519; b) T. Masquelin, E. Broger, K. Müller, R. Schmid, D. Obrecht, *Helv. Chim. Acta* **1994**, *77*, 1395–1411; c) C. Ducho, R. B. Hamed, E. T. Batchelar, J. L. Sorensen, B. Odell, C. J. Schofield, *Org. Biomol. Chem.* **2009**, *7*, 2770–2779.
- [17] a) Y. Mitsuoka, T. Kodama, R. Ohnishi, Y. Hari, T. Imanishi, S. Obika, *Nucleic Acids Res.* **2009**, *37*, 1225–1238; b) A. I. S. Holm, L. Munksgaard Nielsen, S. Vronning Hoffmann, S. Brøndsted Nielsen, *Phys. Chem. Chem. Phys.* **2010**, *12*, 9581–9596.
- [18] R. Mazurkiewicz, A. Kuźnik, M. Grymel, N. H. Kuźnik, *Magn. Reson. Chem.* **2005**, *43*, 36–40.
- [19] Y. W. Kim, T. N. Grossmann, G. L. Verdine, *Nat. Protoc.* **2011**, *6*, 761–771.

Manuscript received: September 14, 2017

Accepted manuscript online: October 19, 2017

Version of record online: December 27, 2017

C. Towards Zwitterionic Oligonucleotides with Improved Properties: the NAA/LNA-Gapmer Approach

Manuscript C

The contributions of each author to Manuscript C "Towards Zwitterionic Oligonucleotides with Improved Properties: the NAA/LNA-Gapmer Approach" are listed below:

Melissa Wojtyniak (née Meng): She planned, carried out, analyzed and validated most of the experimental work described in this publication. She re-synthesized the dimeric CxT-building block and prepared the NAA/LNA-gapmer as well as the DNA/LNA control gapmer. She prepared and performed the UV-Vis-monitored melting studies, the CD spectroscopy, the biological stability assays and the ³²P-labelled RNase H assay. Finally, she conceived and wrote the manuscript.

Boris Schmidtgall: He mainly established the synthetic route for the synthesis of the CxT-building block.

Philine Kirsch: She helped to establish the synthesis of the CxT-building block.

Christian Ducho: He was responsible for the project design, supervision and administration and reviewed and edited the manuscript.

This is an open access article under the terms of the Creative Commons Attribution Non-Commercial NoDerivs License, which permits use and distribution in any medium, provided the original work is properly cited, the use is non-commercial and no modifications or adaptations are made.

© 2020 The Authors. Published by Wiley-VCH GmbH.

M. Wojtyniak, B. Schmidtgall, P. Kirsch, C. Ducho, *ChemBioChem*. **2020**, *21*, 3234-3243.

DOI: 10.1002/cbic.202000450



Towards Zwitterionic Oligonucleotides with Improved Properties: the NAA/LNA-Gapmer Approach

Melissa Wojtyniak,^[a] Boris Schmidtgall,^[b] Philine Kirsch,^[a] and Christian Ducho^{*[a, b]}

In memory of Professor Thomas C. Bruice (1925–2019).

Oligonucleotides (ON) are promising therapeutic candidates, for instance by blocking endogenous mRNA (antisense mechanism). However, ON usually require structural modifications of the native nucleic acid backbone to ensure satisfying pharmacokinetic properties. One such strategy to design novel antisense oligonucleotides is to replace native phosphate diester units by positively charged artificial linkages, thus leading to (partially) zwitterionic backbone structures. Herein, we report a “gapmer” architecture comprised of one zwitterionic central segment (“gap”) containing nucleosyl amino acid

(NAA) modifications and two outer segments of locked nucleic acid (LNA). This NAA/LNA-gapmer approach furnished a partially zwitterionic ON with optimised properties: i) the formation of stable ON-RNA duplexes with base-pairing fidelity and superior target selectivity at 37 °C; and ii) excellent stability in complex biological media. Overall, the NAA/LNA-gapmer approach is thus established as a strategy to design partially zwitterionic ON for the future development of novel antisense agents.

Introduction

Oligonucleotides (ON) represent attractive candidates for novel therapeutic agents due to their unique binding mode, that is, hybridisation with complementary endogenous nucleic acids. Hence, they enable interference with protein biosynthesis through several modes of action: i) the antisense mechanism;^[1] ii) the antigene mechanism;^[2] and iii) the RNA interference mechanism.^[3] These unique interaction pathways have already been proven to be clinically useful. For instance, fomivirsen, an antiviral antisense oligonucleotide used against cytomegalovirus retinitis, was approved by the FDA as the very first antisense drug on the market in 1998.^[4a] In the following years, a few other ON were approved for clinical use, such as mipomersen for the treatment of familial hypercholesterolemia,^[4b] nusinersen against spinal muscular atrophy^[4c] and eteplirsen to treat Duchenne muscular dystrophy.^[4d] However, the development of ON into pharmaceuticals is significantly hampered due to several characteristics of their phosphate diester backbone. First, its dense negative charge results in restrained cell permeability. Second, the native phosphate diester linkage is labile towards nuclease-mediated hydrolysis.

In order to overcome these hurdles, a large toolbox of various backbone modifications has been established over the past decades. According artificial backbone structures can be: i) the sole substitution of single atoms within the phosphate diester unit, for example, methylphosphonates^[5] or the broadly used phosphorothioates;^[6] ii) replacement of the phosphate diester with electroneutral groups, for instance with amides^[7] or sulfones;^[8] iii) a complete replacement of the native sugar-phosphate backbone, such as in peptide nucleic acids (PNA).^[9]

Furthermore, modifications of the (2'-deoxy)ribose units can also furnish improved properties of ON analogues. For instance, Wengel and co-workers have developed unnatural locked nucleic acids (LNA) to alter the native ON characteristics (Figure 1A).^[10] The LNA modification is characterised by an additional bridging bond, linking the 2'-oxygen of the ribose with the 4'-position, thus locking it in the 3'-endo conformation. Insertion of this rigid sugar significantly increases binding affinity towards RNA, due to a reduced entropic penalty upon hybridisation. In addition, the LNA modification was shown to significantly enhance stability against nuclease-mediated degradation, thereby improving the overall stability in biological media. As a result, LNA-modified ON have found pronounced attention as potential biomedical agents.^[10c] Yet, the improved affinity for duplex formation was also shown to be accompanied by limited sensitivity towards base mismatches and thus, by decreased binding selectivity. Furthermore, the high melting temperatures of LNA-ON in complex with their RNA targets have been shown to be correlated to increased cytotoxicity resulting from elevated off-target effects, as well as increased hepatotoxic risks.^[11a] To elucidate this toxic potential, Dieckmann et al. have developed an *in vitro* approach to evaluate the hybridisation-dependent toxicity of high-affinity ON, which confirmed a correlation of high melting temperatures (T_m values) and undesired toxic effects.^[11b]

[a] M. Wojtyniak, P. Kirsch, Prof. Dr. C. Ducho
Department of Pharmacy, Pharmaceutical and Medicinal Chemistry, Saarland University
Campus C2 3, 66123 Saarbrücken (Germany)
E-mail: christian.ducho@uni-saarland.de

[b] Dr. B. Schmidtgall, Prof. Dr. C. Ducho
Department of Chemistry, University of Paderborn
Warburger Str. 100, 33098 Paderborn (Germany)

Supporting information for this article is available on the WWW under <https://doi.org/10.1002/cbic.202000450>

© 2020 The Authors. Published by Wiley-VCH GmbH. This is an open access article under the terms of the Creative Commons Attribution Non-Commercial NoDerivs License, which permits use and distribution in any medium, provided the original work is properly cited, the use is non-commercial and no modifications or adaptations are made.

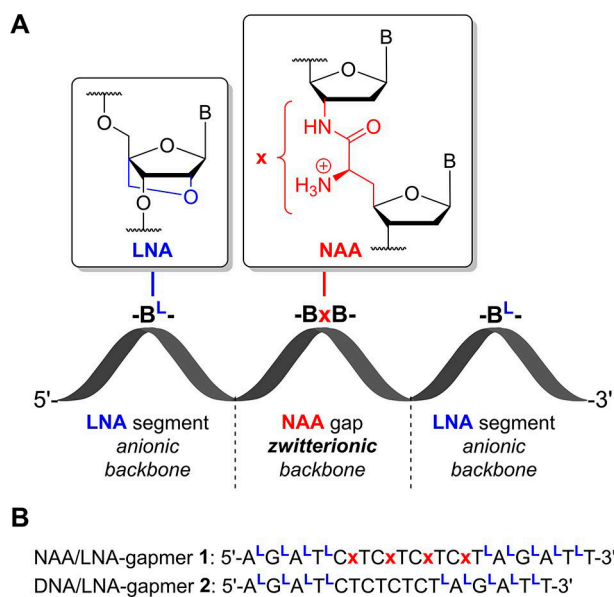


Figure 1. A) Schematic representation of the NAA/LNA-gapmer approach. B = nucleobase, ^L = LNA-modification, x = NAA-modification. B) Sequences of novel NAA/LNA-gapmer 1 and DNA/LNA-gapmer 2 (as reference ON). All unlabelled linkages are native phosphate diesters.

An alternative strategy in the development of backbone-modified ON involves the replacement of the anionic phosphate diester unit with artificial, positively charged linkers, thus creating an either partially zwitterionic^[12] or fully cationic^[13] ON. This approach significantly differs from the introduction of positive charges by modification of the 2'-hydroxy groups (in RNA) or nucleobases, while leaving the phosphate diester backbone unchanged. Such strategies also afford zwitterionic structures, but result in densely charged oligonucleotides.^[14] In contrast, cationic replacements of the anionic phosphate diester enable the synthesis of artificial ON with a reduced net charge due to the compensation for adjacent phosphates. This substitution has been shown to have a positive effect on the ability to penetrate biological barriers such as cellular membranes.^[15] So far, four suitable types of unnatural cationic linkers have been reported: i) Letsinger's phosphoramidate linkages^[16] that carry a positively charged head group connected to the phosphate by an alkyl chain; ii) the guanidine^[17] and iii) 5-methylthiourea^[18] modifications, both first described by Bruice et al.; and the iv) nucleosyl amino acid (NAA) modification (Figure 1A), an amide-derived cationic backbone motif previously reported by our group.^[12,13b,c,19]

The NAA internucleoside structure has been formally derived from the "high-carbon" nucleoside core unit of naturally occurring muraymycin antibiotics and their synthetic analogues.^[12,20] In terms of conformational flexibility, the NAA-linkage is somewhat intermediate to the rather flexible phosphoramidates and the rigid guanidines and 5-methylthioureas. Its peptide-like structure features a primary amino group carrying a positive charge at physiological pH. This unit can be attached with a specific spatial orientation, that is, with stereoselectivity at the 6'-position of the adjacent "high-carbon"

nucleoside.^[12,13b,c] Partially zwitterionic ON including up to four NAA-modifications in an otherwise anionic (i.e., phosphate-based) backbone had previously been proven to form stable helical duplexes with complementary DNA. They were also shown to preserve excellent base-pairing fidelity, as demonstrated by decreasing melting temperatures due to base mismatches in the DNA counterstrand. For hybrid duplexes of NAA-containing DNA-ON with RNA, however, a fairly significant loss in thermal stability was observed (ΔT_m up to $\sim 4.0^\circ\text{C}$ /modification). In this context, the 6'*S*-configured NAA linkage seemed to exert a slightly greater destabilising effect than the 6'*R*-configured congener.^[12a] The biological *in vitro* evaluation of NAA-modified DNA-ON confirmed high stability against cleavage by 3'→5'- and 5'→3'-exonucleases as well as in more complex biological media (human plasma, whole cell lysate).^[19]

For the future development of NAA-containing partially zwitterionic ON towards potential biomedical agents, one major issue was the undesired decrease in thermal stability for duplexes with complementary RNA strands (as these would represent the drug targets in antisense applications). Hence, we have envisioned to overcome this hurdle by using a "gapmer" approach,^[21] that is, a hybrid structure with different internucleoside linkages in the middle of the ON than at its ends. The overall goal was to obtain a chimeric, partially zwitterionic NAA-containing ON that exerts high affinity towards its target RNA, while still showing excellent base-pairing fidelity. LNA units facilitate the formation of thermally highly stable DNA/RNA heteroduplexes (*vide supra*). Hence, it was planned to exploit this feature for the design of according NAA-containing gapmers. We have therefore designed a partially zwitterionic gapmer-ON consisting of LNA segments at the 3'- and the 5'-ends and a block of 6'*R*-configured NAA-modified DNA filling the "gap" in the central section (Figure 1A).

In this work, we report the synthesis of the novel NAA/LNA-gapmer 1 (with a partially zwitterionic backbone) and its properties in comparison with DNA/LNA-gapmer 2 (as a reference ON with a fully anionic backbone, Figure 1B). The identical base sequence of 1 and 2 has been artificially designed in order to study the fundamental principles of a zwitterionic gapmer construct such as 1, that is, its sequence is not (yet) designed to target a specific biologically relevant RNA sequence. The choice of this sequence was based on synthetic considerations and the goal to obtain an ON containing all four canonical bases, while having a reasonable G-C content. The reported results strongly indicate that the NAA/LNA-gapmer approach is a useful strategy to design partially zwitterionic ON with improved properties.

Results

Synthesis of gapmer ON 1 and 2

It was envisioned to prepare both target ON 1 and 2 (Figure 1) by modified automated solid-phase-supported ON synthesis using phosphoramidite methodology. To synthesise the NAA/LNA-gapmer 1, a "dimeric" CxT-NAA phosphoramidite (with

6'*R*-configuration in the NAA linkage) had to be prepared.^[12] Thus, the aforementioned goal to obtain a gapmer ON with reasonable G-C content could be reached, as the only previously reported "dimeric" NAA phosphoramidites had been TxT^[12a] and AxT,^[12b] respectively (with "x" representing the NAA linkage, cf. Figure 1). The synthesis of this novel CxT-NAA phosphoramidite required the preparation of a suitably protected 3'-amino-2',3'-dideoxycytidine building block (Scheme 1). Different synthetic routes towards such a 3'-aminodeoxycytidine building block had been described before.^[22] With respect to its elegance and high stereoselectivity, our synthetic strategy was mainly based on the procedure reported by Richert and co-workers.^[22d]

Thus, 2'-deoxycytidine **3** was *N*-benzoylated at the nucleobase using a standard transient protection protocol,^[23] furnishing *N*-benzoyl-2'-deoxycytidine **4** in 96% yield (Scheme 1). In contrast to the recrystallisation procedure described by Ti et al., compound **4** was purified by column chromatography to remove excess benzoic acid. This was followed by a sequence of two Mitsunobu reactions, with the first one leading to 5'-(*p*-bromobenzoyl) protection and the second one enabling ring closure of the cytosin-2-O and C-3', to give cyclised product **5** in 39% yield. Nucleophilic substitution (S_N2) at C-3' with sodium azide then furnished 3'-azidonucleoside **6** in 66% yield. After saponification of the *p*-bromobenzoyl ester, silylation gave 5'-*O*-TBDMS-protected derivative **7** in 85% yield over two steps from **6**. Finally, reduction of the azido group by transfer hydrogenation^[24] afforded the desired protected 3'-amino-2',3'-dideoxycytidine derivative **8** in 96% yield (Scheme 1).

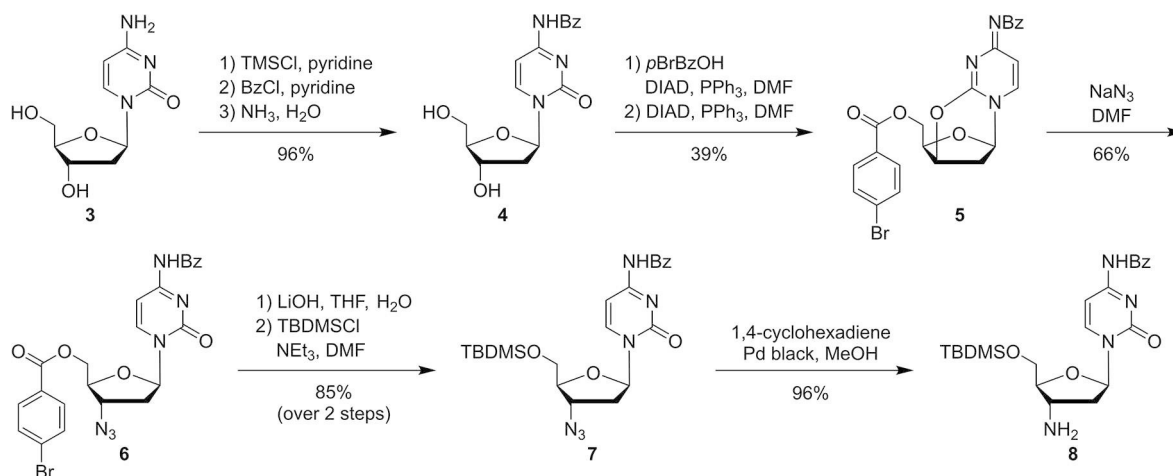
Based on our stereoselective route for the synthesis of uridine-derived nucleosyl amino acids,^[25] we had previously developed the preparation of according thymidine derivatives.^[12,13b] Hence, this reported protocol was used to prepare protected nucleosyl amino acid **9** (Scheme 2, reactions not shown).^[12] Thymidine derivative **9** underwent amide coupling with 3'-aminonucleoside **8** to furnish the bis-silylated NAA-linked C-T dimer **10** in 78% yield. Fluoride-mediated desilylation gave diol **11** in a moderate yield of 53%. Attempts

to improve this deprotection protocol for the TBDMS ethers were not successful, as changes in the reaction conditions always led to more side reactions or even complete decomposition of starting material **10**. Regioselective 5'-*O*-dimethoxytritylation afforded 5'-*O*-DMTr-protected NAA-linked dimer **12** (64% yield), which was then phosphitylated (using diamidite reagent **13**) to give the dimeric NAA-linked C-T phosphoramidite **14** in 78% yield (Scheme 2).

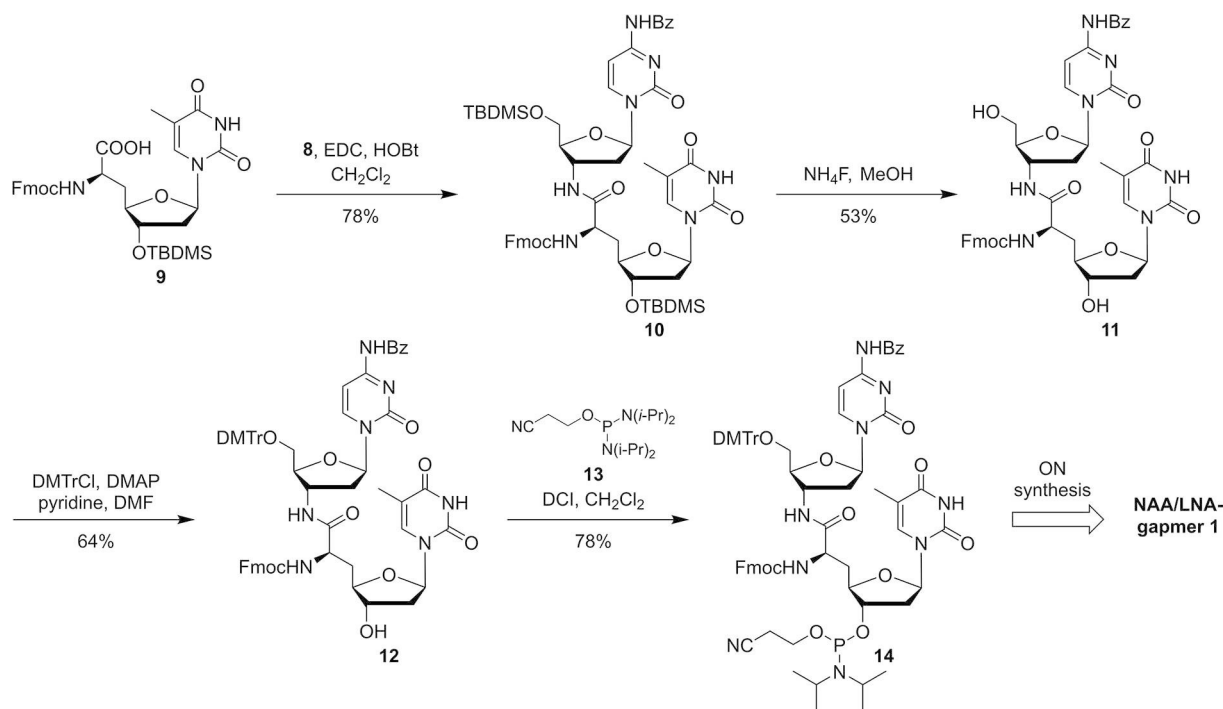
With the NAA-linked C-T phosphoramidite **14** in hand, both gapmers **1** and **2** (Figure 1) were assembled on the DNA synthesiser. Standard protocols were slightly adjusted (see the Supporting Information for details). In general, coupling times for LNA and NAA phosphoramidites were prolonged relative to their commercially available, unmodified DNA congeners, and the number of couplings was increased to enhance the step-to-step yield. With respect to the activator for phosphoramidite coupling, it was found that benzylmercaptotetrazole (BMT) was superior to 4,5-dicyanoimidazole (DCI) as it gave higher yields, in particular when the NAA-linked building block **14** was coupled. Apart from this, standard solvents and reagents for solid-phase-supported DNA synthesis and the usual basic work-up procedure were used. Purification of gapmers **1** and **2** was achieved by polyacrylamide gel electrophoresis (PAGE) with urea as chaotropic component. The identities of gapmers ON **1** and **2** were confirmed by high resolution mass spectrometry (see the Supporting Information).

NAA/LNA-gapmer **1** shows superior hybridisation properties at physiologically relevant temperature

One main goal of the reported gapmer approach was to enhance the stability of NAA-containing DNA-RNA hybrid duplexes, while retaining base-pairing fidelity. Therefore, melting temperature experiments with fully complementary strands as well as with mismatched RNA-ON **X** (base mismatch opposite of one of the LNA segments: 5'-AAUCUAGAGAGAGAG \underline{C} CU-3') and mismatched RNA-ON **Y** (base mismatch opposite of the



Scheme 1. Synthesis of the protected 3'-amino-2',3'-dideoxycytidine building block **8**.



Scheme 2. Synthesis of the "dimeric" NAA-linked C–T phosphoramidite **14** for automated ON synthesis.

central NAA gap: 5'-AAUCUAGAGGGAGAUCU-3') were performed. To eliminate the temperature dependency of the extinction coefficient ϵ , αT_m values were calculated and used to describe the melting temperature of all studied duplexes. Furthermore, $\alpha T_{37^\circ\text{C}}$ values were calculated to investigate the hybridisation at a physiologically relevant temperature of 37 °C (for more details see the Supporting Information). The obtained results are given in Table 1, with selected melting curves shown in Figure 2.

Satisfactorily, the duplex stability of the NAA/LNA-gapmer **1** (Figure 1) with fully complementary DNA was equal to the according native DNA/DNA duplex ($\alpha T_m = 48.5^\circ\text{C}$, entries 9 vs. 1, Table 1), whereas control gapmer **2** furnished an even higher value ($\Delta\alpha T_m = +4.5^\circ\text{C}$, entry 5). This was also the case for the 2-RNA duplex, for which an even stronger increase in melting temperature was observed ($\Delta\alpha T_m = +17.0^\circ\text{C}$, entry 6). This was anticipated as the LNA segments in gapmer **2** were supposed to stabilise duplexes with native RNA.^[10] However, for the hybridisation of the complementary RNA strand with NAA-

Table 1. αT_m values [°C] of native DNA (entries 1–4), DNA/LNA-gapmer **2** (entries 5–8) and NAA/LNA-gapmer **1** (entries 9–12) in complex with either complementary DNA, complementary RNA, mismatched RNA **X**, and mismatched RNA **Y**, respectively. [†] = LNA modification, **x** = NAA modification (Figure 1). All unlabelled linkages are native phosphate diesters. Mismatches in RNA-ON **X** and **Y** are highlighted in bold and underlined.

Duplex	αT_m [°C]	$\Delta\alpha T_m$ [°C] ^[a]	$\alpha T_{37^\circ\text{C}}$	$\alpha T_{37^\circ\text{C}}$ [%]	$1 - \alpha T_{37^\circ\text{C}}$ [%]	
1	DNA + DNA	48.5	–	0.97	97	3
2	DNA + RNA	55.5	–	1.00	100	0
3	DNA + X	50.0	–	0.97	97	3
4	DNA + Y	52.0	–	0.98	98	2
5	gapmer 2 + DNA	53.0	4.5	0.98	98	2
6	gapmer 2 + RNA	72.5	17.0	1.00	100	0
7	gapmer 2 + X	62.5	12.5	1.00	100	0
8	gapmer 2 + Y	68.5	16.5	1.01	100	0
9	gapmer 1 + DNA	48.5	0.0	0.96	96	4
10	gapmer 1 + RNA	49.5	–6.0	0.98	98	2
11	gapmer 1 + X	37.0	–13.0	0.51	51	49
12	gapmer 1 + Y	43.0	–9.0	0.86	86	14

[a] $\Delta\alpha T_m$ values were calculated based on the difference to native duplexes, i.e., αT_m (gapmer + counterstrand) – αT_m (native DNA + counterstrand).

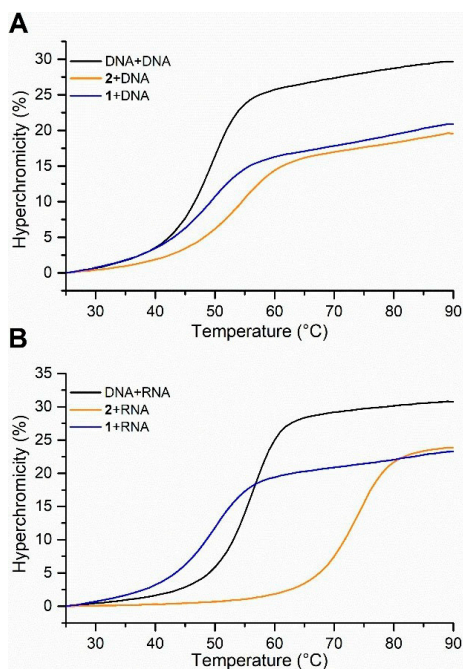


Figure 2. A) Melting curves of native DNA, DNA/LNA-gapmer 2, and NAA/LNA-gapmer 1 in complex with complementary DNA. B) Melting curves of native DNA, DNA/LNA-gapmer 2, and NAA/LNA-gapmer 1 in complex with complementary RNA. All depicted curves are the average of technical triplicates.

containing gapmer 1, this overall stabilising effect was not found. Instead, a slight decrease in the melting temperature was observed ($\Delta\alpha T_m = -6.0^\circ\text{C}$, entry 10). This decrease in duplex stability is equivalent to about -5.8°C per NAA modification (entry 10 vs. entry 6), which is similar to the previously described destabilising effect of the NAA modification on DNA-RNA hybrid duplexes ($\sim 3.5^\circ\text{C}$ per NAA modification for a comparable type of sequence).^[12a] The presence of the stabilising LNA units then limits the overall destabilisation of the 1-RNA duplex to a formal value of -1.5°C per NAA modification (entry 10 vs. entry 2). Therefore, the results obtained with ON 1 demonstrated that the gapmer architecture with two flanking LNA segments indeed furnished an improved duplex stability for hybridisation with RNA.

For a more detailed analysis of the hybridisation properties of gapmer 1, we considered the overall ratio of hybrid duplex to free single strands at physiological human body temperature (37°C), as this property is decisive for any potential *in vivo* application of antisense ON. Thus, the y values of the α -curve for $T=37^\circ\text{C}$ were determined for every thermal denaturation experiment ($\alpha T_{37^\circ\text{C}}$ values, Table 1, see also the Supporting Information for the exact procedure). These values correspond to the amount of duplex present at this given temperature and can therefore also be expressed as a percentage of hybridised (i.e., bound) ON ($\alpha T_{37^\circ\text{C}}$ values in %). Correspondingly, the term $1-\alpha T_{37^\circ\text{C}}$ provides the unbound, single-stranded ON fraction (Table 1). It was found that hybridisation of native DNA and RNA of the given sequence occurred with 100% at 37°C (entry 2, Table 1). This was also the case for the mixture of

reference gapmer 2 and complementary RNA under these conditions (entry 6). For the NAA/LNA-gapmer 1 and complementary RNA, almost quantitative (98%) hybridisation at 37°C was determined, with only $\sim 2\%$ single-stranded fraction (entry 10). This demonstrated the possibility to achieve excellent target engagement by such an NAA-containing gapmer under physiologically relevant conditions.

We then studied the base-pairing fidelity of NAA/LNA-gapmer 1, that is, its hybridisation properties with RNA-ON containing a single base mismatch. Therefore, gapmer 1 as well as both reference ON (2 and native DNA, respectively) were investigated for duplex formation with two different mismatched RNA-ON: i) the aforementioned RNA strand X having a mismatching base opposite one of the LNA segments of 1; ii) the aforementioned RNA strand Y having the mismatch opposite the zwitterionic NAA-modified gap of 1. In all resultant cases (i.e., with gapmers 1 and 2 as well as with native DNA), a decrease in thermal duplex stability due to the introduction of base mismatches was observed (entries 3 and 4 vs. entry 2; entries 7 and 8 vs. entry 6; entries 11 and 12 vs. entry 10, Table 1; also see Figure S7 in the Supporting Information). Furthermore, in all of these experiments, the mismatch-mediated destabilisation of duplex structures was most pronounced when the mismatched base was placed opposite the LNA segment, that is, with RNA-ON X as counterstrand (entries 3, 7, and 11). Interestingly, NAA/LNA-gapmer 1 proved to be highly sensitive towards both mismatched RNA-ON X and Y (entries 11 and 12 vs. entry 10). In this case, mismatch recognition was found to be even better than for the native DNA strand (entries 3 and 4 vs. entry 2), as expressed by a stronger mismatch-induced destabilisation of the duplex structures. Again, the duplex-to-single strand ratio at 37°C was determined from the melting curve data (*vide supra*). Both reference ON (gapmer 2 and native DNA) showed a large percentage of duplex structures at 37°C ($\alpha T_{37^\circ\text{C}} = 97\text{--}100\%$), both with X and Y as counterstrands (entries 3, 4, 7, and 8). Only the NAA/LNA-gapmer 1 was partially dissociated from the mismatched RNA-ON under these conditions (entries 11 and 12). In the presence of Y, 14% of gapmer 1 was not bound to the RNA-ON, and with X, the unbound fraction of the gapmer was even $\sim 50\%$. This selectivity in RNA binding led to the conclusion that the hybridisation properties of NAA/LNA-gapmer 1 are superior relative to both the reference gapmer 2 and to native DNA (*vide infra*), even though the presence of the NAA-modification furnished a moderate decrease of thermal duplex stability.

Circular dichroism spectra of both gapmers in complex with DNA or RNA demonstrate structural resemblance to a DNA-RNA heteroduplex

In order to elucidate the structural properties of the partially zwitterionic NAA/LNA-gapmer 1, circular dichroism (CD) spectra of duplexes of 1 either with complementary DNA (Figure 3A) or RNA (Figure 3B) were recorded and compared to the respective

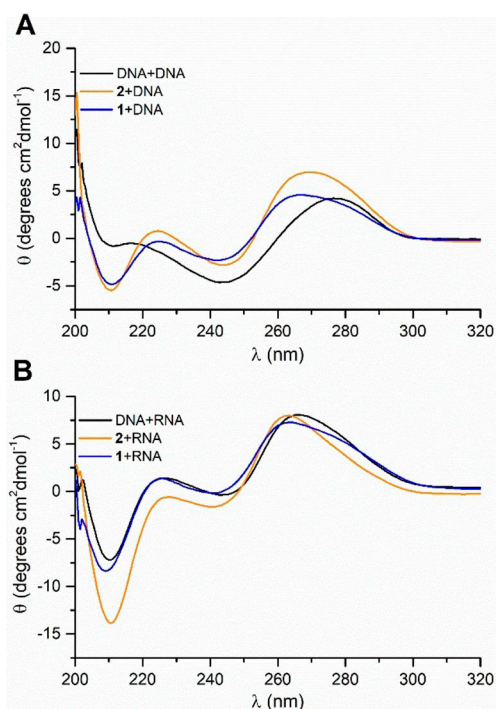


Figure 3. CD spectra of native DNA, DNA/LNA-gapmer 2, and NAA/LNA-gapmer 1 in complex with complementary A) DNA and B) RNA. All depicted curves are the average of technical triplicates.

spectra of DNA/LNA-gapmer 2 with complementary counterstrands.

For the duplexes of either gapmers 1 or 2 with DNA, CD signals indicated more resemblance between both gapmer-containing duplexes than to the unmodified DNA–DNA duplex of the same sequence (Figure 3A). In particular regarding the distinct negative signal at 210 nm and the following positive amplitude at 225 nm – which were almost nonexistent for the DNA–DNA reference duplex – duplexes containing gapmers 1 and 2 showed pronounced similarities. This hints towards substantial structural differences in the conformation of both gapmer–DNA duplexes as compared to the native DNA–DNA helix. However, when according duplexes with a complementary RNA counterstrand were studied, striking similarities to the unmodified DNA–RNA congener were observed (Figure 3B). In this case, the CD signals of the 1–RNA duplex almost perfectly superposed with the native DNA–RNA duplex. This was also the case for reference gapmer 2, with the slight difference that the negative signal at 210 nm was stronger than for the other two duplexes. Furthermore, the CD spectra of the 1–RNA and 2–RNA duplexes show some resemblance to the spectra of the 1–DNA and 2–DNA congeners, respectively (Figure 3B vs. A). Overall, these results therefore demonstrate that both gapmers 1 and 2, either in complex with DNA or RNA, furnish duplexes with topologies similar to a DNA–RNA heteroduplex. Remarkably, this finding was independent of the charge pattern in the ON backbone, that is, the partially zwitterionic nature of gapmer 1.

Both gapmer ON show excellent stability in biological media

Stability in biological media is crucial for any potential *in vivo* application of antisense ON. Therefore, we tested the stability of both gapmers 1 and 2 in pooled human plasma (HP; Figure 4A) as well as in whole cell lysate (WCL) of the human U937 cell line (Figure 4B). Unmodified DNA served as the positive (i.e., degradable) control in both assays.

We had previously reported that NAA-modified ON have potentially excellent stabilities in such media, dependent on the position of the cationic NAA-linkage.^[19] LNA-modified ON are also known to show an improved stability against nuclease-mediated degradation^[26a] and also in human serum, relative to unmodified controls.^[26b] In this work, we have aimed to verify the thus anticipated stability of gapmers 1 and 2 in the aforementioned biological media. Analysis by urea-PAGE demonstrated that both gapmers 1 and 2 show excellent stability against cleavage in HP (Figure 4A) as well as in WCL (Figure 4B) over a time course of eight hours, whereas an unmodified DNA–ON of the same sequence was completely cleaved.

Duplex formation of NAA/LNA-gapmer 1 with complementary RNA results in moderate activation of RNase H

In order to determine whether NAA/LNA-gapmer 1 is capable of triggering RNase H-mediated cleavage of complementary RNA, an assay employing a 5′-³²P-labelled RNA strand was used.^[27] Duplexes of native DNA as well as of DNA/LNA-gapmer 2, respectively, with this RNA strand served as controls, with the

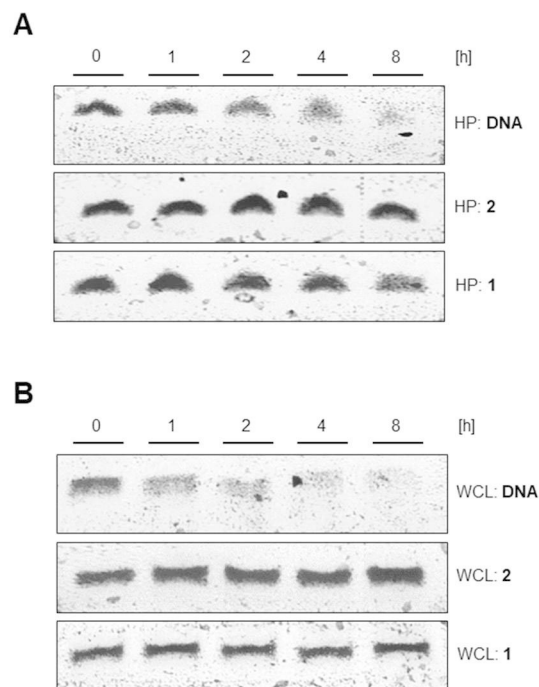


Figure 4. Effect of A) human plasma (HP) and B) human whole-cell lysate (WCL) on native DNA as well as on gapmers 1 and 2, respectively, over a time course of eight hours (analysis by urea-PAGE).

DNA-RNA heteroduplex representing a positive control, that is, a system furnishing RNase H-catalysed RNA degradation.

Figure 5A shows the results of the incubation of the labelled RNA with all three aforementioned strands, respectively, and RNase H over a time course of 60 min. Furthermore, the bottom panel depicts the influence of RNase H on the ^{32}P -labelled RNA strand without the presence of any counterstrand as an additional control experiment. Analyses of the assay mixtures were carried out by urea-PAGE and autoradiography. As anticipated,^[28] DNA/LNA-gapmer 2 induced the activation of RNase H and led to complete degradation of the parent RNA strand within the first 5 min of incubation (Figure 5A, degradation product label b). The timepoint of 0 min shows the intact RNA (Figure 5A, label a) as well as a band of the 2-RNA duplex (label x) which was still present despite the addition of urea as chaotropic agent. Similar observations were made for unmodified DNA that likewise triggered rapid degradation after 5 min, but led to the formation of an additional degradation product. In contrast, single-stranded RNA without a complementary counterstrand remained stable against RNase H over the observed timeframe. Interestingly, NAA/LNA-gapmer 1 also induced RNase H-mediated cleavage of the target RNA, although no uniform phosphate diester backbone was present in its structure. However, the rate of degradation appeared to be significantly slower than for reference gapmer 2.

We therefore performed a second set of experiments to observe RNase H-mediated degradation over an extended time period (Figure 5B). After 24 h, degradation of the labelled RNA was clearly detectable in the assay mixture containing NAA/LNA-gapmer 1, yet nearly the exact same outcome was observed without the presence of 1. To rule out general instability of the chosen RNA sequence over such an extended time period, another control experiment was included: ^{32}P -

labelled RNA was incubated over the full time period (i.e., up to 24 h) in the absence of both a counterstrand and RNase H. However, no RNA cleavage was detected under these conditions (Figure 5B). It has to be noted that the degradation signals observed for the duplex of 1 and ^{32}P -labelled RNA after 30 and 60 min (Figure 5A) could not be visualised in the prolonged incubation experiment (Figure 5B) due to differences in signal intensity.

Discussion

In previous studies,^[12a,19] we reported the generally favourable properties of ON with partially zwitterionic NAA-modified backbone structures, that is, their formation of stable, helical duplexes with complementary DNA, their retention of base-pairing fidelity and their high stability in biological media. However, duplex formation with RNA had been observed to be moderately hampered, that is, decreased thermal stabilities (up to -4.0°C /NAA-modification^[12a]) had been observed. Thus, we have now aspired to modify such zwitterionic NAA-ON in a way that furnishes satisfactory binding affinity towards RNA without compromising base-pairing fidelity, hence potentially enabling an efficient and selective target engagement with endogenous RNA. These considerations have led to the design of NAA/LNA-gapmer 1, in which strongly RNA-binding LNA segments were combined with a zwitterionic NAA-modified gap unit.

Following the successful synthesis of 1 (and an according DNA/LNA-gapmer 2 as a reference with a uniformly anionic backbone), UV-monitored thermal melting studies revealed an improved binding affinity to complementary RNA, relative to previously studied NAA-modified ON (formally -1.5°C /NAA-modification due to the stabilising effect of the LNA units). As a

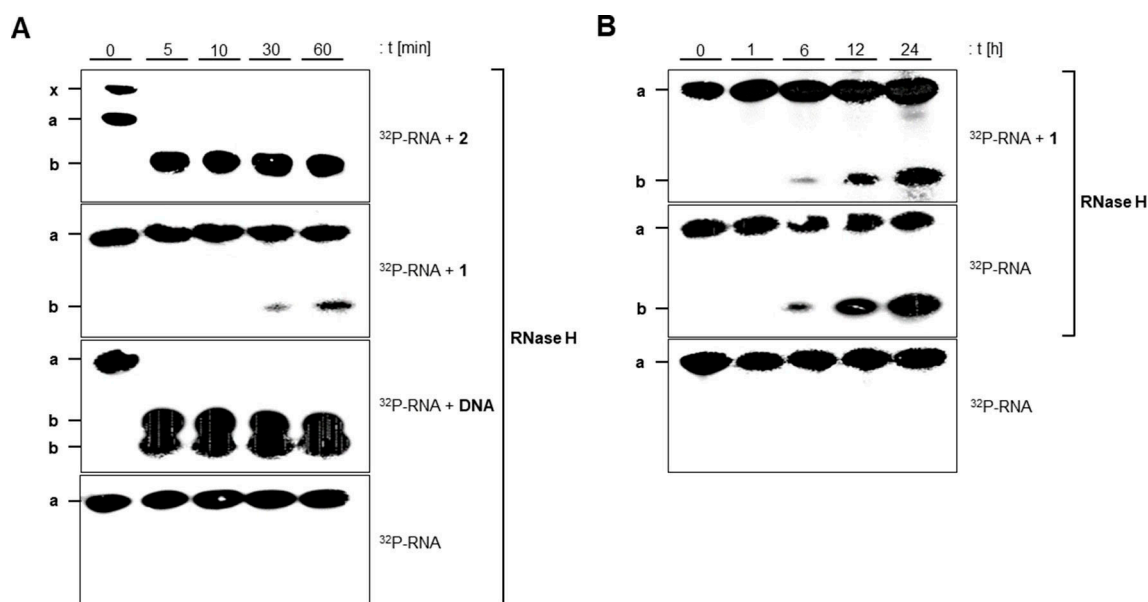


Figure 5. A) RNase H-mediated degradation of ^{32}P -labelled RNA upon hybridisation with 1, 2, native DNA, and without any counterstrand over 60 min (urea-PAGE). B) RNase H-mediated degradation of ^{32}P -labelled RNA with 1, without any counterstrand, and without either counterstrand or RNase H over 24 h (urea-PAGE). x: heteroduplex of 2 and RNA, a: intact RNA, b: RNA degradation products.

result, almost quantitative formation of the 1-RNA duplex at physiologically relevant 37 °C could be demonstrated. Furthermore, gapmer 1 was shown to be sensitive towards single base mismatches in the counterstrand at 37 °C. Experiments with mismatched RNA X resulted in only 50% formation of the 1-RNA duplex at this temperature. With a different mismatched RNA Y, 14% single-stranded gapmer 1 was determined (cf. Table 1). Interestingly, this selectivity was not observed with the DNA/LNA-gapmer 2 (i.e., the polyanionic reference ON) that showed no sensitivity towards base mismatches in the RNA counterstrand at 37 °C. The same was true for unmodified DNA. Binding to RNA off-targets with sequences similar to the actual target mRNA can lead to potential side effects in the pharmaceutical application of antisense ON.^[29] It is therefore of great relevance that backbone-modified ON structures show some sequence selectivity in their hybridisation properties under physiologically relevant conditions (i.e., at 37 °C). With respect to this consideration, the hybridisation properties of NAA/LNA-gapmer 1 are superior relative to those of both the reference gapmer 2 and native DNA, even though the presence of the NAA-modification furnished a decrease of thermal duplex stability. Furthermore, these results give rise to the general question if T_m values might be overrated in the evaluation of hybridisation properties of backbone-modified ON with respect to their potential application as antisense agents. We present herein an alternative parameter for such an evaluation: the target selectivity of the investigated ON (with a suitable length for an antisense agent) at 37 °C. This appears to be superior to a “the more stable, the better” approach for studying the physicochemical hybridisation properties with RNA counterstrands. This hypothesis is also supported by recent findings by Dieckmann et al. who could demonstrate a direct correlation of high T_m values and the hepatotoxic potential of high-affinity ON due to enhanced off-target effects.^[11b] Of course, such an improved target selectivity due to decreased duplex stability can in principle also be achieved by alternative means, for example, designing a shorter sequence of the antisense ON or a lower number of LNA units. However, herein we demonstrate that the NAA-modification is a useful addition to the toolbox of ON modifications to achieve this goal.

CD-spectroscopic analyses confirmed helical topologies for the gapmers 1 and 2, respectively, in complex with complementary DNA or RNA, with the resultant helical structures being similar to a DNA-RNA heteroduplex in all cases. This uniform topological preference was obviously caused by the presence of the LNA segments in the gapmer sequences.^[30] Notably, the partially zwitterionic backbone structure of 1 had no distorting influence on the topologies of its duplexes formed with either DNA or RNA counterstrands. In addition, high stability against degradation of the gapmers in human plasma and whole cell lysate was observed.

The activation of RNase H generally represents a desirable (though not essential feature) of antisense ON, and the NAA/LNA-gapmer 1 was therefore investigated with respect to this property. In a first set of experiments, the RNase H-mediated cleavage of a complementary ³²P-labelled RNA counterstrand was studied over a period of 60 min. Within this time, the two

reference ON (i.e., gapmer 2 and unmodified DNA) both induced rapid degradation of the target RNA by RNase H. Surprisingly, some degradation of the labelled RNA (albeit rather slowly) was also detected in presence of NAA/LNA-gapmer 1, although 1 possesses no uniform phosphate diester backbone (cf. Figure 5). This suggested a very moderate activation of RNase H due to the presence of 1 in the assay mixture. In order to further study this effect, the assay was then performed again with a significantly extended incubation period (up to 24 h). Even though this led to stronger signals for the RNA degradation products with gapmer 1, this result could not solely be linked to the influence of the partially zwitterionic gapmer: the same experimental setup with the absence of 1 resulted in a rather similar outcome. To exclude a general instability of the radiolabelled RNA strand, an additional control containing only the target RNA without RNase H was also incubated for 24 h, but no degradation was recorded. This demonstrated that the employed preparation of RNase H displayed some sort of unspecific nuclease activity. Overall, it was concluded that the aforementioned very moderate activation of RNase H by gapmer 1 became indistinguishable from background reactions over longer incubation periods. This suggests that an NAA/LNA-gapmer of type 1 might exert a potential antisense effect by “steric block” (i.e., binding to endogenous RNA) rather than by “catalytic” RNA degradation, as the latter would probably require a more efficient activation of RNase H. It should also be noted that this part of the reported work generally proves the high relevance of a rigorous set of control experiments in RNase H assays. Otherwise, it is unclear if the described alleged activation of RNase H was genuine or actually resulted (at least partially) from unspecific nuclease activity. This actually might be the case for several reports on ‘RNase H activation’ by modified ON structures in the literature.

Conclusion

In summary, we report the synthesis and properties of a new type of gapmer oligonucleotide architecture featuring a partially zwitterionic backbone structure. This NAA/LNA-gapmer approach furnished a zwitterionic ON 1 with optimised characteristics: gapmer 1 showed superior hybridisation properties with RNA at physiologically relevant 37 °C as well as excellent stability in biological media. In a cellular setting, a gapmer of type 1 might then mainly exert biological activity via a ‘steric block’ mechanism, even though 1 apparently activated RNase H-mediated RNA degradation on a very moderate level. Overall, the NAA/LNA-gapmer approach is thus established as a strategy to design partially zwitterionic ON for the future development of novel antisense agents with a reduced overall charge in the backbone. This is anticipated to furnish improved pharmacokinetic properties of according ON-based drug candidates. Based on the favourable characteristics of 1, the stage is now set for the development of synthetic methodology for the efficient preparation of zwitterionic gapmers of type 1 with biologically relevant base sequences. This will enable future

studies on their antisense efficacy *in cellulo*, with the goal to establish zwitterionic backbone architectures of oligonucleotide analogues as a viable strategy for the development of novel antisense agents.

Experimental Section

Synthesis of oligonucleotides: Based on our previous syntheses of NAA-modified ON,^[12] gapmer ON 1 and 2 were assembled by automated solid phase-supported DNA synthesis. This required the chemical synthesis of "dimeric" NAA-linked phosphoramidite 14 (see the Supporting Information for detailed synthetic procedures). Unmodified DNA phosphoramidites (Glen Research) and LNA phosphoramidites (QIAGEN) were commercially purchased. After completion of ON synthesis and basic workup under standard conditions, purification of 1 and 2 was achieved by urea polyacrylamide gel electrophoresis (urea-PAGE, Figure S1, see the Supporting Information for detailed procedures). The identities of both gapmers 1 and 2 were confirmed by high resolution mass spectrometry (Table S1, Figures S2 and S3). All other oligonucleotides were commercially purchased (Sigma-Aldrich).

Melting temperature experiments: To determine the binding affinity of the NAA/LNA-gapmer 1 towards complementary DNA (5'-AATCTAGAGAGATCT-3') and RNA (5'-AAUCUAGAGAGAU-3'), a 1 μM solution of the gapmer/counterstrand duplex in phosphate buffer (10 mM NaH_2PO_4 , pH 7.4, containing 100 mM NaCl) was prepared. Prior to measurements, the solution was heated to 90 °C and subsequently cooled down to RT to enable duplex formation. Then, three heating and cooling cycles ranging from 25 to 90 °C with a heating rate of 0.7 °C/min were performed and changes in the absorption at $\lambda = 260$ nm were recorded using a Cary 100 UV/Vis spectrometer (Agilent Technologies). Hyperchromicity was plotted against temperature to obtain melting curves, and T_m values were calculated as the maximum of the first derivative. To eliminate the temperature dependency of the extinction coefficient ϵ , αT_m values were calculated and used to describe the melting temperature of all studied duplexes. Furthermore, $\alpha T_{37^\circ\text{C}}$ values were calculated to investigate the hybridisation at a physiologically relevant temperature of 37 °C. Details on the method for the compilation of the α -curves are provided in the Supporting Information (Figures S4 to S6). A similar protocol was used for studies on mismatch sensitivity. Therefore, base mismatches were introduced in the RNA counterstrand opposite of either one of the LNA segment (5'-AAUCUAGAGAGAG $\underline{\text{CCU}}$ -3', mismatched RNA-ON X) or the NAA gap (5'-AAUCUAGAG $\underline{\text{GG}}$ AGAU-3', mismatched RNA-ON Y, mismatches are highlighted in bold and are underlined in the sequences, also see Figure S7). To obtain reference T_m values, according melting temperature experiments were conducted with DNA/LNA-gapmer 2 and a native DNA-ON with the same sequence (5'-AGATCTCTCTAGATT-3').

CD-spectroscopic analysis of duplex structures: Circular dichroism (CD) spectra of duplexes containing the NAA/LNA-gapmer 1 were recorded in phosphate buffer (10 mM NaH_2PO_4 , pH 7.4, containing 100 mM NaCl) on a Jasco 715 spectropolarimeter. The final concentration of the duplex was 1 μM . All measurements were performed at 25 °C in a cuvette with a length of 1 cm and a wavelength range of 200–320 nm. Every sample was scanned 10 times with a scanning speed of 200 nm/min, a bandwidth of 5 nm, response time of 2 s and a data pitch of 0.5 nm. Prior to data analysis, a background correction was performed. Spectra were obtained by plotting the mean residual ellipticity θ against the recording wavelength λ . Reference spectra were recorded using the same protocol and duplexes containing either the DNA/LNA-

gapmer 2 or a native DNA-ON with the same sequence (5'-AGATCTCTCTAGATT-3').

Stability assays in biological media: The stabilities of both gapmer ON 1 and 2 in biological media was studied using pooled human plasma and whole-cell lysate of the U937 cell line as described before.^[19] As a positive control for the degradation of ON in these media, a native DNA-ON with the same sequence (5'-AGATCTCTCTAGATT-3') was used. In contrast to the previously reported protocol,^[19] incubation times for both ON were increased to a total of 8 h. Samples were taken at the time points shown in Figure 4 (*vide supra*). Pooled human plasma was obtained from BIOTREND Chemikalien GmbH. U937 cells were purchased from Sigma-Aldrich and the whole-cell lysate was prepared as reported.^[19]

RNase H assays: An RNA-ON with a sequence (5'-AAUCUAGAGAGAGAU-3') complementary to the gapmer sequence was radiolabelled at the 5'-end using γ -³²P-ATP (Hartmann Analytics, 500 μCi). The phosphorylation reaction was catalysed by T4 polynucleotide kinase according to the manufacturer's protocol (kit for DNA/RNA 5'-end labelling, Thermo Scientific). The resultant 5'-radiolabelled RNA was purified on an illustra NAP-5 gravity flow column (GE Healthcare) using water (Milli-Q) as eluent. The solvent was evaporated under reduced pressure and the dry 5'-³²P-labelled RNA was redissolved in water to a final concentration of 10 μM . The labelled RNA (2.5 pmol) was then combined with the NAA/LNA-gapmer 1 (5 pmol), diluted with 10x Reaction Buffer (Thermo Scientific) to a total volume of 25 μL and incubated at 37 °C for 15 min to allow formation of the hybrid duplex. Subsequently, RNase H from *E. coli* MRE-600 cells (Thermo Scientific, 1 μL , 10 U) was added and the mixture was incubated at 37 °C. Samples were taken at the time points shown in Figure 5 (*vide supra*) and the reaction was quenched by addition of stop-mix (50 mM EDTA, 90% formamide, 5 mg bromophenol blue). The resultant final samples were analysed on a urea-PAGE gel^[19] and bands were visualised using a Typhoon 9410 phosphoimager (GE Healthcare, Figure 5). DNA/LNA-gapmer 2 and a native DNA-ON with the same sequence (5'-AGATCTCTCTAGATT-3') were used as positive controls. Furthermore, two negative controls were included: i) incubation under the conditions described above, but lacking the gapmer strand, to determine the influence of the activating strand; ii) incubation under the conditions described above, but lacking both the gapmer strand and RNase H, to elucidate potential unspecific RNase activity of the RNase H preparation.

Acknowledgements

We thank the Deutsche Forschungsgemeinschaft (DFG, grant DU 1095/2-1), the Fonds der Chemischen Industrie (FCI, Sachkostenzuschuss) and the Studienstiftung des deutschen Volkes (doctoral fellowship for B.S.) for financial support. Open access funding enabled and organized by Projekt DEAL.

Conflict of Interest

The authors declare no conflict of interest.

Keywords: antisense · backbone modification · gapmers · oligonucleotides · zwitterions

- [1] a) X. Shen, D. R. Corey, *Nucleic Acids Res.* **2018**, *46*, 1584–1600; b) C. F. Bennett, *Annu. Rev. Med.* **2019**, *70*, 307–321.
- [2] a) B. A. Armitage, *Nat. Chem. Biol.* **2005**, *1*, 185–186; b) V. K. Sharma, P. Rungta, A. K. Prasad, *RSC Adv.* **2014**, *4*, 16618–16631.
- [3] a) Y. Dong, D. J. Siegwart, D. G. Anderson, *Adv. Drug Delivery Rev.* **2019**, *144*, 133–147; b) M. Caillaud, M. El Madani, L. Massaad-Massade, *J. Controlled Release* **2020**, *321*, 616–628.
- [4] a) J. Tamsamani, G. S. Pari, P. Guinot, *Expert Opin. Invest. Drugs* **1997**, *9*, 1157–67; b) J. S. Parham, A. C. Goldberg, *Expert Opin. Pharmacother.* **2019**, *2*, 127–131; c) K. Goodkey, T. Aslesh, R. Maruyama, T. Yokota, *Methods Mol. Biol.* **2018**, 69–76; d) M. Rodrigues, T. Yokota, *Methods Mol. Biol.* **2018**, 31–55.
- [5] P. S. Miller, J. Yano, E. Yano, C. Carroll, K. Jayaraman, P. O. P. Ts'o, *Biochemistry* **1979**, *18*, 5134–5143.
- [6] F. Eckstein, *Annu. Rev. Biochem.* **1985**, *54*, 367–402.
- [7] a) J. Lebreton, A. De Mesmaeker, A. Waldner, V. Fritsch, R. M. Wolf, S. M. Freier, *Tetrahedron Lett.* **1993**, *34*, 6383–6386; b) A. De Mesmaeker, A. Waldner, J. Lebreton, P. Hoffmann, V. Fritsch, R. M. Wolf, S. M. Freier, *Synlett* **1993**, 733–736; c) A. De Mesmaeker, A. Waldner, J. Lebreton, P. Hoffmann, V. Fritsch, R. M. Wolf, S. M. Freier, *Angew. Chem. Int. Ed.* **1994**, *33*, 226–229; *Angew. Chem.* **1994**, *106*, 237–240; d) C. Selvam, S. Thomas, J. Abbott, S. D. Kennedy, E. Rozners, *Angew. Chem. Int. Ed.* **2011**, *50*, 2068–2070; *Angew. Chem.* **2011**, *123*, 2116–2118; e) P. Tanui, S. D. Kennedy, B. D. Lunstad, A. Haas, D. Leake, E. Rozners, *Org. Biomol. Chem.* **2014**, *12*, 1207–1210; f) D. Mutisya, C. Selvam, B. D. Lunstad, P. S. Pallan, A. Haas, D. Leake, M. Egli, E. Rozners, *Nucleic Acids Res.* **2014**, *42*, 6542–6551.
- [8] a) Z. Huang, S. A. Benner, *J. Org. Chem.* **2002**, *67*, 3996–4013; b) B. Eschgfäller, J. G. Schmidt, M. König, S. A. Benner, *Helv. Chim. Acta* **2003**, *86*, 2959–2997.
- [9] a) P. E. Nielsen, M. Egholm, R. H. Berg, O. Buchardt, *Science* **1991**, *254*, 1497–1500; b) Z. V. Zhilina, A. J. Ziemba, S. W. Ebbinghaus, *Curr. Top. Med. Chem.* **2005**, *5*, 1119–1131.
- [10] a) S. K. Singh, A. A. Koshkin, J. Wengel, P. Nielsen, *Chem. Commun.* **1998**, 455–456; b) A. A. Koshkin, S. K. Singh, P. Nielsen, V. K. Rajwanshi, R. Kumar, M. Meldgaard, C. E. Olsen, J. Wengel, *Tetrahedron* **1998**, *54*, 3607–3630; c) J. S. Jepsen, M. D. Sørensen, J. Wengel, *Oligonucleotides* **2004**, *14*, 130–146.
- [11] a) N. Papargyri, M. Pontoppidan, M. R. Andersen, T. Koch, P. H. Hagedorn, *Mol. Ther. Nucleic Acids* **2020**, *19*, 706–717; b) A. Dieckmann, P. H. Hagedorn, Y. Burki, C. Brüggemann, M. Berrera, M. Ebeling, T. Singer, F. Schuler, *Mol. Ther. Nucleic Acids* **2018**, *10*, 45–54.
- [12] a) B. Schmidtgall, A. P. Spork, F. Wachowius, C. Höbartner, C. Ducho, *Chem. Commun.* **2014**, *50*, 13742–13745; b) B. Schmidtgall, C. Höbartner, C. Ducho, *Beilstein J. Org. Chem.* **2015**, *11*, 50–60.
- [13] a) M. L. Jain, P. Y. Bruice, I. E. Szabó, T. C. Bruice, *Chem. Rev.* **2012**, *112*, 1284–1309; b) B. Schmidtgall, A. Kuepper, M. Meng, T. N. Grossmann, C. Ducho, *Chem. Eur. J.* **2018**, *24*, 1544–1553; c) M. Meng, C. Ducho, *Beilstein J. Org. Chem.* **2018**, *14*, 1293–1308.
- [14] a) J. K. Strauss, C. Roberts, M. G. Nelson, C. Switzer, L. J. Maher III, *Proc. Natl. Acad. Sci. USA* **1996**, *93*, 9515–9520; b) T. P. Prakash, A. M. Kawasaki, E. A. Lesnik, N. Sioufi, M. Manoharan, *Tetrahedron* **2003**, *59*, 7413–7422; c) M. Prhvac, T. P. Prakash, G. Minasov, P. D. Cook, M. Egli, M. Manoharan, *Org. Lett.* **2003**, *5*, 2017–2020; d) S. Milton, D. Honcharenko, C. S. J. Rocha, P. M. D. Moreno, C. I. E. Smith, R. Strömberg, *Chem. Commun.* **2015**, *51*, 4044–4047.
- [15] a) G. Deglane, S. Abes, T. Michel, A. Laurent, M. Naval, C. Martinand-Mari, P. Prevot, E. Vives, I. Robbins, I. Barvik, Jr., B. Lebleu, F. Debart, J.-J. Vasseur, *Collection Symposium Series* **2005**, *7*, 143–147; b) G. Deglane, S. Abes, T. Michel, P. Prevot, E. Vives, F. Debart, I. Barvik, B. Lebleu, J.-J. Vasseur, *ChemBioChem* **2006**, *7*, 684–692.
- [16] R. L. Letsinger, C. N. Singman, G. Histan, M. Salunkhe, *J. Am. Chem. Soc.* **1988**, *110*, 4470–4471.
- [17] a) A. Blasko, R. O. Dempcy, E. E. Minyat, T. C. Bruice, *J. Am. Chem. Soc.* **1996**, *118*, 7892–7899; b) D. A. Barawkar, T. C. Bruice, *Proc. Natl. Acad. Sci. USA* **1998**, *95*, 11047–11052; c) B. A. Linkletter, I. E. Szabo, T. C. Bruice, *J. Am. Chem. Soc.* **1999**, *121*, 3888–3896; d) H. Challa, T. C. Bruice, *Bioorg. Med. Chem. Lett.* **2001**, *11*, 2423–2427.
- [18] a) D. P. Arya, T. C. Bruice, *J. Am. Chem. Soc.* **1998**, *120*, 6619–6620; b) H. Challa, T. C. Bruice, *Bioorg. Med. Chem. Lett.* **2001**, *11*, 2423–2427.
- [19] M. Meng, B. Schmidtgall, C. Ducho, *Molecules* **2018**, *23*, 2941.
- [20] a) L. A. McDonald, L. R. Barbieri, G. T. Carter, E. Lenoy, J. Lotvin, P. J. Petersen, M. M. Siegel, G. Singh, R. T. Williamson, *J. Am. Chem. Soc.* **2002**, *124*, 10260–10261; b) D. Wiegmann, S. Koppermann, M. Wirth, G. Niro, K. Leyerer, C. Ducho, *Beilstein J. Org. Chem.* **2016**, *12*, 769–795; c) T. Tanino, B. Al-Dabbagh, D. Mengin-Lecreux, A. Bouhss, H. Oyama, S. Ichikawa, A. Matsuda, *J. Med. Chem.* **2011**, *54*, 8421–8439; d) A. P. Spork, M. Büschleb, O. Ries, D. Wiegmann, S. Boettcher, A. Mihalyi, T. D. H. Bugg, C. Ducho, *Chem. Eur. J.* **2014**, *20*, 15292–15297; e) S. Koppermann, Z. Cui, P. D. Fischer, X. Wang, J. Ludwig, J. S. Thorson, S. G. Van Lanen, C. Ducho, *ChemMedChem* **2018**, *13*, 779–784.
- [21] C. I. E. Smith, R. Zain, *Annu. Rev. Pharmacol. Toxicol.* **2019**, *59*, 605–630.
- [22] a) A. Matsuda, M. Satoh, T. Ueda, H. Machida, T. Sasaki, *Nucleosides Nucleotides* **1990**, *9*, 587–597; b) P. Herdewijn, J. Balzarini, M. Baba, R. Pauwels, A. Van Aerschot, G. Janssen, E. De Clercq, *J. Med. Chem.* **1988**, *31*, 2040–2048; c) S. Czernecki, J.-M. Valery, *Synthesis* **1991**, 239–240; d) R. Eisenhuth, C. Richert, *J. Org. Chem.* **2008**, *74*, 26–37.
- [23] G. S. Ti, B. L. Gaffney, R. A. Jones, *J. Am. Chem. Soc.* **1982**, *104*, 1316–1319.
- [24] A. M. Felix, E. P. Heimer, T. J. Lambros, C. Tzougraki, J. Meienhofer, *J. Org. Chem.* **1978**, *43*, 4194–4196.
- [25] a) A. P. Spork, C. Ducho, *Org. Biomol. Chem.* **2010**, *8*, 2323–2326; b) A. P. Spork, D. Wiegmann, M. Granitzka, D. Stalke, C. Ducho, *J. Org. Chem.* **2011**, *76*, 10083–10098.
- [26] a) J. Toulmé, *Nat. Biotechnol.* **2001**, *20*, 17; b) J. Kurreck, E. Wyszko, C. Gillen, V. A. Erdmann, *Nucleic Acids Res.* **2002**, *30*, 1911–1918.
- [27] a) A. Novogrodsky, J. Hurwitz, *J. Biol. Chem.* **1966**, *241*, 2923–2932; b) C. C. Richardson, *Proc. Natl. Acad. Sci. USA* **1965**, *54*, 158–165; c) S. T. Crooke, K. M. Lemonidis, L. Neilson, R. Griffey, E. A. Lesnik, B. P. Monia, *Biochem. J.* **1995**, *312*, 599–608.
- [28] C. Wahlestedt, P. Salmi, L. Good, J. Kela, T. Johnsson, T. Hökfelt, C. Broberger, F. Porreca, J. Lai, K. Ren, M. Ossipov, A. Koshkin, N. Jakobsen, J. Skouf, H. Henrik Oerum, M. H. Jacobsen, J. Wengel, *Proc. Natl. Acad. Sci. USA* **2000**, *97*, 5633–5638.
- [29] X. Chi, P. Gatti, T. Papoian, *Drug Discovery Today* **2017**, *22*, 823–833.
- [30] a) A. A. Koshkin, P. Nielsen, M. Meldgaard, V. K. Rajwanshi, S. K. Singh, J. Wengel, *J. Am. Chem. Soc.* **1998**, *120*, 13252–13253; b) K. Bondensgaard, M. Petersen, S. K. Singh, V. K. Rajwanshi, R. Kumar, J. Wengel, J. P. Jacobsen, *Chem. Eur. J.* **2000**, *6*, 2687–2695.

Manuscript received: July 8, 2020

Accepted manuscript online: July 13, 2020

Version of record online: August 28, 2020

4. Final Discussion

A continuously rising number of concepts on how to transform ONs into agents that are suitable for therapeutic use have been presented over the last five decades.^[146] Still, despite the large number of studies that have been devoted to this subject, a satisfactory solution in all respects has yet to be found. Nonetheless, the immense potential of ON drugs, together with the constant need for novel druggable targets, must not allow an innovation gap in this field. Consequently, the work presented in this thesis aimed at the validation and improvement of the NAA-linkage, a novel cationic backbone modification conceptualized by *Ducho* et al.^[143,144] Since essential insights regarding the duplex formation and mismatch recognition properties of partially NAA-modified oligomers have already been described,^[143] it was now aspired to gain a more detailed understanding of the potential of this positively charged system. Firstly, the impact of the NAA-linkage on the overall biological stability of partially modified sequences should be evaluated. Secondly, fully NAA-modified and thus completely cationic oligomers should be synthesized and the consequences for hybridization and base-pairing fidelity should be assessed. Finally, it was envisioned to create an NAA/LNA-gapmer structure to improve the binding affinity towards complementary RNA and thus obtain a prototype of a potential antisense agent.

4.1 Evaluation of the Biological Stability of Partially Zwitterionic NAA-Modified Oligomers (Manuscript A)

The surface of most nucleases is covered with a large number of basic residues to efficiently bind the negatively charged nucleic acid backbone and enable successful cleavage.^[147] Considering this mechanism, the replacement of the anionic phosphodiester linkage by cationic units appears to be an elegant method to increase an ON's biological stability. However, only limited information on the stability of (partially) cationic nucleic acids in the presence of nucleases are available. Some insights concerning simple nuclease stability assays are provided e.g. by *Letsinger* et al.^[148] and *Bruice* et al.^[149,150]. Still, more in-depth studies that also cover the influence of more complex biological media remained elusive. Thus, the study published in Manuscript **A** was divided into a systematic analysis of the effect of position and configuration of the cationic NAA-modification on the ON-cleavage by either 3'- or 5'-exonucleases as well as a more detailed investigation of the influence of human plasma and whole cell lysate (WCL). Based on the results of *Bruice* and *Letsinger*, the resistance of the NAA-modification to nuclease-mediated degradation was assumed. Therefore, the focus was on how the presence of the positive charge would impact the stability of the remaining sequence. In a first set of experiments with 3'→5' snake venom phosphodiesterase (SVP)^[151–153] and 5'→3' bovine spleen phosphodiesterase (BSP)^[151,152], both terminally modified ONs (Manuscript **A**, *Figure 1*) showed remarkable stability when the end carrying the positive charge was attacked (Manuscript **A**, *Figure 2a* and *2b*). In fact, no degradation was detectable whereas the unmodified full-length control was cleaved within minutes. It has to be noted that, due to the method of synthesis, the NAA-modification is not completely terminal, but both the 3'- and the 5'-modified variants carry an additional unit linked by a phosphodiester at the 3'- and 5'-end, respectively. Since the available amounts of NAA-ON were not sufficient for mass spectrometry, an analysis method using a high-resolution sequencing PAGE was applied to detect possible single-nucleotide cleavage. Here, it was shown that in both terminally modified sequences the single phosphodiester-linked nucleoside was indeed cleaved (Manuscript **A**, *Figure 2c*), raising the hypothesis that the positively charged NAA-modification serves as a 'stopper' for nuclease activity. This theory was slightly adjusted through the significantly slowed degradation of the single terminally NAA-modified ONs upon exonuclease attack from the respective unaltered end, compared to the native control sequence (Manuscript **A**, *Figure*

2a and 2b). Here, although cleavage was not fully prevented, the considerable deceleration suggests a general stabilizing effect that can act across multiple nucleotides. This might either be a result of charge-mediated repulsion hindering nuclease activity or the formation of (possibly transient) intra-strand structures of the NAA-ON due to electrostatic attraction between the oppositely charged backbone segments. However, the stabilizing effect could also be confirmed for internally NAA-modified sequences (Manuscript A, *Figure 1*) whereas an influence of the configuration of the NAA-modification could not be verified (Manuscript A, *Figure 3*). Subsequently, the impact of less artificial media was evaluated. Thereby, compared to the native control, incubation of an internally modified NAA-ON with human plasma resulted in a significantly slowed degradation, which came to a halt when the modification was reached (Manuscript A, *Figure 4a*). Accordingly, a decelerating long-distance effect of the positive charge towards nuclease activity can be concluded in this environment as well. Similarly slow cleavage was observed for the 5'-modified sequence, whereas the 3'-modified ON showed high stability after initial minimal degradation, which probably resulted from the terminally unmodified nucleotide (Manuscript A, *Figure 4b*). This suggests that 3'-exonuclease activity is higher in human plasma and alteration of the corresponding sequence end with the cationic NAA-linkage can drastically increase the ON's half-life. Comparable observations were made for the experiments with WCL, with the difference that in this model system the terminal 5'-NAA-modification protected the downstream sequence over the complete incubation period (Manuscript A, *Figure 4c* and *4d*).

The findings obtained from these stability studies point towards great potential of the positively charged NAA-backbone modification. Together with the previously verified beneficial properties of NAA-containing systems^[143], these results justify a closer investigation of this artificial backbone linkage.

4.2 Analysis of the Hybridization Properties of Cationic Fully NAA-Modified Oligomers (Manuscript B)

As noted above, partially zwitterionic NAA-modified ONs have been proven to possess characteristics that are useful for the development of potential biomedical agents.^[143,154] However, more detailed insights regarding a fully cationic NAA-structure were not yet available. Thus, the focus of Manuscript B was set on the synthesis of an *all*-NAA-modified oligomer and on how the completely cationic backbone structure might affect fundamental properties of nucleic acids. Since a completely cationic backbone is not accessible using the dimeric phosphoramidite building blocks designed for zwitterionic ONs^[143–145], the synthetic route was adapted to the monomeric building blocks **B-(S)-2** and **B-(R)-2** in analogy to solid-phase peptide synthesis (Manuscript B, *Figure 1, Scheme 1* and *Supporting Information*). The resulting amide-linked fully cationic thymidinyl amino acids (6'-*all*-(S)-14-mer **B-1a** and 6'-*all*-(R)-14-mer **B-1b**, Manuscript B, *Figure 1*) showed considerably increased thermal stability in melting experiments with complementary DNA compared to a native DNA-DNA duplex (Manuscript B, *Table 1*). These results are in good agreement with former studies on fully cationic ONs by *Letsinger et al.*^[148,151] and *Bruice et al.*^[155,156], who also reported about extremely stable duplexes between fully cationic ONs and their DNA counterstrands due to electrostatic attraction of the oppositely charged backbones. Regarding the structural hybridization behavior of the two positively charged DNA congeners, circular dichroism (CD) spectroscopy could confirm the formation of helical duplexes with complementary DNA, showing only a slight signal shift for the duplex containing (6'*R*)-configured **B-1b** (Manuscript B, *Figure 3*). A further analogy to the findings reported by *Letsinger* and *Bruice* was a destabilization of the NAA-ON/DNA duplex with increasing ionic strength as a result of salt-mediated shielding of the backbone charges (Manuscript B, *Table 1*). However, in contrast to the fully cationic oligomers synthesized by *Bruice et al.*^[157,158], which have been found to recognize single-base mismatches, both *all*-NAA-ONs were nearly insensitive towards single mismatched counterstrands (Manuscript B, *Table 1*). So, in this case, the attraction between the two backbones appeared to overrule Watson-Crick base pairing. Yet, it has to be mentioned that the sequence of **B-1a** and **B-1b** was significantly longer than the positively charged systems investigated by *Bruice et al.*, which might most probably have an impact on the sensitivity towards single mismatching bases. Still, in melting studies with a completely mismatched DNA sequence, no duplex

formation could be confirmed. Yet, a distinct increase in hyperchromicity was still observable (Manuscript **B**, *Figure 2*). This may be a result of unspecific, charge-mediated aggregation of the two oppositely charged strands that again slowly dissociates due to the rising temperature. Additional insights supporting this theory were provided by CD spectroscopic analysis of the interactions of **B-1a** and **B-1b** with the fully mismatched DNA sequence that gave no signals that would support the formation of a helical duplex structure (Manuscript **B**, *Figure 4*).

As shown on the example of the two fully NAA-modified oligomers, the application of cationic DNA mimics has to be planned and assessed with great care. Although Watson-Crick base pairing still seemed to play a role in counterstrand recognition and duplex formation, it was strongly hampered by charge-mediated attraction between the native and cationic backbones. Thus, the resulting influence on specific target recognition is not compatible with the requirements for applicable antisense agents and is also in strong contrast to the results obtained for partially zwitterionic NAA-ONs.^[143] Nonetheless the studies conducted in Manuscript **B** provide valuable insights regarding the influence of a reversely charged backbone on fundamental nucleic acid properties and will contribute to the design process during the conceptualization of ON analogues containing cationic charges.

4.3 Synthesis and Evaluation of an NAA/LNA-Gapmer Structure (Manuscript C)

Partially NAA-modified oligomers selectively discriminate between matched and mismatched strands^[143] while displaying excellent resistance towards nuclease-mediated cleavage (Manuscript A). Yet, duplexes with DNA and RNA showed slight to moderate destabilization compared to native controls. Application of fully cationic NAA-ONs, on the other hand, drastically enhanced counterstrand binding, but also diminished base-pairing fidelity and thus specific target recognition (Manuscript B). Consequently, the work described in Manuscript C was aimed at the creation of an NAA/LNA-gapmer (Figure 4.1) to combine the advantageous properties of the cationic NAA-linkage with the high affinity of the LNA sugar modification towards RNA.^[82,85,159]

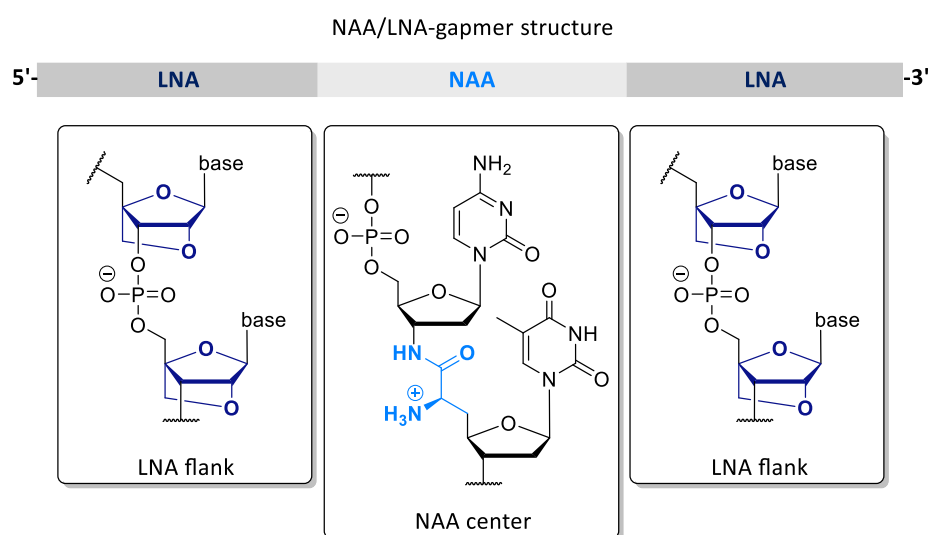


Figure 4.1. Concept of an NAA/LNA-gapmer structure: Simplified illustration of an NAA/LNA-gapmer with focus on position and type of the incorporated backbone modifications. **LNA:** Flank region consisting of anionic LNA-modified DNA. **NAA:** Gap region with a zwitterionic NAA-backbone.

Therefore, gapmer **C-1** and control **C-2** (Manuscript C, Figure 1B) were assembled using automated DNA synthesis (Manuscript C, Supporting Information) and compared regarding their biophysical and biochemical properties. CD-spectroscopic analysis of both **C-1** and **C-2** with complementary DNA (Manuscript C, Figure 3A) and RNA (Manuscript C, Figure 3B) confirmed the formation of helical duplexes with a topology comparable to a DNA-RNA hybrid duplex. Subsequent melting experiments with complementary RNA uncovered a slight destabilization of the **C-1**-RNA duplex, which was in strong contrast to the extremely stable structure formed with **C-2** (Manuscript C, Table 1 and Figure 2B). However, since

the measured T_m values did not reflect physiological conditions, the single-strand-to-duplex-ratio at 37 °C was calculated for RNA duplexes containing either native DNA, **C-1** or **C-2** as counterstrand (Manuscript **C**, *Table 1*). Here, nearly quantitative duplex formation was verified for all three systems, demonstrating excellent target binding of **C-1** at physiological temperature. Also, calculations for duplexes containing either an internally or peripherally located single mismatch unveiled a significant drop in duplex formation for the **C-1**-RNA combination (Manuscript **C**, *Table 1*). It has to be noted that the base mismatch opposite of the LNA-flank induced a more pronounced decrease in stability than the one placed opposite of the NAA-gap. This supported the hypothesis that the LNA-modification was indeed crucial for RNA binding of **C-1**. However, a comparable sensitivity for single mismatches could neither be confirmed for the native DNA-RNA, nor for the **C-2**-RNA duplex (Manuscript **C**, *Table 1*). With respect to the increased cytotoxic potential arising from off-target binding^[96,159], these findings underline the great potential of chimeric ONs such as **C-1** relative to other LNA-modified systems. The biochemical evaluation of **C-1** proved excellent stability of the whole gapmer towards degradation in human plasma and WCL (Manuscript **C**, *Figure 4*). Further, a moderate activation of RNase H-induced RNA cleavage was confirmed (Manuscript **C**, *Figure 5*). This finding was unexpected, since RNA degradation by RNase H was shown to require at least five adjacent DNA nucleosides.^[18] However, as cleavage only occurred on a very moderate level, it can be assumed that the main potential antisense activity of a gapmer such as **C-1** would result from a steric block of ribosomal translation.

In summary, the interplay between the high-affinity LNA- and the mismatch-sensitive NAA-linkage yielded a scaffold for possible antisense agents with remarkable capabilities concerning target recognition, target affinity and selectivity. The latter has only scarcely been discussed in the literature before. As the zwitterionic character of the NAA/LNA-gapmer architecture is also assumed to improve the overall pharmacokinetic behavior of ONs, subsequent work should be focused on the cellular uptake as well as the antisense activity of such oligomers *in cellulo*. It is anticipated that the partially zwitterionic character of **C-1** and the resultant masking of some negative charges might improve permeation over the lipophilic cellular membrane. Furthermore, considering the beneficial characteristics of cationic CPPs^[160], an advantageous effect of the positively charged NAA-modification on cellular uptake might be possible.

4.4 Conclusion and Outlook

Overall, the results obtained in this work revealed further valuable characteristics of the cationic NAA-modification and highlight the concept of a partially zwitterionic NAA/LNA-gapmer structure as a promising template for potential antisense applications. Nonetheless, in subsequent studies, the influence of the zwitterionic NAA-linkage on cellular uptake still has to be verified. For this purpose, the synthesis of a fluorophore-labeled version of **C-1** might be useful to not only evaluate the cellular uptake but also potential endosomal release of the DNA analogue. Additionally, first antisense experiments should be considered. Therefore, a gapmer suitable for hybridization to a distinct cellular target should be synthesized and evaluated regarding its influence on protein expression. A third approach to gain further insights into the potential of the NAA-linkage might be the implementation of new synthetic routes for the assembly of further NAA-building blocks, suitable for automated DNA synthesis. This would facilitate the construction of partially zwitterionic ONs with arbitrary sequences and hence enable access to a larger panel of cellular targets.

In summary, the insights obtained within this thesis underline the great value of the NAA-linkage as 'tool' for the synthesis of artificial antisense ONs and will serve as a guideline for future studies on this positively charged backbone modification.

5. References

- [1] J. D. Watson, F. H. C. Crick; Molecular Structure of Nucleic Acids: A Structure for Deoxyribose Nucleic Acid; *Nature* **1953**, *171*, 737–738.
- [2] M. L. Stephenson, P. C. Zamecnik; Inhibition of Rous sarcoma viral RNA translation by a specific oligodeoxyribonucleotide.; *Proc. Natl. Acad. Sci. U.S.A.* **1978**, *75*, 285–288.
- [3] P. C. Zamecnik, M. L. Stephenson; Inhibition of Rous sarcoma virus replication and cell transformation by a specific oligodeoxynucleotide; *Proc. Natl. Acad. Sci. U.S.A.* **1978**, *75*, 280–284.
- [4] L. J. Maher; Prospects for the Therapeutic Use of Antigene Oligonucleotides; *Cancer Investig.* **1996**, *14*, 66–82.
- [5] H. Moser, P. Dervan; Sequence-specific cleavage of double helical DNA by triple helix formation; *Science* **1987**, *238*, 645–650.
- [6] T. Le Doan, L. Perrouault, D. Praseuth, N. Habhoub, J. L. Decout, N. T. Thuong, J. Lhomme, C. Hélène; Sequence-specific recognition, photocrosslinking and cleavage of the DNA double helix by an oligo-[alpha]-thymidylate covalently linked to an azidoproflavine derivative; *Nucleic Acids Res.* **1987**, *15*, 7749–7760.
- [7] P. E. Nielsen, M. Egholm, O. Buchardt; Evidence for (PNA)₂/DNA triplex structure upon binding of PNA to dsDNA by strand displacement; *J. Mol. Recognit.* **1994**, *7*, 165–170.
- [8] K. Hoogsteen; The crystal and molecular structure of a hydrogen-bonded complex between 1-methylthymine and 9-methyladenine; *Acta Cryst.* **1963**, *16*, 907–916.
- [9] E. M. McGuffie, D. Pacheco, G. M. Carbone, C. V. Catapano; Antigene and antiproliferative effects of a c-myc-targeting phosphorothioate triple helix-forming oligonucleotide in human leukemia cells; *Cancer Res.* **2000**, *60*, 3790–3799.
- [10] M. Egholm, L. Christensen, K. L. Deuholm, O. Buchardt, J. Coull, P. E. Nielsen; Efficient pH-independent sequence-specific DNA binding by pseudoisocytosine-containing bis-PNA; *Nucleic Acids Res.* **1995**, *23*, 217–222.
- [11] C. I. E. Smith, R. Zain; Therapeutic Oligonucleotides: State of the Art; *Annu. Rev. Pharmacol. Toxicol.* **2019**, *59*, 605–630.

- [12] C. F. Bennett, E. E. Swayze; RNA Targeting Therapeutics: Molecular Mechanisms of Antisense Oligonucleotides as a Therapeutic Platform; *Annu. Rev. Pharmacol. Toxicol.* **2010**, *50*, 259–293.
- [13] The commercial tipping point; *Nat. Biotechnol.* **2017**, *35*, 181–181.
- [14] C. M. Perry, J. A. Barman Balfour; Fomivirsen; *Drugs* **1999**, *57*, 375–380.
- [15] W. F. Lima, J. G. Nichols, H. Wu, T. P. Prakash, M. T. Migawa, T. K. Wyrzykiewicz, B. Bhat, S. T. Crooke; Structural requirements at the catalytic site of the heteroduplex substrate for human RNase H1 catalysis; *J. Biol. Chem.* **2004**, *279*, 36317–36326.
- [16] S. M. Cerritelli, R. J. Crouch; Ribonuclease H: the enzymes in eukaryotes; *FEBS J.* **2009**, *276*, 1494–1505.
- [17] H. Stein, P. Hausen; Enzyme from calf thymus degrading the RNA moiety of DNA-RNA Hybrids: effect on DNA-dependent RNA polymerase; *Science* **1969**, *166*, 393–395.
- [18] B. P. Monia, E. A. Lesnik, C. Gonzalez, W. F. Lima, D. McGee, C. J. Guinasso, A. M. Kawasaki, P. D. Cook, S. M. Freier; Evaluation of 2'-modified oligonucleotides containing 2'-deoxy gaps as antisense inhibitors of gene expression; *J. Biol. Chem.* **1993**, *268*, 14514–14522.
- [19] T. Ogawa, T. Okazaki; Function of RNase H in DNA replication revealed by RNase H defective mutants of *Escherichia coli*; *Mol. Genet. Genom.* **1984**, *193*, 231–237.
- [20] G. J. Hannon; RNA interference; *Nature* **2002**, *418*, 244–251.
- [21] A. Grishok, A. E. Pasquinelli, D. Conte, N. Li, S. Parrish, I. Ha, D. L. Baillie, A. Fire, G. Ruvkun, C. C. Mello; Genes and Mechanisms Related to RNA Interference Regulate Expression of the Small Temporal RNAs that Control *C. elegans* Developmental Timing; *Cell* **2001**, *106*, 23–34.
- [22] R. F. Ketting, S. E. J. Fischer, E. Bernstein, R. H. A. Plasterk; Dicer functions in RNA interference and in synthesis of small RNA involved in developmental timing in *C. elegans*; *Genes Dev.* **2001**, *15*, 2654–2659.
- [23] A. Fire, S. Xu, M. K. Montgomery, S. A. Kostas, S. E. Driver, C. C. Mello; Potent and specific genetic interference by double-stranded RNA in *Caenorhabditis elegans*; *Nature* **1998**, *391*, 806–811.
- [24] Y. Zhao, D. Srivastava; A developmental view of microRNA function; *Trends Biochem. Sci.* **2007**, *32*, 189–197.

- [25] E. Bernstein, A. A. Caudy, S. M. Hammond, G. J. Hannon; Role for a bidentate ribonuclease in the initiation step of RNA interference; *Nature* **2001**, *409*, 363–366.
- [26] J. K. W. Lam, M. Y. T. Chow, Y. Zhang, S. W. S. Leung; siRNA Versus miRNA as Therapeutics for Gene Silencing; *Mol. Ther. - Nucleic Acids* **2015**, *4*, e252.
- [27] S. M. Hammond, E. Bernstein, D. Beach, G. J. Hannon; An RNA-directed nuclease mediates post-transcriptional gene silencing in *Drosophila* cells; *Nature* **2000**, *404*, 293–296.
- [28] O. Bagasra, K. R. Prilliman; RNA interference: the molecular immune system; *J. Mol. Histol.* **2004**, *35*, 545–553.
- [29] Q. Liu, T. A. Rand, S. Kalidas, F. Du, H.-E. Kim, D. P. Smith, X. Wang; R2D2, a bridge between the initiation and effector steps of the *Drosophila* RNAi pathway; *Science* **2003**, *301*, 1921–1925.
- [30] A. J. Pratt, I. J. MacRae; The RNA-induced silencing complex: a versatile gene-silencing machine; *J. Biol. Chem.* **2009**, *284*, 17897–17901.
- [31] R. I. Gregory, T. P. Chendrimada, N. Cooch, R. Shiekhattar; Human RISC couples microRNA biogenesis and posttranscriptional gene silencing; *Cell* **2005**, *123*, 631–640.
- [32] S. Shukla, C. S. Sumaria, P. I. Pradeepkumar; Exploring Chemical Modifications for siRNA Therapeutics: A Structural and Functional Outlook; *ChemMedChem* **2010**, *5*, 328–349.
- [33] J. Krützfeldt, N. Rajewsky, R. Braich, K. G. Rajeev, T. Tuschl, M. Manoharan, M. Stoffel; Silencing of microRNAs in vivo with ‘antagomirs’; *Nature* **2005**, *438*, 685–689.
- [34] A. Wittrup, J. Lieberman; Knocking down disease: a progress report on siRNA therapeutics; *Nat. Rev. Genet.* **2015**, *16*, 543–552.
- [35] S. Davis, S. Propp, S. M. Freier, L. E. Jones, M. J. Serra, G. Kinberger, B. Bhat, E. E. Swayze, C. F. Bennett, C. Esau; Potent inhibition of microRNA in vivo without degradation; *Nucleic Acids Res.* **2009**, *37*, 70–77.
- [36] A. G. Torres, M. M. Fabani, E. Vigorito, M. J. Gait; MicroRNA fate upon targeting with anti-miRNA oligonucleotides as revealed by an improved Northern-blot-based method for miRNA detection; *RNA*. **2011**, *17*, 933–943.
- [37] J. Stenvang, A. Petri, M. Lindow, S. Obad, S. Kauppinen; Inhibition of microRNA function by antimiR oligonucleotides; *Silence*. **2012**, *3*, 1.

- [38] F. Petrocca, J. Lieberman; Promise and challenge of RNA interference-based therapy for cancer; *J Clin Oncol.* **2011**, *29*, 747–754.
- [39] J. C. Burnett, J. J. Rossi; RNA-based therapeutics: current progress and future prospects; *Chem. Biol.* **2012**, *19*, 60–71.
- [40] S. M. Nimjee, R. R. White, R. C. Becker, B. A. Sullenger; Aptamers as Therapeutics; *Annu. Rev. Pharmacol. Toxicol.* **2017**, *57*, 61–79.
- [41] J. Zhou, J. Rossi; Aptamers as targeted therapeutics: current potential and challenges; *Nat. Rev. Drug Discovery* **2017**, *16*, 181–202.
- [42] P. Mallikaratchy; Evolution of Complex Target SELEX to Identify Aptamers against Mammalian Cell-Surface Antigens; *Molecules* **2017**, *22*, 215–227.
- [43] Q. Pan, Q. Wang, X. Sun, X. Xia, S. Wu, F. Luo, X.-L. Zhang; Aptamer Against Mannose-capped Lipoarabinomannan Inhibits Virulent Mycobacterium tuberculosis Infection in Mice and Rhesus Monkeys; *Mol. Ther.* **2014**, *22*, 940–951.
- [44] A. Zhang, D. Chang, Z. Zhang, F. Li, W. Li, X. Wang, Y. Li, Q. Hua; In Vitro Selection of DNA Aptamers that Binds Geniposide; *Molecules* **2017**, *22*, 383.
- [45] S. R. Jaffrey; RNA-Based Fluorescent Biosensors for Detecting Metabolites in vitro and in Living Cells; *Adv. Pharmacol.* **2018**, *82*, 187–203.
- [46] G. Felsenfeld, D. R. Davies, A. Rich; Formation of a Three-Stranded Polynucleotide Molecule; *J. Am. Chem. Soc.* **1957**, *79*, 2023–2024.
- [47] M. Cooney, G. Czernuszewicz, E. H. Postel, S. J. Flint, M. E. Hogan; Site-specific oligonucleotide binding represses transcription of the human c-myc gene in vitro; *Science* **1988**, *241*, 456–459.
- [48] G. M. Samadashwily, S. M. Mirkin; Trapping DNA polymerases using triplex-forming oligodeoxyribonucleotides; *Gene* **1994**, *149*, 127–136.
- [49] P. Herdewijn; Heterocyclic Modifications of Oligonucleotides and Antisense Technology; *Antisense and Nucleic Acid Drug Dev.* **2000**, *10*, 297–310.
- [50] R. W. Wagner, M. D. Matteucci, D. Grant, T. Huang, B. C. Froehler; Potent and selective inhibition of gene expression by an antisense heptanucleotide; *Nat. Biotechnol.* **1996**, *14*, 840–844.
- [51] R. W. Wagner, M. D. Matteucci, J. G. Lewis, A. J. Gutierrez, C. Moulds, B. C. Froehler; Antisense gene inhibition by oligonucleotides containing C-5 propyne pyrimidines; *Science* **1993**, *260*, 1510–1513.

- [52] L. Ötvös, J. Sági, Gy. Sági, A. Szemző, F. D. Tóth, A. Jeney; Enzymatic Hydrolysis and Biological Activity of Oligonucleotides Containing 5-Substituted Pyrimidine Bases; *Nucleosides and Nucleotides*. **1999**, *18*, 1665–1666.
- [53] F. B. Howard, H. T. Miles; 2NH₂A.T helices in the ribo- and deoxypolynucleotide series. Structural and energetic consequences of 2NH₂A substitution; *Biochemistry* **1984**, *23*, 6723–6732.
- [54] M. Manoharan, K. S. Ramasamy, V. Mohan, P. D. Cook; Oligonucleotides bearing cationic groups: *N*²-(3-aminopropyl)deoxyguanosine. Synthesis, enhanced binding properties and conjugation chemistry; *Tetrahedron Lett.* **1996**, *37*, 7675–7678.
- [55] H. Liu, J. Gao, S. R. Lynch, Y. D. Saito, L. Maynard, E. T. Kool; A four-base paired genetic helix with expanded size; *Science* **2003**, *302*, 868–871.
- [56] K.-Y. Lin, R. J. Jones, M. Matteucci; Tricyclic 2'-Deoxycytidine Analogs: Syntheses and Incorporation into Oligodeoxynucleotides Which Have Enhanced Binding to Complementary RNA; *J. Am. Chem. Soc.* **1995**, *117*, 3873–3874.
- [57] C. A. Buhr, M. D. Matteucci, B. C. Froehler; Synthesis of a tetracyclic 2'-deoxyadenosine analog; *Tetrahedron Lett.* **1999**, *40*, 8969–8970.
- [58] Y. Doi, J. Chiba, T. Morikawa, M. Inouye; Artificial DNA Made Exclusively of Nonnatural C-Nucleosides with Four Types of Nonnatural Bases; *J. Am. Chem. Soc.* **2008**, *130*, 8762–8768.
- [59] B. D. Heuberger, C. Switzer; An Alternative Nucleobase Code: Characterization of Purine-Purine DNA Double Helices Bearing Guanine-Isoguanine and Diaminopurine 7-Deaza-Xanthine Base Pairs; *ChemBioChem* **2008**, *9*, 2779–2783.
- [60] J. Plavec, W. Tong, J. Chattopadhyaya; How do the gauche and anomeric effects drive the pseudorotational equilibrium of the pentofuranose moiety of nucleosides?; *J. Am. Chem. Soc.* **1993**, *115*, 9734–9746.
- [61] J. Plavec, C. Thibaudeau, J. Chattopadhyaya; How Does the 2'-Hydroxy Group Drive the Pseudorotational Equilibrium in Nucleoside and Nucleotide by the Tuning of the 3'-Gauche Effect?; *J. Am. Chem. Soc.* **1994**, *116*, 6558–6560.
- [62] C. Thibaudeau, J. Plavec, N. Garg, A. Papchikhin, J. Chattopadhyaya; How Does the Electronegativity of the Substituent Dictate the Strength of the Gauche Effect?; *J. Am. Chem. Soc.* **1994**, *116*, 4038–4043.
- [63] A. Rich; DNA comes in many forms; *Gene* **1993**, *135*, 99–109.

- [64] L. L. Cummins, S. R. Owens, L. M. Risen, E. A. Lesnik, S. M. Freier, D. McGee, C. J. Guinosso, P. D. Cook; Characterization of fully 2'-modified oligoribonucleotide hetero- and homoduplex hybridization and nuclease sensitivity; *Nucleic Acids Res.* **1995**, *23*, 2019–2024.
- [65] B. P. Monia, J. F. Johnston, H. Sasmor, L. L. Cummins; Nuclease Resistance and Antisense Activity of Modified Oligonucleotides Targeted to Ha-ras; *J. Biol. Chem.* **1996**, *271*, 14533–14540.
- [66] M. Robbins, A. Judge, L. Liang, K. McClintock, E. Yaworski, I. MacLachlan; 2'-O-methyl-modified RNAs Act as TLR7 Antagonists; *Mol. Ther.* **2007**, *15*, 1663–1669.
- [67] K. M. Flanigan, T. Voit, X. Q. Rosales, L. Servais, J. E. Kraus, C. Wardell, A. Morgan, S. Dorricott, J. Nakielny, N. Quarcoo, et al.; Pharmacokinetics and safety of single doses of drisapersen in non-ambulant subjects with Duchenne muscular dystrophy: Results of a double-blind randomized clinical trial; *Neuromuscul. Disord.* **2014**, *24*, 16–24.
- [68] P. Martin; A New Access to 2'-O-Alkylated Ribonucleosides and Properties of 2'-O-Alkylated Oligoribonucleotides.; *Helv. Chim. Acta* **1995**, *78*, 486-504.
- [69] S. T. Crooke, R. S. Geary; Clinical pharmacological properties of mipomersen (Kynamro), a second generation antisense inhibitor of apolipoprotein B; *Br J Clin Pharmacol.* **2013**, *76*, 269–276.
- [70] F. J. Raal, R. D. Santos, D. J. Blom, A. D. Marais, M.-J. Charng, W. C. Cromwell, R. H. Lachmann, D. Gaudet, J. L. Tan, S. Chasan-Taber, et al.; Mipomersen, an apolipoprotein B synthesis inhibitor, for lowering of LDL cholesterol concentrations in patients with homozygous familial hypercholesterolaemia: a randomised, double-blind, placebo-controlled trial; *Lancet.* **2010**, *375*, 998–1006.
- [71] W. K. Hagmann; The Many Roles for Fluorine in Medicinal Chemistry; *J. Med. Chem.* **2008**, *51*, 4359–4369.
- [72] S. Swallow; Fluorine in medicinal chemistry; *Prog. Med. Chem.* **2015**, *54*, 65–133.
- [73] A. M. Kawasaki, M. D. Casper, S. M. Freier, E. A. Lesnik, M. C. Zounes, L. L. Cummins, C. Gonzalez, P. D. Cook; Uniformly modified 2'-deoxy-2'-fluoro phosphorothioate oligonucleotides as nuclease-resistant antisense compounds with high affinity and specificity for RNA targets; *J. Med. Chem.* **1993**, *36*, 831–841.

- [74] P. S. Pallan, E. M. Greene, P. A. Jicman, R. K. Pandey, M. Manoharan, E. Rozners, M. Egli; Unexpected origins of the enhanced pairing affinity of 2'-fluoro-modified RNA; *Nucleic Acids Res.* **2011**, *39*, 3482–3495.
- [75] L. Bellon, F. Morvan, J.-L. Barascut, J.-L. Imbach; Sugar modified oligonucleotides: Synthesis, nuclease resistance and base pairing of oligodeoxynucleotides containing 1-(4'-thio- β -D-ribofuranosyl)-thymine; *Biochem. Biophys. Res. Commun.* **1992**, *184*, 797–803.
- [76] C. Leydier, L. Bellon, J. L. Barascut, F. Morvan, B. Rayner, J. L. Imbach; 4'-Thio-RNA: synthesis of mixed base 4'-thio-oligoribonucleotides, nuclease resistance, and base pairing properties with complementary single and double strand; *Antisense Res. Dev.* **1995**, *5*, 167–174.
- [77] G. Jones; Investigation of some properties of oligodeoxynucleotides containing 4'-thio-2'-deoxynucleotides: duplex hybridization and nuclease sensitivity; *Nucleic Acids Res.* **1996**, *24*, 4117–4122.
- [78] J. K. Watts, B. D. Johnston, K. Jayakanthan, A. S. Wahba, B. M. Pinto, M. J. Damha; Synthesis and Biophysical Characterization of Oligonucleotides Containing a 4'-Selenonucleotide; *J. Am. Chem. Soc.* **2008**, *130*, 8578–8579.
- [79] A. A. Koshkin, P. Nielsen, M. Meldgaard, V. K. Rajwanshi, S. K. Singh, J. Wengel; LNA (Locked Nucleic Acid): An RNA Mimic Forming Exceedingly Stable LNA:LNA Duplexes; *J. Am. Chem. Soc.* **1998**, *120*, 13252–13253.
- [80] A. A. Koshkin, S. K. Singh, P. Nielsen, V. K. Rajwanshi, R. Kumar, M. Meldgaard, C. E. Olsen, J. Wengel; LNA (Locked Nucleic Acids): Synthesis of the adenine, cytosine, guanine, 5-methylcytosine, thymine and uracil bicyclonucleoside monomers, oligomerisation, and unprecedented nucleic acid recognition; *Tetrahedron* **1998**, *54*, 3607–3630.
- [81] S. Obika, D. Nanbu, Y. Hari, J. Andoh, K. Morio, T. Doi, T. Imanishi; Stability and structural features of the duplexes containing nucleoside analogues with a fixed N-type conformation, 2'-O,4'-C-methylenribonucleosides; *Tetrahedron Lett.* **1998**, *39*, 5401–5404.
- [82] S. K. Singh, A. A. Koshkin, J. Wengel, P. Nielsen; LNA (locked nucleic acids): synthesis and high-affinity nucleic acid recognition; *Chem. Commun.* **1998**, 455–456.

- [83] E. T. Kool; Preorganization of DNA: Design Principles for Improving Nucleic Acid Recognition by Synthetic Oligonucleotides; *Chem. Rev.* **1997**, *97*, 1473–1488.
- [84] A. Eichert, K. Behling, C. Betzel, V. A. Erdmann, J. P. Fürste, C. Förster; The crystal structure of an “All Locked” nucleic acid duplex; *Nucleic Acids Res.* **2010**, *38*, 6729–6736.
- [85] J. Wengel, M. Petersen, M. Frieden, T. Koch; Chemistry of locked nucleic acids (LNA): Design, synthesis, and bio-physical properties; *Int. J. Pept. Res. Ther.* **2003**, *10*, 237–253.
- [86] E. E. Swayze, A. M. Siwkowski, E. V. Wancewicz, M. T. Migawa, T. K. Wyrzykiewicz, G. Hung, B. P. Monia, C. F. Bennett; Antisense oligonucleotides containing locked nucleic acid improve potency but cause significant hepatotoxicity in animals; *Nucleic Acids Res.* **2007**, *35*, 687–700.
- [87] J. K. Watts, D. R. Corey; Silencing disease genes in the laboratory and the clinic; *J. Pathol.* **2012**, *226*, 365–379.
- [88] P. P. Seth, A. Siwkowski, C. R. Allerson, G. Vasquez, S. Lee, T. P. Prakash, E. V. Wancewicz, D. Witchell, E. E. Swayze; Short antisense oligonucleotides with novel 2'-4' conformationally restricted nucleoside analogues show improved potency without increased toxicity in animals; *J. Med. Chem.* **2009**, *52*, 10–13.
- [89] E. M. Straarup, N. Fisker, M. Hedtjärn, M. W. Lindholm, C. Rosenbohm, V. Aarup, H. F. Hansen, H. Ørum, J. B. R. Hansen, T. Koch; Short locked nucleic acid antisense oligonucleotides potently reduce apolipoprotein B mRNA and serum cholesterol in mice and non-human primates; *Nucleic Acids Res.* **2010**, *38*, 7100–7111.
- [90] J. B. Bramsen, M. B. Laursen, C. K. Damgaard, S. W. Lena, B. R. Babu, J. Wengel, J. Kjems; Improved silencing properties using small internally segmented interfering RNAs; *Nucleic Acids Res.* **2007**, *35*, 5886–5897.
- [91] R. L. Beane, R. Ram, S. Gabillet, K. Arar, B. P. Monia, D. R. Corey; Inhibiting gene expression with locked nucleic acids (LNAs) that target chromosomal DNA; *Biochemistry* **2007**, *46*, 7572–7580.
- [92] R. Beane, S. Gabillet, C. Montaillier, K. Arar, D. R. Corey; Recognition of chromosomal DNA inside cells by locked nucleic acids; *Biochemistry* **2008**, *47*, 13147–13149.

- [93] J. T. Nielsen, P. C. Stein, M. Petersen; NMR structure of an α -L-LNA:RNA hybrid: structural implications for RNase H recognition; *Nucleic Acids Res.* **2003**, *31*, 5858–5867.
- [94] M. D. Sørensen, L. Kværnø, T. Bryld, A. E. Håkansson, B. Verbeure, G. Gaubert, P. Herdewijn, J. Wengel; α -L-ribo-Configured Locked Nucleic Acid (α -L-LNA): Synthesis and Properties; *J. Am. Chem. Soc.* **2002**, *124*, 2164–2176.
- [95] J. K. Watts; Locked nucleic acid: tighter is different; *Chem. Commun.* **2013**, *49*, 5618.
- [96] A. Dieckmann, P. H. Hagedorn, Y. Burki, C. Brüggmann, M. Berrera, M. Ebeling, T. Singer, F. Schuler; A Sensitive In Vitro Approach to Assess the Hybridization-Dependent Toxic Potential of High Affinity Gapmer Oligonucleotides; *Mol. Ther. Nucleic Acids* **2018**, *10*, 45–54.
- [97] F. Westheimer; Why nature chose phosphates; *Science* **1987**, *235*, 1173–1178.
- [98] S. A. Benner, D. Hutter; Phosphates, DNA, and the Search for Nonterrestrial Life: A Second Generation Model for Genetic Molecules; *Bioorg. Chem.* **2002**, *30*, 62–80.
- [99] T. Lindahl; Instability and decay of the primary structure of DNA; *Nature* **1993**, *362*, 709–715.
- [100] F. Eckstein; Nucleoside phosphorothioates; *Annu. Rev. Biochem.* **1985**, *54*, 367–402.
- [101] S. Spitzer, F. Eckstein; Inhibition of deoxyribonucleases by phosphorothioate groups in oligodeoxyribonucleotides; *Nucleic Acids Res.* **1988**, *16*, 11691–11704.
- [102] F. Eckstein; Phosphorothioate oligodeoxynucleotides: what is their origin and what is unique about them?; *Antisense Nucleic Acid Drug Dev.* **2000**, *10*, 117–121.
- [103] S. Agrawal, J. Temsamani, J. Y. Tang; Pharmacokinetics, biodistribution, and stability of oligodeoxynucleotide phosphorothioates in mice.; *Proc. Natl. Acad. Sci. U.S.A.* **1991**, *88*, 7595–7599.
- [104] P. J. Furdon, Z. Dominski, R. Kole; RNase H cleavage of RNA hybridized to oligonucleotides containing methylphosphonate, phosphorothioate and phosphodiester bonds; *Nucleic Acids Res.* **1989**, *17*, 9193–9204.
- [105] C. M. Miller, A. J. Donner, E. E. Blank, A. W. Egger, B. M. Kellar, M. E. Østergaard, P. Seth, E. N. Harris; Stabilin-1 and Stabilin-2 are specific receptors for the cellular internalization of phosphorothioate-modified antisense oligonucleotides (ASOs) in the liver; *Nucleic Acids Res.* **2016**, *44*, 2782–2794.

- [106] H. Yanai, S. Chiba, T. Ban, Y. Nakaima, T. Onoe, K. Honda, H. Ohdan, T. Taniguchi; Suppression of immune responses by nonimmunogenic oligodeoxynucleotides with high affinity for high-mobility group box proteins (HMGBs); *Proc. Natl. Acad. Sci. U.S.A.* **2011**, *108*, 11542–11547.
- [107] Z. J. Lesnikowski; Stereocontrolled Synthesis of P-Chiral Analogues of Oligonucleotides; *Bioorg. Chem.* **1993**, *21*, 127–155.
- [108] N. Oka, M. Yamamoto, T. Sato, T. Wada; Solid-Phase Synthesis of Stereoregular Oligodeoxyribonucleoside Phosphorothioates Using Bicyclic Oxazaphospholidine Derivatives as Monomer Units; *J. Am. Chem. Soc.* **2008**, *130*, 16031–16037.
- [109] N. Oka, T. Wada, K. Saigo; An Oxazaphospholidine Approach for the Stereocontrolled Synthesis of Oligonucleoside Phosphorothioates; *J. Am. Chem. Soc.* **2003**, *125*, 8307–8317.
- [110] N. Iwamoto, N. Oka, T. Sato, T. Wada; Stereocontrolled solid-phase synthesis of oligonucleoside H-phosphonates by an oxazaphospholidine approach; *Angew. Chem. Int. Ed. Engl.* **2009**, *48*, 496–499; N. Iwamoto, N. Oka, T. Sato, T. Wada; Stereocontrolled solid-phase synthesis of oligonucleoside H-phosphonates by an oxazaphospholidine approach; *Angew. Chem.* **2009**, *121*, 504–507.
- [111] W. B. Wan, M. T. Migawa, G. Vasquez, H. M. Murray, J. G. Nichols, H. Gaus, A. Berdeja, S. Lee, C. E. Hart, W. F. Lima, et al.; Synthesis, biophysical properties and biological activity of second generation antisense oligonucleotides containing chiral phosphorothioate linkages; *Nucleic Acids Res.* **2014**, *42*, 13456–13468.
- [112] S. M. Gryaznov, D. H. Lloyd, J. K. Chen, R. G. Schultz, L. A. DeDionisio, L. Ratmeyer, W. D. Wilson; Oligonucleotide N3'-->P5' phosphoramidates.; *Proc. Natl. Acad. Sci. U.S.A.* **1995**, *92*, 5798–5802.
- [113] H. An, T. Wang, M. A. Maier, M. Manoharan, B. S. Ross, P. D. Cook; Synthesis of novel 3'-C-methylene thymidine and 5-methyluridine/cytidine H-phosphonates and phosphoramidites for new backbone modification of oligonucleotides; *J. Org. Chem.* **2001**, *66*, 2789–2801.
- [114] O. Heidenreich, S. Gryaznov, M. Nerenberg; RNase H-independent antisense activity of oligonucleotide N3'-->P5' phosphoramidates; *Nucleic Acids Res.* **1997**, *25*, 776–780.

- [115] P. S. Miller, J. Yano, E. Yano, C. Carroll, K. Jayaraman, P. O. Ts'ao; Nonionic nucleic acid analogues. Synthesis and characterization of dideoxyribonucleoside methylphosphonates; *Biochemistry* **1979**, *18*, 5134–5143.
- [116] V. Thiviyanathan, K. V. Vyazovkina, E. K. Gozansky, E. Bichenchova, T. V. Abramova, B. A. Luxon, A. V. Lebedev, D. G. Gorenstein; Structure of hybrid backbone methylphosphonate DNA heteroduplexes: effect of R and S stereochemistry; *Biochemistry* **2002**, *41*, 827–838.
- [117] M. A. Reynolds, R. I. Hogrefe, J. A. Jaeger, D. A. Schwartz, T. A. Riley, W. B. Marvin, W. J. Daily, M. M. Vaghefi, T. A. Beck, S. K. Knowles, et al.; Synthesis and Thermodynamics of Oligonucleotides Containing Chirally Pure R_P Methylphosphonate Linkages; *Nucleic Acids Res.* **1996**, *24*, 4584–4591.
- [118] K. C. Schneider, S. A. Benner; Building blocks for oligonucleotide analogs with dimethylene-sulfide, -sulfoxide, and -sulfone groups replacing phosphodiester linkages; *Tetrahedron Lett.* **1990**, *31*, 335–338.
- [119] C. Richert, A. L. Roughton, S. A. Benner; Nonionic Analogs of RNA with Dimethylene Sulfone Bridges; *J. Am. Chem. Soc.* **1996**, *118*, 4518–4531.
- [120] Y. S. Sanghvi, E. E. Swayze, D. Peoc'h, B. Bhat, S. Dimock; Concept, Discovery and Development of MMI Linkage: Story of a Novel Linkage: for Antisense Constructs; *Nucleosides and Nucleotides* **1997**, *16*, 907–916.
- [121] A. De Mesmaeker, A. Waldner, J. Lebreton, P. Hoffmann, V. Fritsch, R. M. Wolf, S. M. Freier; Amides as a New Type of Backbone Modification in Oligonucleotides; *Angew. Chem. Int. Ed. Engl.* **1994**, *33*, 226–229; A. De Mesmaeker, A. Waldner, J. Lebreton, P. Hoffmann, V. Fritsch, R. M. Wolf, S. M. Freier; Amidverbrückung, eine neue Art der Modifizierung von Oligonucleotidrückgraten; *Angew. Chem.* **1994**, *106*, 237–240.
- [122] A. De Mesmaeker, C. Lesueur, M.-O. Bévière, A. Waldner, V. Fritsch, R. M. Wolf; Amide Backbones with Conformationally Restricted Furanose Rings: Highly Improved Affinity of the Modified Oligonucleotides for Their RNA Complements; *Angew. Chem. Int. Ed. Engl.* **1996**, *35*, 2790–2794; A. De Mesmaeker, C. Lesueur, M.-O. Bévière, A. Waldner, V. Fritsch, R. M. Wolf; Stark erhöhte Affinität modifizierter Oligonucleotide mit in ihrer Konformation eingeschränkten Furanose-Ringen für komplementäre RNA-Stränge; *Angew. Chem.* **1996**, *108*, 2960–2964.

- [123] M. Nina, R. Fonné-Pfister, R. Beaudegnies, H. Chekatt, P. M. J. Jung, F. Murphy-Kessabi, A. De Mesmaeker, S. Wendeborn; Recognition of RNA by amide modified backbone nucleic acids: molecular dynamics simulations of DNA-RNA hybrids in aqueous solution; *J. Am. Chem. Soc.* **2005**, *127*, 6027–6038.
- [124] D. Mutisya, C. Selvam, B. D. Lunstad, P. S. Pallan, A. Haas, D. Leake, M. Egli, E. Rozners; Amides are excellent mimics of phosphate internucleoside linkages and are well tolerated in short interfering RNAs; *Nucleic Acids Res.* **2014**, *42*, 6542–6551.
- [125] P. Nielsen, M. Egholm, R. Berg, O. Buchardt; Sequence-selective recognition of DNA by strand displacement with a thymine-substituted polyamide; *Science* **1991**, *254*, 1497–1500.
- [126] M. Egholm, O. Buchardt, L. Christensen, C. Behrens, S. M. Freier, D. A. Driver, R. H. Berg, S. K. Kim, B. Norden, P. E. Nielsen; PNA hybridizes to complementary oligonucleotides obeying the Watson-Crick hydrogen-bonding rules; *Nature* **1993**, *365*, 566–568.
- [127] S. C. Brown, S. A. Thomson, J. M. Veal, D. G. Davis; NMR solution structure of a peptide nucleic acid complexed with RNA; *Science* **1994**, *265*, 777–780.
- [128] M. Eriksson, P. E. Nielsen; Solution structure of a peptide nucleic acid-DNA duplex; *Nat. Struct. Mol. Biol.* **1996**, *3*, 410–413.
- [129] V. V. Demidov, M. D. Frank-Kamenetskii; Sequence-Specific Targeting of Duplex DNA by Peptide Nucleic Acids via Triplex Strand Invasion; *Methods* **2001**, *23*, 108–122.
- [130] D. F. Doyle, D. A. Braasch, B. A. Janowski, D. R. Corey; Inhibition of Gene Expression Inside Cells by Peptide Nucleic Acids: Effect of mRNA Target Sequence, Mismatched Bases, and PNA Length; *Biochemistry* **2001**, *40*, 53–64.
- [131] C. J. Nulf, D. Corey; Intracellular inhibition of hepatitis C virus (HCV) internal ribosomal entry site (IRES)-dependent translation by peptide nucleic acids (PNAs) and locked nucleic acids (LNAs); *Nucleic Acids Res.* **2004**, *32*, 3792–3798.
- [132] A. M. Siwkowski, L. Malik, C. C. Esau, M. A. Maier, E. V. Wancewicz, K. Albertshofer, B. P. Monia, C. F. Bennett, A. B. Eldrup; Identification and functional validation of PNAs that inhibit murine CD40 expression by redirection of splicing; *Nucleic Acids Res.* **2004**, *32*, 2695–2706.

- [133] R. W. Taylor, P. F. Chinnery, D. M. Turnbull, R. N. Lightowers; Selective inhibition of mutant human mitochondrial DNA replication in vitro by peptide nucleic acids; *Nat. Genet.* **1997**, *15*, 212–215.
- [134] H. J. Larsen, P. E. Nielsen; Transcription-Mediated Binding of Peptide Nucleic Acid (PNA) to Double-Stranded DNA: Sequence-Specific Suicide Transcription; *Nucleic Acids Res.* **1996**, *24*, 458–463.
- [135] K. Albertshofer, A. M. Siwkowski, E. V. Wancewicz, C. C. Esau, T. Watanabe, K. C. Nishihara, G. A. Kinberger, L. Malik, A. B. Eldrup, M. Manoharan, et al.; Structure-activity relationship study on a simple cationic peptide motif for cellular delivery of antisense peptide nucleic acid; *J. Med. Chem.* **2005**, *48*, 6741–6749.
- [136] M. A. Maier, C. C. Esau, A. M. Siwkowski, E. V. Wancewicz, K. Albertshofer, G. A. Kinberger, N. S. Kadaba, T. Watanabe, M. Manoharan, C. F. Bennett, et al.; Evaluation of Basic Amphipathic Peptides for Cellular Delivery of Antisense Peptide Nucleic Acids; *J. Med. Chem.* **2006**, *49*, 2534–2542.
- [137] E. V. Wancewicz, M. A. Maier, A. M. Siwkowski, K. Albertshofer, T. M. Winger, A. Berdeja, H. Gaus, T. A. Vickers, C. F. Bennett, B. P. Monia, et al.; Peptide Nucleic Acids Conjugated to Short Basic Peptides Show Improved Pharmacokinetics and Antisense Activity in Adipose Tissue; *J. Med. Chem.* **2010**, *53*, 3919–3926.
- [138] R. M. Hudziak, E. Barofsky, D. F. Barofsky, D. L. Weller, S. B. Huang, D. D. Weller; Resistance of morpholino phosphorodiamidate oligomers to enzymatic degradation; *Antisense Nucleic Acid Drug Dev.* **1996**, *6*, 267–272.
- [139] J. Summerton, D. Stein, S. B. Huang, P. Matthews, D. Weller, M. Partridge; Morpholino and Phosphorothioate Antisense Oligomers Compared in Cell-Free and In-Cell Systems; *Antisense and Nucleic Acid Drug Dev.* **1997**, *7*, 63–70.
- [140] E. Swayze, B. Bhat; The Medicinal Chemistry of Oligonucleotides; *Antisense Drug Technology Principles, Strategies, and Applications* 2nd Edition, (Ed.: S. Crooke), CRC Press, **2007**, 143–182.
- [141] J. Kurreck, E. Wyszko, C. Gillen, V. A. Erdmann; Design of antisense oligonucleotides stabilized by locked nucleic acids; *Nucleic Acids Res.* **2002**, *30*, 1911–1918.
- [142] C. F. Bennett, B. F. Baker, N. Pham, E. Swayze, R. S. Geary; Pharmacology of Antisense Drugs; *Annu. Rev. Pharmacol. Toxicol.* **2017**, *57*, 81–105.

- [143] B. Schmidtgall, A. P. Spork, F. Wachowius, C. Höbartner, C. Ducho; Synthesis and properties of DNA oligonucleotides with a zwitterionic backbone structure; *Chem. Commun. (Camb.)* **2014**, *50*, 13742–13745.
- [144] B. Schmidtgall, C. Höbartner, C. Ducho; NAA-modified DNA oligonucleotides with zwitterionic backbones: stereoselective synthesis of A-T phosphoramidite building blocks; *Beilstein J. Org. Chem.* **2015**, *11*, 50–60.
- [145] P. Kirsch Elea; Synthese NAA-modifizierter Oligonucleotide mit zwitterionischen Rückgrat-Strukturen; *Master Thesis, Pharmaceutical and Medicinal Chemistry, Saarland University* **2016**.
- [146] V. V. Oberemok, K. V. Laikova, A. I. Repetskaya, I. M. Kenyo, M. V. Gorlov, I. N. Kasich, A. M. Krasnodubets, N. V. Gal'chinsky, I. I. Fomochkina, A. S. Zaitsev, et al.; A Half-Century History of Applications of Antisense Oligonucleotides in Medicine, Agriculture and Forestry: We Should Continue the Journey; *Molecules* **2018**, *23*, 1302-1325.
- [147] T. Nishino, K. Morikawa; Structure and function of nucleases in DNA repair: shape, grip and blade of the DNA scissors; *Oncogene* **2002**, *21*, 9022–9032.
- [148] R. L. Letsinger, C. N. Singman, Gary. Histand, Manikrao. Salunkhe; Cationic oligonucleotides; *J. Am. Chem. Soc.* **1988**, *110*, 4470–4471.
- [149] D. A. Barawkar, T. C. Bruice; Synthesis, biophysical properties, and nuclease resistance properties of mixed backbone oligodeoxynucleotides containing cationic internucleoside guanidinium linkages: Deoxynucleic guanidine/DNA chimeras; *Proc. Natl. Acad. Sci. U.S.A.* **1998**, *95*, 11047–11052.
- [150] H. Challa, T. C. Bruice; Incorporation of positively charged deoxynucleic S-Methylthiourea linkages into oligodeoxyribonucleotides; *Bioorg. Med. Chem. Lett.* **2001**, *11*, 2423–2427.
- [151] R. L. Letsinger, S. A. Bach, J. S. Eadie; Effects of pendant groups at phosphorus on binding properties of d-APa analogues; *Nucleic Acids Res.* **1986**, *14*, 3487–3499.
- [152] H. Saneyoshi, K. Seio, M. Sekine; A General Method for the Synthesis of 2'-O-Cyanoethylated Oligoribonucleotides Having Promising Hybridization Affinity for DNA and RNA and Enhanced Nuclease Resistance; *J. Org. Chem.* **2005**, *70*, 10453–10460.

- [153] E. J. Williams, S. C. Sung, M. Laskowski; Action of venom phosphodiesterase on deoxyribonucleic acid; *J. Biol. Chem.* **1961**, *236*, 1130–1134.
- [154] M. Meng, B. Schmidtgall, C. Ducho; Enhanced Stability of DNA Oligonucleotides with Partially Zwitterionic Backbone Structures in Biological Media; *Molecules* **2018**, *23*, 2941-2952.
- [155] D. P. Arya, T. C. Bruice; Positively Charged Deoxynucleic Methylthioureas: Synthesis and Binding Properties of Pentameric Thymidyl Methylthiourea; *J. Am. Chem. Soc.* **1998**, *120*, 12419–12427.
- [156] R. O. Dempcy, K. A. Browne, T. C. Bruice; Synthesis of the Polycation Thymidyl DNG, Its Fidelity in Binding Polyanionic DNA/RNA, and the Stability and Nature of the Hybrid Complexes; *J. Am. Chem. Soc.* **1995**, *117*, 6140–6141.
- [157] D. P. Arya, T. C. Bruice; Fidelity of Deoxynucleic S-Methylthiourea (DNmt) Binding to DNA Oligomers: Influence of C Mismatches; *J. Am. Chem. Soc.* **1999**, *121*, 10680–10684.
- [158] B. A. Linkletter, I. E. Szabo, T. C. Bruice; Solid-Phase Synthesis of Deoxynucleic Guanidine (DNG) Oligomers and Melting Point and Circular Dichroism Analysis of Binding Fidelity of Octameric Thymidyl Oligomers with DNA Oligomers; *J. Am. Chem. Soc.* **1999**, *121*, 3888–3896.
- [159] N. Papargyri, M. Pontoppidan, M. R. Andersen, T. Koch, P. H. Hagedorn; Chemical Diversity of Locked Nucleic Acid-Modified Antisense Oligonucleotides Allows Optimization of Pharmaceutical Properties; *Mol. Ther. - Nucleic Acids* **2020**, *19*, 706–717.
- [160] R. Brock; The Uptake of Arginine-Rich Cell-Penetrating Peptides: Putting the Puzzle Together; *Bioconjugate Chem.* **2014**, *25*, 863–868.
- [161] R. L. Juliano, X. Ming, K. Carver, B. Laing; Cellular uptake and intracellular trafficking of oligonucleotides: implications for oligonucleotide pharmacology; *Nucleic Acid Ther.* **2014**, *24*, 101–113.
- [162] F. Debart, S. Abes, G. Deglane, H. Moulton, P. Clair, M. Gait, J.-J. Vasseur, B. Lebleu; Chemical Modifications to Improve the Cellular Uptake of Oligonucleotides; *Curr. Top. Med. Chem.* **2007**, *7*, 727–737.
- [163] Y. Wang, L. Miao, A. Satterlee, L. Huang; Delivery of oligonucleotides with lipid nanoparticles; *Adv. Drug Delivery Rev.* **2015**, *87*, 68–80.

- [164] M. A. Lysik, S. Wu-Pong; Innovations in oligonucleotide drug delivery; *J. Pharm. Sci.* **2003**, *92*, 1559–1573.
- [165] J. Soutschek, A. Akinc, B. Bramlage, K. Charisse, R. Constien, M. Donoghue, S. Elbashir, A. Geick, P. Hadwiger, J. Harborth, et al.; Therapeutic silencing of an endogenous gene by systemic administration of modified siRNAs; *Nature* **2004**, *432*, 173–178.
- [166] A. Astriab-Fisher, D. Sergueev, M. Fisher, B. R. Shaw, R. L. Juliano; Conjugates of antisense oligonucleotides with the Tat and antennapedia cell-penetrating peptides: effects on cellular uptake, binding to target sequences, and biologic actions; *Pharm. Res.* **2002**, *19*, 744–754.
- [167] M. Pooga, M. Hällbrink, M. Zorko, U. Langel; Cell penetration by transportan; *FASEB J.* **1998**, *12*, 67–77.
- [168] U. Koppelhus, S. K. Awasthi, V. Zachar, H. U. Holst, P. Ebbesen, P. E. Nielsen; Cell-dependent differential cellular uptake of PNA, peptides, and PNA-peptide conjugates; *Antisense Nucleic Acid Drug Dev.* **2002**, *12*, 51–63.
- [169] P. L. Iversen, K. M. Aird, R. Wu, M. M. Morse, G. R. Devi; Cellular uptake of neutral phosphorodiamidate morpholino oligomers; *Curr. Pharm. Biotechnol.* **2009**, *10*, 579–588.
- [170] K. Skakuj, K. E. Bujold, C. A. Mirkin; Mercury-Free Automated Synthesis of Guanidinium Backbone Oligonucleotides; *J. Am. Chem. Soc.* **2019**, *141*, 20171–20176.
- [171] R. O. Dempcy, O. Almarsson, T. C. Bruice; Design and synthesis of deoxynucleic guanidine: a polycation analogue of DNA; *Proc. Natl. Acad. Sci. U.S.A.* **1994**, *91*, 7864–7868.
- [172] M. Meng, C. Ducho; Oligonucleotide analogues with cationic backbone linkages; *Beilstein J. Org. Chem.* **2018**, *14*, 1293–1308.
- [173] M. L. Jain, P. Y. Bruice, I. E. Szabó, T. C. Bruice; Incorporation of positively charged linkages into DNA and RNA backbones: a novel strategy for antigene and antisense agents; *Chem. Rev.* **2012**, *112*, 1284–1309.
- [174] E. Linnane, P. Davey, P. Zhang, S. Puri, M. Edbrooke, E. Chiarparin, A. S. Revenko, A. R. Macleod, J. C. Norman, S. J. Ross; Differential uptake, kinetics and mechanisms of

- intracellular trafficking of next-generation antisense oligonucleotides across human cancer cell lines; *Nucleic Acids Res.* **2019**, *47*, 4375–4392.
- [175] M. Frigerio, M. Santagostino, S. Sputore; A User-Friendly Entry to 2-Iodoxybenzoic Acid (IBX); *J. Org. Chem.* **1999**, *64*, 4537–4538.
- [176] U. Schmidt, A. Lieberknecht, U. Schanbacher, T. Beuttler, J. Wild; Facile Preparation of *N*-Acyl-2-(diethoxyphosphoryl)glycine Esters and Their Use in the Synthesis of Dehydroamino Acid Esters; *Angew. Chem. Int. Ed. Engl.* **1982**, *21*, 776–777; U. Schmidt, A. Lieberknecht, U. Schanbacher, T. Beuttler, J. Wild; Einfache Herstellung von *N*-Acyl-2-(diethoxyphosphoryl)-glycinestern und ihre Verwendung zum Aufbau von Dehydroaminosäureestern; *Angew. Chem.* **1982**, *94*, 797-798.
- [177] U. Schmidt, A. Lieberknecht, J. Wild; Amino Acids and Peptides; XLIII¹. Dehydroamino Acids; XVIII². Synthesis of Dehydroamino Acids and Amino Acids from *N*-Acyl-2-(dialkyloxyphosphinyl)-glycin Esters; II; *Synthesis* **1984**, *1984*, 53–60.
- [178] U. Schmidt, J. Wild; Synthesen von Peptidalkaloiden, 11. Über Aminosäuren und Peptide, 51. — Dehydroaminosäuren, 19. Totalsynthese von Hexaacetylcelenamid A; *Liebigs Ann. Chem.* **1985**, *1985*, 1882–1894.

6. Appendix

6.1 Studies on the Cellular Uptake of the Partially Zwitterionic NAA/LNA-Gapmer

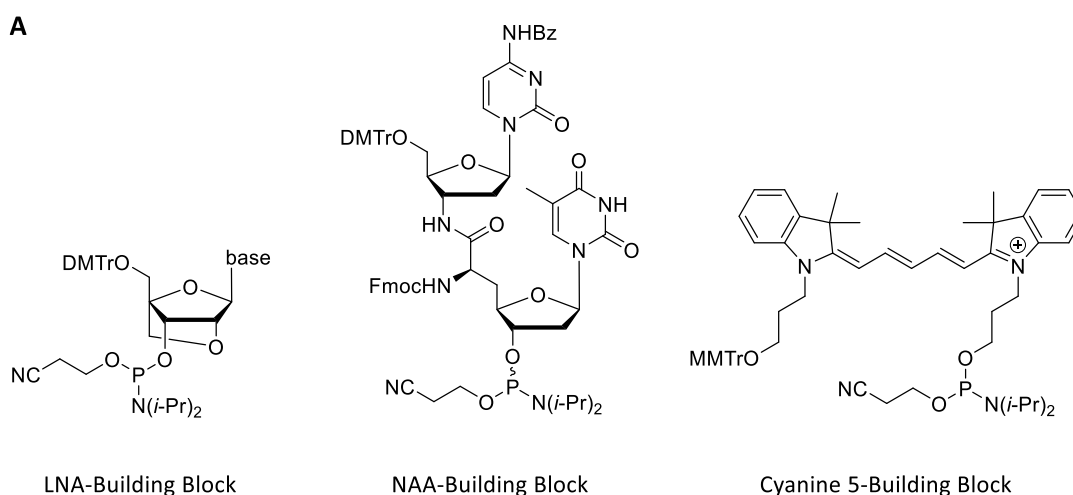
Insufficient cellular uptake represents one of the main obstacles hampering the efficacy of ONs as biomedical agents.^[161] Due to their anionic backbone structure, in combination with their hydrophilic sugar units, native ONs represent extremely polar oligomers. Consequently, diffusion over lipophilic cellular membranes is strongly hindered what again prohibits interaction with intracellular targets. In recent years, many attempts have been made to overcome this issue.^[162] The most prominent approaches include (i) the transport of ONs in macromolecular vesicles, like cationic lipids^[163] or cyclodextrins^[164], (ii) formation of ON-conjugates with *e.g.* cholesterol^[165] or CPPs^[166,167] at the 3'- or 5'-end and (iii) the chemical modification of the overall ON structure to yield artificial DNA congeners with improved uptake properties, as in PNA^[168], PMOs^[169] or for deoxyribonucleic guanidines (DNGs)^[170]. However, a detailed overview of the above-named strategies would be beyond the scope of this work. Therefore, a brief summary regarding DNG-modified oligomers is provided, as their backbone charge pattern is comparable with the cationic NAA-modification.^[171] In this context, a successful approach demonstrating the enhanced cellular uptake of a DNG ON was reported by *Mirkin* and co-workers.^[170] They explored a new synthetic procedure for the preparation of completely cationic DNG ONs, first conceptualized by *Bruice* et al.,^[172,173] and subsequently evaluated their cellular uptake. Interestingly, *Mirkin* et al. were able to show that a fully cationic DNG 10-mer surpasses the lipophilic membrane of human C166 cells significantly better than a native DNA ON of the same sequence.^[170] A possible explanation for the increased uptake of the positively charged DNG might be the mimicry of arginine-rich CPPs.^[160] In any case, this concept showed great similarity, in terms of the backbone charge pattern, to the idea of the NAA-modification. Still, the efficient use of completely cationic systems as antisense agents remains questionable, especially with respect to the results obtained for fully NAA-modified ONs (Manuscript **B**). Here, although a drastic increase of counterstrand affinity was confirmed, a significant loss in mismatch sensitivity could be observed. Thus, the focus of the cellular uptake studies on NAA-modified oligomers was set on the partially zwitterionic gapmer structure **C-1**, which was proven to possess extremely beneficial

properties regarding its biological stability, target recognition and mismatch sensitivity (Manuscript **C**). Consequently, it was aspired to synthesize gapmer **A** (Figure 6.1 B), a 5'-fluorophore labeled version of **C-1**, to examine the effect of the zwitterionic gap on lipophilicity and membrane penetration. Furthermore, it was planned to construct a fluorophore-labeled version of the anionic DNA/LNA-gapmer **C-2** (gapmer **B**, Figure 6.1 B), to obtain a directly comparable control to the zwitterionic NAA/LNA-chimera. As fluorophore for the tracking of the cellular uptake process, cyanine 5 (Cy5, Figure 6.1 B) was chosen. This was the case because attachment of a fluorophore phosphoramidite to the 5'-end of the gapmer would result in an additional phosphodiester bond and thus, in another negative charge. Cy5, however, possesses a permanently cationic moiety, which can compensate for the additional negative backbone linkage. Furthermore, Cy5 represents a rather small fluorescent unit. It was therefore anticipated to create an intracellularly trackable compound without too much alteration of the structure and charge pattern of the actual gapmer. The synthesis and evaluation of gapmers **A** and **B** are described in the following chapters.

6.1.1 Synthesis of the Fluorophore-Labeled NAA/LNA- and DNA/LNA-Gapmers

The synthesis of the Cy5-labeled gapmers **A** and **B** (*Figure 6.1 B*) was performed following a protocol very similar to that of the non-fluorescent gapmers **C-1** and **C-2** described in Manuscript **C**. Like for **C-1**, the dimeric CxT-phosphoramidite building block (NAA (x)-Building Block, *Figure 6.1 A*) was assembled starting from thymidine and 2'-deoxycytidine, respectively. With this building block in hand, automated DNA synthesis was performed to furnish gapmers **A** and **B**. The CxT-module (for **A**), commercially available DNA phosphoramidites in case of gapmer **B**, LNA phosphoramidites as well as the 4-monomethoxytrityl (MMTr)-protected Cy5-phosphoramidite (*Figure 6.1 A*) were used for the automated synthesis. Prior to synthesis, the CxT-building block was dissolved in a 1:1 mixture of dry MeCN/CH₂Cl₂ to a final concentration of 0.05 M. It has to be noted that higher concentrations of the CxT-phosphoramidite always led to precipitation on the synthesizer and thus, had to be avoided. DNA synthesis was performed in the usual 3'- to 5'-direction, with the Cy5-fluorophore being the last phosphoramidite to be coupled. Different coupling protocols, depending on the applied phosphoramidite, were used. In case of gapmer **B**, coupling times for the DNA phosphoramidites placed in the gap region of the ON were set to 2 min. The LNA phosphoramidites positioned in the flanks of the sequence were coupled for 5 min. Concerning the NAA CxT-building block used for gapmer **A**, a triple-coupling procedure was utilized. Therefore, the phosphoramidite/activator mix was flushed over the column and coupled for 90 seconds. Subsequently, the mixture was replaced by a fresh amount of CxT/activator mix, which was again coupled for another 90 seconds. Lastly, fresh mixture was once more flushed over to column and coupled for 3 min. Consequently, the three coupling steps added up to a total coupling time of 6 min for the NAA-building block. The same procedure was applied for the Cy5-fluorophore building block. Unreacted 5'-OH groups were capped by typical acetylation procedure. The oxidation step to furnish the phosphodiester backbone was performed by addition of iodine solution. The efficiency of every coupling step was observed *via* trityl monitoring. It has to be noted that the efficiency of the coupling of the Cy5-phosphoramidite could not be determined by this procedure for two reasons: (i) the Cy5-label possesses a strong blue color, which interfered with the detection method and (ii) the Cy5-building block carried a MMTr-protection group instead of a DMTr-unit, which requires a different wavelength

region. Hence, trityl monitoring constantly recorded poor yields for the last coupling step (diagram not shown).



B

Gapmer **A**: 5'-**Cy5**-A^LG^LA^LT^LC^xTC^xTC^xTC^xTA^LG^LA^LT^L-3'

Gapmer **B**: 5'-**Cy5**-A^LG^LA^LT^LCTCTCTCTA^LG^LA^LT^L-3'

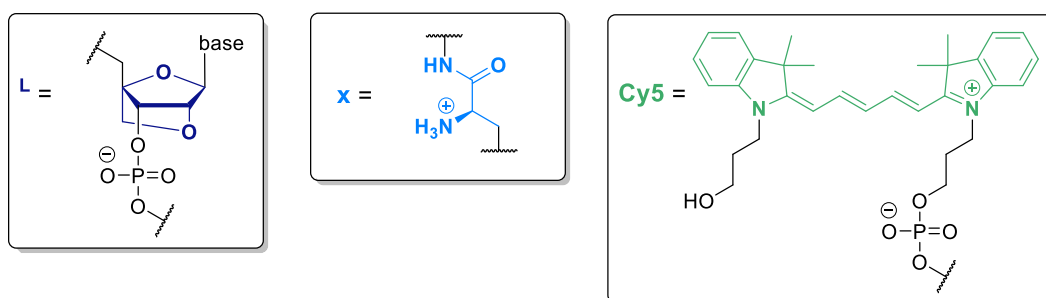


Figure 6.1. Cy5-labeled gapmers for studies on cellular uptake. **A**: Building blocks required for the automated DNA synthesis of gapmers **A** and **B**. **B**: Base sequence and modification pattern of gapmers **A** and **B**. ^L = LNA-modification, ^x = NAA-modification, **Cy5** = Cyanine 5 fluorophore label.

Following these conditions, gapmers **A** and **B** were assembled. Thereby, the same sequences as used for **C-1** and **C-2** were chosen, with the additional introduction of the 5'-fluorophore label (*Figure 6.1*). After completion of all synthetic cycles, gapmers **A** and **B** were globally deprotected and cleaved from the CPG resin. Therefore, standard conditions (NH₃(25%)/EtOH 3:1, 55 °C, 22 h) were first tested on gapmer **B**, with the addition of aluminum foil wrapped around the Eppendorf tube to protect the fluorophore label against light-mediated degradation. Here, with regard to the small quantities that were available of both gapmers, this established protocol was chosen to obtain efficient global deprotection. Subsequent ureaPAGE (not shown) and mass spectrometry analysis (*Table*

6.1) of **B** showed satisfying cleavage of all remaining protection groups as well as high stability of the Cy5-label towards the basic conditions. Thus, no adjustments regarding the newly introduced Cy5-fluorophore were made. After cleavage of both gapmers from the CPG resin, the obtained crude ONs were purified and desalted using the ureaPAGE protocol also used for gapmers **C-1** and **C-2** in Manuscript **C**. The identity of each gapmer was then confirmed *via* high resolution mass spectrometry (HRMS). Considering the large size of the ONs, in combination with the limited available amounts, both gapmers were directly injected into the ion source. For better comparability, the expected masses of **A** and **B** were calculated from their chemical structures, respectively. Masses found were deconvoluted and compared to the predicted masses. The resulting data are given in *Table 6.1*.

Table 6.1. High resolution mass data of gapmer **A** and **B**. Calculated values correspond to the exact masses of **A** and **B**, found values refer to the respective deconvoluted mass spectra.

Gapmer Sequence 5'→3'	Chemical Formula	Calculated	Found
A: Cy5-A ^L G ^L A ^L T ^L CxTCxTCxTCxTA ^L G ^L A ^L T ^L T	C ₂₁₃ H ₂₆₀ N ₆₆ Na ₂ O ₁₀₃ P ₁₃ ⁺	5838.3515	5838.3442
B: Cy5-A ^L G ^L A ^L T ^L CTCTCTCTA ^L G ^L A ^L T ^L T	C ₂₀₅ H ₂₅₀ N ₅₈ O ₁₁₅ P ₁₇ ⁺	5890.1031	5890.1029

Satisfactorily, the masses for both gapmers were found and could be confirmed through the calculated values. Concerning gapmer **A**, the mass with the highest abundance was a positively charged species incorporating two sodium ions (*Table 6.1*). Regarding **B**, the cationic parental mass without sodium was primarily detectable (*Table 6.1*).

Following the successful synthesis of **A** and **B**, the capability of both gapmeric structures to surpass lipophilic barriers was evaluated. Therefore, two different methods were applied to monitor the cellular uptake of the Cy5-gapmers into living cells: (i) fluorescence-activated cell sorting (FACS) and (ii) entrance-tracking through confocal microscopy. Thereby, FACS analysis should be used to provide information about the approximate amount of the intracellularly accumulated partially zwitterionic gapmer **A** relative to anionic **B**. On the other hand, the confocal microscopy experiments were chosen to gain insights regarding the intracellular distribution of both gapmers. Here, the focus was set on the question whether the Cy5-ONs remain in endosomes after passing through the cell membrane or appear freely in the cytosol. The respective experiments as well as the according results are described in the following sections.

6.1.2 Evaluation of the Fluorophore-Labeled NAA/LNA- and DNA/LNA-Gapmers

The experiments described in section 6.1.2.1 were performed in cooperation with the group of Prof. A. K. Kiemer at the Department of Pharmacy, Pharmaceutical Biology, Saarland University, and conducted by Dr. J. Hoppstädter. Experiments described in section 6.1.2.2 were performed in cooperation with the group of Prof. C.-M. Lehr, at the Helmholtz Institute for Pharmaceutical Research Saarland, and supervised by Dr. B. Loretz.

6.1.2.1 Fluorescence-Activated Cell Sorting (FACS) Analysis

For FACS analysis of the cellular uptake of the gapmer structures **A** and **B**, A549 cells were utilized. This cell line was chosen based on recent studies regarding the uptake of antisense ONs by Ross and co-workers.^[174] In their work, Ross reviewed a broad spectrum of different cell lines and cell types with respect to their permeability for antisense ONs. In this context, A549 cells were shown to have a well-balanced uptake behavior, meaning that neither too much nor too little of the ON was absorbed. Thus, they represented a suitable module system.

Two different assay setups were designed to investigate the cellular uptake of **A** and **B**. In a first set of experiments, it was envisioned to gain insights regarding the required amounts of the Cy5 fluorophore-labeled gapmers to produce a sufficiently strong signal. Furthermore, the expected concentration-dependent uptake behavior of **A** and **B** should be confirmed (*Figure 6.2 A*). Therefore, the A549 cells were treated with three different concentrations of **A** and **B** (100 nM, 300 nM, 500 nM). The initial incubation time was set to 1 h. Satisfactorily, a robust signal could already be achieved for the lowest tested amount of 100 nM. Hence, this concentration was also applied for the second, subsequent study. These following experiments concerned the influence of the incubation time on cellular uptake. Here the contact time with the A549 cells was set to be either 1 h, 4 h or 8 h (*Figure 6.2 B*). For both setups, every data point represents the mean value of technical triplicates. The resulting data after FACS analysis were normalized against the average mean area (APC-A) of the measured fluorescent signal of either **B** (100 nM, *Figure 6.2 A*) or **B** (1 h, *Figure 6.2 B*), to obtain easily comparable results.

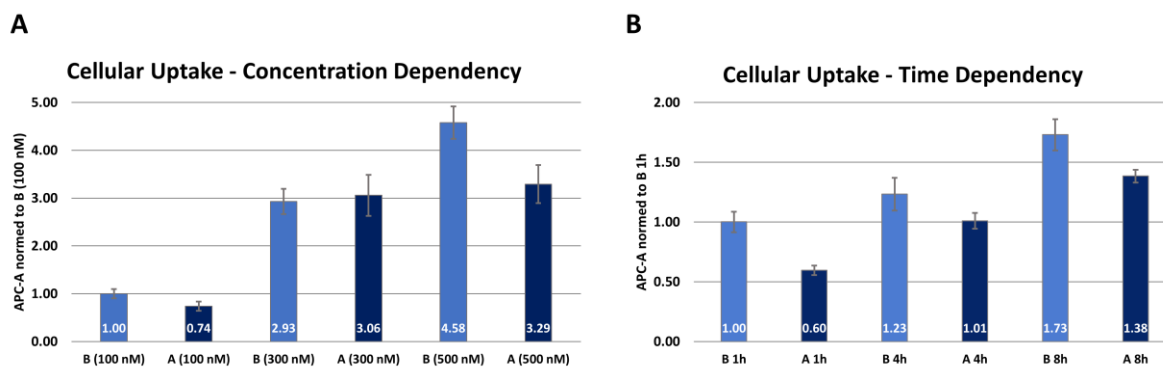


Figure 6.2. Tracking of the cellular uptake of the fluorophore-labeled gapmers **A** and **B** through FACS analysis. **A:** Cellular uptake of **A** and **B** as a function of the applied concentration (100, 300 and 500 nM). All values were obtained after 1 h of incubation and normalized to the APC-A value measured for **B** (100 nM). **B:** Cellular uptake of **A** and **B** as a function of the incubation time (1, 4 and 8 h). All values were obtained after incubation with 100 nM of either **A** or **B**, respectively, and normalized to the APC-A value measured for **B** (1 h).

Interestingly, neither in the concentration- (*Figure 6.2 A*) nor in the time-dependent assay setup (*Figure 6.2 B*) cellular uptake of **A** was observed to be superior to **B**. This was unexpected, since former studies had reported an improved uptake of ONs carrying positively charged segments.^[162] A possible explanation might be that, due to the alternating charge pattern in the central gap, **A** adopts a coiled topology, which then hampers uptake into the cell. Nevertheless, the data shown for the FACS analysis are only preliminary and further experiments, including the usage other cell types, have to be performed in order to make substantiated statements regarding the cellular uptake of **A**.

6.1.3.2 Confocal Microscopy

For tracing of the cellular uptake of **A** and **B** *via* confocal microscopy, a protocol utilizing three different dyes was applied. Staining of the actin filaments was achieved using A488 – phalloidin and cell nuclei were visualized through application of 4',6-diamidino-2-phenylindole (DAPI) staining solution. Finally, the two gapmers were made visible through their attached Cy5-fluorophore. To obtain results comparable to those of the FACS analysis experiments, A549 cells were also used for the confocal microscopy-monitored uptake studies on gapmers **A** and **B**. To obtain an initial overview regarding the required amounts of Cy5-labeled gapmer to generate an adequate fluorescence signal, three different concentrations of **A** and **B** were chosen (50 nM, 100 nM, 500 nM). Additionally, to achieve a first impression about the cellular uptake of the two gapmer structures, the incubation time was set to 1 h. This rather short time frame was selected with the aim to reduce the

overall stress put on the cells and hence, to increase the chance of recording preliminary, informative results. As positive control, two different amounts of the NAA/LNA-gapmer **A** (500 nM and 50 nM, *Figure 6.3*) were transfected into the A549 cells to mimic cellular uptake and thus, the signals that can be expected after successful permeation of the ONs over the cellular membrane. As negative control, cells solely stained with phalloidin and DAPI were used.

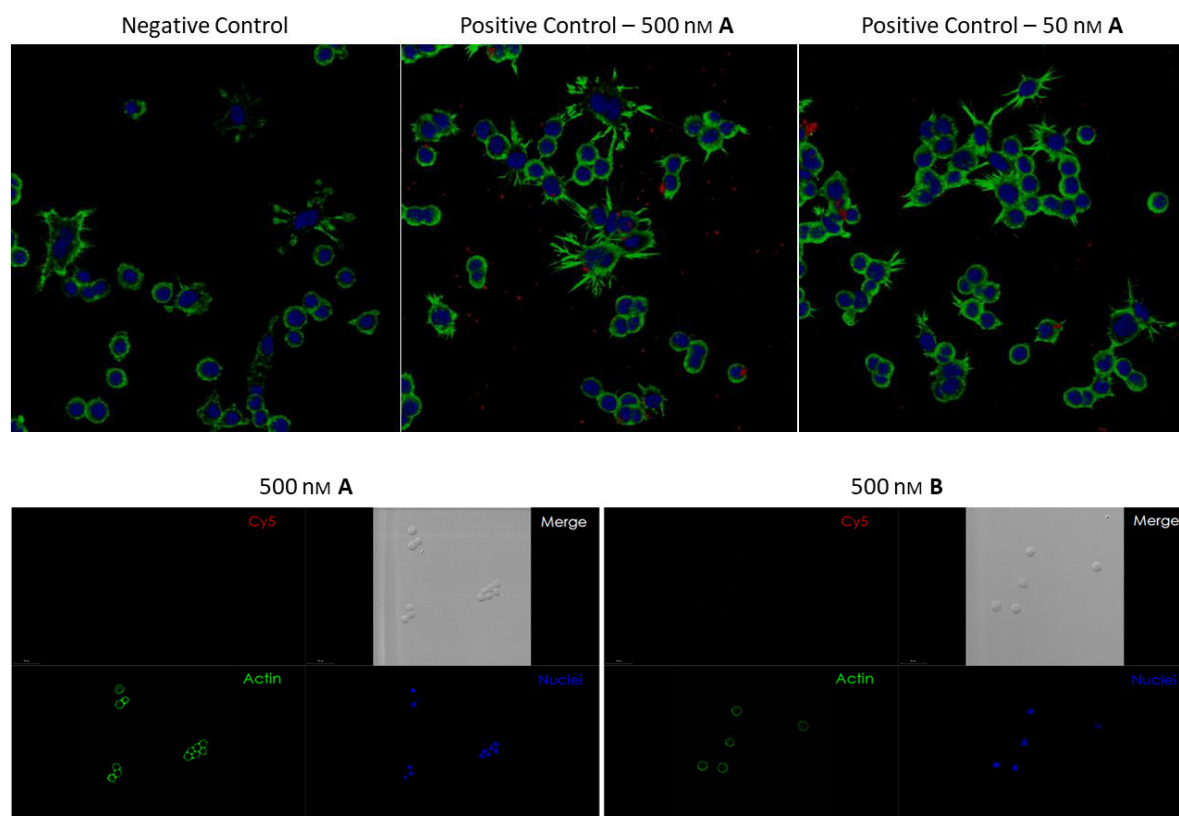


Figure 6.3. Results of the first confocal microscopy analysis of the cellular uptake of gapmers **A** and **B**. The upper panel shows the merged images of the negative control (left) and the two positive controls containing 500 nM and 50 nM of **A**, respectively. Actin filaments appear in green, nuclei in blue and gapmers in red. The second panel depicts the merged, as well as the individual signals recorded for **A** (left) and **B** (right).

The results achieved for this initial experiment are given in *Figure 6.3*. All panels depicted in *Figure 6.3* demonstrate the successful staining of the cellular cytoskeleton (green) as well as an effective DAPI-staining of the nuclei (blue). Furthermore, the two positive controls, as seen in the upper row, show satisfying signals corresponding to the transfected gapmer **A** at both 500 nM and 50 nM (red). However, with respect to the untransfected cells, none of the applied amounts of either **A** or **B** resulted in observable fluorescence signals (bottom row, *Figure 6.3*), which again means that no cellular uptake had taken place. Here, it has to

be noted that, due to a combination of undesirable events, the number of remaining cells on the chamber slides after the fixation and staining procedure was extremely low. A possible explanation for the loss of most of the cells is the uncoated surface of the used chamber slides, which prevented sufficient support of the A549 cells. Furthermore, some of the numerous washing steps might have been too harsh for the loosely attached cells. As a result, many cells might have been lost due to the PBS washing circles. Thus, it should be emphasized that the preliminary data shown in *Figure 6.3* cannot be considered as representative for the uptake of the two gapmers.

In summary, the results obtained from this study are only preliminary and the overall procedure still requires some improvement. For instance, future confocal measurements should be carried out with the cells attached to another type of chamber slides, preferably with a rougher surface structure. As described above, the slides used during this first analysis were non-coated and did not support an adherent growth of the A549 cells, which again led to loss of most of the cells due to the required washing steps. Consequently, no signals implicating the cellular entrance of neither gapmer **A** nor **B** could be confirmed. Furthermore, the remaining cells were shown to have adapted a rather roundish shape, which is not representative for alveolar epithelial cells. Thus, for subsequent experiments a fresh batch of A549 should be used. Also, to achieve an additional boost in signal intensity, it might be beneficial to enhance the incubation time when applying the Cy5 gapmers. In the aforementioned procedure, a time frame of 1 h was chosen to gain a first impression of the uptake of **A** and **B**. However, with respect to the results obtained by *Mirkin* and co-workers,^[170] it might be appropriate to enhance the duration of incubation to at least 2.5 h to ensure the emergence of robust signals. Nonetheless, both positive controls incorporating concentrations of either 500 nM or 50 nM of the transfected Cy5-labeled NAA/LNA-gapmer **A** resulted in nicely detectable signals. This confirmed that a sufficient signal can be obtained by utilizing small concentrations of ON, which is an important insight regarding compound sustainability. Altogether, it can be concluded that the first attempt to visualize the cellular uptake of the two Cy5-labeled gapmers did not provide any reliable information regarding the improved capability of gapmer **A** to surpass lipophilic barriers. However, valuable insights concerning the overall setup of future confocal microscopy studies could be obtained and thus, will be useful in the design of upcoming experiments.

6.1.3 Experimental Section

6.1.3.1 Synthesis of Cy5-labeled Gapmers A and B

Gapmers **A** and **B** were synthesized using a H-8 standard synthesizer (*K&A*) from 3'→5' direction under strict exclusion of oxygen (argon atmosphere) on columns with nucleoside-loaded CPG resin (200 nmol of 5'-*O*-DMTr-nucleoside/g matrix, *K&A*). Unmodified DNA phosphoramidites (*Glen Research*), LNA phosphoramidites (*QIAGEN*) and MMTr-protected Cyanine 5 phosphoramidite (*Sigma Aldrich*) were purchased and prepared according to the manufacturers' protocol. Before usage, the CxT phosphoramidite was dissolved in a mixture of MeCN/CH₂Cl₂ (1:1) to a final concentration of 0.05 M. Cleavage of the 5'-DMTr protection group of the CPG-bound nucleoside through 3% trichloroacetic acid (TCA) in CH₂Cl₂ started the first reaction cycle. Subsequent flushing of the column with MeCN and argon removed excess of acid. Then, a mixture of activator and phosphoramidite (benzylmercaptotetrazole (BMT), 0.25 M, *EMP Biotech*) were flushed on the column. Coupling times varied depending on the applied phosphoramidite: unmodified DNA phosphoramidites (2 min), LNA phosphoramidites (5 min), CxT phosphoramidite and Cy5 phosphoramidite (triple coupling: 2 x 90 s, 1 x 3 min). After every coupling step excess of reagents was removed with MeCN and argon. Unreacted 5'-OH groups were deactivated through a capping step ('Cap A', acetic anhydride, 2,6-dimethylpyridine, THF, *Sigma Aldrich* and 'Cap B', 1-methylimidazole, THF, *Sigma Aldrich*). Subsequent oxidation with 0.1 M iodine solution (iodine, THF, *Sigma Aldrich*) furnished the final phosphate diester backbone. Lastly, application of 3% TCA in CH₂Cl₂ caused deprotection of the new 5'-end and started the next reaction cycle. Trityl monitoring was used to measure the coupling efficiency. ON cleavage and global deprotection were achieved through application of the standard deprotection protocol (NH₃(25%)-EtOH, 3:1, 55 °C, 22 h) in an aluminum foil wrapped Eppendorf tube. After incubation, the remaining CPG resin was removed through centrifugation and washed three times with 50 µL ultrapure water. The resulting solvent mixture was removed *in vacuo* and the residual crude solid was dissolved in ultrapure water (100 µL). A NanoDrop 2000 Spectrophotometer (*Thermo Scientific*) was used to define the amount of crude ON mixture before further purification. Crude ON concentration before UreaPAGE (assuming hypothetical purity): Gapmer **A**: 92 nmol, Gapmer **B**: 61 nmol.

6.1.3.2 Purification of Gapmers A and B

For purification of gapmers **A** and **B** electrophoresis with a sequencing ureaPAGE gel was used (1.5 mm thickness, 28 cm isolating distance, 20% polyacrylamide, 7 M urea). The crude ON mixture was mixed with loading buffer (90% formamide, 10% glycerol, bromophenol blue) (2:1), applied on the gel (20 nmol per well) and run in 0.5 x TBE buffer for 2.5 h at 35 W (10 x TBE-running buffer: 890 mM Tris, 890 mM boric acid, 20 mM EDTA, pH 8.3). Position of the Cy5-labeled gapmers was visible through the blue color of the Cy5-fluorophore. Subsequently, the blue band was cut from the gel and incubated two times with TEN extraction buffer (300 μ L, 0.01 M Tris (pH 8.0), 0.001 M EDTA (pH 8.0), 0.3 M NaCl) for 16 h. The resultant mixture was dried *in vacuo* and the solid was dissolved in ultrapure water (300 μ L). For desalination, NaOAc solution (30 μ L, 3 M, pH 5.2) and EtOH (1.2 mL, 99%, -25 $^{\circ}$ C) were added and the mixture was stored at -80 $^{\circ}$ C for 24 h to initiate precipitation. Next, centrifugation (-4 $^{\circ}$ C, 60 min, 13000 rpm) led to pellet formation. The supernatant was removed, the pellet was washed twice with EtOH (95%, -25 $^{\circ}$ C) and subsequently dried under reduced pressure. This yielded 6.2 nmol of gapmer **A** (3.1% over all coupling steps and purification) and 5.1 nmol of gapmer **B** (2.3% over all coupling steps and purification). The identities of **A** and **B** were obtained by HRMS (direct injection of 100 μ L, 4 μ M). Data were obtained using an Ultimate 3000 system by *Thermo Scientific* with a Dionex UltiMate 3000 UHPLC system in positive mode. The system contained a pump, autosampler, column department, diode array detector and a *Thermo Scientific* Q Exactive Orbitrap.

6.1.3.3 Fluorescence-Activated Cell Sorting (FACS) Analysis

A549 cells were seeded in 12-well plates using RPMI 1640 medium containing 10% FCS and grown for two days until a confluent layer was formed (5% CO₂, 37 $^{\circ}$ C). Next, the medium was aspirated, cells were washed with PBS buffer (500 μ L per well) and the Cy5-labeled gapmers **A** (*concentration-dependent setup*: 100 nM, 300 nM, 500 nM of **A** in PBS, 500 μ L per well, 60 min, 37 $^{\circ}$ C; *time-dependent setup*: 100 nM of **A** in PBS, 500 μ L per well, 1 h/4 h/8 h, 37 $^{\circ}$ C) and **B** (*concentration-dependent setup*: 100 nM, 300 nM, 500 nM of **B** in PBS, 500 μ L per well, 60 min, 37 $^{\circ}$ C; *time-dependent setup*: 100 nM of **B** in PBS, 500 μ L per well, 1 h/4 h/8 h, 37 $^{\circ}$ C) were added, respectively. After incubation, gapmer-containing PBS

was aspirated and cells were washed twice with PBS (500 μ L per well). Then, cells were harvested using a cell scraper, collected in FACS tubes and stored on ice until they were used. Cells not incubated with the Cy5-gapmers served as negative control and calibration standard for the FACS measurements. For every FACS run, 10000 singlet-events were recorded. FACS analysis was performed on a BD LRS Fortessa (*BD Biosciences*).

6.1.3.4 Confocal Microscopy

A549 cells were seeded in chamber slides (40.000 cells per slide, μ -Slide 8 well, uncoated, *ibidi*) using RPMI 1640 medium containing 10% FCS and grown for two days until a confluent layer was formed (5% CO₂, 37 °C). Next, the medium was aspirated, cells were washed twice with PBS buffer (2 x 200 μ L per well) and then fixed using freshly prepared paraformaldehyde (PFA) solution (3% in PBS, 200 μ L per well, 20 min, RT). Subsequently, PFA was removed through two washing steps with PBS (200 μ L per well) and blocking and permeabilization (B/P) solution (1% bovine serum albumin (BSA) and 0.05% saponin in PBS, 150 μ L per well, 20 min, RT) were added. For staining of the actin filaments, phalloidin (stock of 1000x, *Invitrogen*, diluted to 1x in PBS, 150 μ L per well, 20 min, RT) was added to the B/P solution. Afterwards, the staining solution was aspirated and cells were washed twice with PBS buffer (200 μ L per well) to remove residual dye. DAPI solution (0.5 mg/mL in PBS, *Sigma*, 200 μ L per well, 20 min, RT) for staining of the nuclei was applied and the cells were again incubated. After aspiration of the DAPI solution and two washing steps with PBS (200 μ L per well), the gapmers **A** (50 nM, 100 nM and 500 nM in PBS, 100 μ L per well, 60 min, RT) and **B** (50 nM, 100 nM and 500 nM in PBS, 100 μ L per well, 60 min, RT) were added. As positive control, gapmer **A** (500 nM and 50 nM, respectively) was transfected to the A549 cells using the jetPRIME® in vitro DNA & siRNA transfection reagent (*Polyplus transfection*) according to the manufacturer's protocol. As negative control, cells only stained with phalloidin and DAPI were used. All incubation conditions were performed as triplicates. After incubation, cells were washed with PBS buffer (2 x 200 μ L per well) and analyzed under the confocal microscope. The microscope consisted of a confocal laser scanning microscope (CLSM) Leica TCS SP8 (*Leica Microsystems*, Mannheim, Germany) and the Leica Application Suite (LAS X) software bundle. As objective a 25x objective lens (Fluotar VISIR 25x/0.95 WATER) was used. Channel-settings for 1) Cy5 label: 633 nm laser

(3% power); 660-680 nm filter (100% HyD gain), 2) AF488-phalloidin: 488 nm laser (2% power); 510-550 nm filter (830 V PMT gain), 3) DAPI: 405 nm laser (5% power); 430-490 nm filter (100% HyD gain), 4) transmitted light: 430 V PMT gain, were applied.

6.2 Supporting Information

6.2.1 Manuscript B: Oligonucleotides with Cationic Backbone and Their Hybridization with DNA: Interplay of Base Pairing and Electrostatic Attraction

Supporting information and the ORCID identification numbers for the authors of this article can be found under:

<https://doi.org/10.1002/chem.201704338>.

CHEMISTRY

A **European** Journal

Supporting Information

Oligonucleotides with Cationic Backbone and Their Hybridization with DNA: Interplay of Base Pairing and Electrostatic Attraction

Boris Schmidtgall,^[a, b] Arne Kuepper,^[c, d] Melissa Meng,^[a] Tom N. Grossmann,^{*[c, d, e]} and Christian Ducho^{*[a, b]}

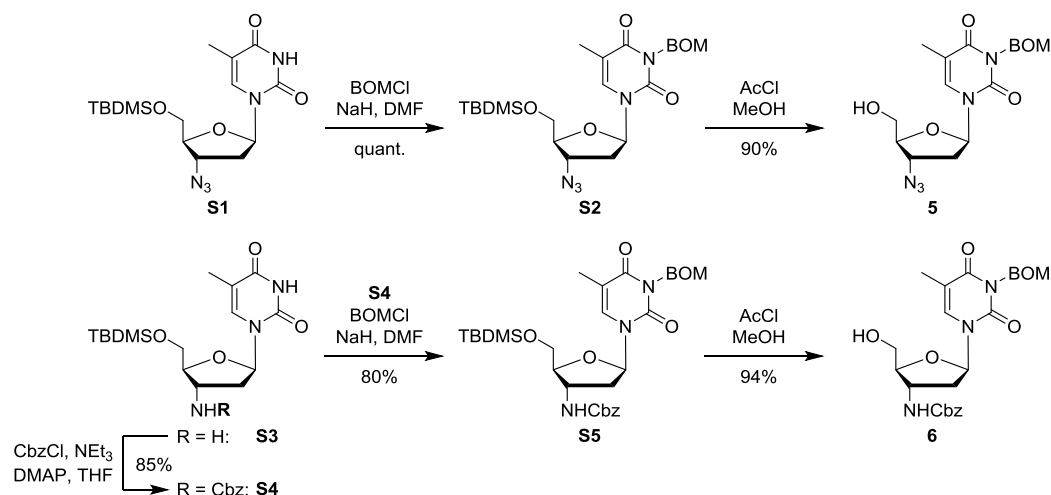
chem_201704338_sm_miscellaneous_information.pdf

Table of contents

Additional syntheses.....	S2
^1H , ^{13}C and ^{31}P NMR spectra of synthesized compounds.....	S10
Analytical data of oligonucleotide analogues.....	S27
Melting temperature experiments.....	S29
Additional CD spectrum.....	S32
References.....	S33

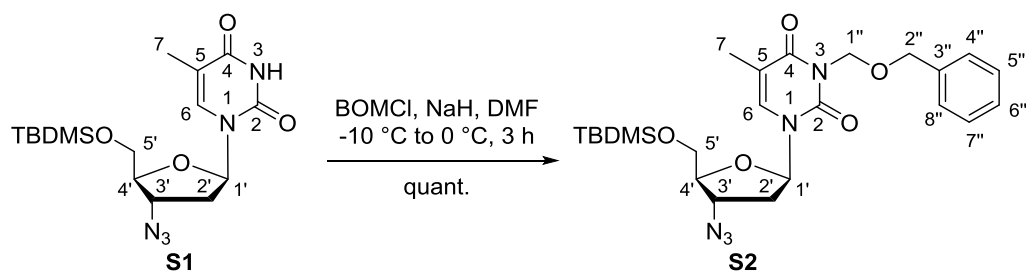
Additional syntheses

For the synthesis of starting materials **5** and **6**, 5'-*O*-silylated 3'-azido-3'-deoxythymidine **S1**^{S1,S2} was treated with benzyloxymethyl chloride (BOMCl) to give the *N*-3-alkylated product **S2** in quantitative yield (Scheme S1). Acidic desilylation of **S2** then furnished 3'-azido congener **5** in 90% yield. In order to obtain 3'-*N*-Cbz-amino analogue **6**, **S1** was first reduced to amine **S3**^{S1,S2} (not displayed), which was then Cbz-protected under non-aqueous conditions to afford **S4** in 85% yield. Protection of the nucleobase using BOMCl gave **S5** in 80% yield, and acidic desilylation finally led to **6** in 94% yield (Scheme S1). For the synthesis of phosphonate **7**, saponification of the corresponding methyl ester **S6**^{S3-S6} was followed by benzylation of the carboxylate under basic conditions (*vide infra*). Compounds **S1**^{S1,S2}, **S3**^{S1,S2} and **S6**^{S3-S6} were prepared according to established procedures.



Scheme S1. Synthesis of starting materials **5** and **6**.

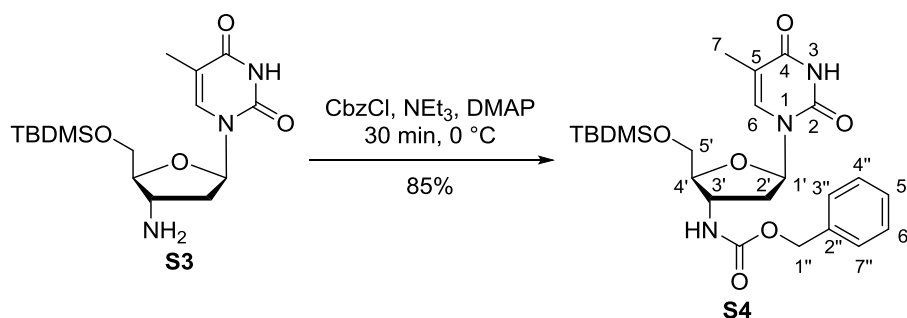
5'-O-TBDMS-3'-N-BOM-3'-azido-3'-deoxythymidine **S2**



A solution of 5'-O-TBDMS-3'-azido-3'-deoxythymidine **S1**^{S1,S2} (2.04 g, 5.35 mmol) in dry DMF (8 mL) was added to a suspension of NaH (231 mg, 60% dispersion in mineral oil, 9.63 mmol) in dry DMF (15 mL) at -10 °C. The suspension was stirred for 30 min at -3 °C to -5 °C, after which benzyl chloromethyl ether (1.00 mL, 1.01 g, 6.42 mmol) was slowly added. The reaction mixture was stirred for 3 h at 0 °C. It was then diluted with EtOAc (100 mL), and water (30 mL) was slowly added to quench unreacted NaH. The organic layer was washed with sat. aq. NH₄Cl (50 mL), sat. aq. NaHCO₃ (50 mL), water (2 x 50 mL) and brine (50 mL). It was then dried over Na₂SO₄, filtered and evaporated under reduced pressure. The resultant slurry was coevaporated with toluene (3 x 50 mL). The thus obtained crude product was purified by column chromatography (4:1 *iso*-hexanes-EtOAc) to give **S2** as a colorless viscous oil (2.68 g, quant.). TLC: R_f = 0.22 (8:2 *iso*-hexanes-EtOAc). [α]_D²⁰ = +44.4 (c 1.0, CHCl₃). ¹H NMR (300 MHz, CDCl₃): δ = 0.13 (s, 6H, SiCH₃), 0.94 (s, 9H, SiC(CH₃)₃), 1.92 (d, *J* = 1.2 Hz, 3H, 7-H), 2.19 (ddd, *J* = 13.7, 7.0, 6.7 Hz, 1H, 2'-H_a), 2.44 (ddd, *J* = 13.7, 6.3, 4.4 Hz, 1H, 2'-H_b), 3.78-3.82 (m, 1H, 5'-H_a), 3.92-3.97 (m, 2H, 4'-H, 5'-H_b), 4.20 (ddd, *J* = 7.0, 4.4, 4.4 Hz, 1H, 3'-H), 4.70 (s, 2H, 2''-H), 5.49 (s, 2H, 1''-H), 6.21 (dd, *J* = 6.7, 6.3 Hz, 1H, 1'-H), 7.23-7.27 (m, 1H, 4''-H), 7.29-7.33 (m, 2H, 3''-H, 5''-H), 7.36-7.38 (m, 2H, 2''-H, 6''-H), 7.39 (q, *J* = 1.2 Hz, 1H, 6-H) ppm. ¹³C NMR (75 MHz, CDCl₃): δ = -5.4 (SiCH_{3a}), -5.3 (SiCH_{3b}), 13.2 (C-7), 18.4 (SiC(CH₃)₃), 25.9 (SiC(CH₃)₃), 38.1 (C-2'), 60.3 (C-3'), 62.8 (C-5'), 70.6 (C-1''), 72.3 (C-2''), 84.5 (C-4'), 85.2 (C-1'), 110.3 (C-5), 127.6 (C-6''), 127.6 (C-4'', C-8''), 128.3 (C-5'', C-7''), 133.7 (C-6), 138.1 (C-3''), 150.8 (C-2), 163.4

(C-4) ppm. IR (ATR): $\nu = 2101, 1709, 1652, 1461, 1256, 1075, 832, 774, 731, 698 \text{ cm}^{-1}$. UV (MeCN): $\lambda_{\text{max}} (\log \epsilon) = 208 (4.36), 267 (4.07) \text{ nm}$. HRMS (ESI): calcd for $\text{C}_{24}\text{H}_{35}\text{N}_5\text{NaO}_5\text{Si}$ 524.2300, found 524.2296 $[\text{M} + \text{Na}]^+$.

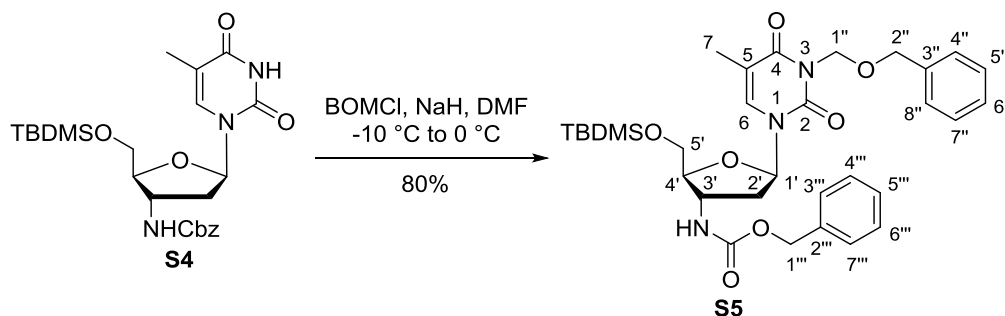
5'-O-TBDMS-3'-N-Cbz-amino-3'-deoxythymidine **S4**



To a precooled ($0 \text{ }^\circ\text{C}$) solution of 5'-O-TBDMS-3'-amino-3'-deoxythymidine **S3**^{S1,S2} (6.00 g, 17.0 mmol) in THF (150 mL) were added DMAP (10 mg, 82 μmol), NEt_3 (5.89 mL, 4.30 g, 42.0 mmol) and benzyl chloroformate (2.66 mL, 3.18 g, 18.7 mmol). The reaction mixture was stirred for 30 min at $0 \text{ }^\circ\text{C}$. It was then diluted with EtOAc (500 mL) and washed with sat. aq. NaHCO_3 (2 x 200 mL) and brine (200 mL). The organic layer was dried over Na_2SO_4 , filtered and evaporated. The resultant residue was purified by column chromatography (40:1 CH_2Cl_2 -MeOH) to give **S4** as a colorless foam (7.05 g, 85%). Mp $79 \text{ }^\circ\text{C}$. TLC: $R_f = 0.36$ (20:1 CH_2Cl_2 -MeOH). $[\alpha]_{\text{D}}^{20} = -28.8$ (c 1.0, CHCl_3). ^1H NMR (500 MHz, CD_3OD , $50 \text{ }^\circ\text{C}$): $\delta = 0.09$ (s, 6H, SiCH_3), 0.92 (s, 9H, $\text{SiC}(\text{CH}_3)_3$), 1.87 (d, $J = 1.0 \text{ Hz}$, 3H, 7-H), 2.29 (dd, $J = 6.6, 6.6 \text{ Hz}$, 2H, 2'-H), 3.77-3.85 (m, 1H, 5'-H_a), 3.88-3.95 (m, 2H, 4'-H, 5'-H), 4.29 (ddd, $J = 6.6, 6.6, 5.5 \text{ Hz}$, 1H, 3'-H), 5.06 (d, $J = 13.0 \text{ Hz}$, 1H, 1''-H_a), 5.10 (d, $J = 13.0 \text{ Hz}$, 1H, 1''-H_b), 6.17 (dd, $J = 6.6 \text{ Hz}$, 1H, 1'-H), 7.22-7.37 (m, 5H, aryl-H), 7.57 (d, $J = 1.0 \text{ Hz}$, 1H, 6-H) ppm. ^{13}C NMR (126 MHz, CD_3OD , $50 \text{ }^\circ\text{C}$): $\delta = -5.3$ (SiCH_3), -5.2 (SiCH_3), 12.6 (C-7), 19.3 ($\text{SiC}(\text{CH}_3)_3$), 26.5 ($\text{SiC}(\text{CH}_3)_3$), 39.3 (C-2'), 52.2 (C-3'), 64.2 (C-5'), 67.7 (C-1''), 86.0 (C-1'), 86.5 (C-4'), 111.5 (C-5), 128.9 (C-3'',C-7''), 129.0 (C-4'', C-5'', C-6''), 129.5 (C-2''), 137.4

(C-6), 152.3 (C-2), 166.2 (C-4) ppm. IR (ATR): $\nu = 1680, 1466, 1256, 1123, 1065, 1003, 831, 774, 698 \text{ cm}^{-1}$. UV (MeCN): $\lambda_{\text{max}} (\log \epsilon) = 207 (4.19), 265 (3.91) \text{ nm}$. HRMS (ESI): calcd for $\text{C}_{24}\text{H}_{34}\text{N}_3\text{O}_6\text{Si}$ 488.2222, found 488.2219 $[\text{M} - \text{H}]^-$.

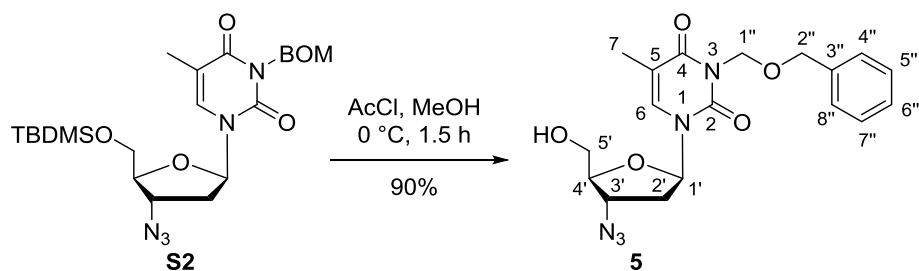
5'-O-TBDMS-3'-N-Cbz-amino-3'-deoxythymidine **S5**



A solution of 5'-O-TBDMS-3'-N-Cbz-amino-3'-deoxythymidine **S4** (6.94 g, 14.2 mmol) in dry DMF (22 mL) was added to a suspension of NaH (572 mg, 60% dispersion in mineral oil, 14.3 mmol) in dry DMF (23 mL) at $-10 \text{ }^\circ\text{C}$. The suspension was stirred for 30 min at $-3 \text{ }^\circ\text{C}$ to $-5 \text{ }^\circ\text{C}$, after which benzyl chloromethyl ether (2.10 mL, 2.30 g, 14.3 mmol) was slowly added. The reaction mixture was stirred for 3 h at $0 \text{ }^\circ\text{C}$. It was then diluted with EtOAc (300 mL), and water (30 mL) was slowly added to quench unreacted NaH. The organic layer was washed with sat. aq. NH_4Cl (50 mL), sat. aq. NaHCO_3 (150 mL), water (2 x 150 mL) and brine (150 mL). It was then dried over Na_2SO_4 , filtered and evaporated under reduced pressure. The resultant slurry was coevaporated with toluene (3 x 50 mL). The thus obtained crude product was purified by column chromatography (7:3 *iso*-hexanes-EtOAc) to give **S5** as a colorless viscous oil (6.94 g, 80%). TLC: $R_f = 0.27$ (7:3 *iso*-hexanes-EtOAc). $[\alpha]_{\text{D}}^{20} = +6.5$ (c 1.2, CHCl_3). ^1H NMR (500 MHz, CD_3OD , $50 \text{ }^\circ\text{C}$): $\delta = 0.12$ (s, 6H, $\text{Si}(\text{CH}_3)_2$), 0.94 (s, 9H, $\text{SiC}(\text{CH}_3)_3$), 1.89 (d, $J = 0.8 \text{ Hz}$, 3H, 7-H), 2.26 (ddd, $J = 13.8, 7.4, 6.3 \text{ Hz}$, 1H, 2'-H_a), 2.33 (ddd, $J = 13.8, 6.4, 5.8 \text{ Hz}$, 1H, 2'-H_b), 3.80-3.87 (m, 1H, 5'-H), 3.92-3.98 (m, 2H, 4'-H, 5'-H), 4.29 (ddd, $J = 8.0, 5.8, 5.7 \text{ Hz}$, 1H, 3'-H), 4.67 (s, 2H, 1''-H), 5.10 (d, $J = 12.5 \text{ Hz}$, 1H, 1'''-H_a),

5.13 (d, $J = 12.5$ Hz, 1H, 1'''-H_b), 5.48 (d, $J = 9.9$ Hz, 1H, 2''-H_a), 5.51 (d, $J = 9.9$ Hz, 1H, 2''-H_b), 6.17 (dd, $J = 6.4, 6.3$ Hz, 1H, 1'-H), 7.21-7.39 (m, 10H, aryl-H), 7.56 (s, 1H, 6-H) ppm. ^{13}C NMR (126 MHz, CD₃OD, 50 °C): $\delta = -6.7$ (SiCH₃), -6.6 (SiCH₃), 11.8 (C-7), 17.9 (SiC(CH₃)₃), 25.1 (SiC(CH₃)₃), 38.1 (C-2'), 50.7 (C-3'), 62.8 (C-5'), 66.3 (C-1'''), 70.6 (C-1'''), 71.9 (C-2'''), 85.3 (C-1'), 85.5 (C-4'), 109.3 (C-5), 126.6, 126.8, 127.1, 127.3, 127.5, 127.7, 127.9, 128.1 (aryl-C), 134.9 (C-6), 138.3 (Cbz-C=O), 150.9 (C-2), 163.8 (C-4) ppm. IR (ATR): $\nu = 1704, 1637, 1255, 1070, 1022, 827, 769, 731, 698$ cm⁻¹. UV (MeCN): λ_{max} (log ϵ) = 207 (4.55), 268 (4.08) nm. HRMS (ESI): calcd for C₃₂H₄₃N₃NaO₇Si 632.2768, found 632.2760 [M + Na]⁺.

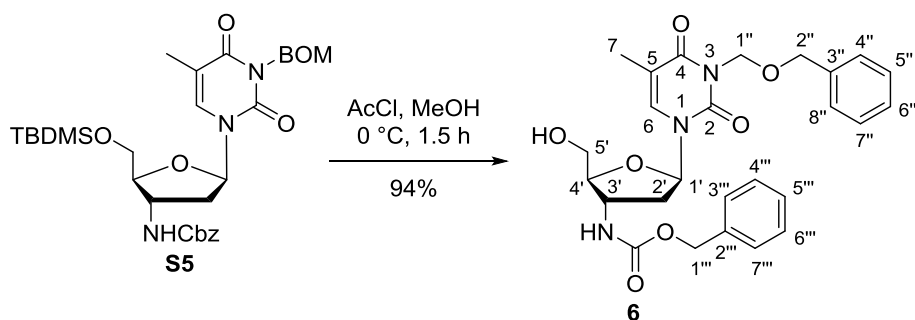
3-*N*-BOM-3'-azido-3'-deoxythymidine **5**



To a precooled (0 °C) solution of 5'-*O*-TBDMS-3-*N*-BOM-3'-azido-3'-deoxythymidine **S2** (2.60 g, 5.19 mmol) in dry MeOH (100 mL), acetyl chloride (202 mg, 183 μL , 2.59 mmol) was added under stirring. The solution was brought to rt and then stirred for 1.5 h. Subsequently, sat. aq. NaHCO₃ (5 mL) was added and the reaction mixture was stirred for further 15 min. The resultant suspension was diluted with EtOAc (150 mL) and washed with water (1 x 80 mL) and brine (1 x 80 mL). The organic layer was evaporated under reduced pressure. The resultant crude product was purified by column chromatography (3:2 *iso*-hexanes-EtOAc) to give **5** as a viscous colorless oil (1.81 g, 90%). TLC: $R_f = 0.43$ (9:1 CH₂Cl₂-MeOH). $[\alpha]_{\text{D}}^{20} = +49.1$ (c 1.1, CHCl₃). ^1H NMR (500 MHz, CDCl₃): $\delta = 1.90$ (d, $J = 1.2$ Hz, 3H, 7-H), 2.36 (ddd, $J = 13.8, 6.7, 5.3$ Hz, 1H, 2'-H_a), 2.42 (ddd, $J = 13.8, 7.4,$

6.2 Hz, 1H, 2'-H_b), 3.75-3.81 (m, 1H, 5'-H_a), 3.91-3.97 (m, 2H, 4'-H, 5'-H_b), 4.33 (ddd, $J = 7.4, 5.3, 5.3$ Hz, 1H, 3'-H), 4.69 (s, 2H, 2''-H), 5.47 (s, 2H, 1''-H), 6.07 (dd, $J = 6.4, 6.4$ Hz, 1H, 1'-H), 7.22-7.27 (m, 1H, 6''-H), 7.28-7.32 (m, 2H, 5''-H, 7''-H), 7.33-7.35 (m, 2H, 4''-H, 8''-H), 7.43 (q, $J = 1.2$ Hz, 1H, 6-H) ppm. ¹³C NMR (126 MHz, CDCl₃): $\delta = 13.2$ (C-7), 37.5 (C-2'), 59.9 (C-3'), 61.9 (C-5'), 70.6 (C-1''), 72.3 (C-2''), 84.5 (C-4'), 86.8 (C-1'), 110.4 (C-5), 127.6 (C-6''), 127.7 (C-4'', C-8''), 128.3 (C-5'', C-7''), 135.3 (C-6), 137.9 (C-3''), 150.9 (C-2), 163.4 (C-4) ppm. IR (ATR): $\nu = 2101, 1704, 1637, 1466, 1266, 1093, 1070, 774, 731, 698$ cm⁻¹. UV (MeCN): λ_{max} (log ϵ) = 208 (4.14), 267 (3.89) nm. HRMS (ESI): calcd for C₁₄H₂₀N₅O₅Si 388.1615, found 388.1610 [M + H]⁺.

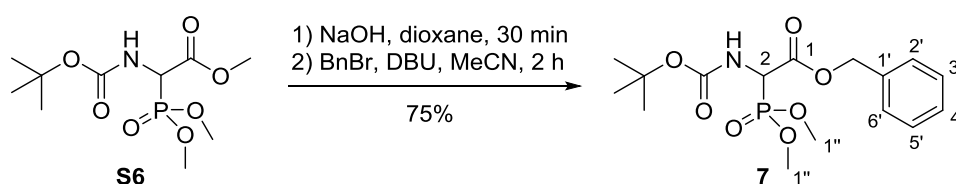
3-*N*-BOM-3'-*N*-Cbz-amino-3'-deoxythymidine **6**



To a precooled (0 °C) solution of 5'-*O*-TBDMS-3-*N*-BOM-3'-*N*-Cbz-amino-3'-deoxythymidine **S5** (6.94 g, 11.5 mmol) in dry MeOH (100 mL), acetyl chloride (180 mg, 164 μ L, 2.23 mmol) was added under stirring. The solution was brought to rt and then stirred for 1.5 h. Subsequently, sat. aq. NaHCO₃ (5 mL) was added and the reaction mixture was stirred for further 15 min. The resultant suspension was diluted with EtOAc (300 mL) and washed with water (1 x 100 mL) and brine (1 x 100 mL). The organic layer was evaporated under reduced pressure. The resultant crude product was purified by column chromatography (98:2 CH₂Cl₂-MeOH) to give **6** as a viscous colorless foam (5.31 g, 94%). Mp 57 °C. TLC: $R_f = 0.28$ (1:1 *iso*-hexanes-EtOAc). $[\alpha]_{\text{D}}^{20} = +25.8$ (c 1.0, CHCl₃). ¹H NMR (500 MHz, CDCl₃): $\delta = 1.92$ (s,

3H, 7-H), 2.28-2.38 (m, 2H, 2'-H), 3.74-3.86 (m, 2H, 4'-H, 5'-H_a), 3.91-3.98 (m, 1H, 5'-H_b), 4.29 (ddd, $J = 7.8, 7.8, 7.6$ Hz, 1H, 3'-H), 4.68 (s, 2H, 1'''-H), 5.08 (d, $J = 12.1$ Hz, 1H, 1''-H_a), 5.13 (d, $J = 12.1$ Hz, 1H, 1''-H_b), 5.23 (d, $J = 7.6$ Hz, 1H, 3'-NH), 5.47 (s, 2H, 2''-H), 6.13 (dd, $J = 5.5, 4.9$ Hz, 1H, 1'-H), 7.21-7.38 (m, 10H, aryl-H), 7.63 (s, 1H, 6-H) ppm. ¹³C NMR (126 MHz, CDCl₃): $\delta = 13.3$ (C-7), 38.1 (C-2'), 49.3 (C-3'), 61.3 (C-5'), 67.4 (C-1'''), 70.5 (C-1'''), 72.3 (C-2'''), 85.0 (C-1'), 85.6 (C-4'), 110.1 (C-5), 127.7, 128.2, 128.3, 128.5, 128.7 (aryl-C), 134.5 (C-6), 135.8 (aryl-C), 138.0 (Cbz-C=O), 150.9 (C-2), 163.4 (C-4) ppm. IR (ATR): $\nu = 1695, 1632, 1452, 1255, 1083, 1065, 1022, 774, 736, 698$ cm⁻¹. UV (MeCN): λ_{max} (log ϵ) = 207 (4.43), 268 (4.00) nm. HRMS (ESI): calcd for C₂₆H₂₉N₃NaO₇ 518.1902, found 518.1898 [M + Na]⁺.

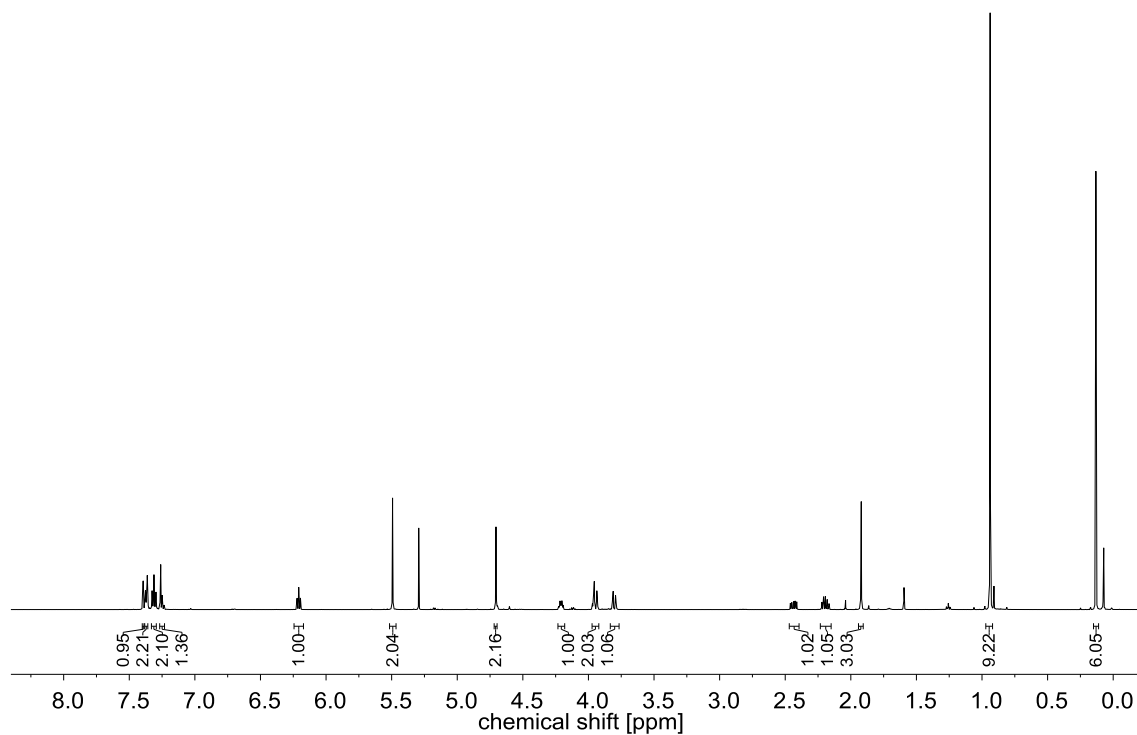
***N*-Boc-2-(dimethylphosphoryl)-glycine benzyl ester 7**



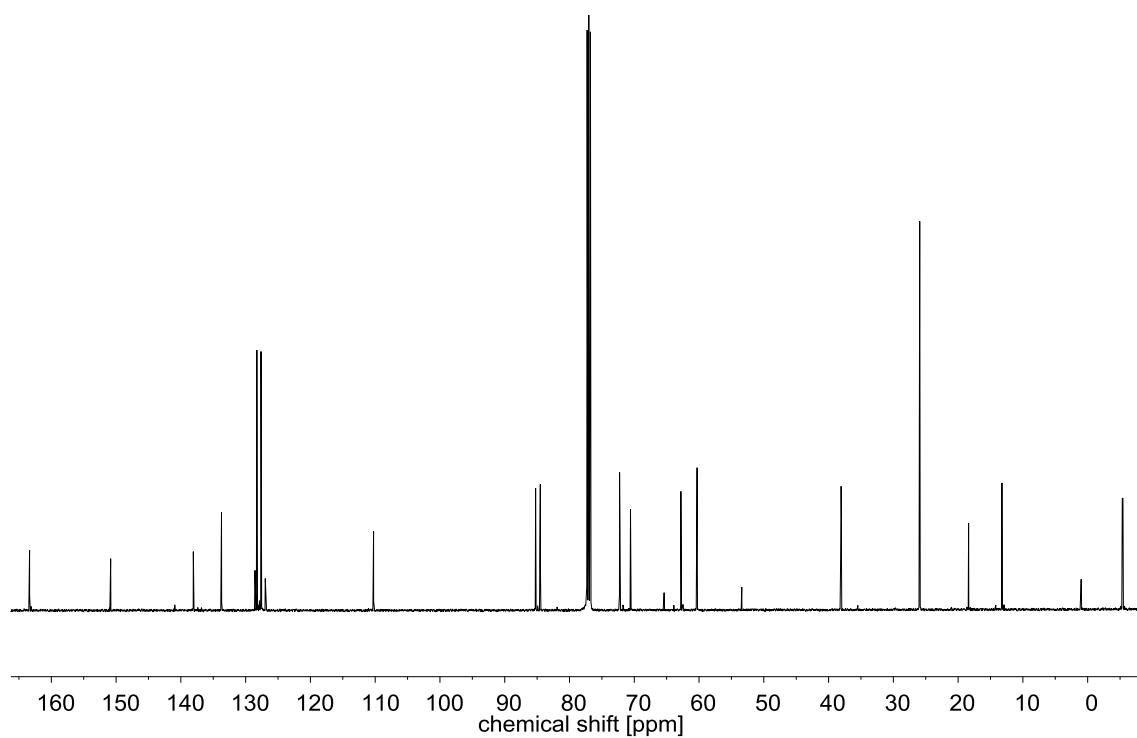
A solution of methyl ester **S6**^{S3-S6} (1.77 g, 5.96 mmol) in dioxane (1.35 mL) was cooled to 15 °C and 2 M aq. NaOH (2.98 mL, 5.96 mmol) was added. The reaction mixture was stirred for 30 min at 15 °C. It was then cooled to 0 °C, and precooled (0 °C) 5 M aq. HCl was added until the pH was adjusted to 2. The resultant solution was diluted with water (11 mL) and EtOAc (20 mL). The aqueous layer was extracted with EtOAc (5 x 10 mL). The combined organics were dried over Na₂SO₄, filtered and evaporated. The resultant residue was kept under high vacuum for several hours to remove remaining volatiles and give a colorless solid. The thus obtained intermediate carboxylic acid (1.53 g, 5.41 mmol) was coevaporated with dry MeCN (3 x 3 mL) and then dissolved in MeCN (3 mL). DBU (823 mg, 807 μ L, 5.41 mmol) was added and the solution was stirred for 5 min at rt. Subsequently, benzyl

bromide (971 mg, 671 μ L, 5.68 mmol) was added and the reaction mixture was stirred for 2 h. It was then diluted with brine (20 mL) and extracted with EtOAc (3 x 10 mL). The combined organics were washed with 1 M aq. HCl, dried over Na₂SO₄, filtered and evaporated. The resultant residue was purified by column chromatography (1:1 *iso*-hexanes-EtOAc) to give **7** as a colorless oil (1.51 g, 75% over 2 steps from **S6**). TLC: R_f = 0.33 (30:1 CH₂Cl₂-MeOH). ¹H NMR (300 MHz, CDCl₃): δ = 1.40 (s, 9H, C(CH₃)₃), 3.68 (d, J_{HP} = 9.5 Hz, 3H, 1''-H_a), 3.71 (d, J_{HP} = 10.9 Hz, 3H, 1''-H_b), 4.87 (dd, J_{HP} = 22.6 Hz, J = 9.0 Hz, 1H, 2-H), 5.21 (d, J = 12.2 Hz, 1H, BnCHH_a), 5.27 (d, J = 12.2 Hz, 1H, BnCHH_b), 5.43 (d, J = 9.0 Hz, 1H, NH), 7.26-7.40 (m, 5H, aryl-H) ppm. ¹³C NMR (126 MHz, CDCl₃): δ = 28.1 (C(CH₃)₃), 51.9 (d, J_{CP} = 148.5 Hz, C-2), 53.9 (d, J_{CP} = 6.6 Hz, C_a-1''), 53.5 (d, J_{CP} = 6.2 Hz, C_b-1''), 68.0 (BnCH₂), 80.9 (C(CH₃)₃), 128.4 (C-2', C-6'), 128.5 (C-4'), 128.5 (C-3', C-5'), 134.8 (C-1'), 154.9 (d, J_{CP} = 8.2 Hz, Boc-C=O), 166.81 (d, J_{CP} = 2.9 Hz, C-1) ppm. ³¹P NMR (121 MHz, CDCl₃): δ = 18.84 ppm; IR (KBr): ν = 1747, 1709, 1494, 1303, 1250, 1156, 1022, 741, 698 cm⁻¹. UV (MeCN): λ_{max} (log ϵ) = 205 (3.14) nm. HRMS (ESI): calcd for C₁₃H₁₈NNaO₇P 396.1183, found 396.1183 [M+Na]⁺.

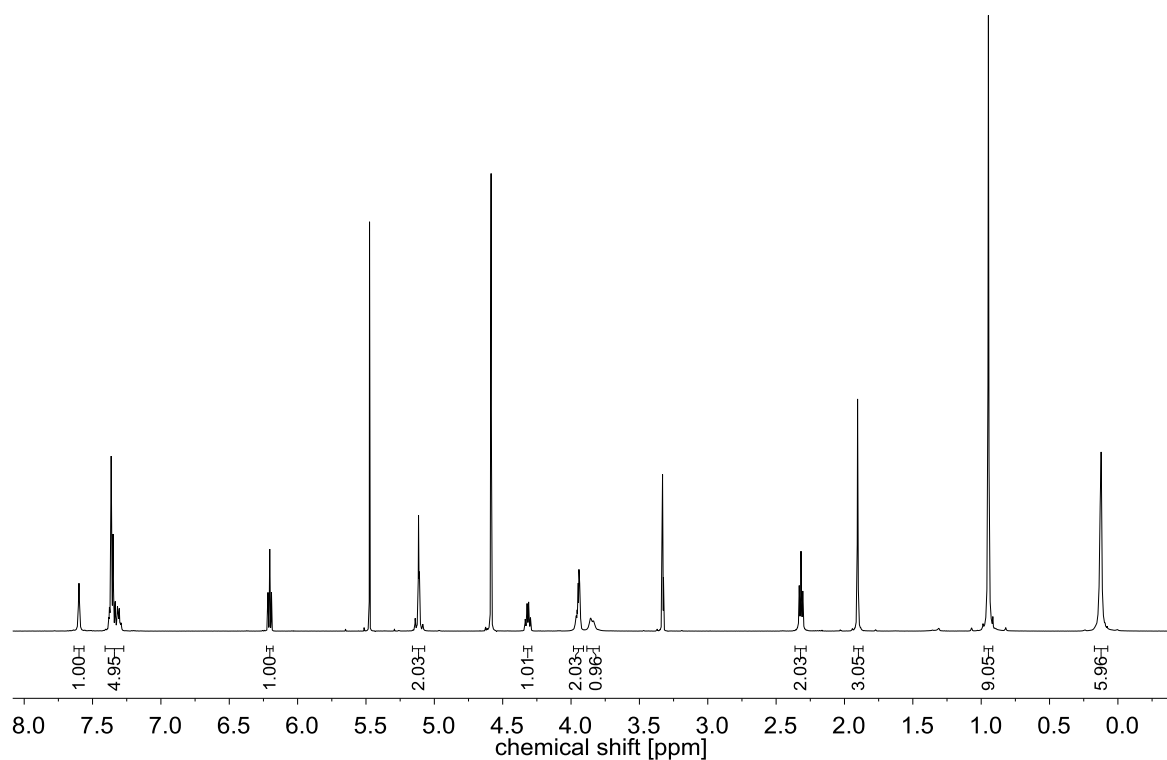
^1H , ^{13}C and ^{31}P NMR spectra of synthesized compounds



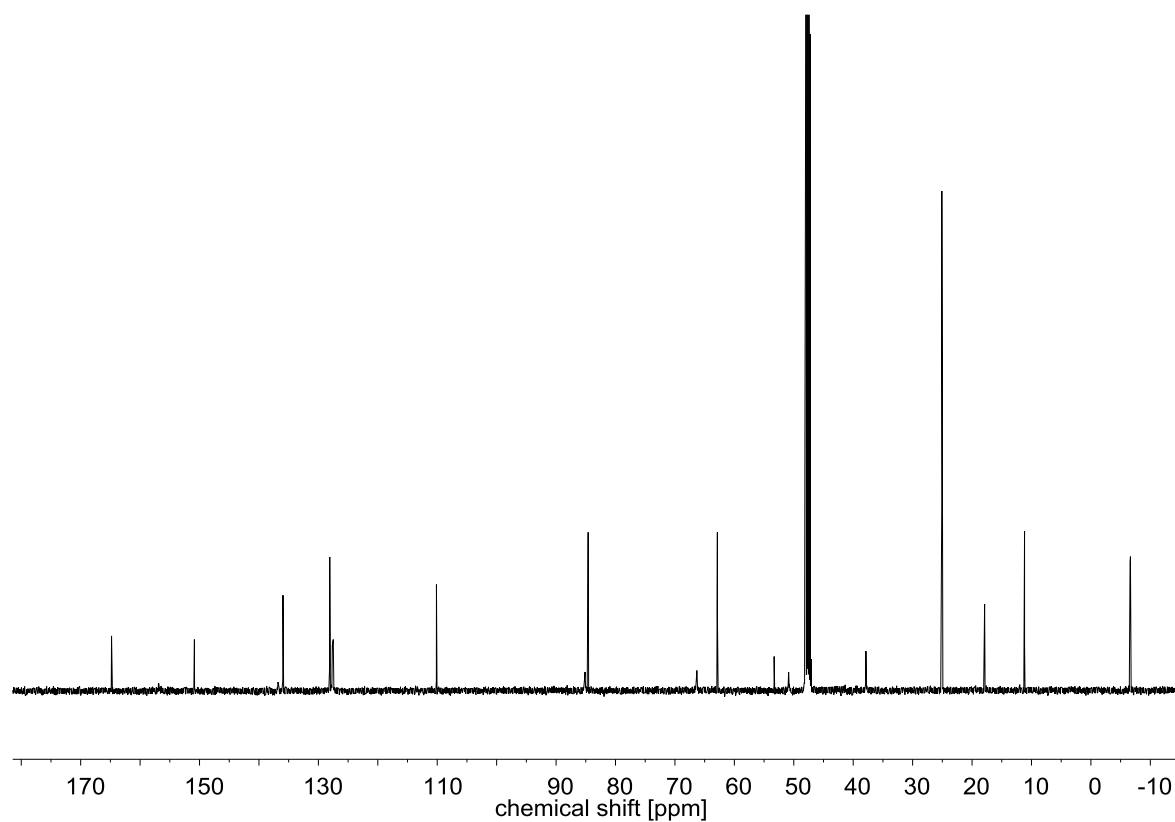
^1H NMR spectrum of **S2** (300 MHz, CDCl_3)



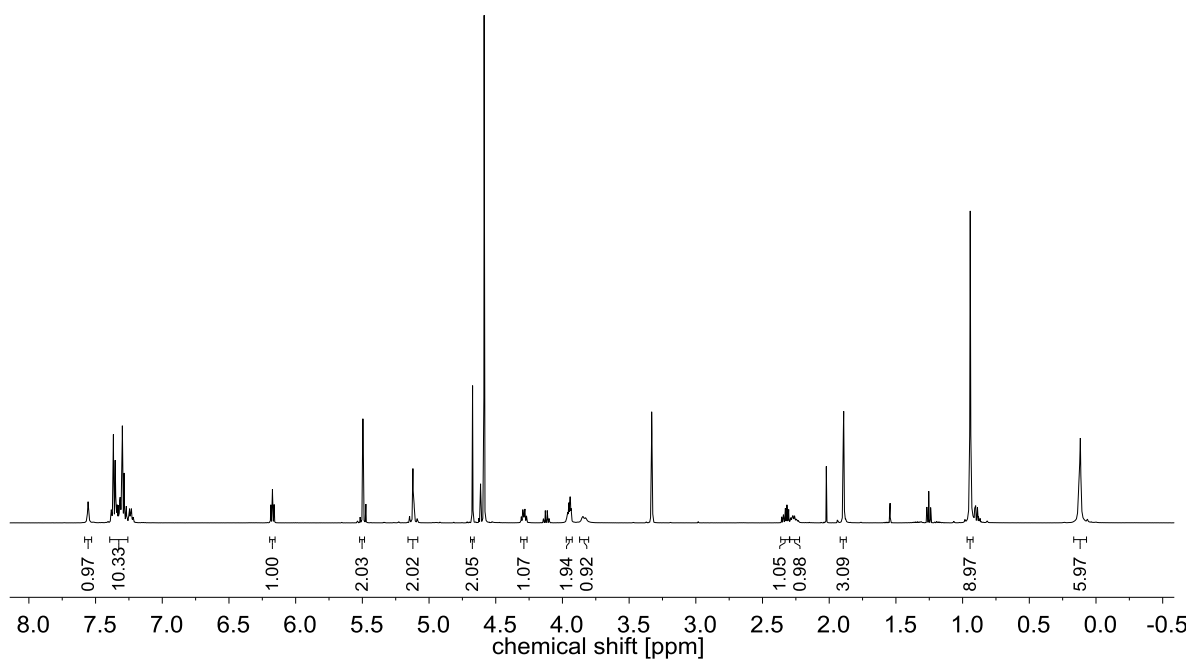
^{13}C NMR spectrum of **S2** (75 MHz, CDCl_3)



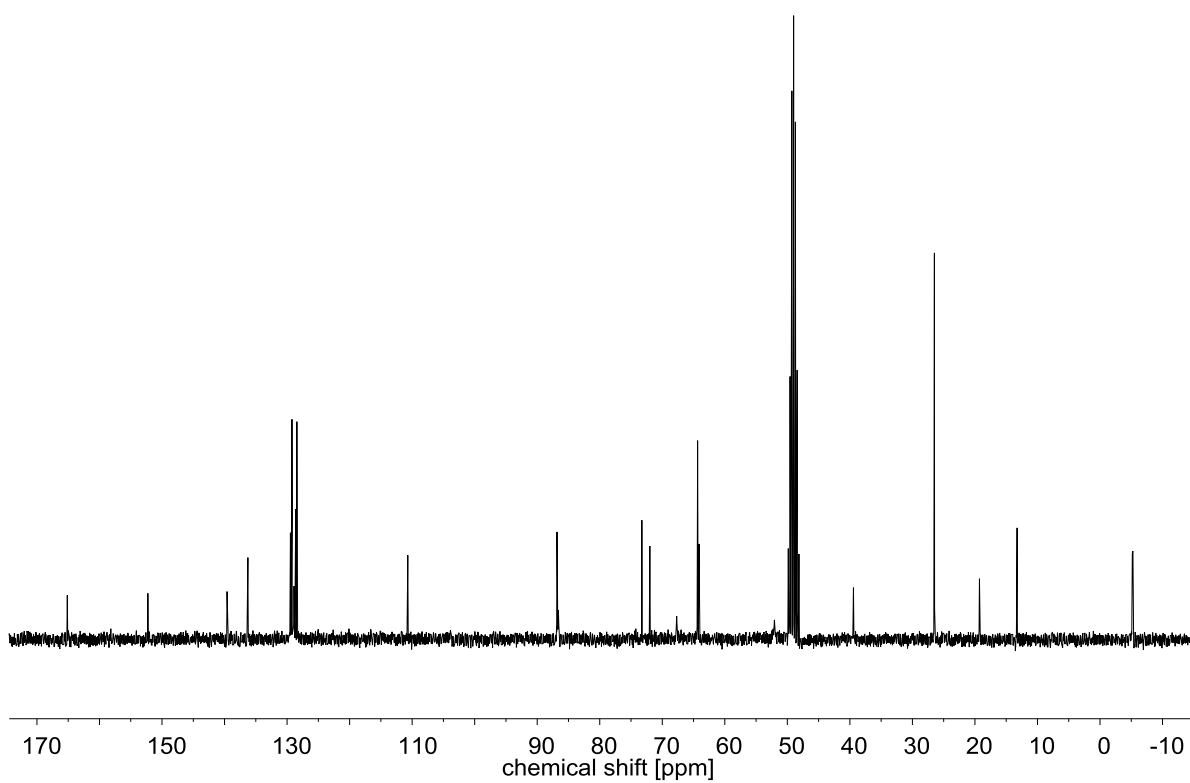
¹H NMR spectrum of **S4** (500 MHz, MeOD, 50 °C)



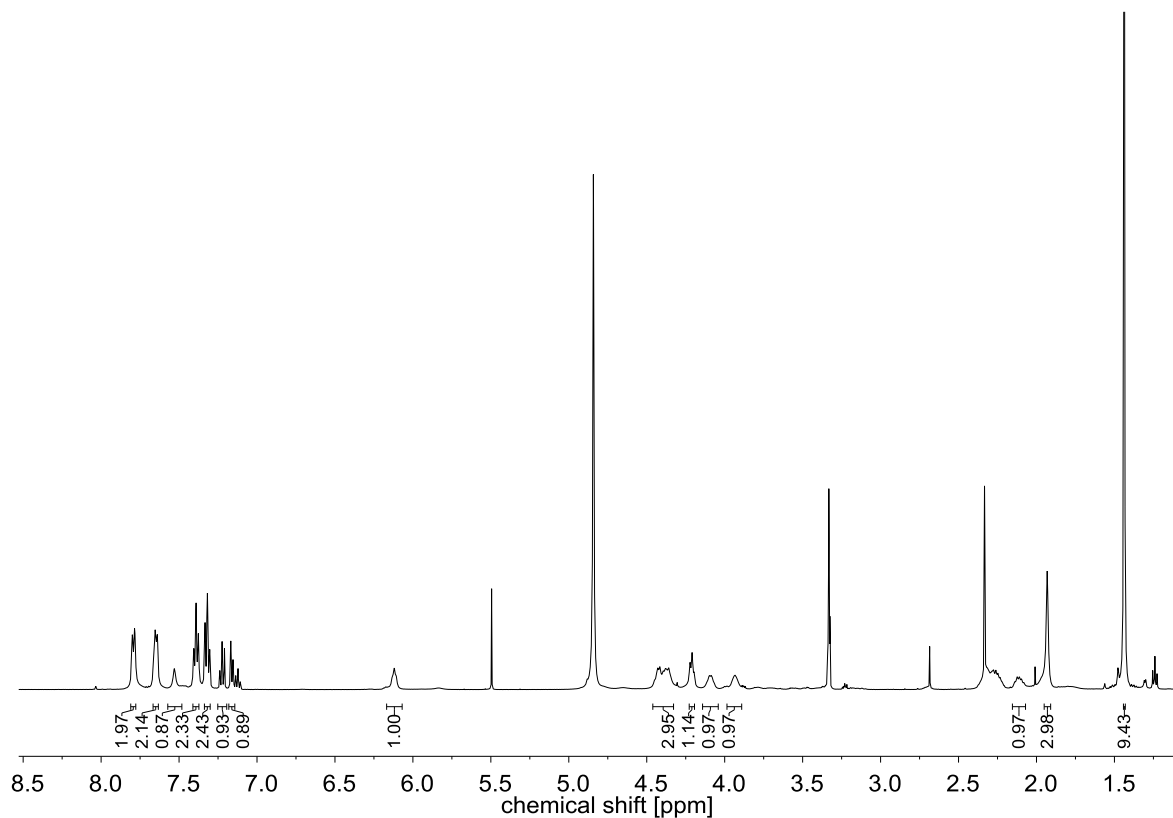
¹³C NMR spectrum of **S4** (126 MHz, MeOD, 50 °C)



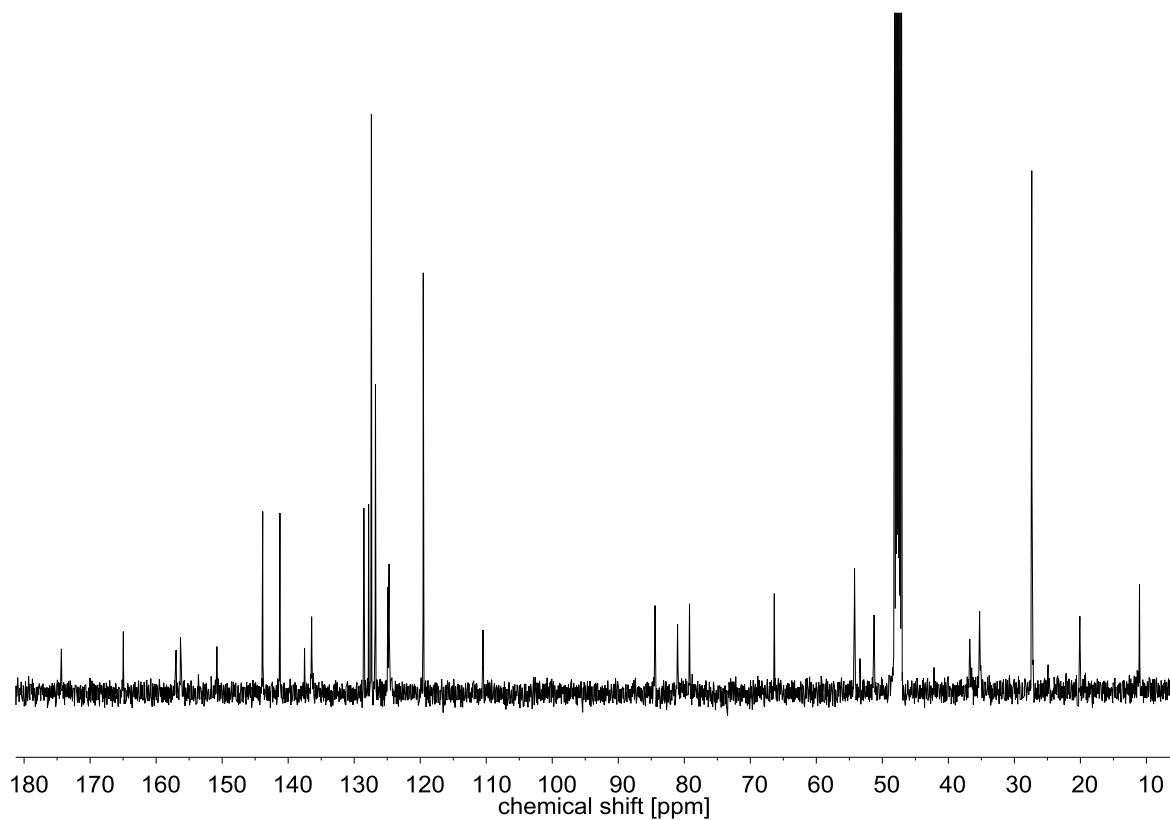
¹H NMR spectrum of **S5** (500 MHz, MeOD, 50 °C)



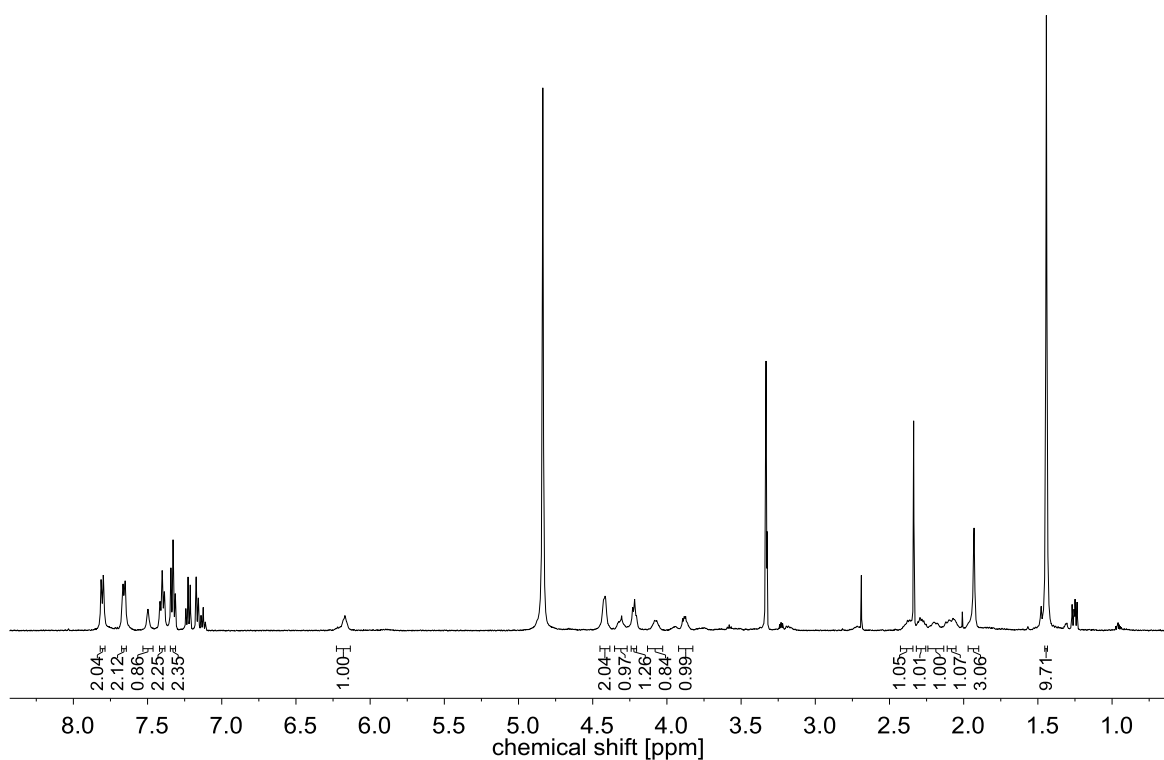
¹³C NMR spectrum of **S5** (126 MHz, MeOD, 50 °C)



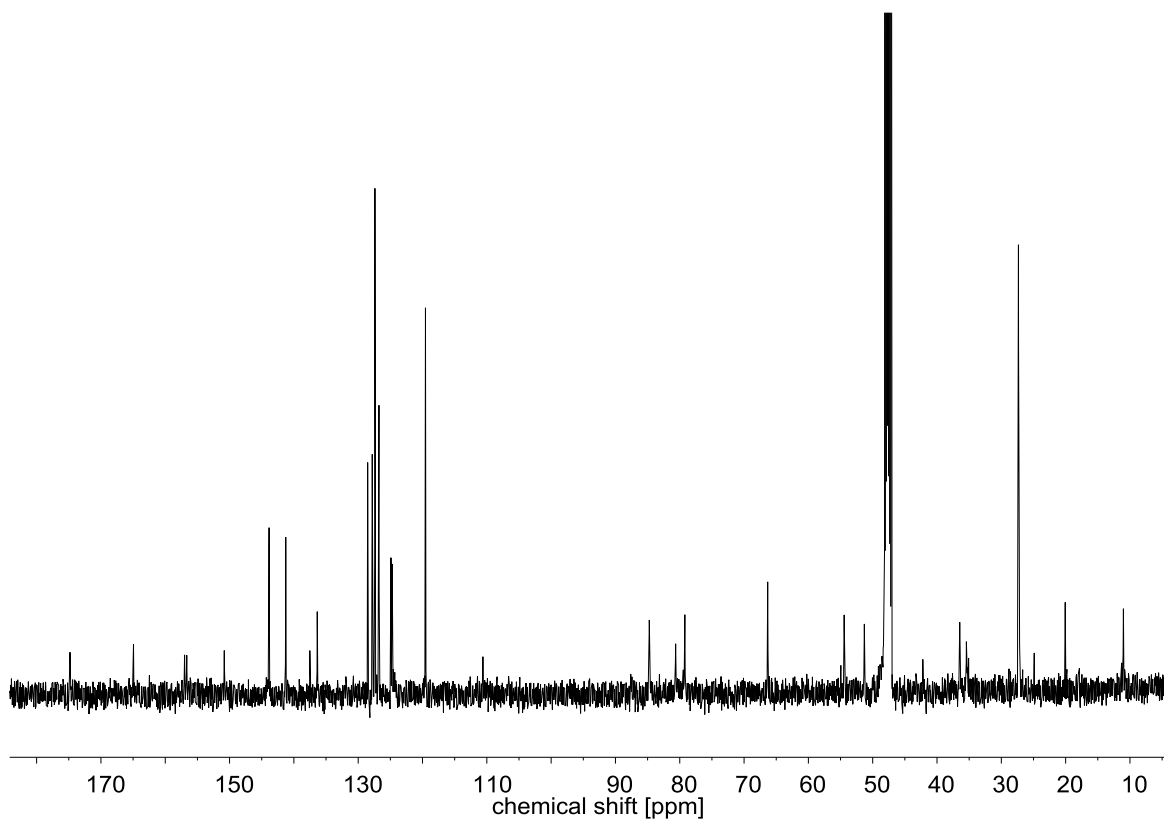
^1H NMR spectrum of (*S*)-**2** (500 MHz, MeOD)



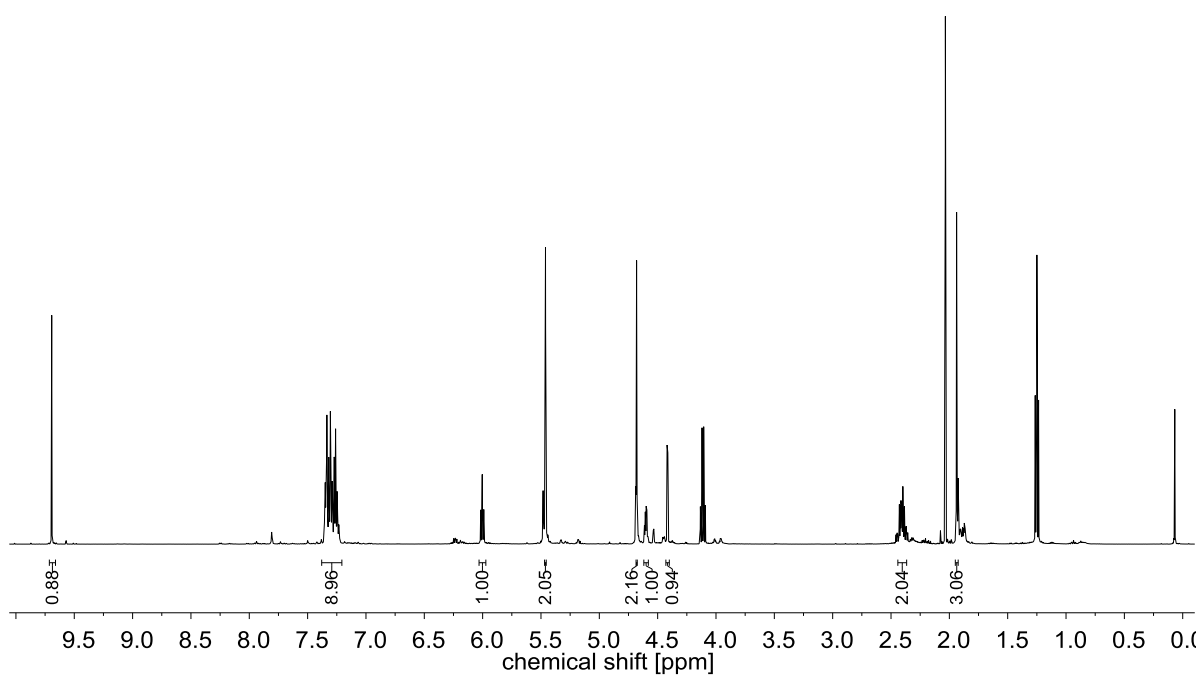
^{13}C NMR spectrum of (*S*)-**2** (126 MHz, MeOD)



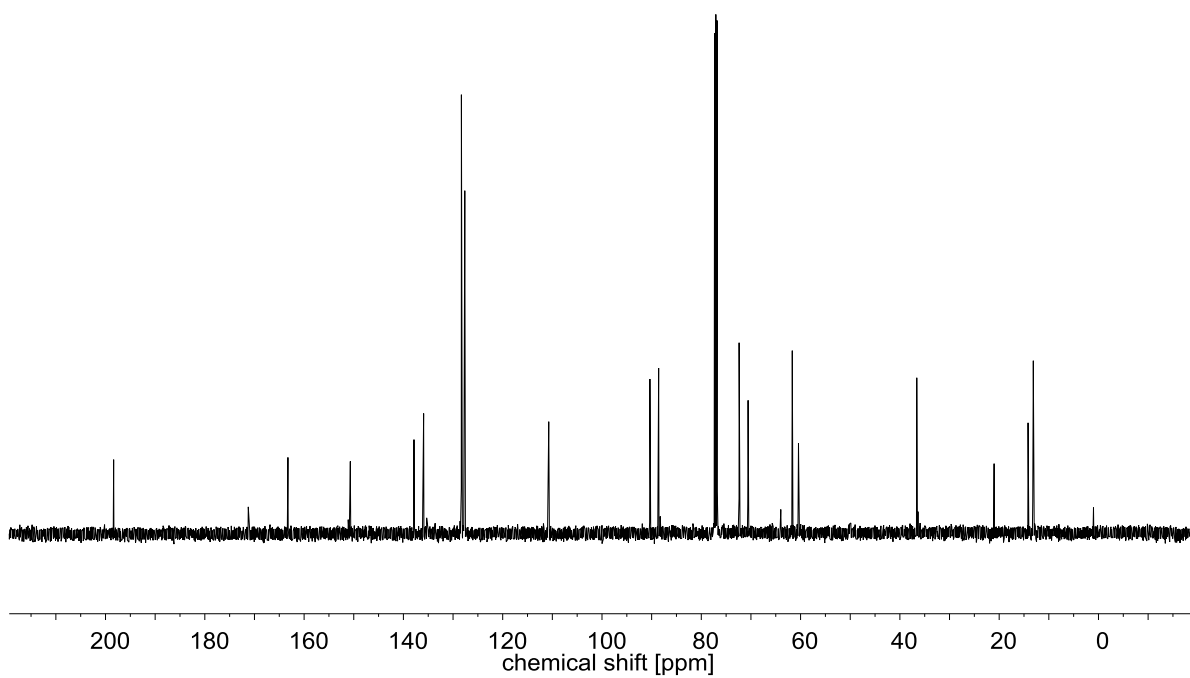
^1H NMR spectrum of (*R*)-**2** (500 MHz, MeOD)



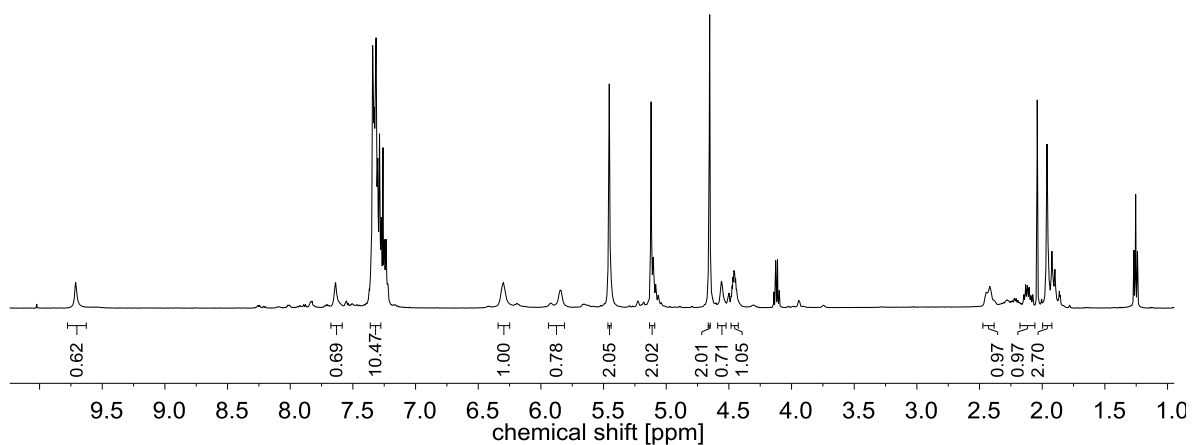
^{13}C NMR spectrum of (*R*)-**2** (126 MHz, MeOD)



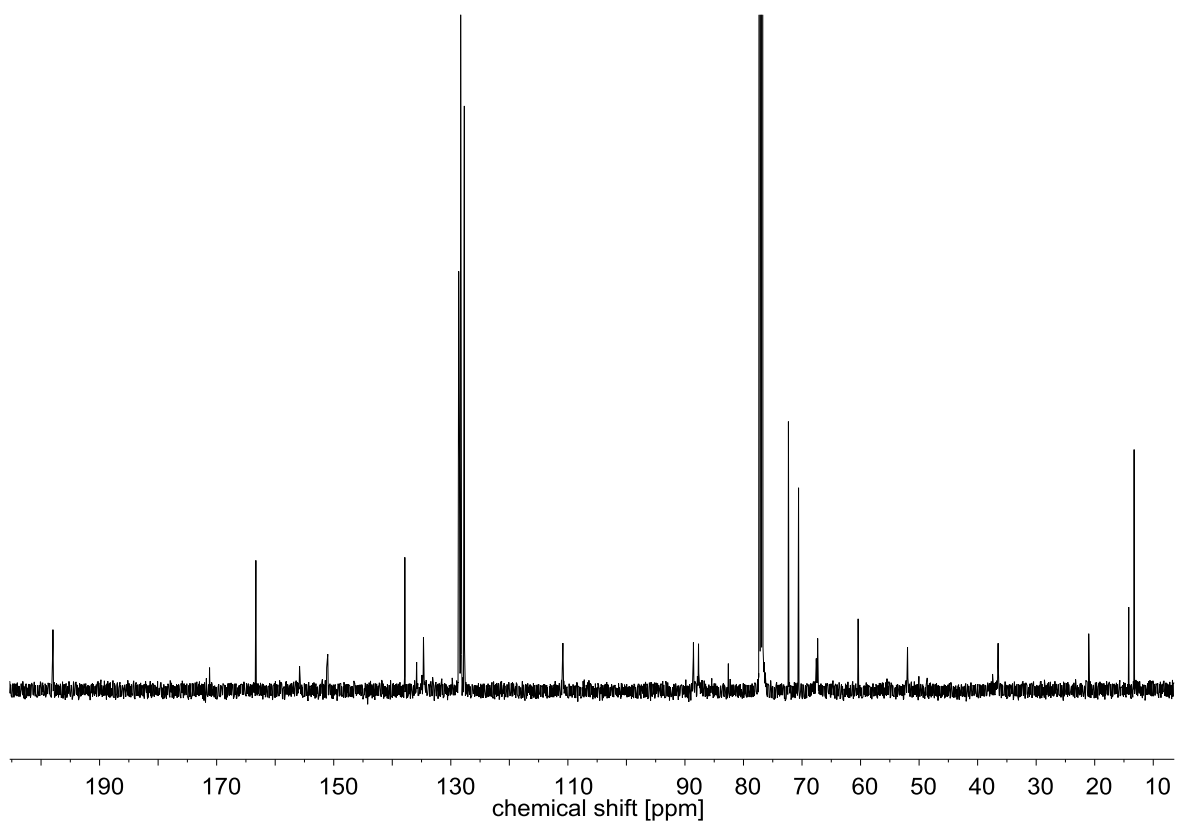
^1H NMR spectrum of **3** (500 MHz, CDCl_3)



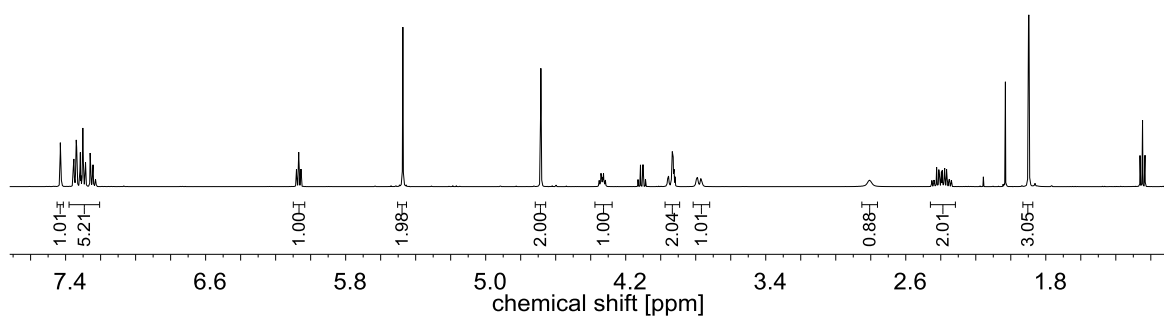
^{13}C NMR spectrum of **3** (126 MHz, CDCl_3)



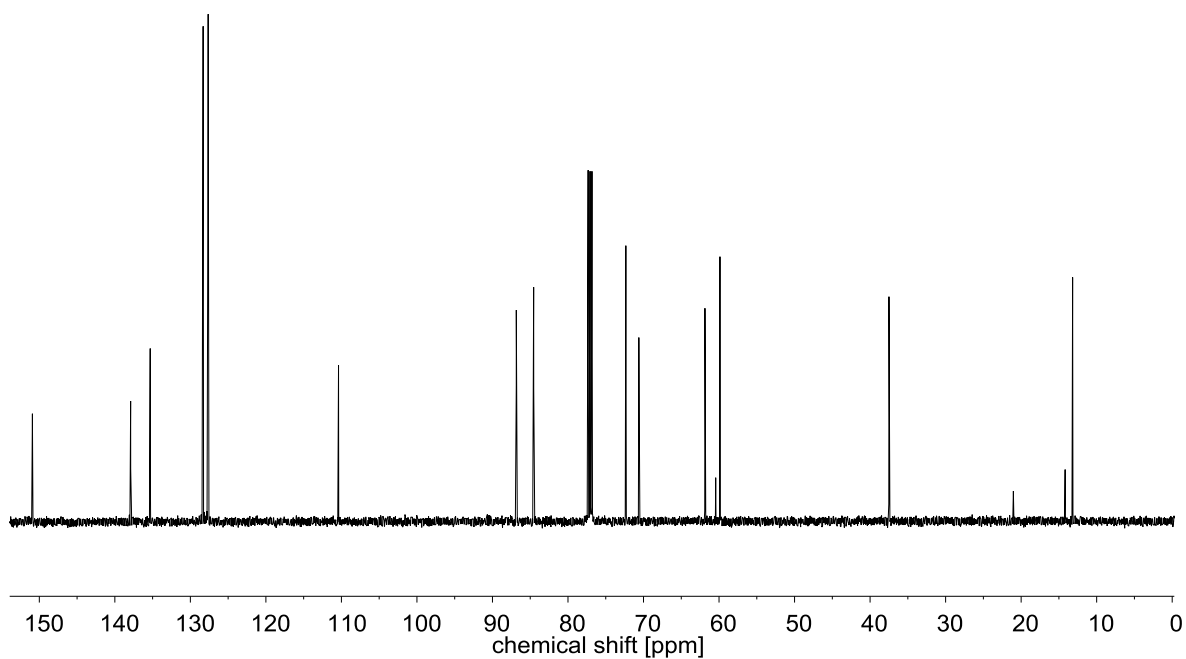
^1H NMR spectrum of **4** (500 MHz, CDCl_3)



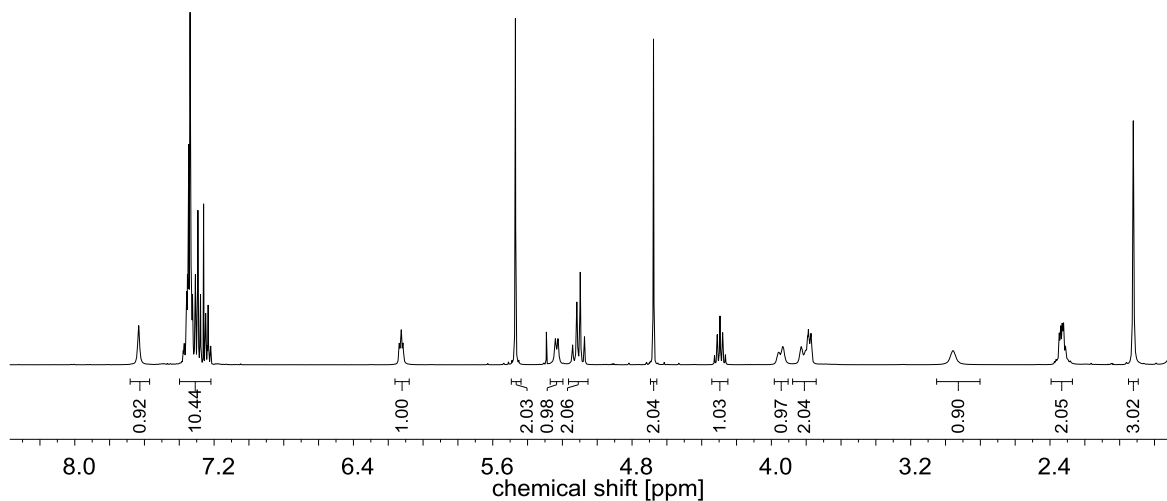
^{13}C NMR spectrum of **4** (126 MHz, CDCl_3)



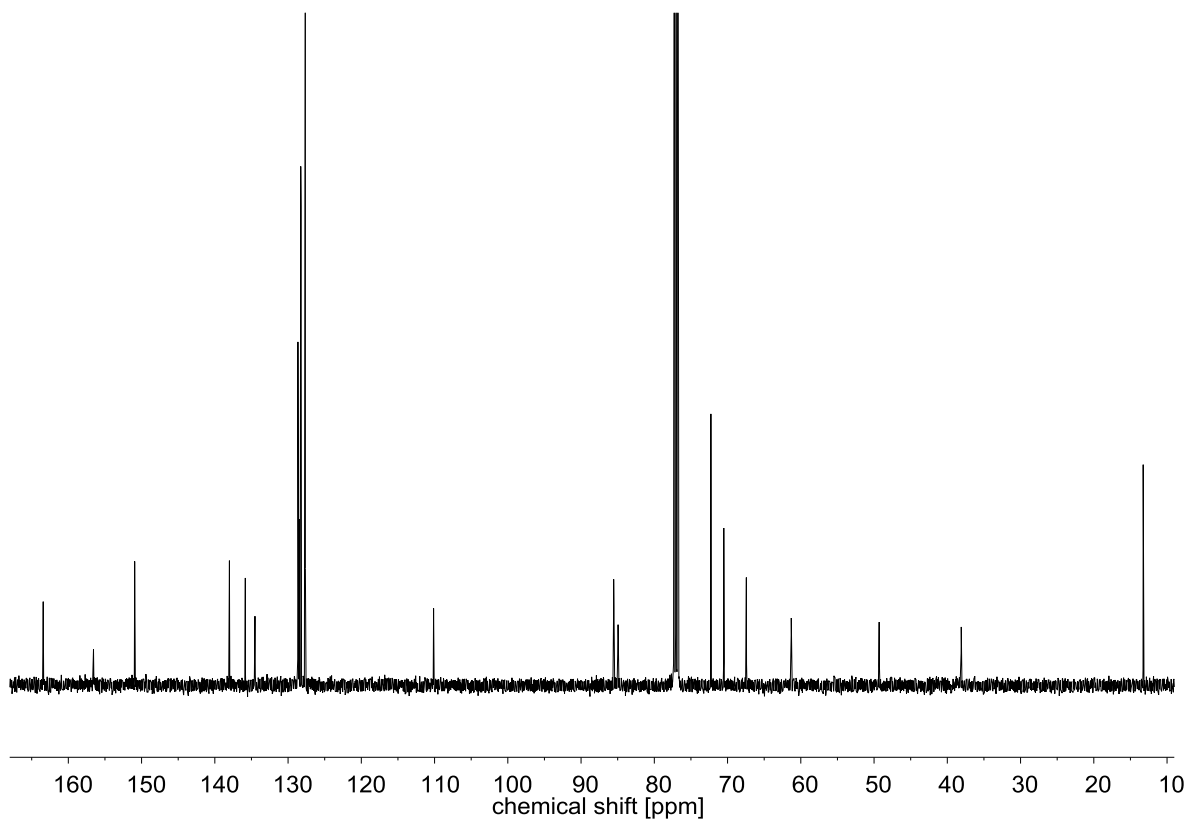
^1H NMR spectrum of **5** (500 MHz, CDCl_3)



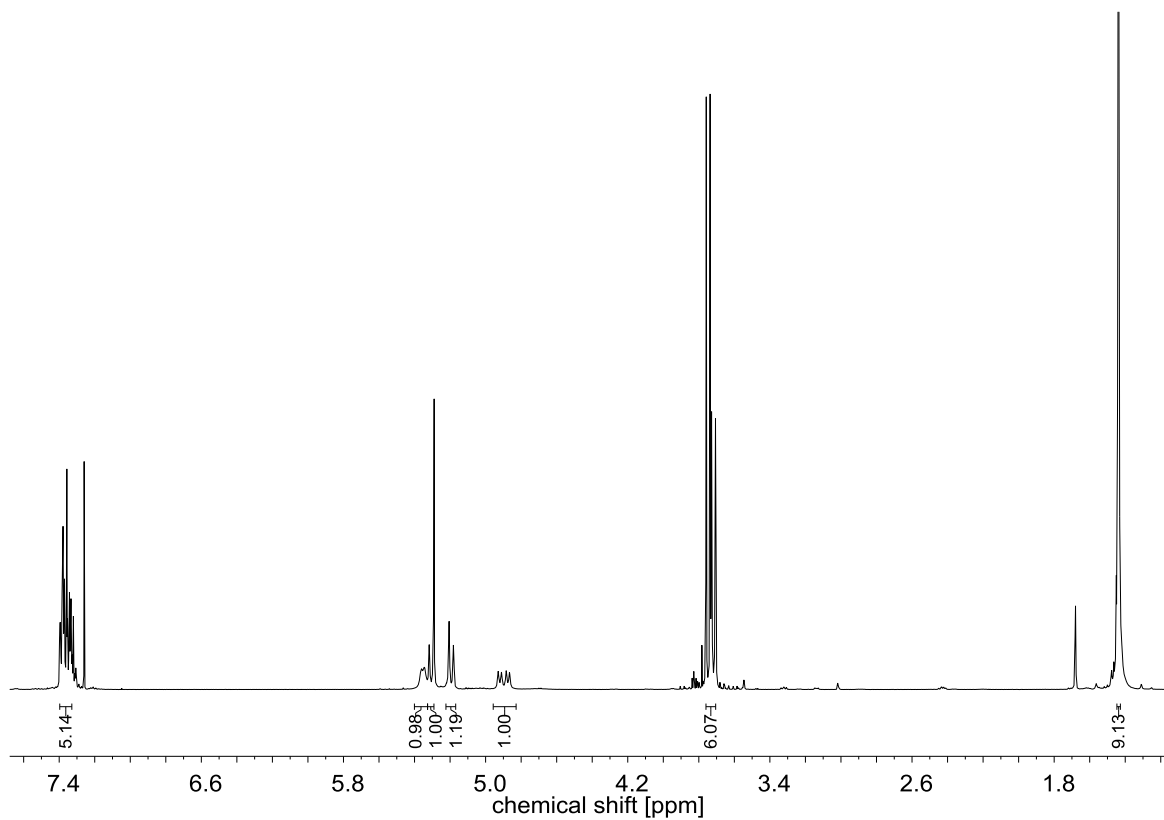
^{13}C NMR spectrum of **5** (126 MHz, CDCl_3)



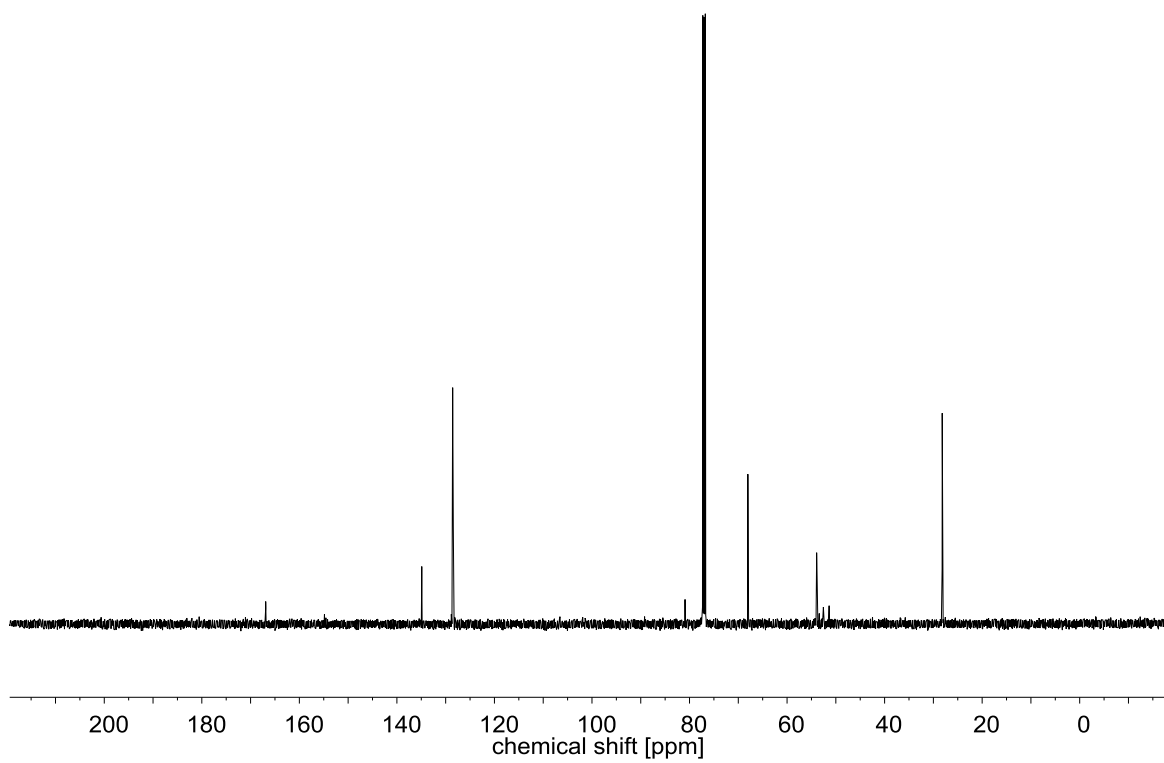
^1H NMR spectrum of **6** (300 MHz, CDCl_3)



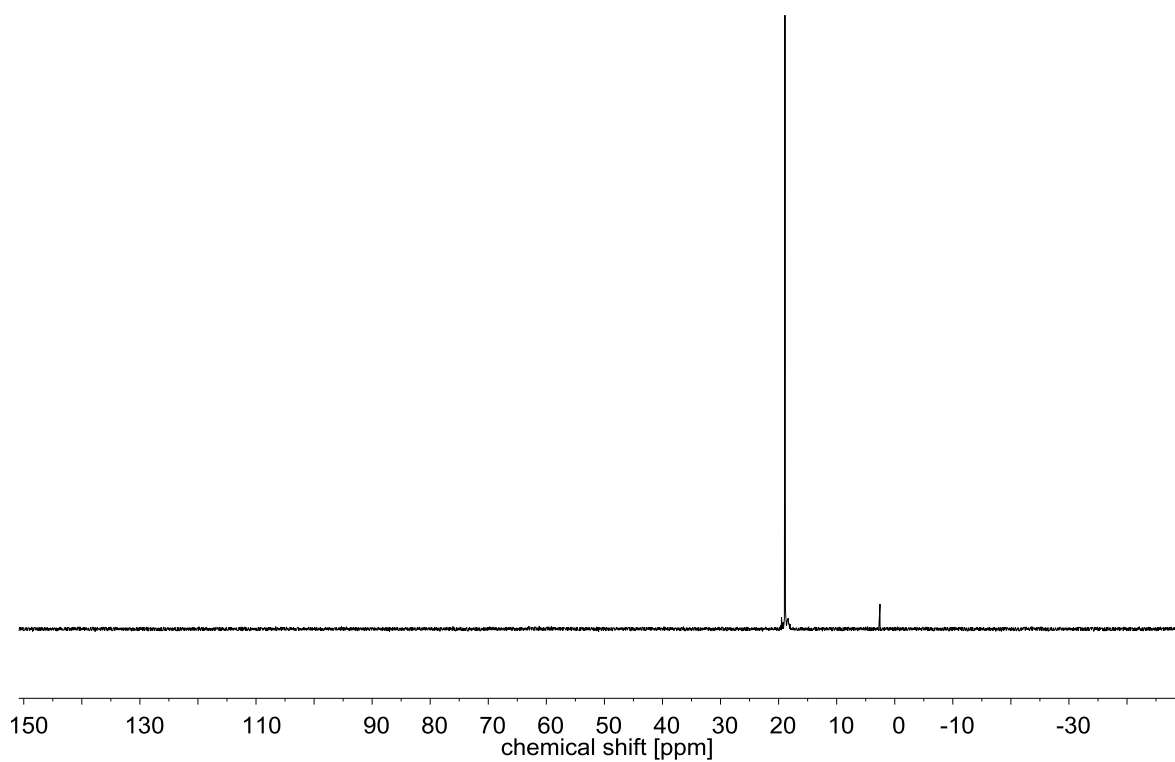
^{13}C NMR spectrum of **6** (126 MHz, CDCl_3)



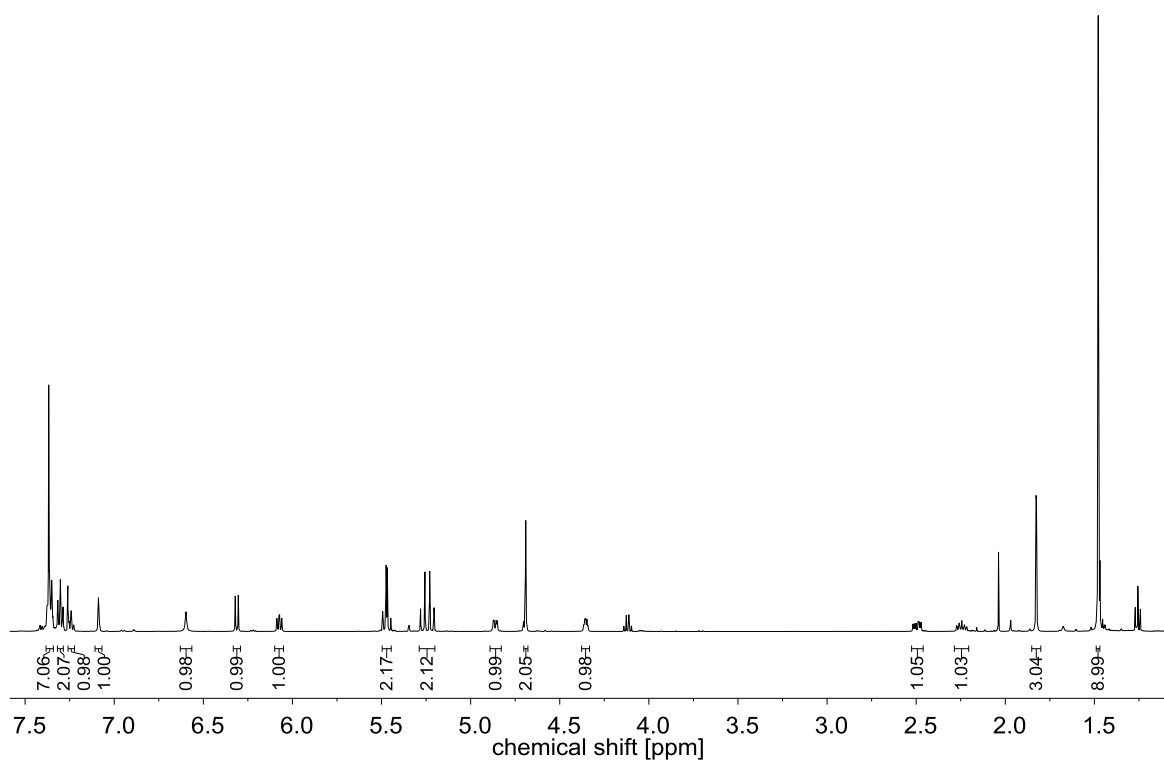
^1H NMR spectrum of **7** (300 MHz, CDCl_3)



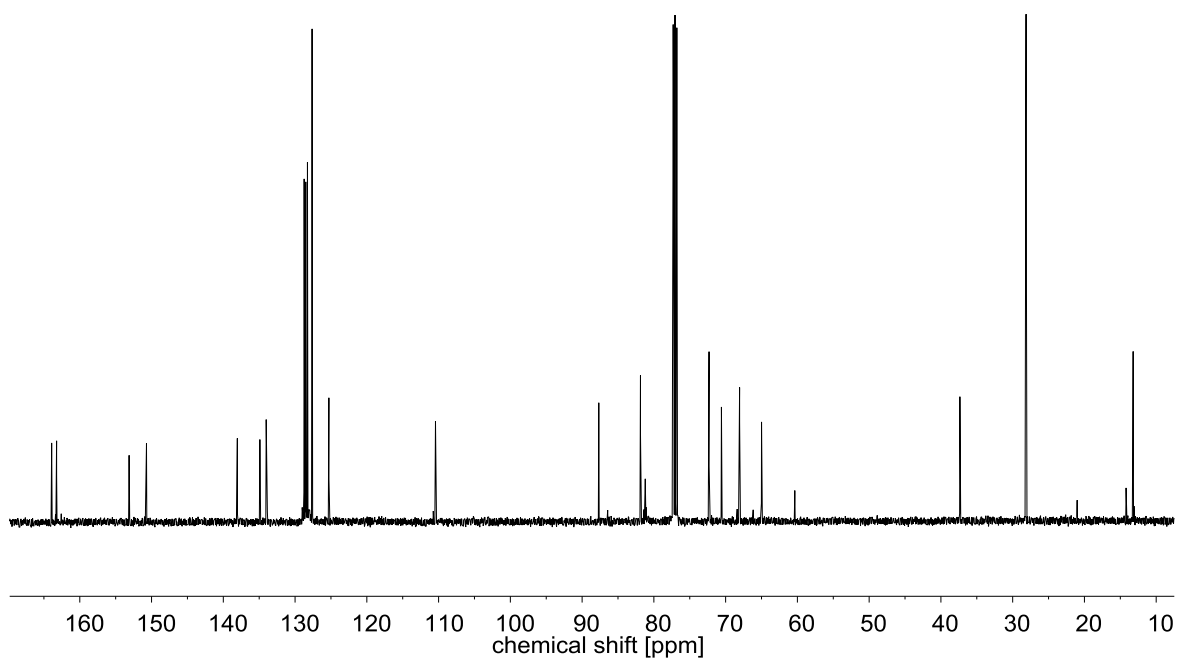
^{13}C NMR spectrum of **7** (126 MHz, CDCl_3)



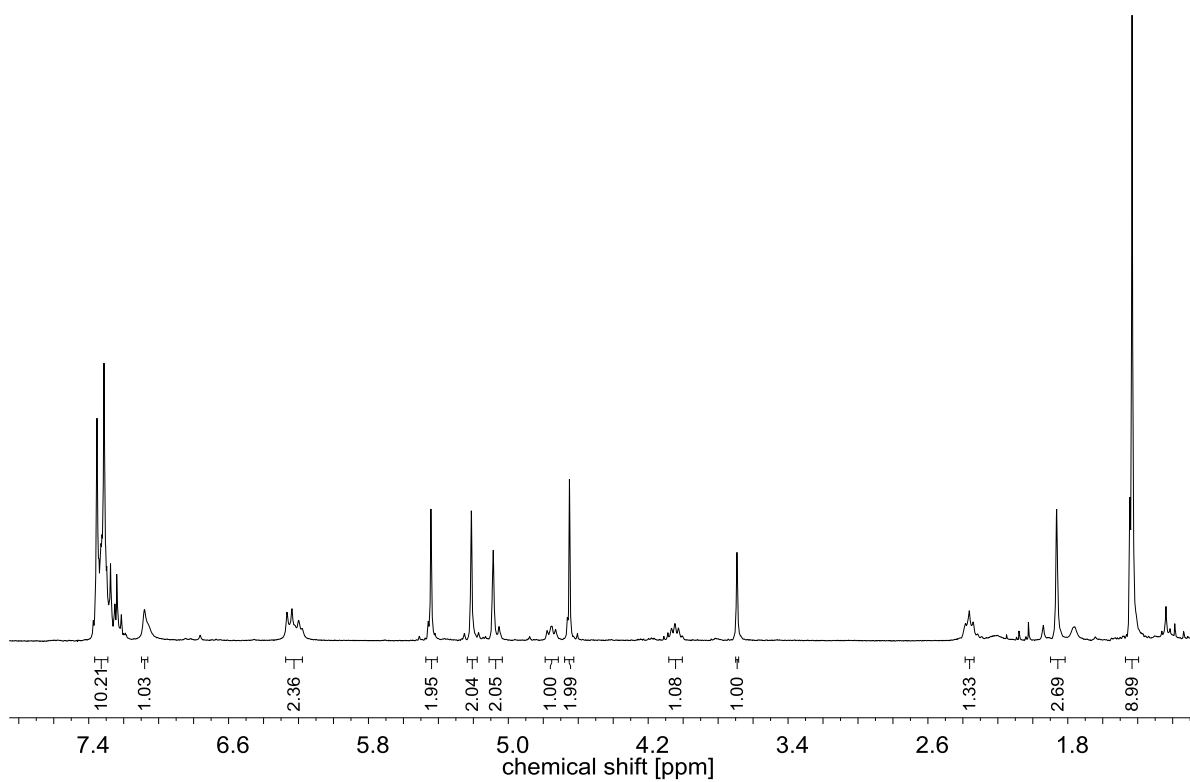
^{31}P NMR spectrum of **7** (121 MHz, CDCl_3)



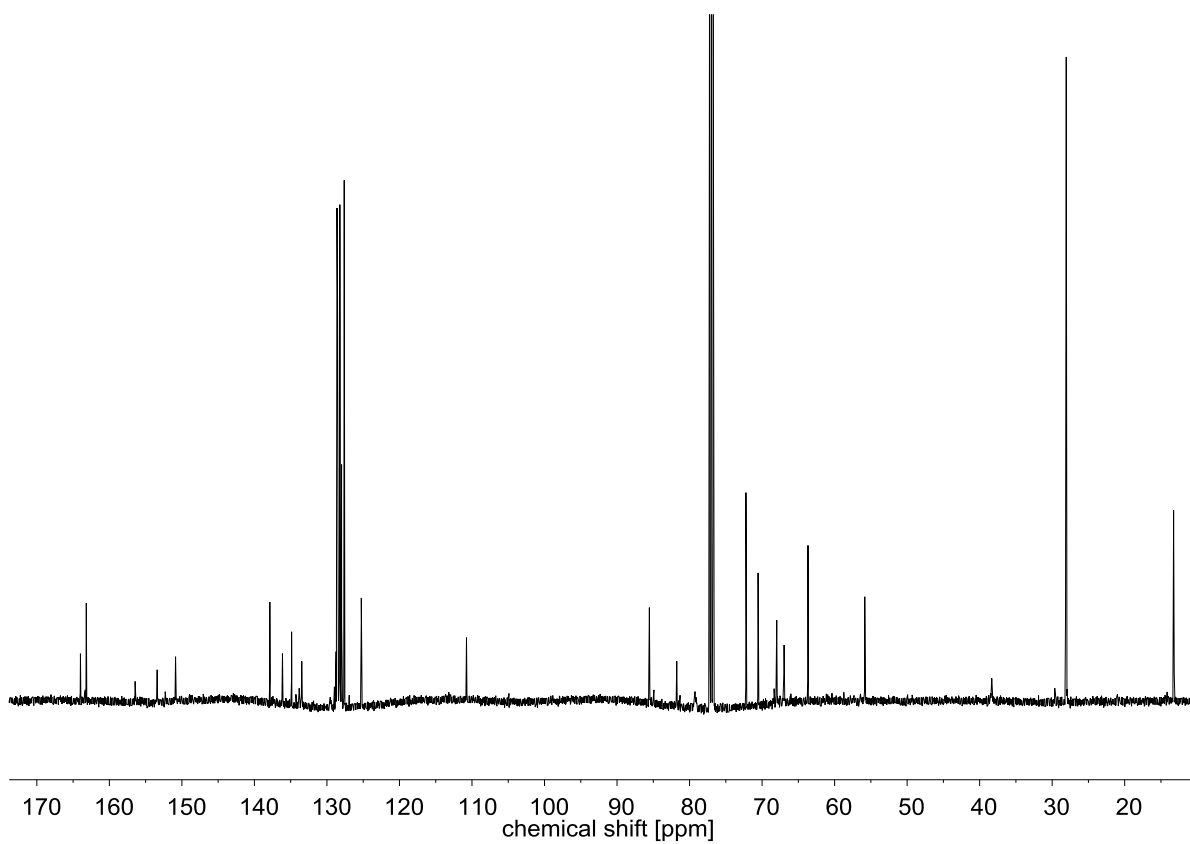
^1H NMR spectrum of **8** (500 MHz, CDCl_3)



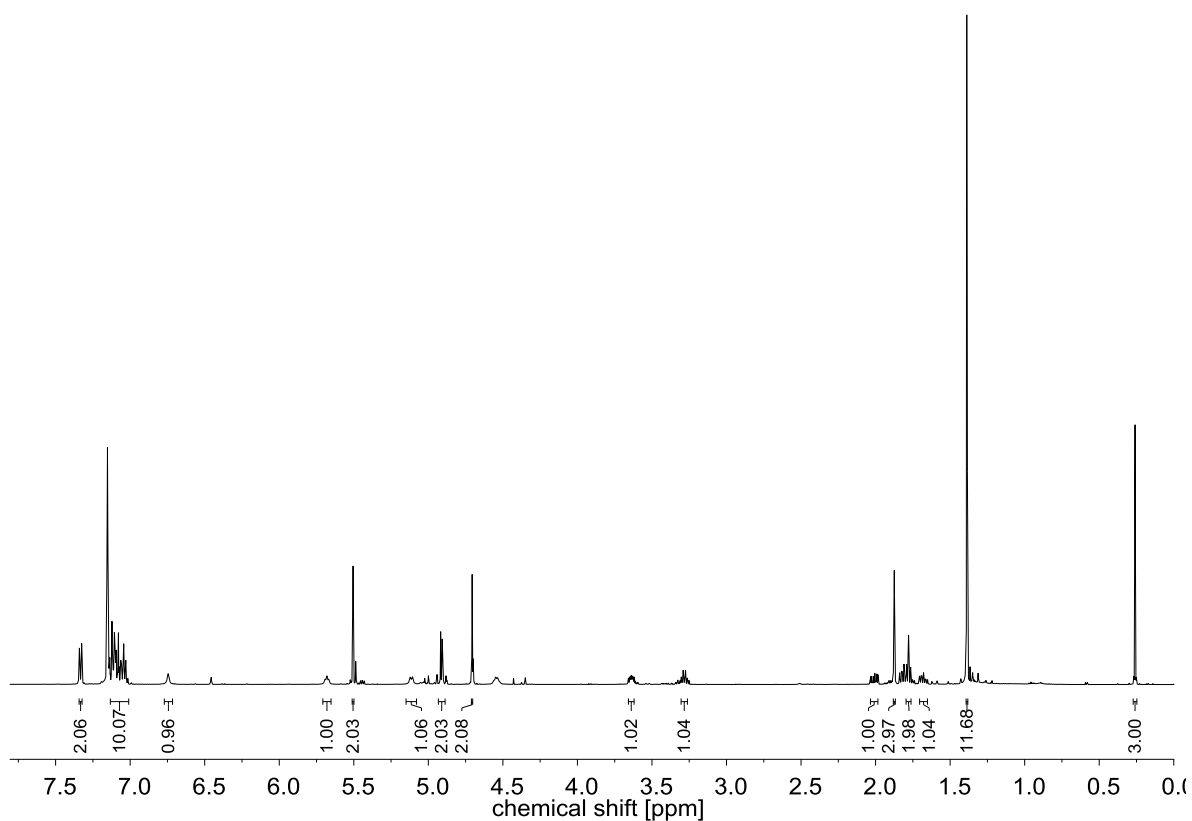
^{13}C NMR spectrum of **8** (126 MHz, CDCl_3)



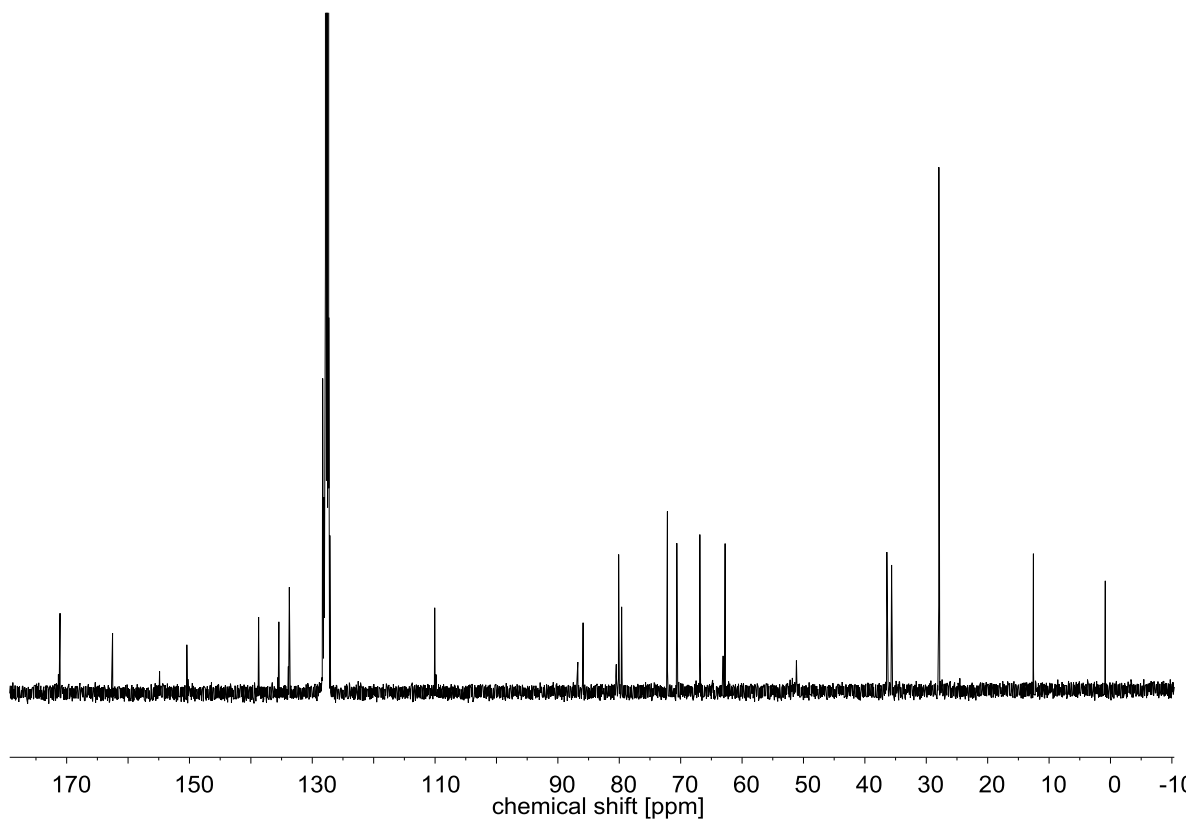
^1H NMR spectrum of **9** (500 MHz, CDCl_3)



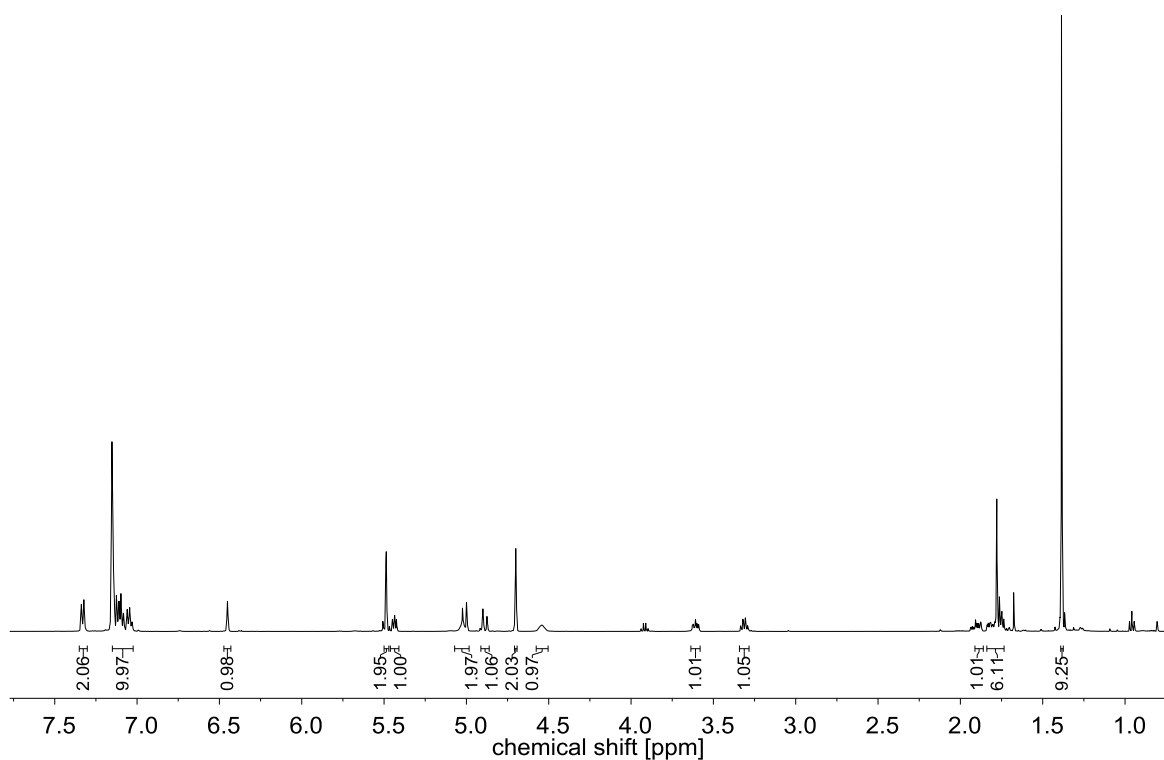
^{13}C NMR spectrum of **9** (126 MHz, CDCl_3)



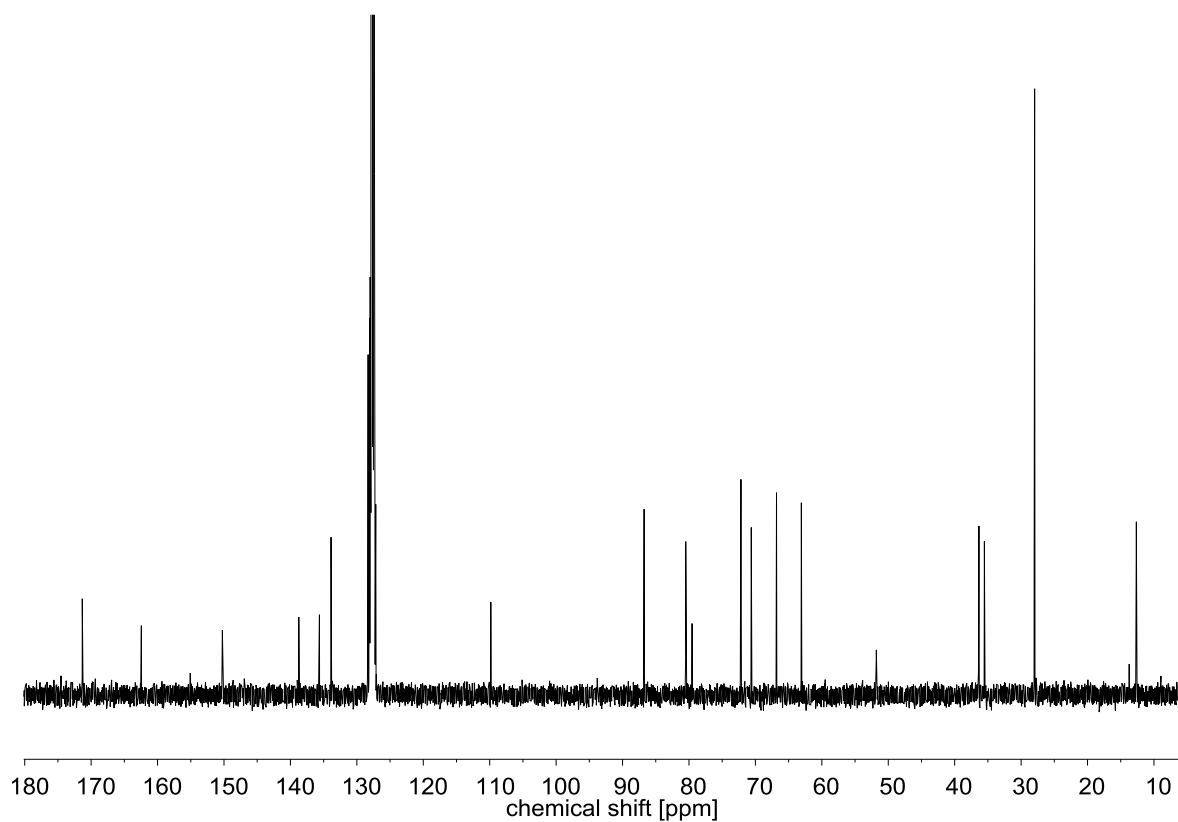
^1H NMR spectrum of (*S*)-**10** (300 MHz, CDCl_3)



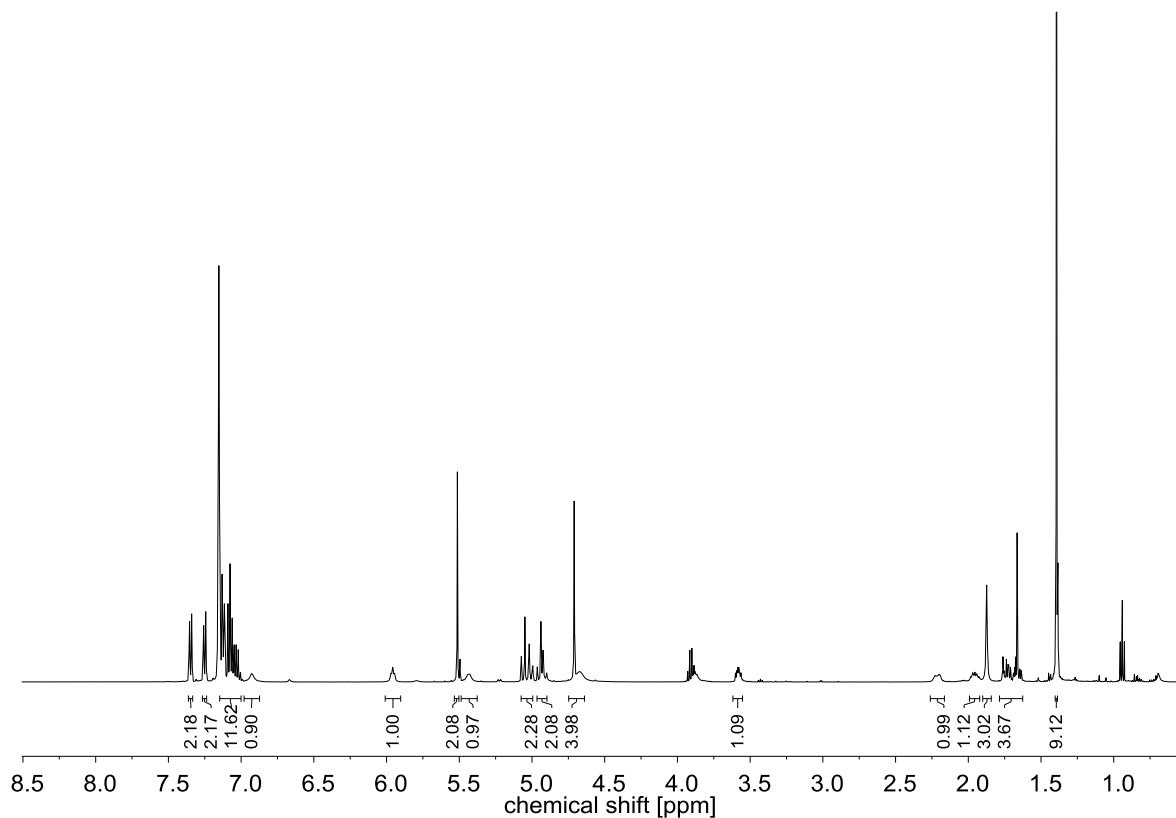
^{13}C NMR spectrum of (*S*)-**10** (126 MHz, CDCl_3)



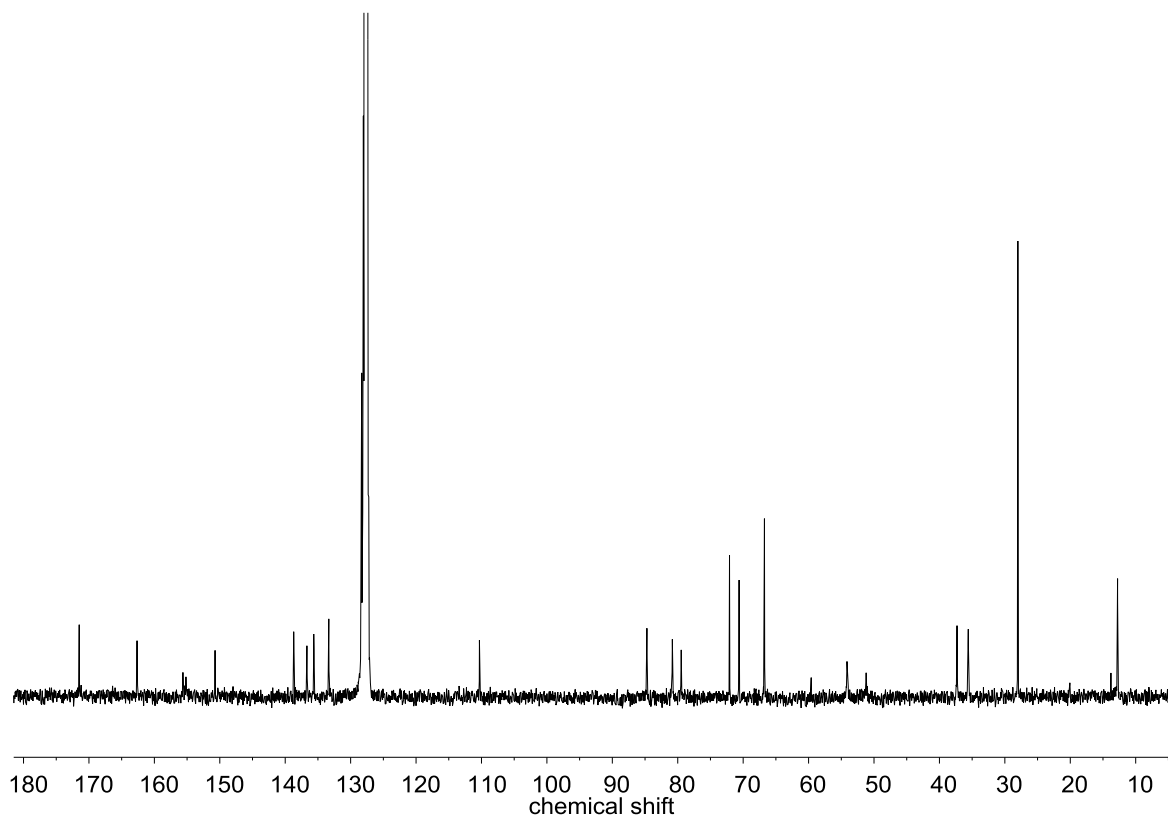
^1H NMR spectrum of (*R*)-**10** (300 MHz, CDCl_3)



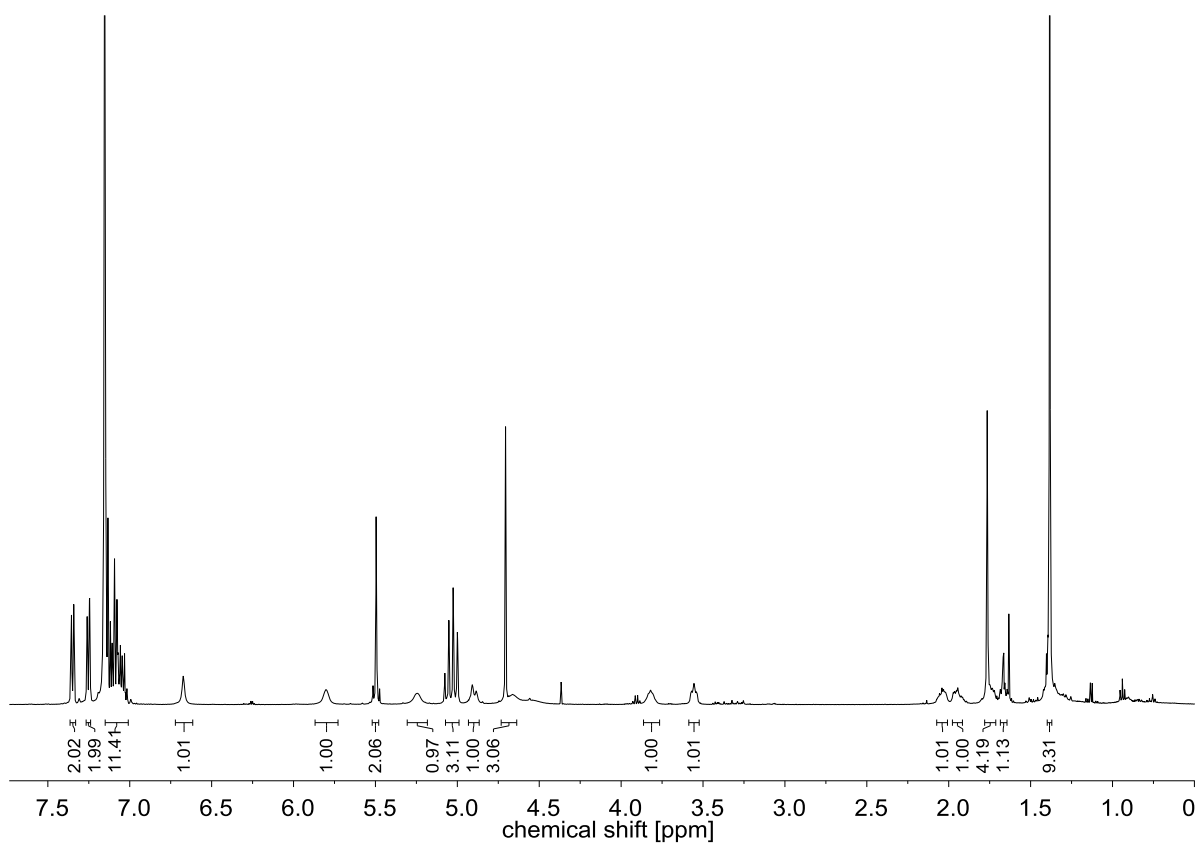
^{13}C NMR spectrum of (*R*)-**10** (126 MHz, CDCl_3)



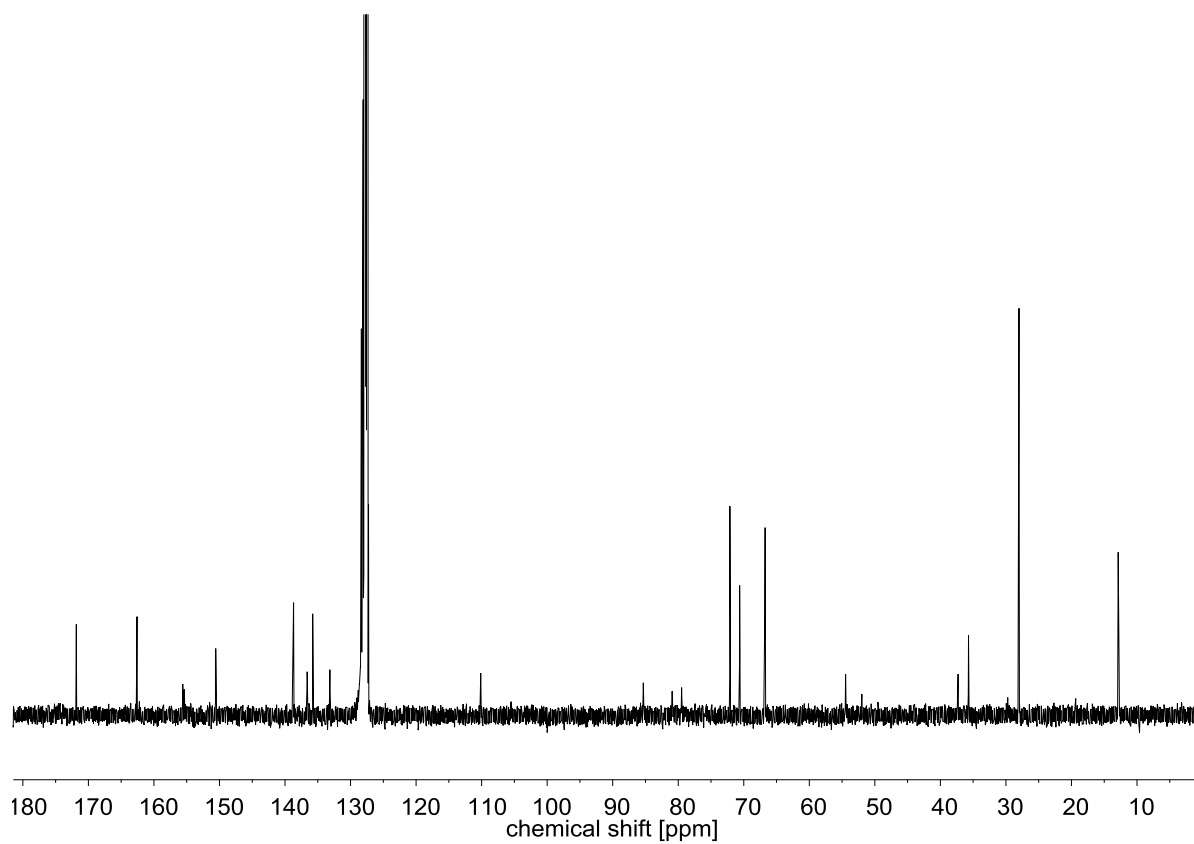
¹H NMR spectrum of (S)-11 (500 MHz, C₆D₆, 50 °C)



¹³C NMR spectrum of (S)-11 (126 MHz, C₆D₆, 50 °C)



^1H NMR spectrum of (*R*)-**11** (500 MHz, C_6D_6 , 50 °C)



^{13}C NMR spectrum of (*R*)-**11** (126 MHz, C_6D_6 , 50 °C)

Analytical data of oligonucleotide analogues

After SPPS, product identification and purity was assessed using an HPLC/ESI-MS 1200 system equipped with a Zorbax Eclipse XDB-C18 reverse-phase column (4.6 x 150 mm, particle size 5 μm , Agilent Technologies; solvent A: water + 0.1% TFA, solvent B: MeCN + 0.1% TFA; flow rate: 1 mL min⁻¹) connected to a liquid chromatography quadrupole Advantage Max (FinniganTM) mass spectrometer. According analytical data are shown in Table S1 and Figure S1. High-resolution mass spectrometry (HRMS) using a quadrupole linear ion trap Orbitrap mass spectrometer connected to an Accela HPLC system equipped with a Hypersyl GOLD column (50 mm x 1 mm, particle size 1.9 μm , Thermo Scientific) was also carried out (Figure S1). Oligonucleotide analogues were photometrically quantified using a NanoDrop 2000c (Thermo Scientific). The UV absorbance measurement was accomplished in water and a molar extinction coefficient at $\lambda = 260$ nm (λ_{260}) according to the computing program of the enterprise Proligo (nearest-neighbour-method)^{S7} was calculated treating the building block as thymidine monomers.

Table S1. Mass spectral data of synthesized oligonucleotide analogues; sequences from 5'- to 3'-end (corresponds to direction from C- to N-terminus, C-terminal amide (NH₂), N-terminal acetylation (Ac)), S = (6'S)-configured building block, R = (6'R)-configured building block; molecular formula (MF), molecular weight (MW), calculated molecular masses (m/z) for charged ions ($[\text{M} + 2\text{H}]^{2+}/[\text{M} + 3\text{H}]^{3+}/[\text{M} + 4\text{H}]^{4+}$), and found masses (m/z).

no.	sequence	MF	MW [g/mol]	calculated	found
1a	5'-NH ₂ -SSSSSSSSSSSSSS-Ac-3'	C ₁₇₀ H ₂₂₉ N ₅₇ O ₅₇	3983.04	1992.5 (2+)	1994.3
				1328.7 (3+)	1329.5
				996.8 (4+)	996.9
1b	5'-NH ₂ -RRRRRRRRRRRRRR-Ac-3'	C ₁₇₀ H ₂₂₉ N ₅₇ O ₅₇	3983.04	1992.5 (2+)	1994.7
				1328.7 (3+)	1330.7
				996.8 (4+)	998.6

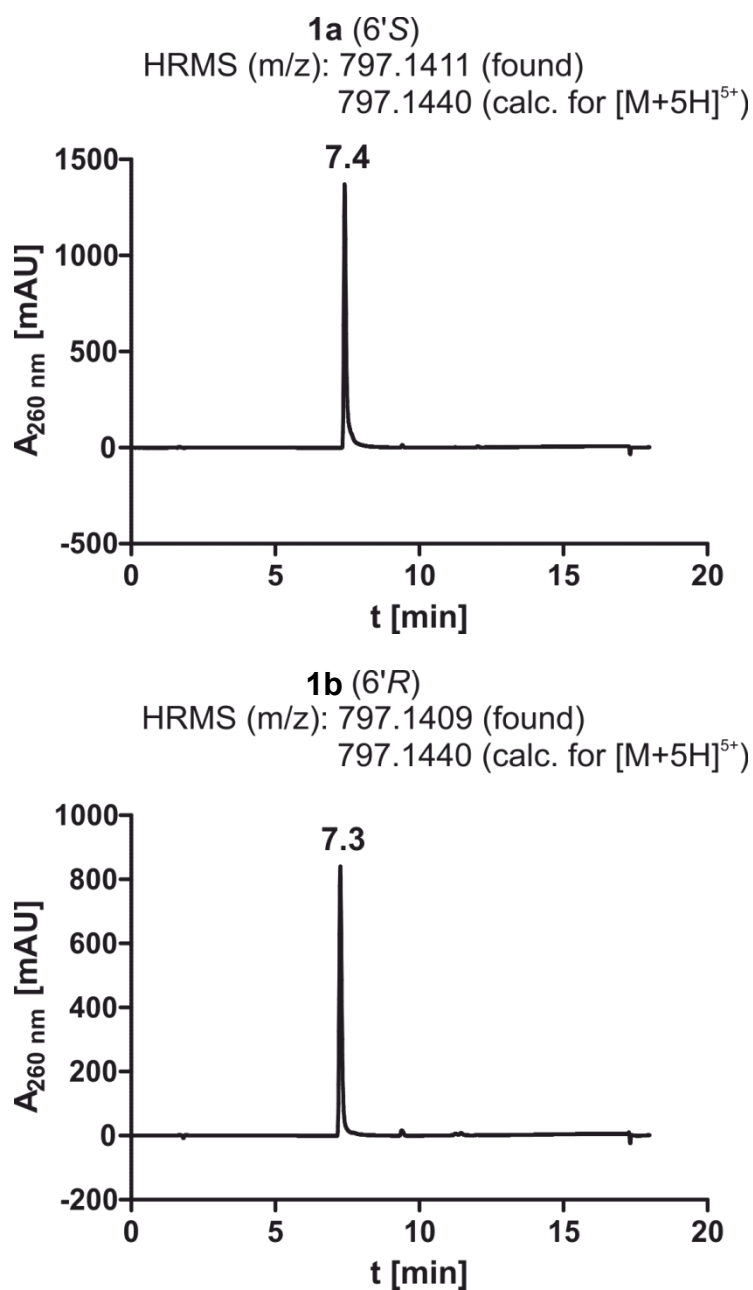


Figure S1. Analytical data of synthesized oligonucleotide analogues. Purity and identity were validated by HPLC/ESI-MS showing the eluting peak in the HPLC chromatogram with corresponding HRMS data. Retention times in min are denoted. Found and calculated masses by HRMS for charged ions ($[M + 5H]^{5+}$) are stated.

Melting temperature experiments

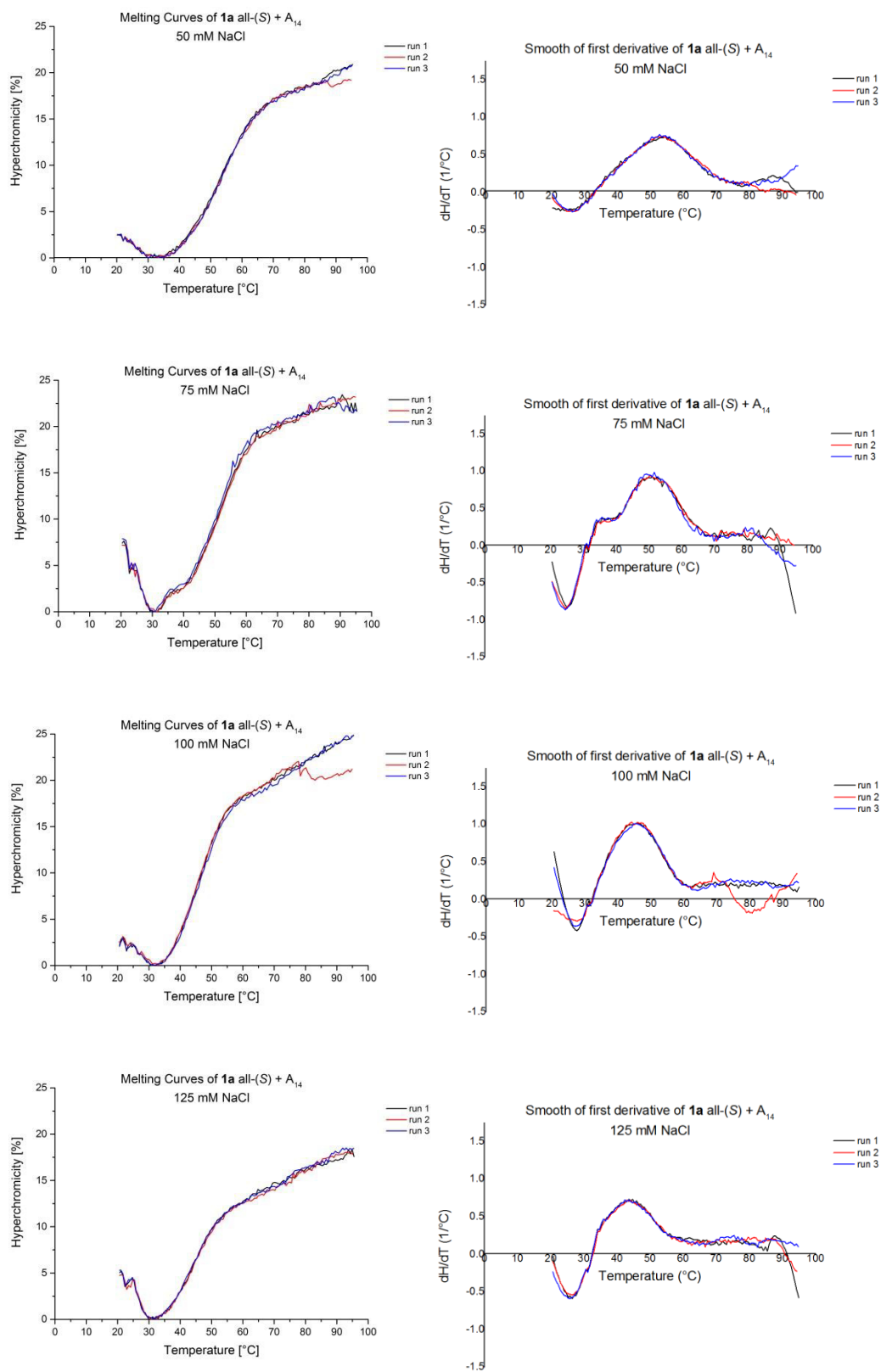


Figure S2. Melting curves (triplicates) and smoothed first derivatives for oligonucleotide analogue **1a** (6'S) with complementary native DNA at increasing NaCl concentrations.

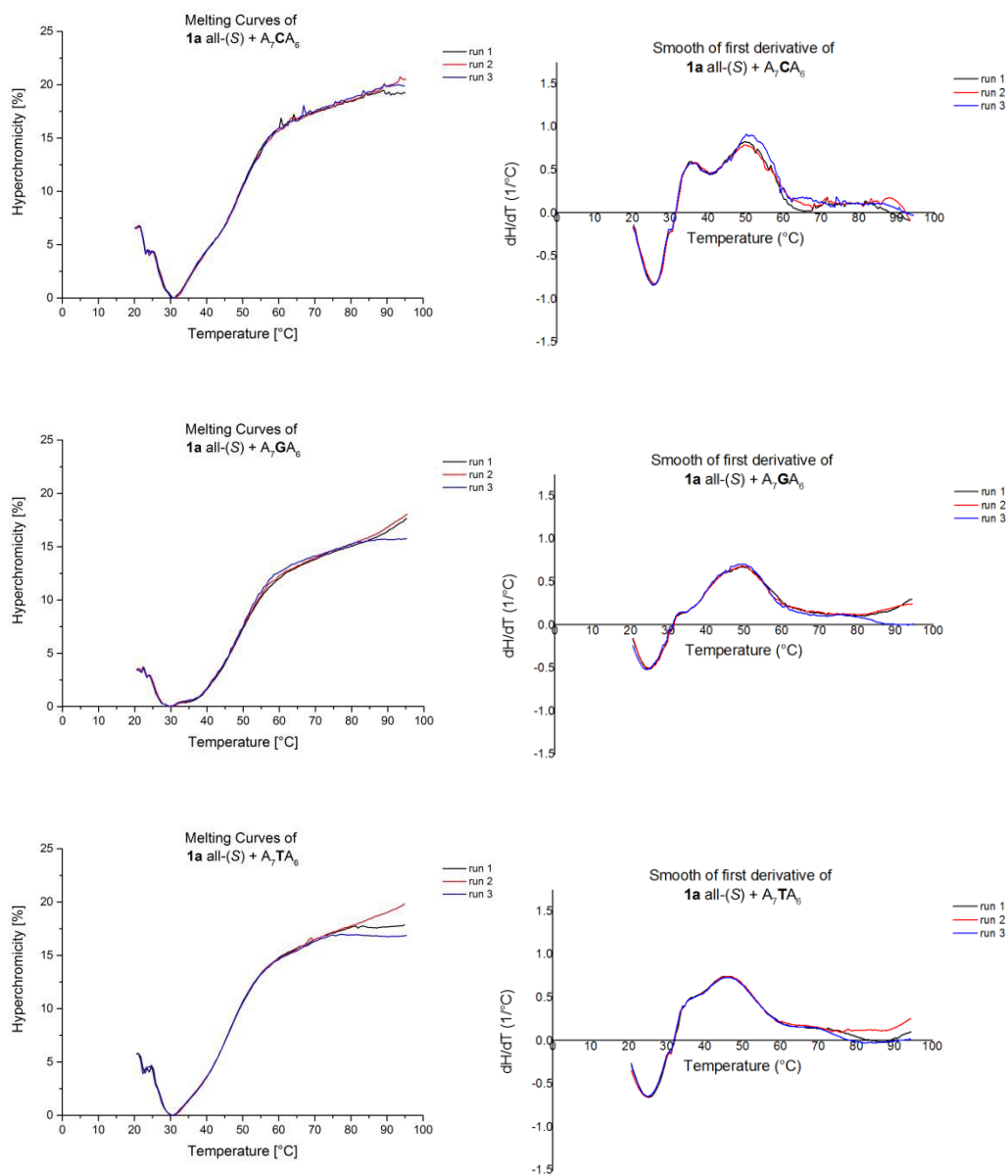


Figure S3. Melting curves (triplicates) and smoothed first derivatives for oligonucleotide analogue **1a** (6'S) with native DNA containing a single base mismatch.

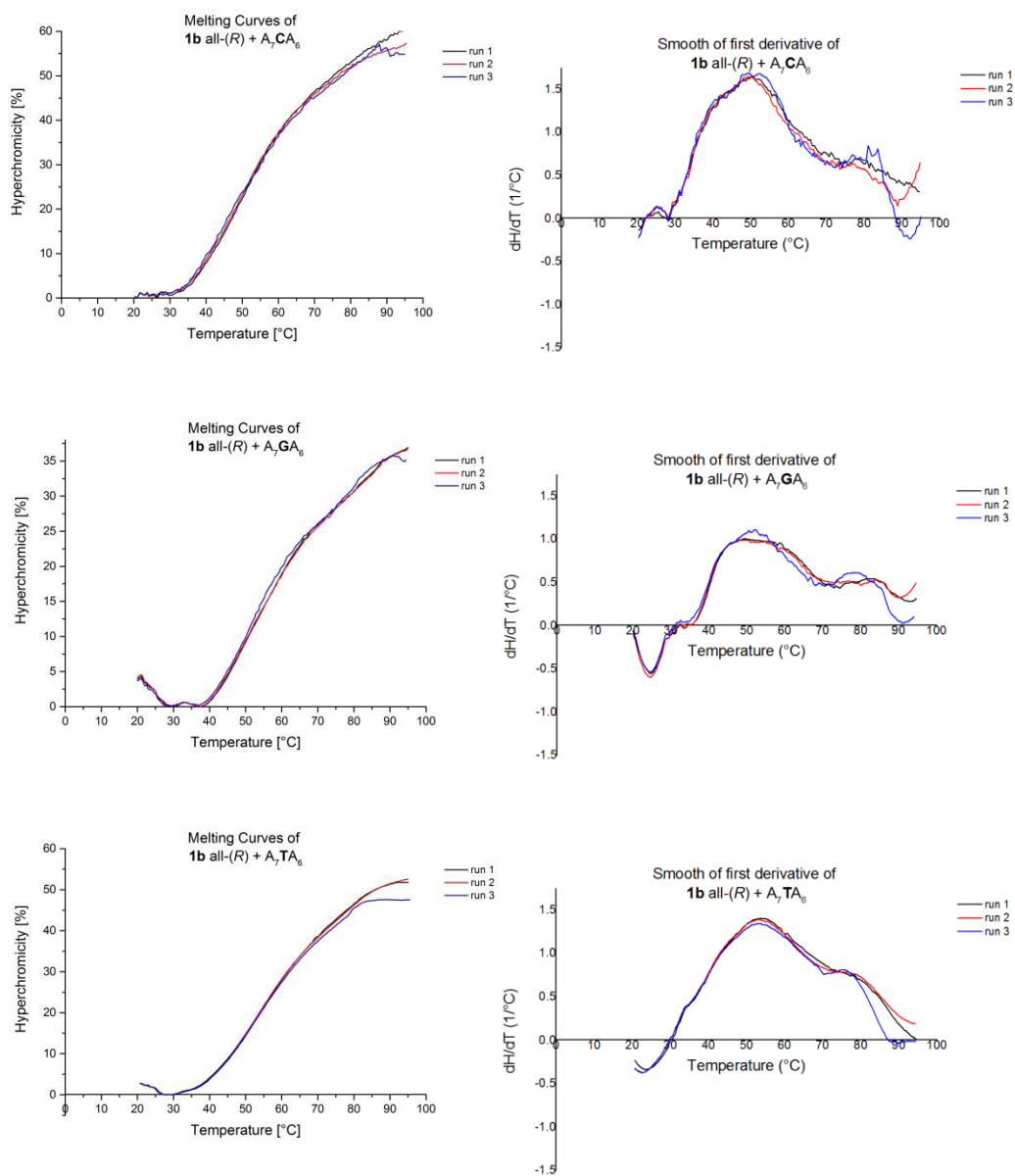


Figure S4. Melting curves (triplicates) and smoothed first derivatives for oligonucleotide analogue **1b** (6'R) with native DNA containing a single base mismatch.

Additional CD spectrum

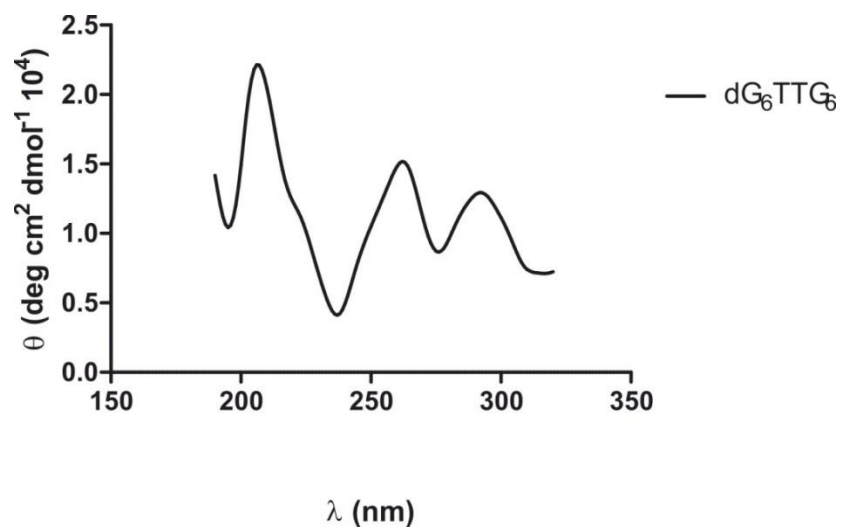


Figure S5. CD spectrum of native single-stranded DNA oligonucleotide G₆TTG₆.

References

- S1 S. Czernecki, J.-M. Valéry, *Synthesis* **1991**, 239-240.
- S2 R. Eisenhuth, C. Richert, *J. Org. Chem.* **2008**, *74*, 26-37.
- S3 U. Schmidt, A. Lieberknecht, U. Schanbacher, T. Beuttler, J. Wild, *Angew. Chem.* **1982**, *94*, 797-798; *Angew. Chem. Int. Ed.* **1982**, *21*, 776-777.
- S4 U. Schmidt, A. Lieberknecht, J. Wild, *Synthesis* **1984**, 53-60.
- S5 U. Schmidt, J. Wild, *Liebigs Ann. Chem.* **1985**, 1882-1894.
- S6 R. Hamzavi, F. Dolle, B. Tavitian, O. Dahl, P. E. Nielsen, *Bioconjugate Chem.* **2003**, *14*, 941-954.
- S7 <http://proligo2.prolig.com/calculation/calculation.html>.

6.2.2 Manuscript C: Towards Zwitterionic Oligonucleotides with Improved Properties: the NAA/LNA-Gapmer Approach

Supporting information for this article is available on the WWW under:
<https://doi.org/10.1002/cbic.202000450>.

ChemBioChem

Supporting Information

Towards Zwitterionic Oligonucleotides with Improved Properties: the NAA/LNA-Gapmer Approach

Melissa Wojtyniak, Boris Schmidtgall, Philine Kirsch, and Christian Ducho*

Table of Contents

Synthesis.....	S2
^1H , ^{13}C and ^{31}P NMR spectra of synthesised compounds.....	S14
Oligonucleotide synthesis, purification and analytical data.....	S23
Melting temperature experiments.....	S28
References.....	S31

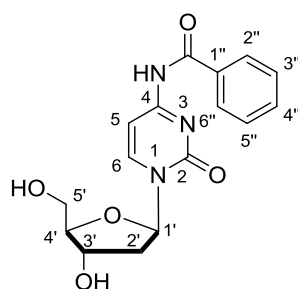
Synthesis

General methods

The synthesis of thymidinyI amino acid building block **9** was carried out as reported before [S1,S2]. All other chemicals were purchased from standard suppliers. Reactions involving oxygen and/or moisture sensitive reagents were carried out under an atmosphere of nitrogen or argon using anhydrous solvents. Anhydrous solvents were obtained in the following manner: THF, MeCN, CH₂Cl₂, Et₂O and DMF were dried with a solvent purification system (MBRAUN MB SPS 800). Pyridine was dried over CaH₂ and distilled. MeOH was dried over activated molecular sieves (4 Å) and degassed. All other solvents were of technical quality and distilled prior to use, and deionised water was used throughout. Column chromatography was carried out on silica gel 60 (0.040-0.063 mm, 230-400 mesh ASTM, VWR) under flash conditions (with air, in case of phosphoramidite **14** with nitrogen) except where indicated. TLC was performed on aluminium plates precoated with silica gel 60 F₂₅₄ (VWR). Visualisation of the spots was carried out using UV light (254 nm) and/or staining under heating (H₂SO₄ staining solution: 4 g vanillin, 25 mL conc. H₂SO₄, 80 mL AcOH and 680 mL MeOH). Analytical RP-HPLC-MS was performed on a Thermo Scientific Spectra System consisting of an SN 4000 controller, an SCM 1000 mixer, a P4000 pump system, an AS3000 autosampler, an UV2000 detector and a Surveyor MSQ Plus ESI mass spectrometer (Finnigan) using MeCN-water mixtures (containing 0.1% TFA if needed) as eluents. 500 MHz-¹H, 126 MHz-¹³C and 202 MHz-³¹P NMR spectra were recorded on Bruker Avance I 500, Avance DRX 500 or Avance III 500 (with TCI cryoprobe) spectrometers. All ¹³C NMR spectra are ¹H-decoupled. All spectra were recorded at room temperature except where indicated and were referenced internally to solvent reference frequencies wherever possible. Chemical shifts (δ) are quoted in ppm and coupling constants (*J*) are reported in Hz.

Assignment of signals was carried out using H,H-COSY, HSQC, and HMBC spectra obtained on the spectrometers mentioned above. High resolution mass spectra were measured on a Bruker Maxis 4G (UPLC-coupled with Dionex/Thermo Scientific RSLC3000 Ultimate) or on a Thermo Scientific Q Exactive Orbitrap (HPLC-coupled) mass spectrometer with ESI ionisation mode.

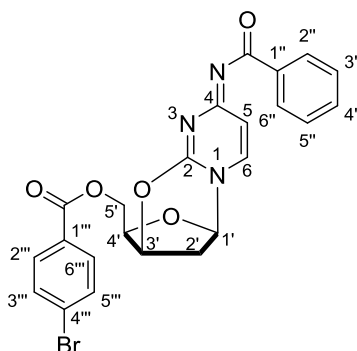
4-*N*-Benzoyl-2'-deoxycytidine **4**



2'-Deoxycytidine **3** (7.00 g, 30.8 mmol) was coevaporated with pyridine (40 mL) and pyridine (100 mL) was added. Trimethylsilyl chloride (TMSCl, 18.1 g, 167 mmol) was slowly added and the mixture was stirred at rt for 60 min, after which benzoyl chloride (23.5 g, 167 mmol) was added and the solution was stirred at rt for another 24 h. After cooling to 0 °C, water (30 mL) was added and the mixture was stirred at 0 °C for 10 min. Then, aq. NH₃ (25%, 100 mL) was added and the solution was stirred for further 30 min while warming to rt. The solvent was evaporated under reduced pressure and the resultant crude product was purified by column chromatography (CH₂Cl₂-MeOH, 9:1) to give **4** (9.80 g, 96%). ¹H NMR (500 MHz, DMSO-d₆): δ = 2.02-2.09 (m, 1H, 2'-H_a), 2.28-2.34 (m, 1H, 2'-H_b), 3.58 (d, *J* = 10.1 Hz, 1H, 5'-H_a), 3.64 (d, *J* = 11.8 Hz, 1H, 5'-H_b), 3.88 (ddd, *J* = 3.7, 3.7, 3.6 Hz, 1H, 4'-H), 4.21-4.27 (m, 1H, 3'-H), 5.09 (brs, 1H, OH), 5.29 (brs, 1H, OH), 6.14 (dd, *J* = 6.3, 6.3 Hz, 1H, 1'-H), 7.30-7.39 (m, 1H, 5-H), 7.46-7.54 (m, 2H, 3''-H, 5''-H), 7.58-7.65 (m, 1H, 4''-H), 8.00 (dd, *J* = 8.3, 1.1 Hz, 2H, 2''-H, 6''-H), 8.40 (d, *J* = 7.6 Hz, 1H, 6-H), 11.25 (brs, 1H, NH). ¹³C NMR (126 MHz, DMSO-d₆): δ = 40.88 (C-2'), 60.91 (C-5'), 69.88 (C-3'), 86.17

(C-1'), 87.91 (C-4'), 96.01 (C-5), 128.41, 129.21, 132.68, 133.18 (aryl-C), 144.89 (C-6), 156.34 (C-2), 162.89 (C-4), 167.59 (Bz-C=O). HRMS (ESI): calcd. for C₁₆H₁₈N₃O₅ [M+H]⁺ 332.1241, found 332.1224. TLC (CH₂Cl₂-MeOH, 9:1): R_f = 0.21.

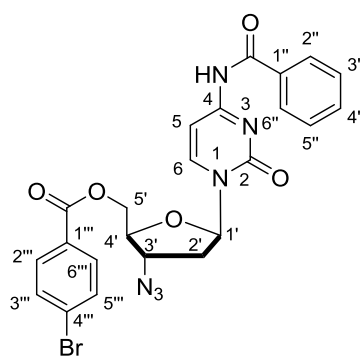
O*-2,3'-Anhydro-4-*N*-benzoyl-5'-*O*-(*p*-bromobenzoyl)-2'-deoxycytidine **5*



4-*N*-Benzoyl-2'-deoxycytidine **4** (4.75 g, 14.3 mmol) was dissolved in DMF (60 mL) and cooled to 0 °C. Triphenylphosphine (7.37 g, 28.1 mmol), 4-bromobenzoic acid (5.63 g, 28.0 mmol) and diisopropyl azodicarboxylate (DIAD, 5.67 g, 28.0 mmol) were added and the reaction mixture was stirred at rt for 1 h. The solution was then cooled to 0 °C, and more triphenylphosphine (7.37 g, 28.1 mmol) and DIAD (5.67 g, 28.0 mmol) were added. The reaction mixture was stirred for 3 h while warming to rt, cooled to 0 °C again, mixed with Et₂O (600 mL) and stored at 0 °C for 24 h. The precipitated solid was filtered off and washed with Et₂O (4 x 50 mL, 0 °C). The solvent of the combined filtrates was evaporated under reduced pressure to give **5** (2.77 g, 39%). ¹H NMR (500 MHz, DMSO-d₆): δ = 2.54-2.60 (m, 1H, 2'-H_a), 2.65-2.71 (m, 1H, 2'-H_b), 4.38-4.47 (m, 1H, 5'-H_a), 4.53-4.65 (m, 2H, 4'-H, 5'-H), 5.44-5.50 (m, 1H, 3'-H), 6.00 (d, *J* = 3.5 Hz, 1H, 1'-H), 6.46 (d, *J* = 7.4 Hz, 1H, 5-H), 7.42 (dd, *J* = 7.5, 7.5 Hz, 2H, 3''-H, 5''-H), 7.51 (t, *J* = 7.4 Hz, 1H, 4''-H), 7.66 (d, *J* = 7.4 Hz, 1H, 6-H), 7.72 (d, *J* = 8.4 Hz, 2H, 2'''-H, 6'''-H), 7.81 (d, *J* = 8.5 Hz, 2H, 3'''-H, 5'''-H), 7.91-7.96 (m, 2H, 2''-H, 6''-H). ¹³C NMR (126 MHz, DMSO-d₆): δ = 32.62 (C-2'), 62.37 (C-5'), 78.00 (C-3'), 81.89 (C-4'), 87.20 (C-1'), 105.76 (C-5), 127.65 (C-4''), 128.07 (C-2'', C-6''), 128.87

(C-4'''), 129.20 (C-3'', C-5''), 131.12 (C-3''', C-5'''), 131.54 (C-1''), 131.91 (C-2''', C-6'''), 136.59 (C-1'''), 139.83 (C-6), 152.91 (C-2), 161.96 (C-4), 164.70 (Bz-C=O), 177.29 (ester-C=O). HRMS (ESI): calcd. for C₂₃H₁₉BrN₃O₅ [M+H]⁺ 496.0503, found 496.0531. TLC (CH₂Cl₂-MeOH, 4:1): R_f = 0.30.

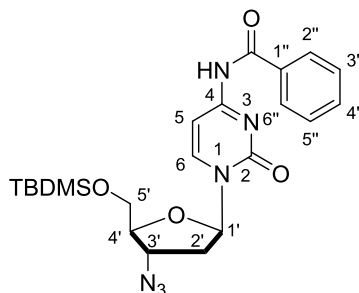
3'-Azido-4-N-benzoyl-5'-O-(*p*-bromobenzoyl)-2',3'-dideoxycytidine **6**



Sodium azide (1.42 g, 21.8 mmol) and *O*-2,3'-anhydro-4-*N*-benzoyl-5'-*O*-(*p*-bromobenzoyl)-2'-deoxycytidine **5** (2.70 g, 5.44 mmol) were dissolved in DMF (69 mL) and the reaction mixture was stirred at 130 °C for 45 min. It was then added to sat. NH₄Cl solution (240 mL) and extracted with EtOAc (3 x 200 mL). The organic layer was dried over Na₂SO₄ and the solvent was evaporated under reduced pressure. The resultant crude product was purified by column chromatography (petroleum ether-EtOAc, 1:6) to give **6** (1.93 g, 66%). ¹H NMR (500 MHz, CDCl₃): δ = 2.46 (ddd, *J* = 14.1, 7.2, 5.0 Hz, 1H, 2'-H_a), 2.80 (ddd, *J* = 13.0, 10.2, 6.3 Hz, 1H, 2'-H_b), 4.22 (dd, *J* = 12.5, 6.4 Hz, 1H, 3'-H), 4.25-4.31 (m, 1H, 4'-H), 4.60-4.67 (m, 2H, 5'-H), 6.08-6.15 (m, 1H, 1'-H), 7.44-7.53 (m, 3H, 5-H, 3''-H, 5''-H), 7.55-7.65 (m, 3H, 4''-H, 2'''-H, 6'''-H), 7.79-7.91 (m, 4H, 2''-H, 6''-H, 3'''-H, 5'''-H), 7.97-8.04 (m, 1H, 6-H). ¹³C NMR (126 MHz, CDCl₃): δ = 38.96 (C-2'), 60.17 (C-3'), 63.80 (C-5'), 87.86 (C-1'), 97.13 (C-5), 127.75 (C-4''), 128.06 (C-2'', C-6''), 128.93 (C-4'''), 129.25 (C-3'', C-5''), 131.21 (C-2''', C-6'''), 132.28 (C-1'', C-2''', C-6'''), 133.53 (C-1'''), 142.98 (C-6), 153.73 (C-2), 162.47 (C-4),

165.53 (Bz-C=O), 175.04 (ester-C=O). HRMS (ESI): calcd. for $C_{23}H_{20}BrN_6O_5$ $[M+H]^+$ 539.0673, found 539.0641. TLC (petroleum ether-EtOAc, 1:6): $R_f = 0.35$.

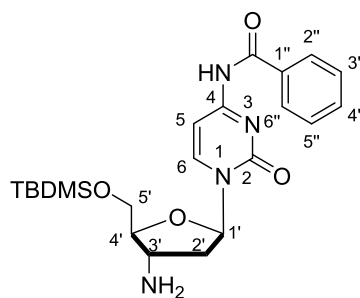
3'-Azido-4-*N*-benzoyl-5'-*O*-TBDMS-2',3'-dideoxycytidine **7**



A solution of 3'-azido-4-*N*-benzoyl-5'-*O*-(*p*-bromobenzoyl)-2',3'-dideoxycytidine **6** (1.45 g, 2.68 mmol) in THF (17 mL) was cooled to 0 °C. An aqueous solution of LiOH-hydrate (1 M, 10.7 mL, 10.7 mmol LiOH-hydrate) was added dropwise over 2 h, and the reaction mixture was then stirred at 0 °C for 3 h until complete conversion was observed by TLC. The reaction mixture was diluted with CH_2Cl_2 (110 mL) and washed with sat. NH_4Cl solution and brine. The solvent of the organic layer was evaporated under reduced pressure to give the crude 5'-alcohol (947 mg). This material (1.23 g, 3.50 mmol, from several reaction batches) was then coevaporated with toluene (2 x 10 mL) and dissolved in DMF (6 mL). NEt_3 (1.06 g, 10.5 mmol) and *tert*-butyldimethylsilyl chloride (TBDMSCl, 1.06 g, 7.00 mmol) were added and the reaction mixture was stirred at rt for 16 h. Then, EtOAc (15 mL) was added, the solution was washed with brine, dried over Na_2SO_4 and the solvent was evaporated under reduced pressure. The resultant crude product was purified by column chromatography (petroleum ether-EtOAc, 2:3) to give **7** (1.39 g, 85% over 2 steps from **6**). 1H NMR (500 MHz, $CDCl_3$): $\delta = 0.14$ (s, 3H, $SiCH_3$), 0.15 (s, 3H, $SiCH_3$), 0.94 (s, 9H, $SiC(CH_3)_3$), 2.41 (ddd, $J = 13.8, 6.9, 4.1$ Hz, 1H, 2'- H_a), 2.66 (ddd, $J = 13.8, 6.9, 6.9$ Hz, 1H, 2'- H_b), 3.84 (dd, $J = 11.8, 1.9$ Hz, 1H, 5'- H_a), 3.98-4.03 (m, 1H, 4'-H), 4.06 (dd, $J = 11.8, 2.2$ Hz, 1H, 5'- H_b), 4.19 (ddd, $J = 6.9, 6.9, 6.9$ Hz, 1H, 3'-H), 6.20 (dd, $J = 10.5, 4.9$ Hz, 1H, 1'-H), 7.48-

7.56 (m, 3H, 5-H, 3''-H, 5''-H), 7.58-7.64 (m, 1H, 4''-H), 7.89 (d, $J = 7.4$ Hz, 2H, 2''-H, 6''-H), 8.43 (d, $J = 7.5$ Hz, 1 H, 6-H), 8.71 (brs, 1H, NH). ^{13}C NMR (126 MHz, CDCl_3): $\delta = -5.41$ (SiCH_3), -5.26 (SiCH_3), 18.51 ($\text{SiC}(\underline{\text{C}}\text{H}_3)_3$), 26.02 ($\text{SiC}(\underline{\text{C}}\text{H}_3)_3$), 39.23 (C-2'), 58.51 (C-3'), 61.91 (C-5'), 85.41 (C-4'), 86.75 (C-1'), 96.20 (C-5), 127.64 (C-4''), 129.21 (C-2'', C-3'', C-5'', C-6''), 133.36 (C-1''), 144.66 (C-6), 153.59 (C-2), 162.34 (C-4). HRMS (ESI): calcd. for $\text{C}_{22}\text{H}_{31}\text{N}_6\text{O}_4\text{Si}$ $[\text{M}+\text{H}]^+$ 471.2171, found 471.2180. TLC (petroleum ether-EtOAc, 2:3): $R_f = 0.20$.

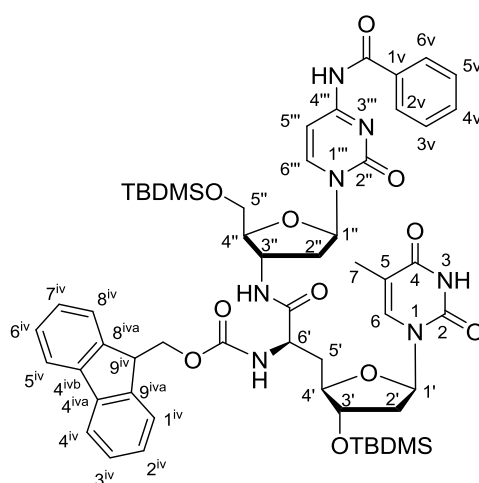
3'-Amino-4-*N*-benzoyl-5'-*O*-TBDMS-2',3'-dideoxycytidine **8**



To a solution of 3'-azido-4-*N*-benzoyl-5'-*O*-TBDMS-2',3'-dideoxycytidine **7** (135 mg, 0.287 mmol) in MeOH (1.5 mL), 1,4-cyclohexadiene (232 mg, 2.90 mmol) and Pd black (spatula tip) were added. The reaction was stirred at rt for 1.5 h and monitored by TLC (petroleum ether-EtOAc, 3:2). After complete conversion, the solution was filtered and the solvent of the filtrate was evaporated under reduced pressure. The resultant crude product was purified by column chromatography (CH_2Cl_2 -MeOH, 9:1) to give **8** (125 mg, 98%). ^1H NMR (500 MHz, CDCl_3): $\delta = 0.13$ (s, 3H, SiCH_3), 0.15 (s, 3H, SiCH_3), 0.95 (s, 9H, $\text{SiC}(\text{CH}_3)_3$), 1.51 (brs, 2H, NH_2), 2.33 - 2.39 (m, 2H, 2'-H), 3.58 (dd, $J = 15.3, 7.6$ Hz, 1H, 3'-H), 3.76 (d, $J = 7.1$ Hz, 1H, 4'-H), 3.88 (dd, $J = 11.6, 1.3$ Hz, 1H, 5'- H_a), 4.06 (dd, $J = 11.5, 2.3$ Hz, 1H, 5'- H_b), 6.19 (dd, $J = 9.4, 5.1$ Hz, 1H, 1'-H), 7.47 - 7.55 (m, 3H, 3''-H, 4''-H, 5''-H), 7.60 (dd, $J = 10.8, 4.0$ Hz, 1H, 5-H), 7.90 (d, $J = 7.6$ Hz, 2''-H, 6''-H), 8.56 (d, $J = 7.4$ Hz, 1H, 6-H). ^{13}C NMR (126 MHz, CDCl_3): $\delta = -5.53$ (SiCH_3), -5.24 (SiCH_3), 18.60 ($\text{SiC}(\underline{\text{C}}\text{H}_3)_3$), 26.07

(SiC(CH₃)₃), 43.17 (C-2'), 49.27 (C-3'), 61.57 (C-5'), 86.65 (C-4'), 88.32 (C-1'), 95.98 (C-5), 127.65 (C-4''), 129.18 (C-2'', C-3'', C-5'', C-6''), 133.27 (C-1''), 145.28 (C-6), 156.90 (C-2), 162.20 (C-4). HRMS (ESI): calcd. for C₂₂H₃₃N₄O₄Si [M+H]⁺ 445.2266, found 445.2251. TLC (CH₂Cl₂-MeOH, 9:1): R_f = 0.21.

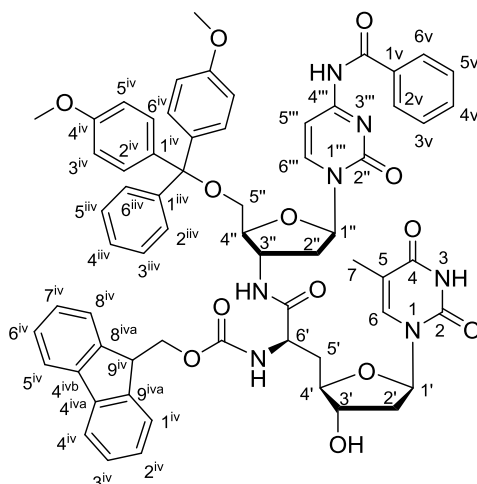
(5''-O-TBDMS-3''-aminocytidinyl)-(6'-N-Fmoc-3'-O-TBDMS)-(R)-thymidinyl amino acid amide 10



To a solution of 6'-N-Fmoc-3'-O-TBDMS-(R)-thymidinyl amino acid **9** [S1,S2] (406 mg, 0.639 mmol) in CH₂Cl₂ (8 mL), 1-hydroxybenzotriazole (HOBt, 91 mg, 0.67 mmol) and 1-ethyl-3-(3-dimethylaminopropyl)carbodiimide hydrochloride (EDC, 129 mg, 0.673 mmol) were added and the reaction mixture was stirred at rt for 20 min. Then, 3'-amino-4-N-benzoyl-5'-O-TBDMS-2',3'-dideoxycytidine **8** (301 mg, 0.678 mmol) was added and the reaction mixture was stirred at rt for 24 h. The solvent was then evaporated under reduced pressure and the resultant crude product was purified by column chromatography (CH₂Cl₂-MeOH, 98:2 → 95:5) to give **10** (533 mg, 78%). ¹H NMR (500 MHz, CDCl₃): δ = 0.04 (s, 6H, SiCH₃), 0.17 (s, 6H, SiCH₃), 0.84 (s, 9H, SiC(CH₃)₃), 0.95 (s, 9H, SiC(CH₃)₃), 1.78 (s, 3H, 7-H), 1.95-2.07 (m, 3H, 2'-H_a, 5'-H_a, 2''-H_a), 2.25-2.36 (m, 1H, 2''-H_b), 2.58-2.76 (m, 1H, 5''-H_a), 2.87 (dd, *J* = 13.6, 5.4 Hz, 1H, 2'-H_b), 3.85-3.92 (m, 1H, 9^{iv}-H), 3.94-4.02 (m, 4H,

(5''-O-TBDMS-3''-aminocytidinyl)-(6'-N-Fmoc-3'-O-TBDMS)-(R)-thymidinyl amino acid amide **10** (350 mg, 0.329 mmol) was dissolved in MeOH (11 mL) and dry NH₄F (166 mg, 4.48 mmol) was added. The reaction was stirred at 60 °C for 6 h and monitored by TLC (CH₂Cl₂-MeOH, 9:1). When too much formation of side products was observed, the reaction was quenched by the addition of silica (900 mg). The solvent was evaporated under reduced pressure and the resultant crude product (on silica) was purified by column chromatography (CH₂Cl₂-MeOH, 9:1) to give **11** (146 mg, 53%). ¹H NMR (500 MHz, pyridine-d₅): δ = 1.98 (s, 3H, 7-H), 2.56-2.62 (m, 2H, 2'-H_a, 5'-H_a), 2.63-2.69 (m, 2H, 2'-H_b, 5'-H_b), 2.79-2.58 (m, 1H, 2''-H_a), 3.04 (ddd, *J* = 12.9, 6.3, 6.3 Hz, 1H, 2''-H_b), 4.20-4.26 (m, 2H, 5''-H), 4.27 (t, *J* = 6.8 Hz, 1H, 9^{iv}-H), 4.43-4.48 (m, 2H, 3'-H, 4''-H), 4.54 (dd, *J* = 10.5, 7.3 Hz, 1H, 4'-H), 4.62-4.68 (m, 2H, Fmoc-CH₂), 5.23 (ddd, *J* = 13.5, 6.8, 6.8 Hz, 1H, 6'-H), 5.35-5.41 (m, 1H, 3''-H), 5.71 (brs, 2H, OH), 6.79 (dd, *J* = 6.7, 6.7 Hz, 1H, 1''-H), 6.85 (dd, *J* = 5.7, 5.7 Hz, 1H, 1'-H), 7.24-7.33 (m, 3H, aryl-H), 7.38-7.50 (m, 5H, 6-H, aryl-H), 7.64 (dd, *J* = 17.4, 7.6 Hz, 2H, aryl-H), 7.72 (d, *J* = 7.4 Hz, 1H, 5'''-H), 7.85 (d, *J* = 7.6 Hz, 2H, 4^{iv}-H, 5^{iv}-H), 8.26 (d, *J* = 7.2 Hz, 2H, 1^{iv}-H, 8^{iv}-H), 8.98 (d, *J* = 7.5 Hz, 1H, 6'-NH), 9.20 (d, *J* = 8.3 Hz, 1H, 6'''-H), 9.88 (d, *J* = 7.2 Hz, 1H, 3''-NH), 11.99 (s, 1H, 4'''-NH), 13.20 (s, 1H, 3-NH). ¹³C NMR (126 MHz, pyridine-d₅): δ = 13.24 (C-7), 38.36 (C-5'), 39.07 (C-2''), 40.36 (C-2'), 48.14 (C-9^{iv}), 50.50 (C-3''), 54.12 (C-6'), 62.28 (C-5'), 67.26 (Fmoc-CH₂), 75.07 (C-3'), 84.35 (C-4''), 86.09 (C-4'), 87.95 (C-1'), 88.12 (C-1''), 97.46 (C-5'''), 111.33 (C-5), 120.86 (C-4^{iv}, C-5^{iv}), 124.52 (C-4^v), 126.13 (C-1^{iv}, C-8^{iv}), 127.98 (C-2^v, C-6^v), 128.55 (C-3^v, C-5^v), 129.26, 129.48 (C-2^{iv}, C-3^{iv}, C-6^{iv}, C-7^{iv}), 133.12 (C-1^v), 136.98 (C-6), 142.11 (C-8^{iv}_a, C-9^{iv}_b), 144.98, 145.09 (C-4^{iv}_a, C-4^{iv}_b), 145.51 (C-6'''), 150.76 (3''-amide-C=O), 152.14 (C-2), 164.23 (C-2'''), 165.31 (C-4), 174.12 (Bz-C=O). HRMS (ESI): calcd. for C₄₃H₄₄N₇O₁₁ [M+H]⁺ 834.3093, found 834.3066. TLC (CH₂Cl₂-MeOH, 9:1): *R*_f = 0.20.

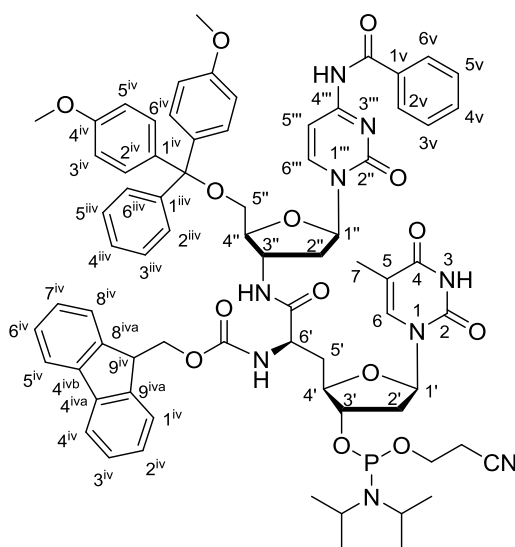
(5'-O-DMTr-3''-aminocytidiny)-(6'-N-Fmoc)-(R)-thymidinyl amino acid amide 12



(3''-Aminocytidiny)-(6'-N-Fmoc)-(R)-thymidinyl amino acid amide **11** (41.5 mg, 49.8 μmol) was coevaporated with pyridine (3 x 1 mL) and then dissolved in a mixture of pyridine and DMF (1:1, 0.4 mL). To this solution, 4-dimethylaminopyridine (DMAP, 0.7 mg, 6 μmol) and 4,4'-dimethoxytrityl chloride (DMTrCl, 18.3 mg, 54.2 μmol) were added and the reaction mixture was stirred at rt for 16 h. The solvent was then evaporated under reduced pressure and the resultant crude product was purified by column chromatography (CH_2Cl_2 -MeOH, 95:5) to give **12** (36.0 mg, 64%). ^1H NMR (500 MHz, pyridine- d_5): δ = 1.98 (s, 3H, 7-H), 2.58-2.63 (m, 2H, 2'-H_a, 5'-H_a), 2.69 (dd, J = 13.4, 8.6 Hz, 2H, 2'-H_b, 5'-H_b), 2.88 (dd, J = 10.7, 7.2 Hz, 1H, 2''-H_a), 2.93-3.01 (m, 1H, 2''-H_b), 3.70 (dd, J = 8.9, 1.8 Hz, 1H, 5''-H_a), 3.72 (s, 3H, OMe), 3.74 (s, 3H, OMe), 3.84 (dd, J = 10.9, 3.3 Hz, 1H, 5''-H_b), 4.31 (t, J = 7.1 Hz, 1H, 9^{iv}-H), 4.42-4.49 (m, 2H, 4'-H, 4''-H), 4.59-4.69 (m, 3H, 3'-H, Fmoc-CH₂), 5.24 (dd, J = 13.7, 8.5 Hz, 1H, 6'-H), 5.47 (dddd, J = 8.2, 8.2, 8.1, 8.1 Hz, 1H, 3''-H), 6.65 (dd, J = 6.5, 3.4 Hz, 1H, 1''-H), 6.77 (dd, J = 6.8, 6.8 Hz, 1H, 1'-H), 7.07 (d, J = 8.9 Hz, 4H, 3^{iv}-H, 5^{iv}-H), 7.24-7.31 (m, 3H, aryl-H), 7.39-7.43 (m, 2H, aryl-H), 7.46-7.50 (m, 4H, aryl-H), 7.53 (d, J = 7.4 Hz, 1H, 5'''-H), 7.63-7.71 (m, 7H, aryl-H), 7.82 (d, J = 7.4 Hz, 2H, aryl-H), 7.86 (d, J = 7.8 Hz, 2H, 1^{iv}-H, 4^{iv}-H), 8.25 (d, J = 7.2 Hz, 2H, 5^{iv}-H, 8^{iv}-H), 8.80 (d, J = 7.5 Hz, 1H, 6'-NH), 9.30 (d, J = 8.4 Hz, 1H, 6'''-H), 9.65 (d, J = 7.8 Hz, 1H, 3''-NH), 12.19 (s, 1H,

4^{'''}-NH), 13.20 (s, 1H, 3-NH). ¹³C NMR (126 MHz, pyridine-d₅): δ = 13.22 (C-7), 38.13 (C-5[']), 40.25 (C-2^{''}), 40.50 (C-2[']), 48.17 (C-9^{iv}), 49.07 (C-3^{''}), 54.27 (C-6[']), 55.64 (OCH₃), 62.74 (C-5[']), 67.27 (Fmoc-CH₂), 75.01 (C-3[']), 84.24 (DMTr-C_{quart}), 85.13 (C-4^{''}), 86.23 (C-4[']), 87.29 (C-1[']), 87.77 (C-1^{''}), 97.40 (C-5^{'''}), 111.36 (C-5), 114.35 (C-3^{iv}, C-5^{iv}), 120.88 (C-4^{iv}, C-5^{iv}), 123.53 (C-4^v, C-4^{vii}), 124.26, 124.51 (C-1^{iv}, C-8^{iv}), 126.15 (C-2^v, C-6^v), 128.00 (C-3^v, C-5^v), 128.56, 128.98 (C-2^{iv}, C-3^{iv}, C-6^{iv}, C-7^{iv}), 129.32, 129.44 (C-2^{iv}_a, C-6^{iv}_a, C-2^{iv}_b, C-6^{iv}_b), 130.99 (C-2^{vii}), 131.27 (C-6^{vii}), 133.14 (C-1^v), 135.56 (C-6), 136.48, 136.97, 137.11 (C-3^{vii}, C-5^{vii}, C-1^{vi}_a, C-1^{vi}_b), 142.12 (C-8^{iv}_a, C-9^{iv}_a), 144.97, 145.09, 145.15 (C-1^{vii}, C-4^{iv}_a, C-4^{iv}_b), 145.79 (C-6^{'''}), 150.76 (C-2, C-2^{'''}), 152.12 (3^{''}-amide-C=O), 159.60 (C-4^{vi}), 164.26 (C-4), 165.30 (C-4^{'''}), 173.98 (Bz-C=O). HRMS (ESI): calcd. for C₆₄H₆₂N₇O₁₃ [M+H]⁺ 1136.4400, found 1136.4370. TLC (CH₂Cl₂-MeOH, 9:1): R_f = 0.20.

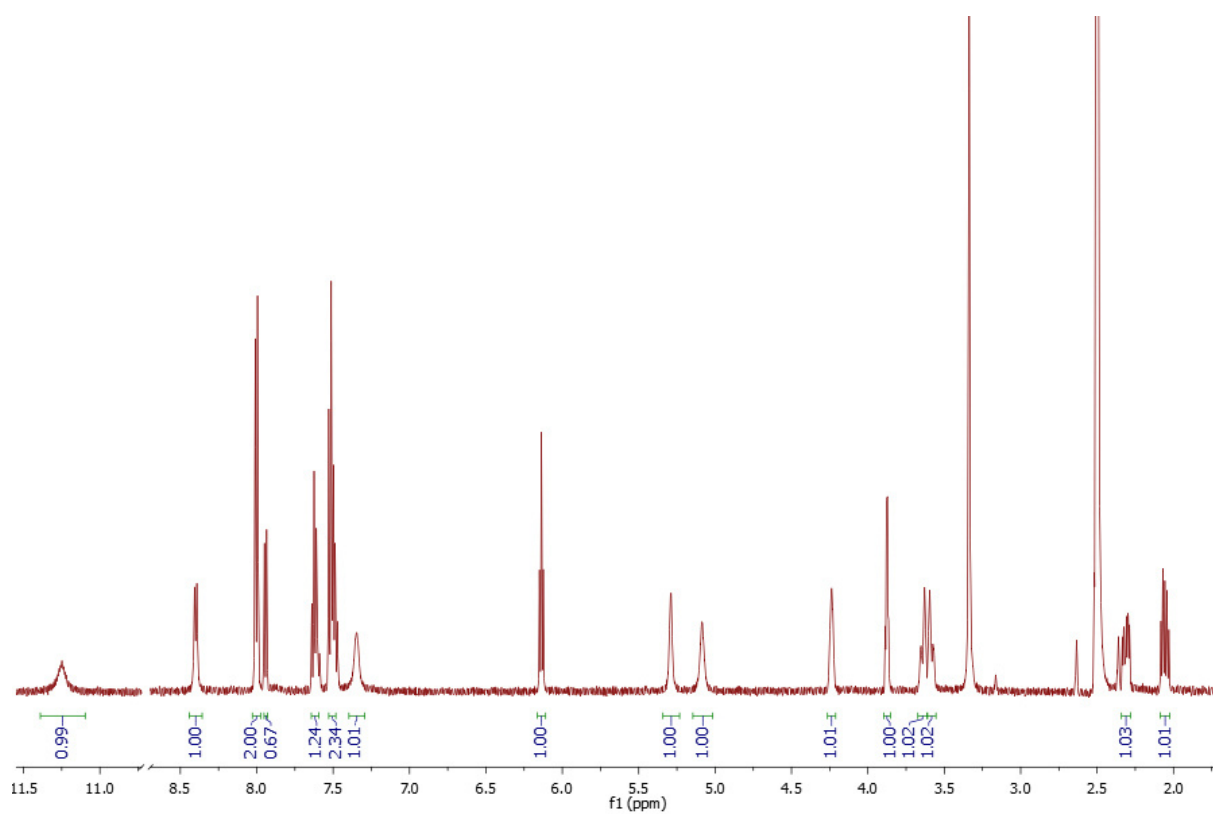
(5'-O-DMTr-3''-aminocytidiny)-(6'-N-Fmoc)-(R)-thymidinyl amino acid phosphoramidite 14



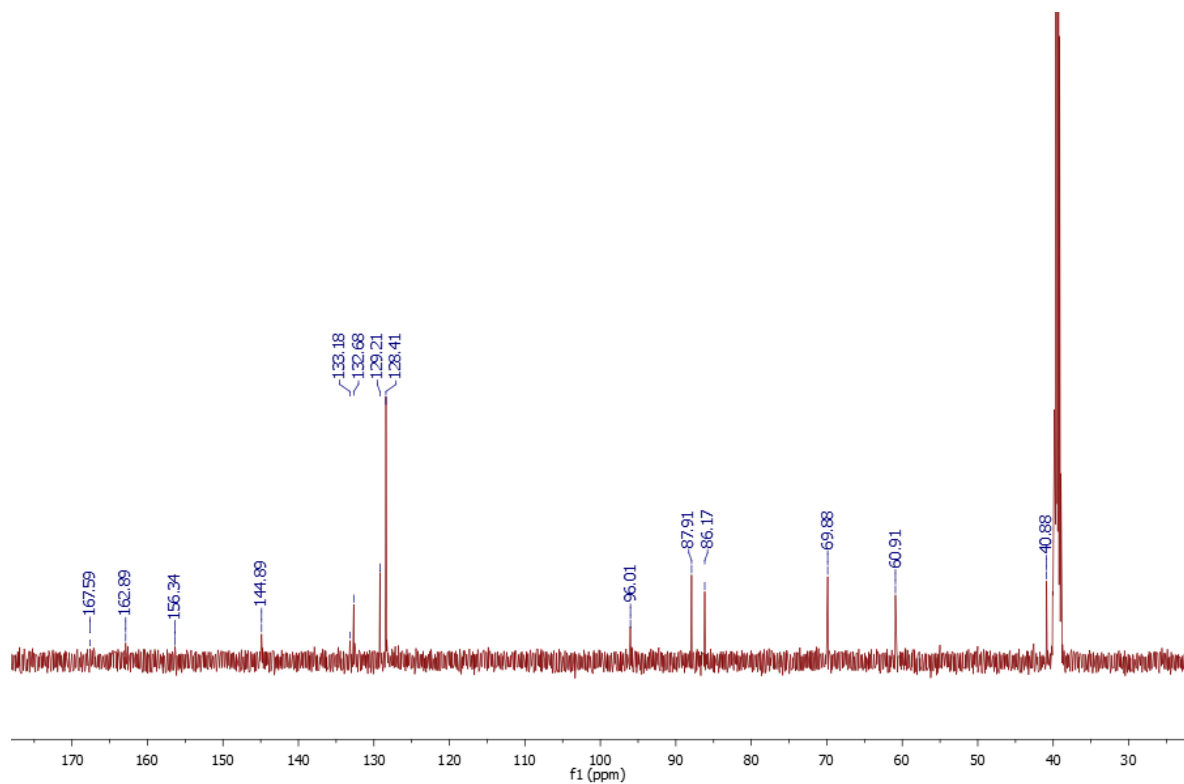
(5'-O-DMTr-3''-Aminocytidiny)-(6'-N-Fmoc)-(R)-thymidinyl amino acid amide **12** (310 mg, 0.273 mmol) was coevaporated with pyridine (1 x 3 mL), toluene (1 x 3 mL), MeCN (1 x 3 mL) and CH₂Cl₂ (1 x 3 mL). It was then dissolved in CH₂Cl₂ (3 mL), 4,5-

dicyanoimidazole (DCI, 32 mg, 0.27 mmol) and 2-cyanoethyl *N,N,N',N'*-tetraisopropyl phosphordiamidite **13** (99 mg, 0.32 mmol) were added to the solution and the reaction mixture was stirred at rt for 90 min. The solvent was evaporated under reduced pressure and the resultant crude product was purified by column chromatography (CH₂Cl₂-MeOH, 15:1 + 0.7% pyridine) under nitrogen atmosphere. The thus obtained solid was dissolved in CH₂Cl₂ (2 mL), and this solution was added dropwise to *n*-hexane (20 mL) at -20 °C, which led to precipitation of the product. The mixture was centrifuged at -9 °C and 4500 rpm for 5 min, and the resultant pellet was again dissolved in CH₂Cl₂ (0.5 mL). The solvent was evaporated under reduced pressure to give **14** as a mixture (*R_p/S_p*) of two diastereomers (285 mg, 78%). ³¹P NMR (203 MHz, C₆D₆): δ = 161.55, 162.10 ppm. HRMS (ESI): calcd. for C₇₃H₇₉N₉O₁₄P [M+H]⁺ 1336.5479, found 1336.5452. TLC (CH₂Cl₂-MeOH, 30:1): *R_f* = 0.33.

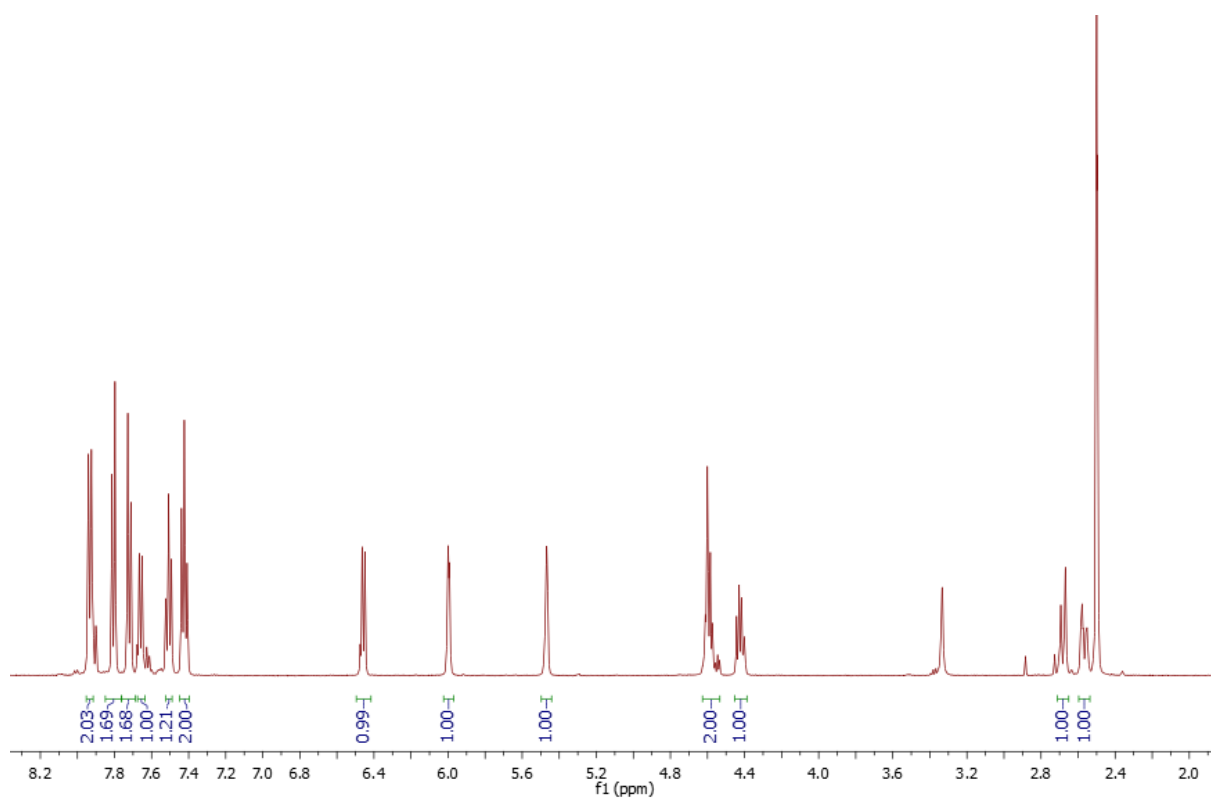
^1H , ^{13}C and ^{31}P NMR spectra of synthesised compounds



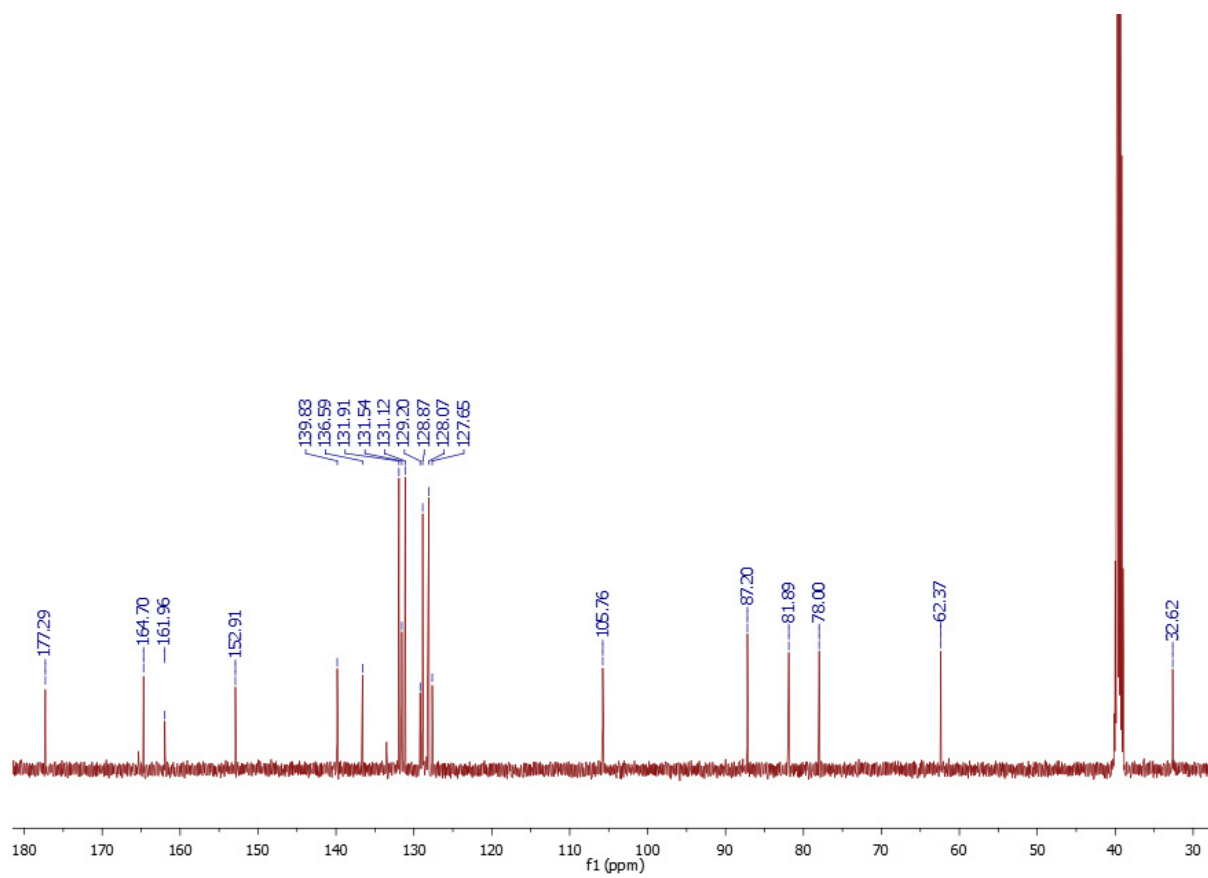
^1H NMR spectrum of **4** (500 MHz, DMSO- d_6)



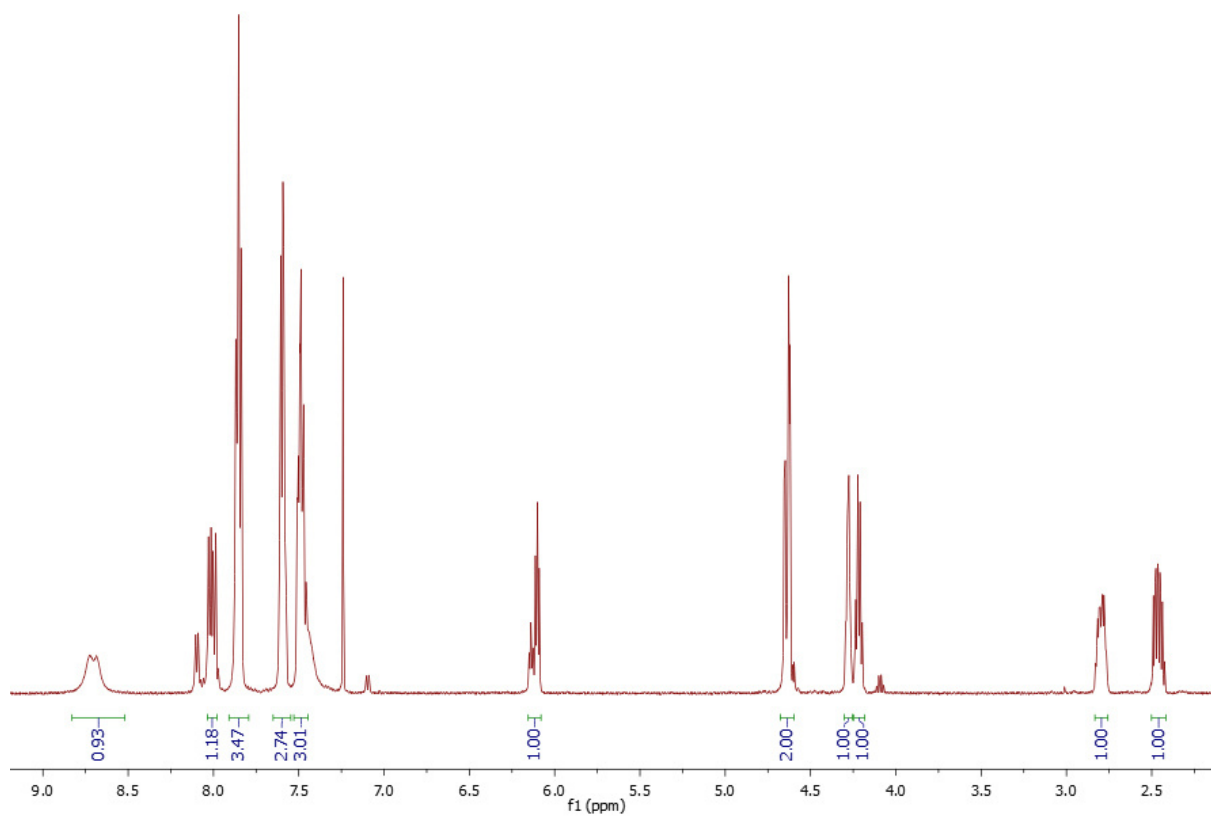
^{13}C NMR spectrum of **4** (126 MHz, DMSO- d_6)



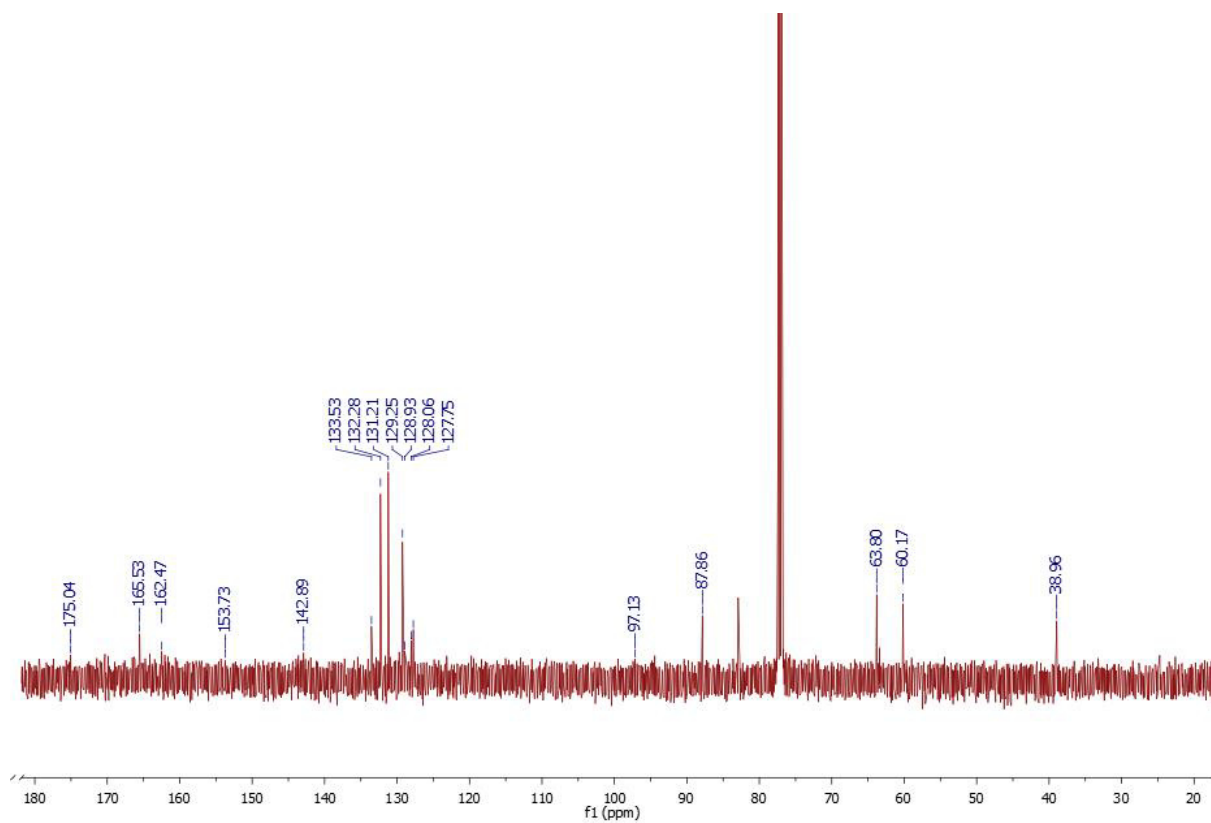
^1H NMR spectrum of **5** (500 MHz, DMSO-d_6)



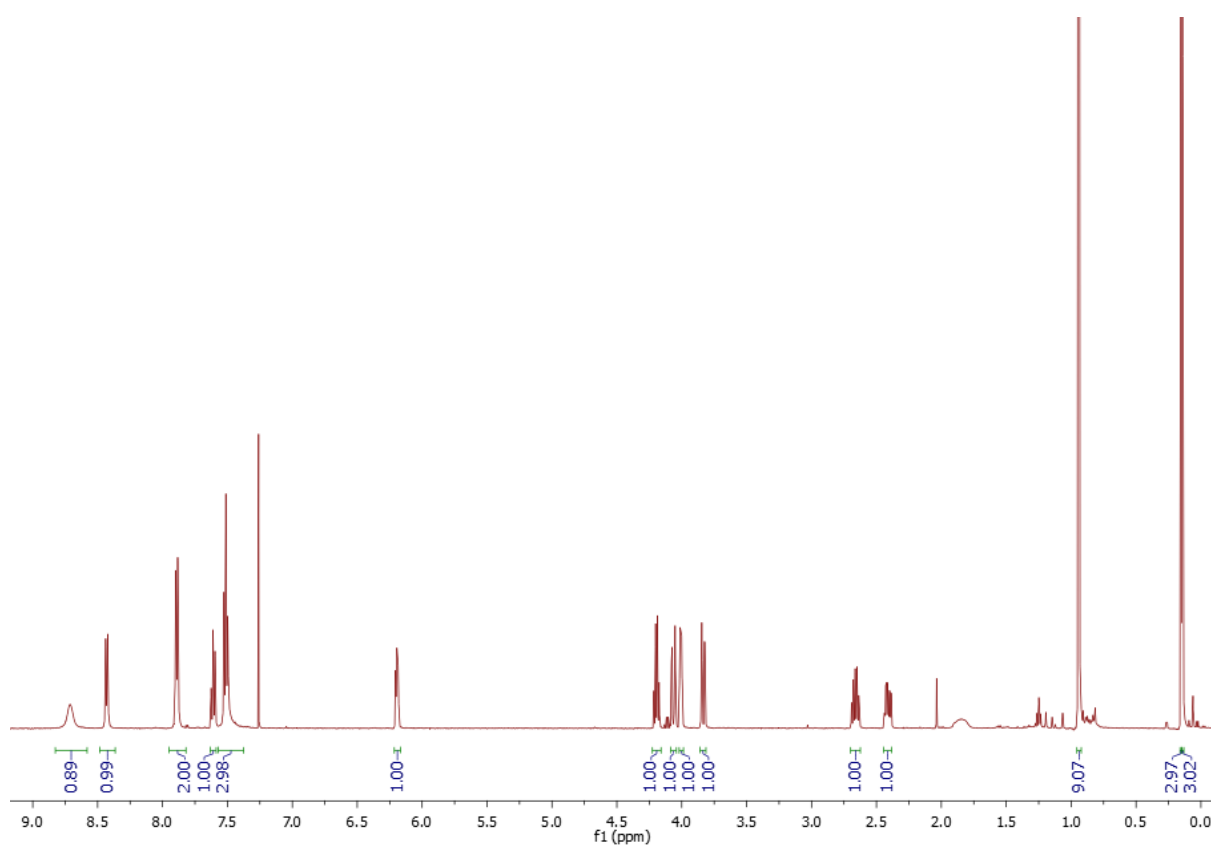
^{13}C NMR spectrum of **5** (126 MHz, DMSO-d_6)



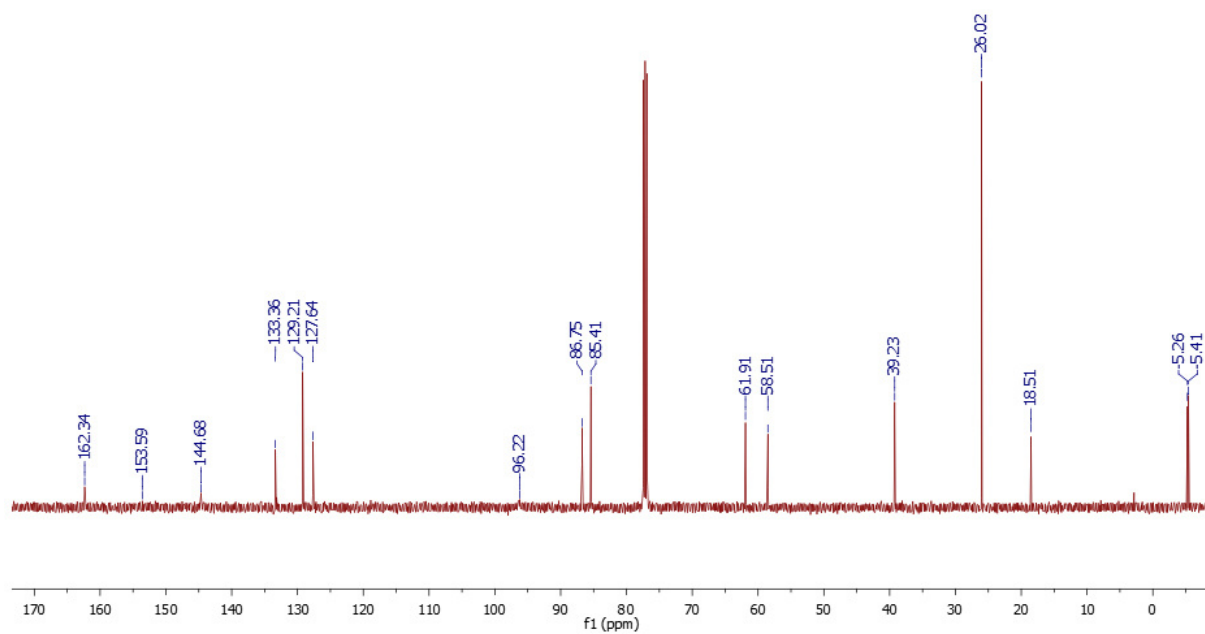
^1H NMR spectrum of **6** (500 MHz, CDCl_3)



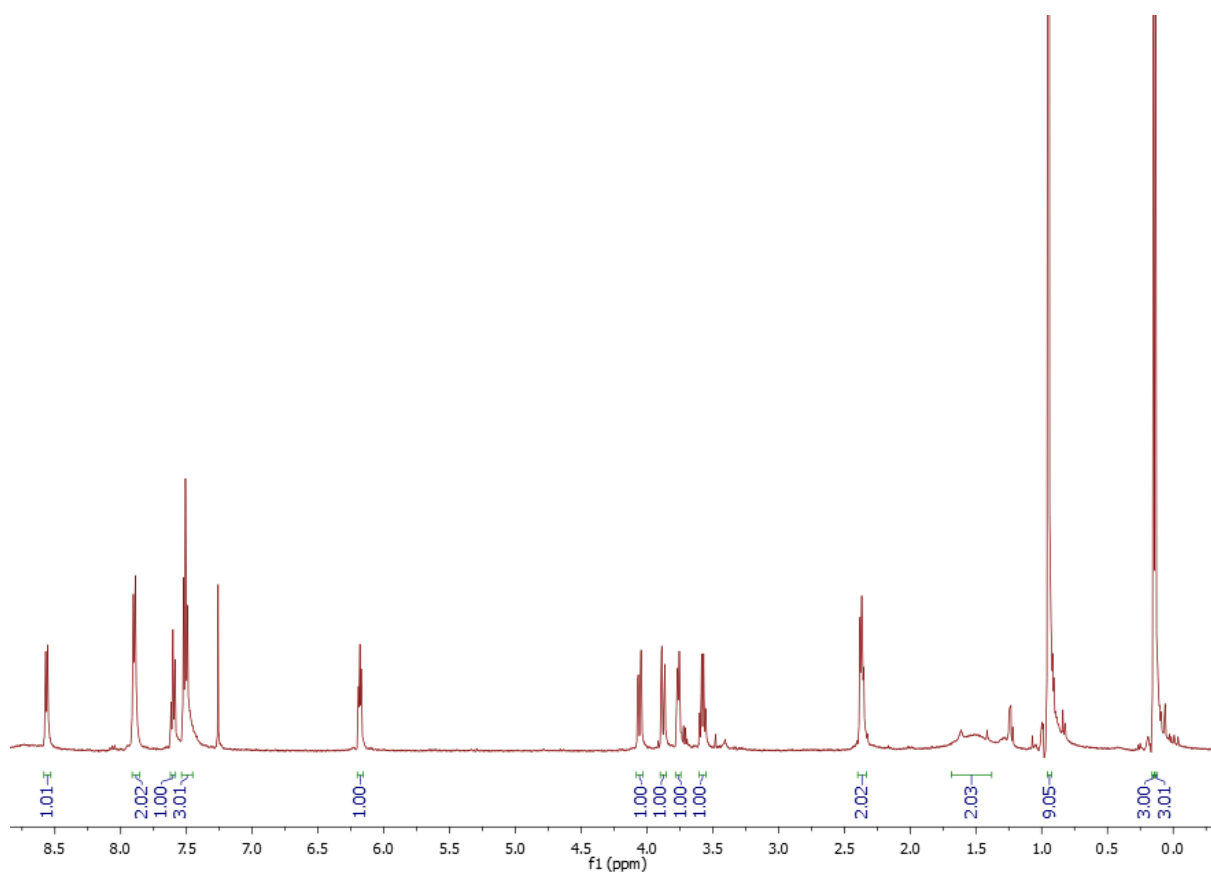
^{13}C NMR spectrum of **6** (126 MHz, CDCl_3)



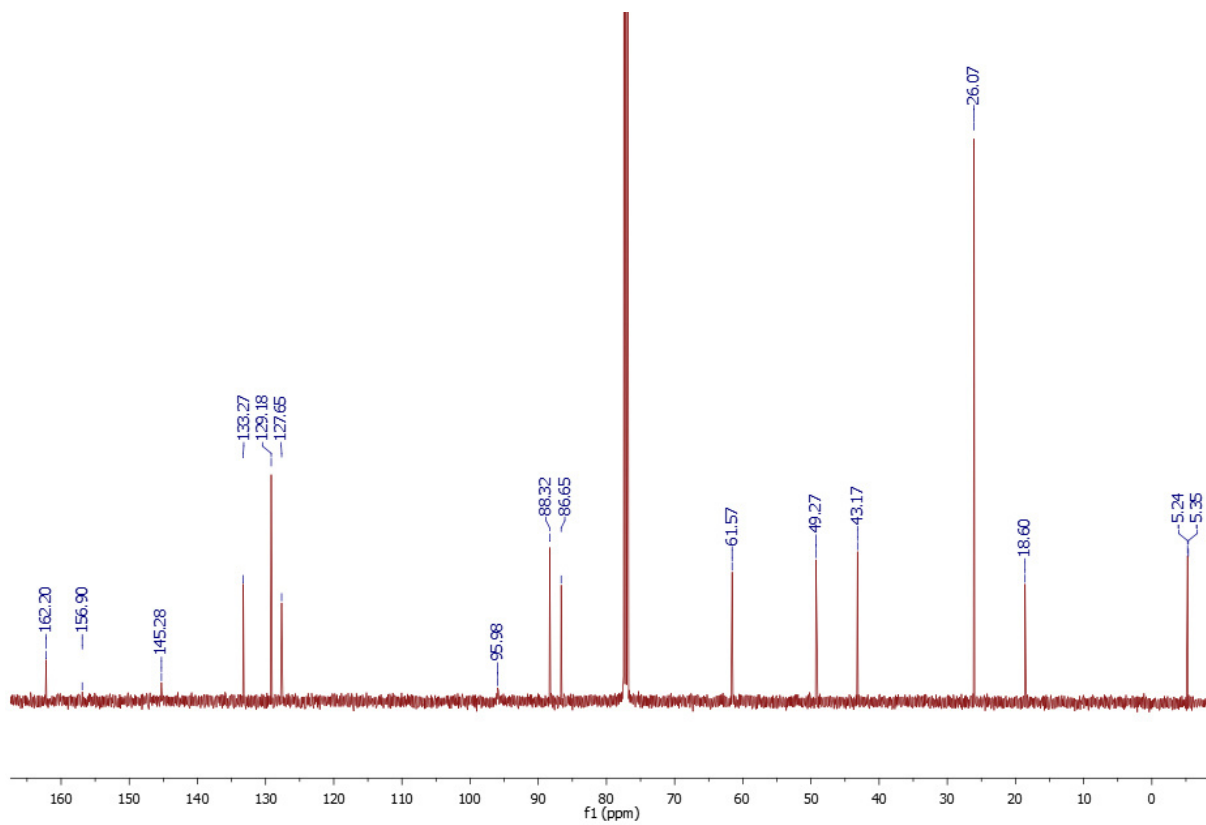
^1H NMR spectrum of **7** (500 MHz, CDCl_3)



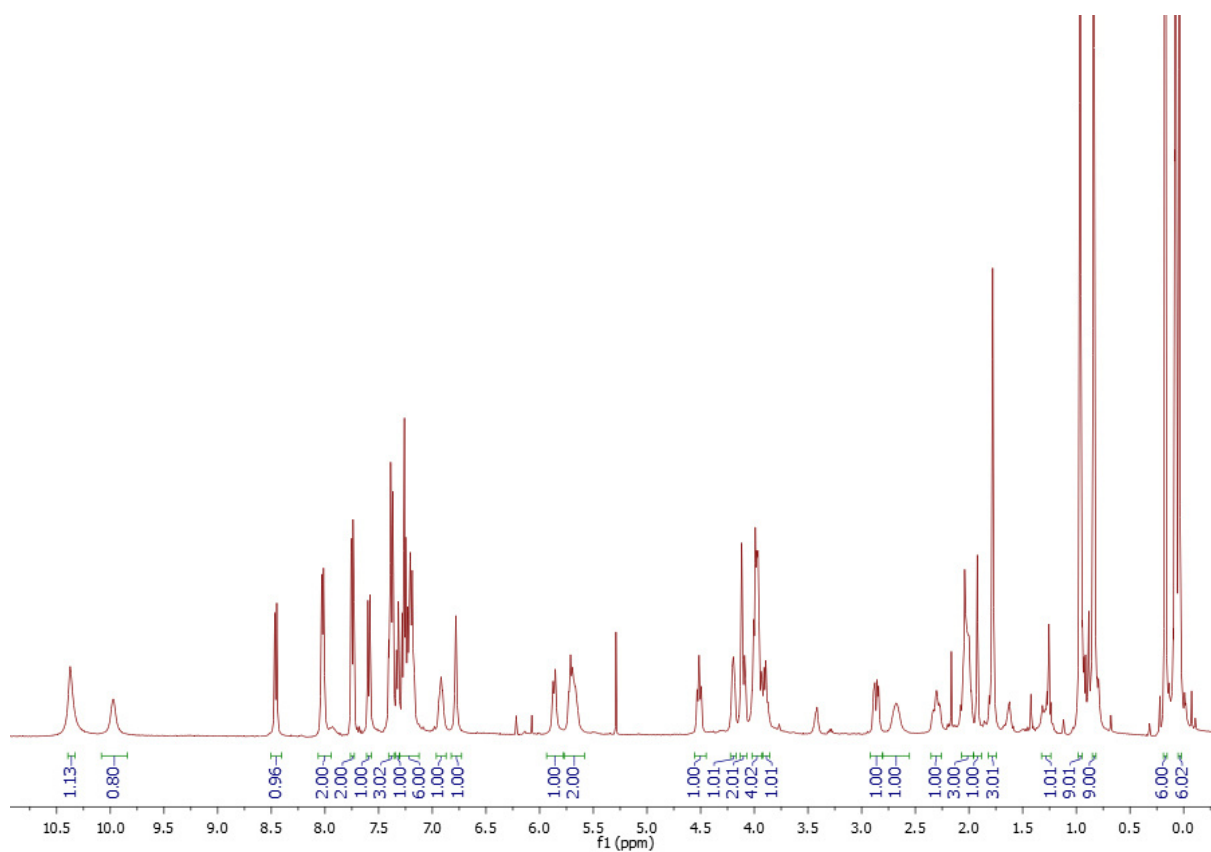
^{13}C NMR spectrum of **7** (126 MHz, CDCl_3)



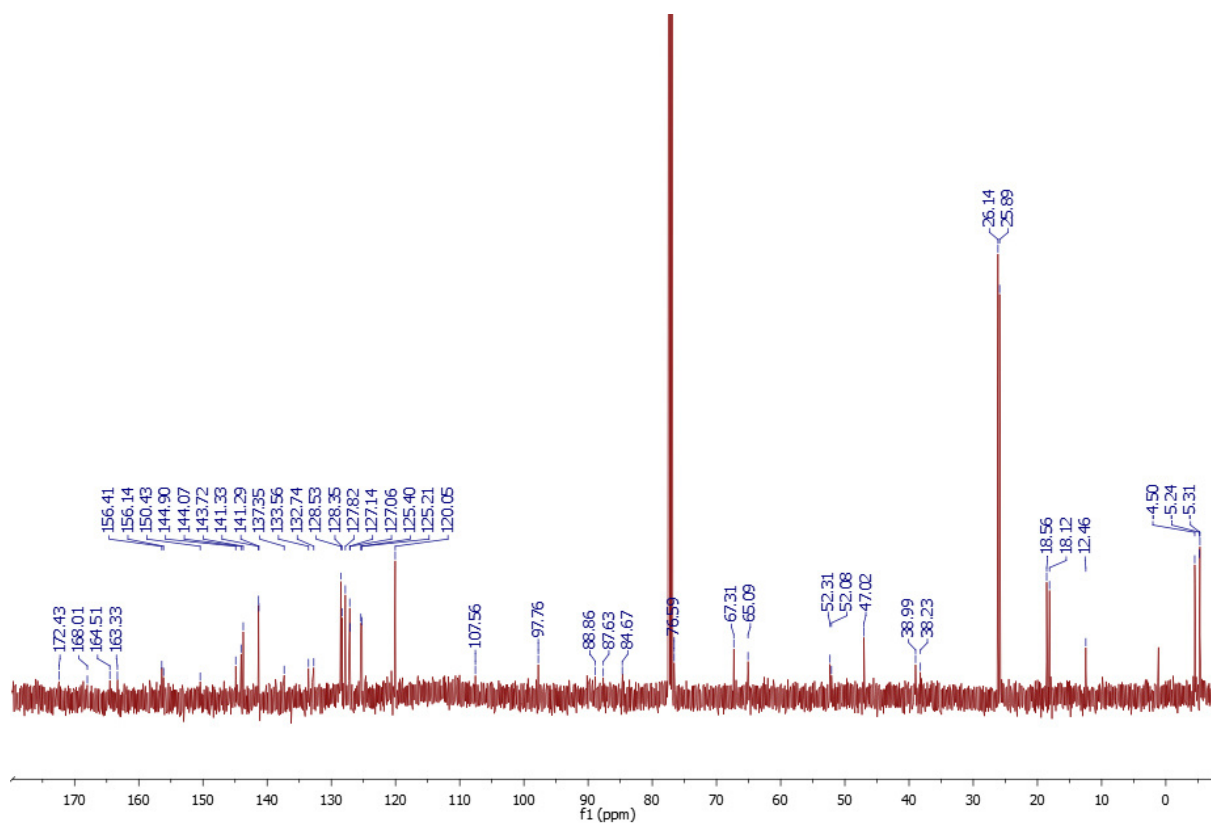
¹H NMR spectrum of **8** (500 MHz, CDCl₃)



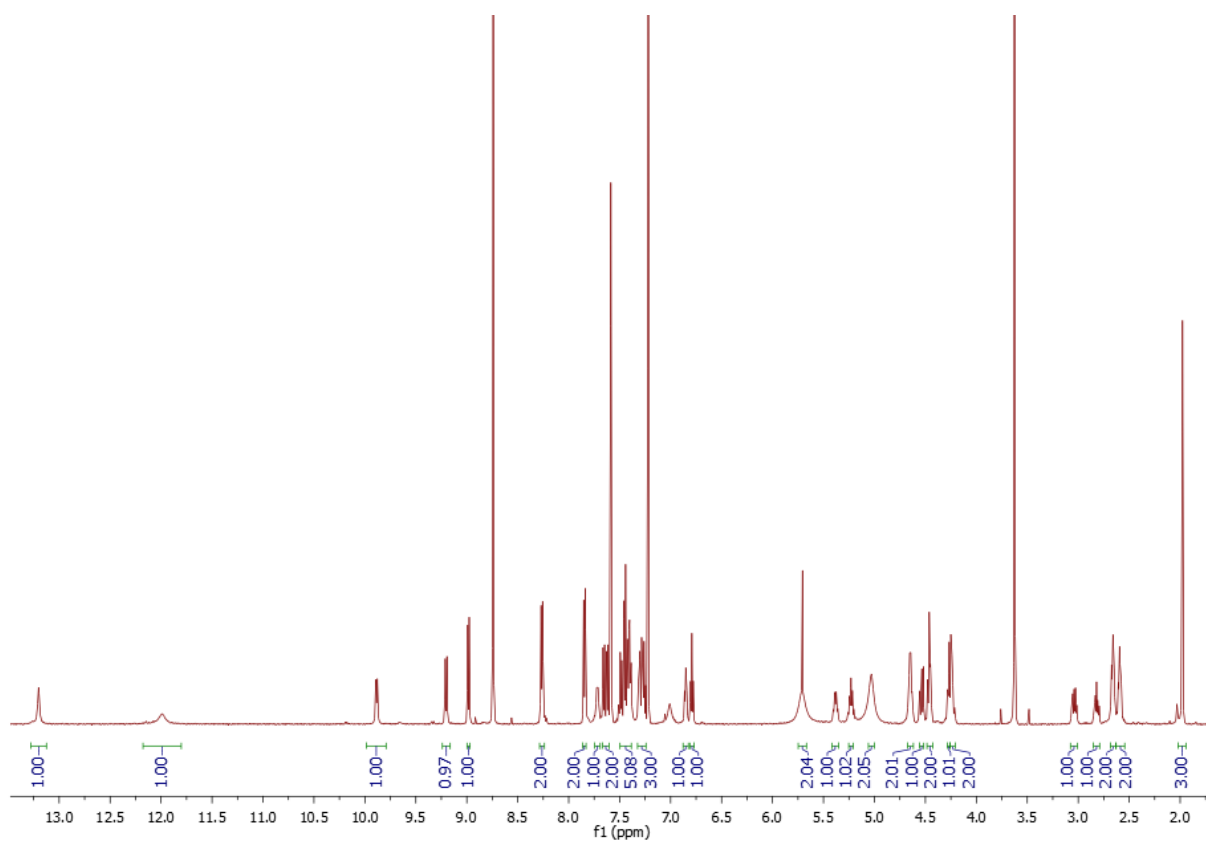
¹³C NMR spectrum of **8** (126 MHz, CDCl₃)



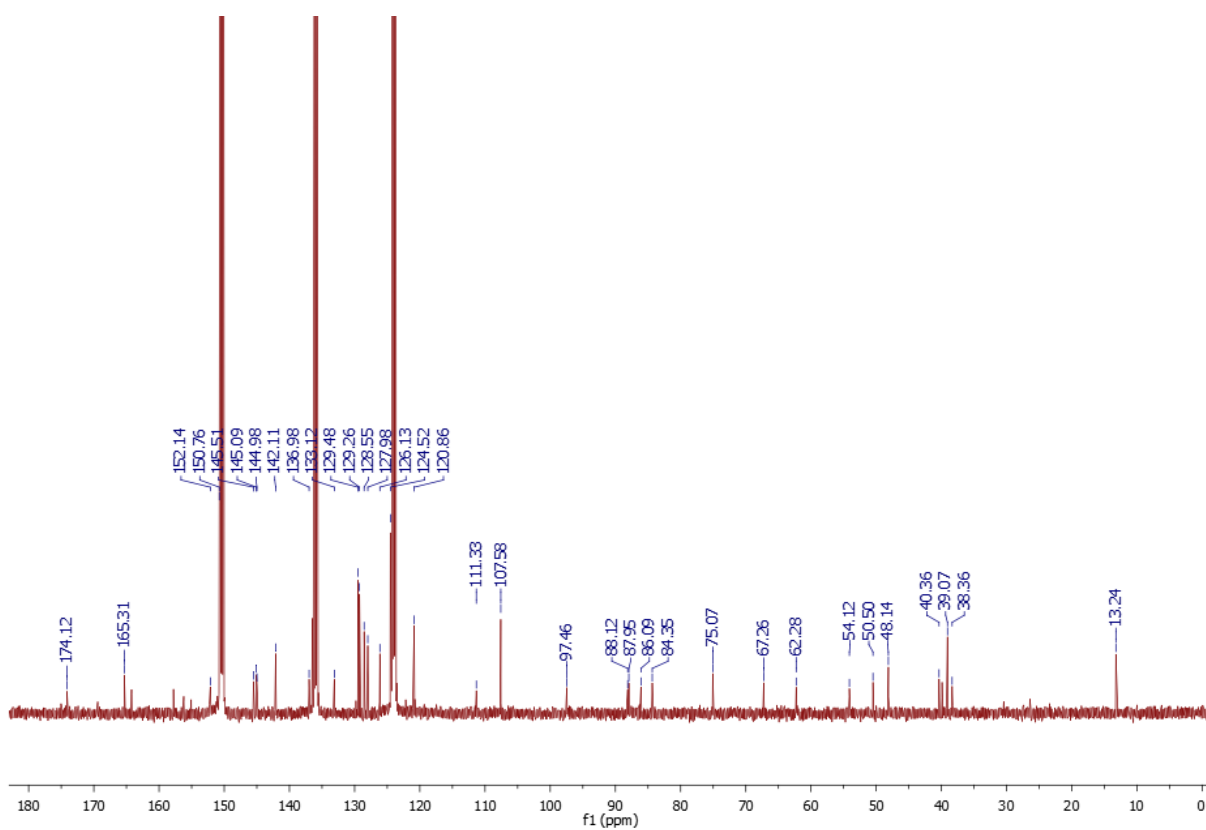
^1H NMR spectrum of **10** (500 MHz, CDCl_3)



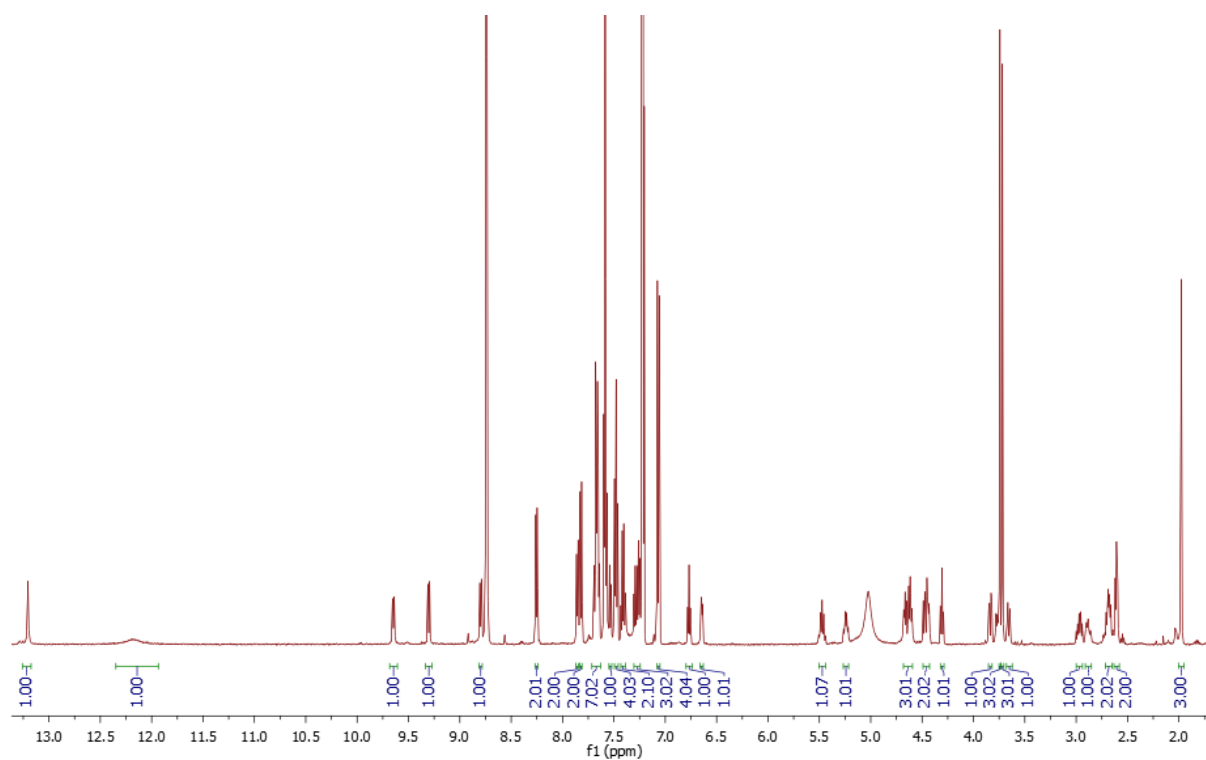
^{13}C NMR spectrum of **10** (126 MHz, CDCl_3)



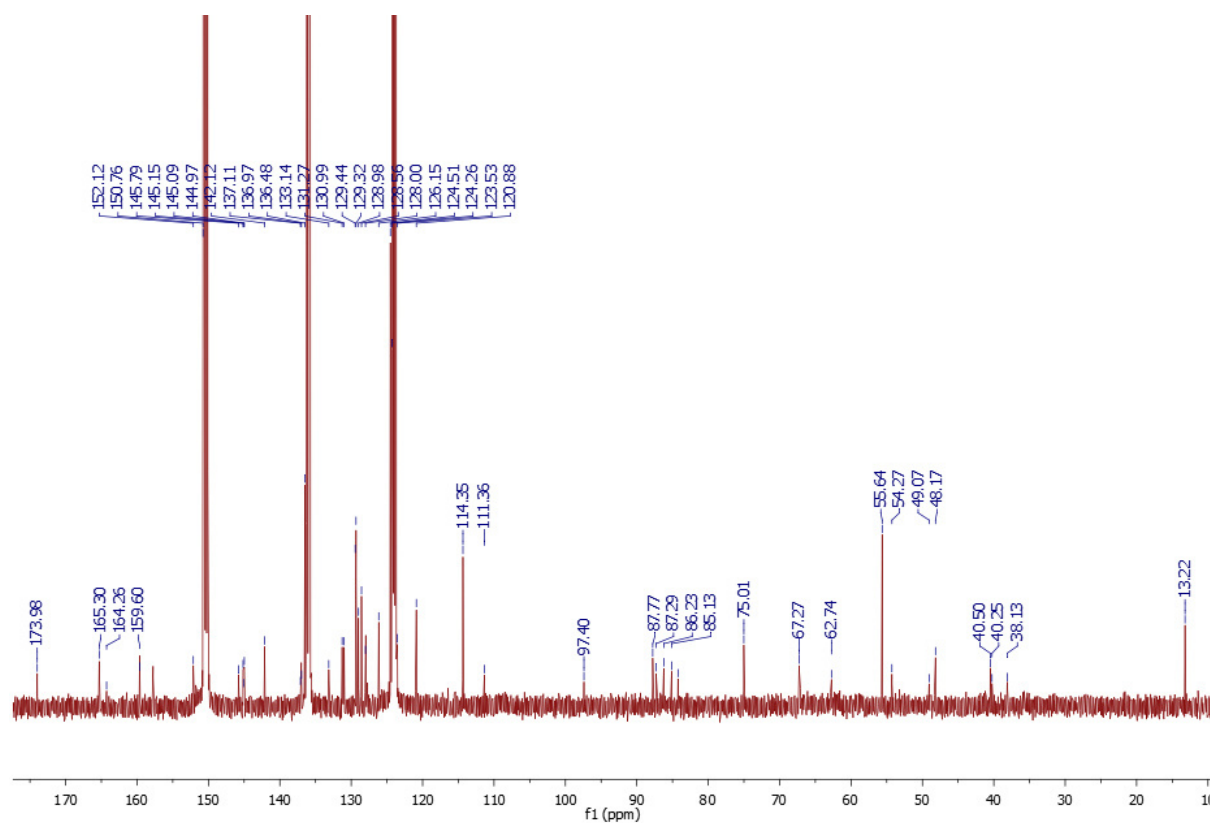
^1H NMR spectrum of **11** (500 MHz, pyridine- d_5)



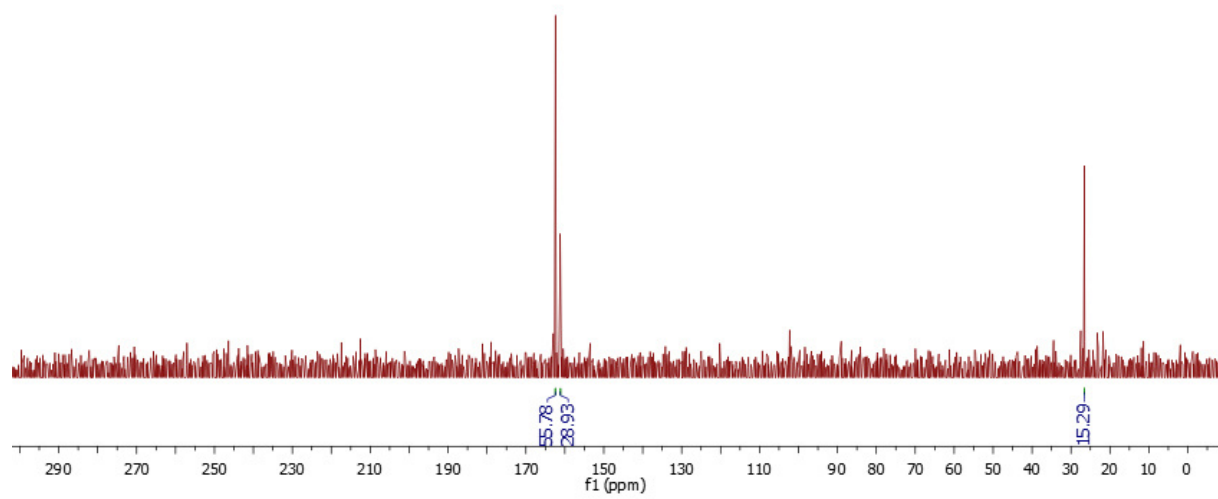
^{13}C NMR spectrum of **11** (126 MHz, pyridine- d_5)



^1H NMR spectrum of **12** (500 MHz, pyridine- d_5).



^{13}C NMR spectrum of **12** (126 MHz, pyridine- d_5).



^{31}P NMR spectrum of **14** (203 MHz, C_6D_6)

Oligonucleotide synthesis, purification and analytical data

Automated oligonucleotide synthesis

Synthesis of the gapmer ON **1** and **2** was performed under strict argon atmosphere using an H-8 standard synthesiser (K&A) with standard 3'→5' synthesis. Unmodified DNA phosphoramidites (Glen Research) and LNA phosphoramidites (QIAGEN) were commercially purchased and prepared according to manufacturers' protocols prior to their use. The 'dimeric' NAA-linked C-T phosphoramidite **14** was dissolved in a MeCN-CH₂Cl₂ mixture (1:1) to a final concentration of 0.05 M. For every ON synthesis, columns with nucleoside-loaded CPG resin (200 nmol of 5'-O-DMTr-nucleoside/g matrix, K&A) were used.

For the first reaction cycle, the DMTr protecting group was cleaved off the starting nucleoside using 3% trichloroacetic acid (TCA) in CH₂Cl₂. Excess of acid was removed by flushing the column with MeCN and argon. The free 5'-OH functionality was then treated with a mixture of phosphoramidite and activator (benzylmercaptotetrazole (BMT), 0.25 M, EMP Biotech). Coupling times differed from 2 min for unmodified DNA phosphoramidites to 5 min for LNA phosphoramidites. In case of the NAA-modified dimeric phosphoramidite **14**, triple couplings gave the best results. Therefore, columns were flushed with activated phosphoramidite **14** three times with a 90 s coupling period between each of the flushes. The final coupling time after the last flush was 3 min, resulting in a total coupling time of 6 min for **14**. Excess reagents were again removed with MeCN and argon. For the capping of unreacted 5'-OH groups, capping solution A ('CapA', i.e. acetic anhydride, 2,6-dimethylpyridine, THF, Sigma Aldrich) and capping solution B ('CapB', 1-methylimidazole, THF, Sigma Aldrich) were used. Oxidation to P(V) was achieved with 0.1 M iodine solution (iodine, THF, Sigma Aldrich). This was followed by deprotection of the new 5'-end to start the next reaction cycle. The efficacy of each coupling step was determined by trityl monitoring.

After completion of all synthetic cycles, treatment of the resin under standard cleavage conditions (NH₃(25%)-EtOH, 3:1, 55 °C, 22 h) led to cleavage of the Fmoc, β-cyanoethyl and nucleobase protecting groups as well as cleavage of the ON from the CPG support. Remaining solids were removed by centrifugation. The solvent was evaporated under reduced pressure and the resultant crude ON were dissolved in ultrapure water (300 μL) for further purification. Final concentrations of ON were determined using a NanoDrop 2000 Spectrophotometer (Thermo Scientific).

Oligonucleotide purification

The crude ON were purified by electrophoresis using a urea-PAGE sequencing gel. Therefore, a polyacrylamide gel containing 7 M urea (1.5 mm, 28 cm isolating distance, 20% polyacrylamide) was prepared. The crude ON solution (20 nmol/well) was applied to the gel and electrophoresis was performed for 2.5 h at 35 W in 0.5 x TBE buffer (10 x TBE-running buffer: 890 mM Tris, 890 mM boric acid, 20 mM EDTA, pH 8.3). Visualisation of the oligonucleotide bands was achieved by irradiation with UV light (254 nm) after placing the gel on a plastic foil-covered TLC plate (aluminum plate precoated with silica gel 60 F254 (VWR)) as shown in Figure S1.

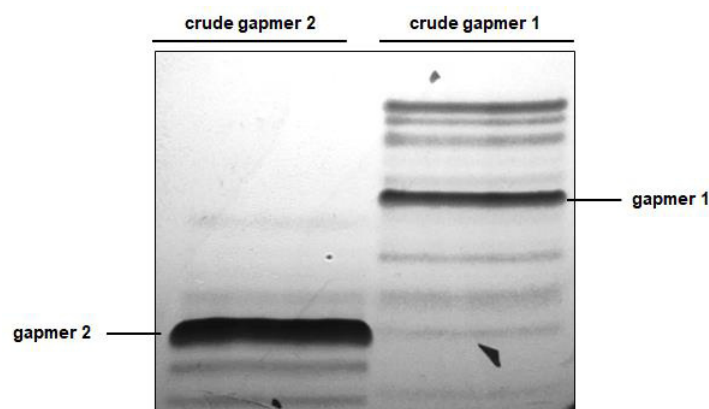


Figure S1. Oligonucleotide purification by urea-PAGE.

Segments containing the desired ON products were separated from the gel and incubated twice with TEN-extraction buffer (300 μ L, 0.01 M Tris (pH 8.0), 0.001 M EDTA (pH 8.0), 0.3 M NaCl) for 16 h. The thus obtained ON fractions were pooled and dried under reduced pressure. Subsequently, ON were desalinated by precipitation from EtOH. Therefore, ON were dissolved in ultrapure water (300 μ L) and mixed with NaOAc solution (30 μ L, 3 M, pH 5.2). After the addition of EtOH (99%, 1.2 mL, cooled to -25 $^{\circ}$ C), standing of the mixture in the freezer (-80 $^{\circ}$ C, 24 h) led to initial precipitation. A pellet was formed by centrifugation (-4 $^{\circ}$ C, 60 min, 13 000 rpm) and washed thoroughly with EtOH (95%, -25 $^{\circ}$ C) twice. The thus obtained pellets were dried under reduced pressure and represented the pure ON.

Analytical data of oligonucleotides

High resolution mass spectra of ON were obtained using an Ultimate 3000 system by Thermo Scientific with a Thermo Scientific Q Exactive OrbiTrap mass spectrometer. For MS analyses, ON were dissolved in ultrapure water (100 μ L, 4 μ M) and directly injected into the ion source. Calculated and found masses are shown in Table S1. For better comparison, expected mass spectra were simulated and used for the evaluation of the recorded mass spectra. The measured and calculated spectra of the fourfold negatively charged species of gapmer **1** as well as its deconvoluted mass spectrum are depicted in Figures S2 **A** and **B**, respectively. Corresponding data for gapmer **2** are shown in Figure S3.

Table S1: Mass spectral data of synthesized gapmer ON **1** and **2** (x = NAA-modification).

gapmer sequence	calculated	found
5'-A ^L G ^L A ^L T ^L C ^x TC ^x TC ^x TA ^L G ^L A ^L T ^L T-3' 1	5261.1312	5261.1395
5'-A ^L G ^L A ^L T ^L CTCTCTCTA ^L G ^L A ^L T ^L T-3' 2	5356.8468	5356.8182

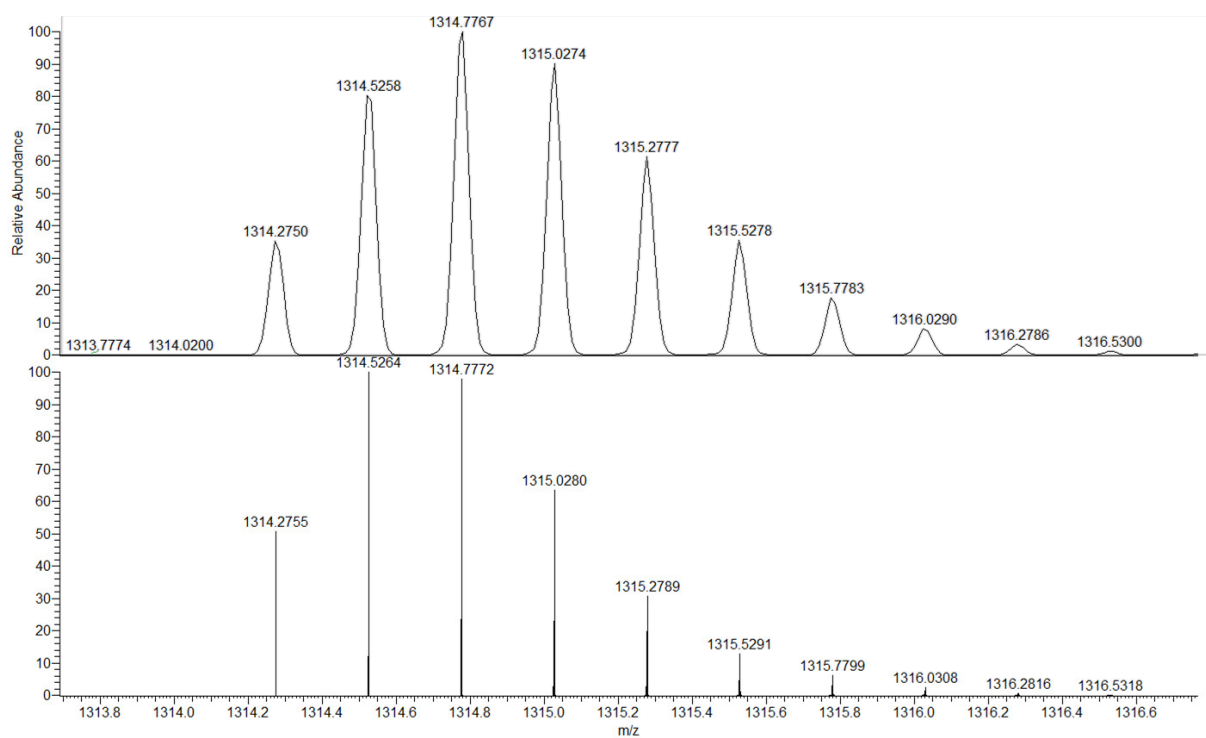
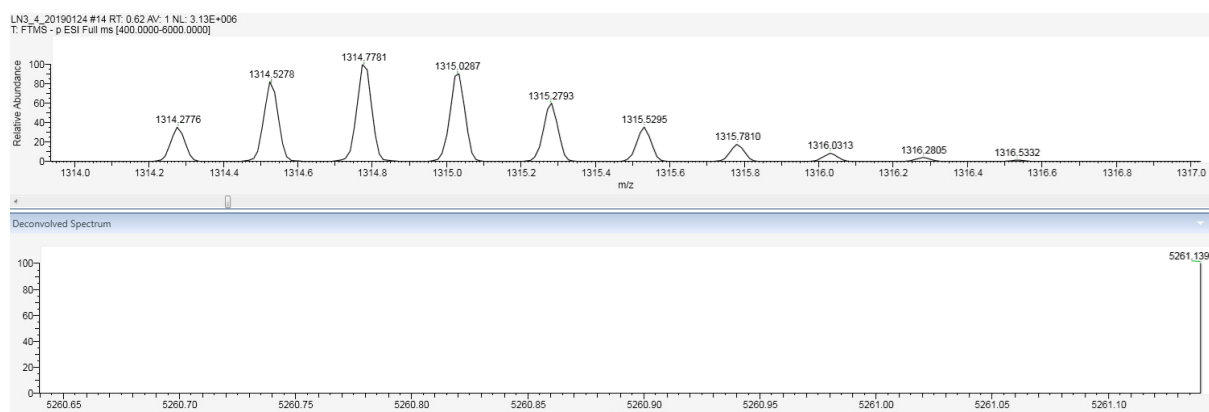
A**B**

Figure S2. A. Mass spectrum of the fourfold negatively charged species of ON 1 (5'-A^LG^LA^LT^LC^xTC^xTC^xTA^LG^LA^LT^LT-3'): measured vs. predicted mass. **B.** Deconvoluted mass spectrum of ON 1.

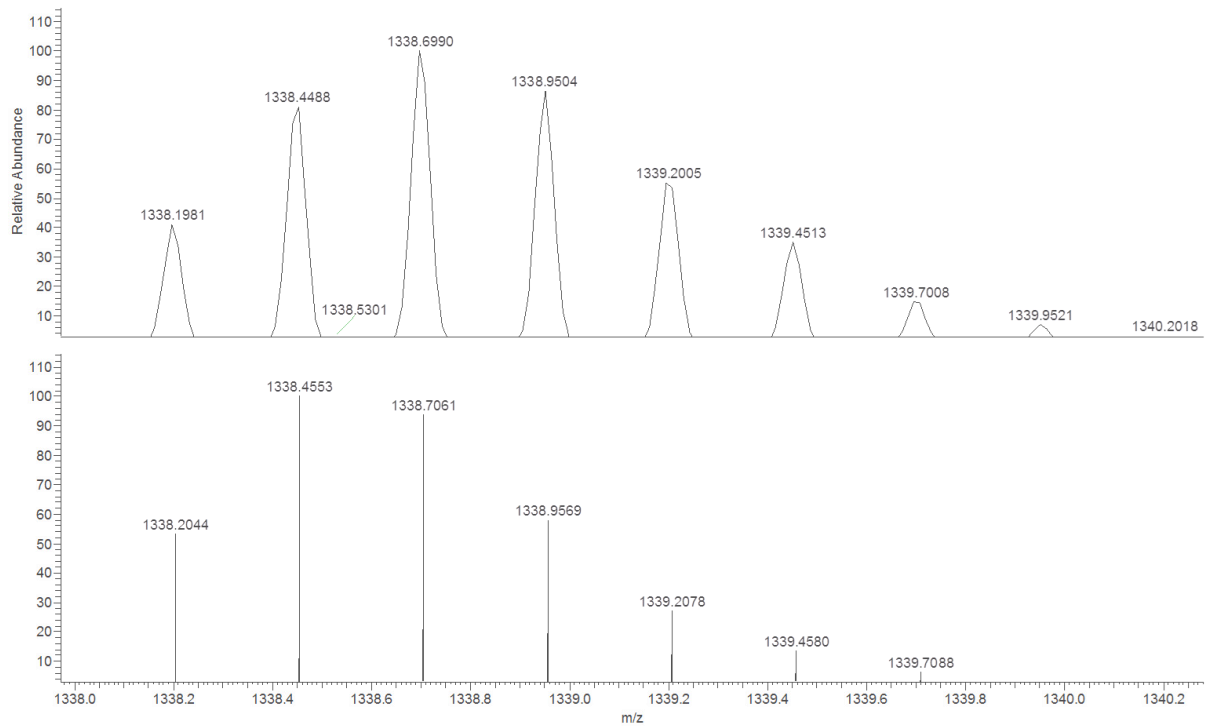
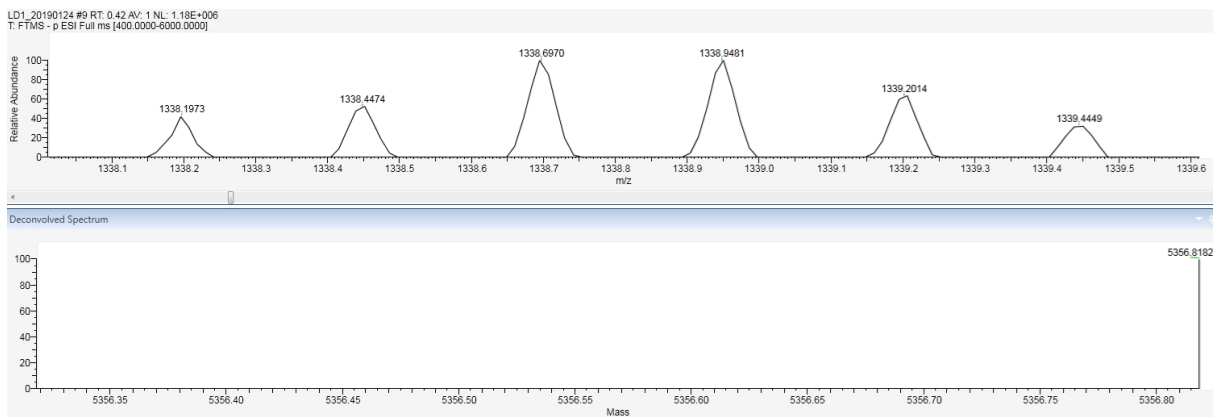
A**B**

Figure S3. A. Mass spectrum of the fourfold negatively charged species of ON 2 (5'-A^LG^LA^LT^LCTCTCTCTA^LG^LA^LT^LT-3'); measured vs. predicted mass. **B.** Deconvoluted mass spectrum of ON 2.

Melting temperature experiments

Compilation of the α -curves

To eliminate the temperature dependency of the extinction coefficient ε , αT -curves were calculated for every melting experiment and subsequently, αT_m values were determined. Therefore, the hyperchromicity h [%] was plotted against the temperature T [°C] to give the typical sigmoidal melting curves. Then, the two pseudo-linear sections of the melting curves (Figure S4, labelled in red and blue) were extrapolated and the matching linear functions (Figure S5, functions $o(y_o)$ and $u(y_u)$ of type $y = m * x + n$) were determined. Next, x_α and y_α were calculated, where x_α corresponds to the amount of hybridised duplex and y_α refers to the abundance of single-stranded ON. Thus, x_α is defined as $x_\alpha = y_o(x) - h(x)$ and y_α as $y_\alpha = h(x) - y_u(x)$. Subsequently, αT values were calculated using the formula $\alpha T = x_\alpha / (x_\alpha + y_\alpha)$ and plotted against the corresponding temperature to give an αT -curve as depicted in Figure S6. From this curve, αT_m values were determined with $\alpha T = 0.5$ (Figure S6).

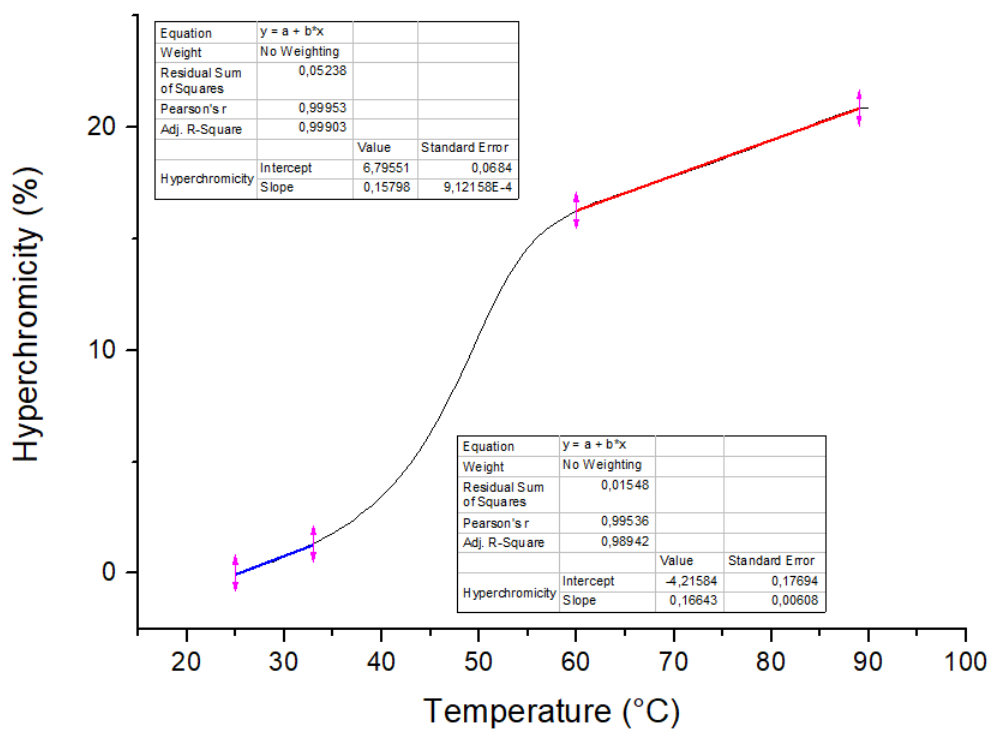


Figure S4. Sigmoidal melting curve with highlighted pseudo-linear sections.

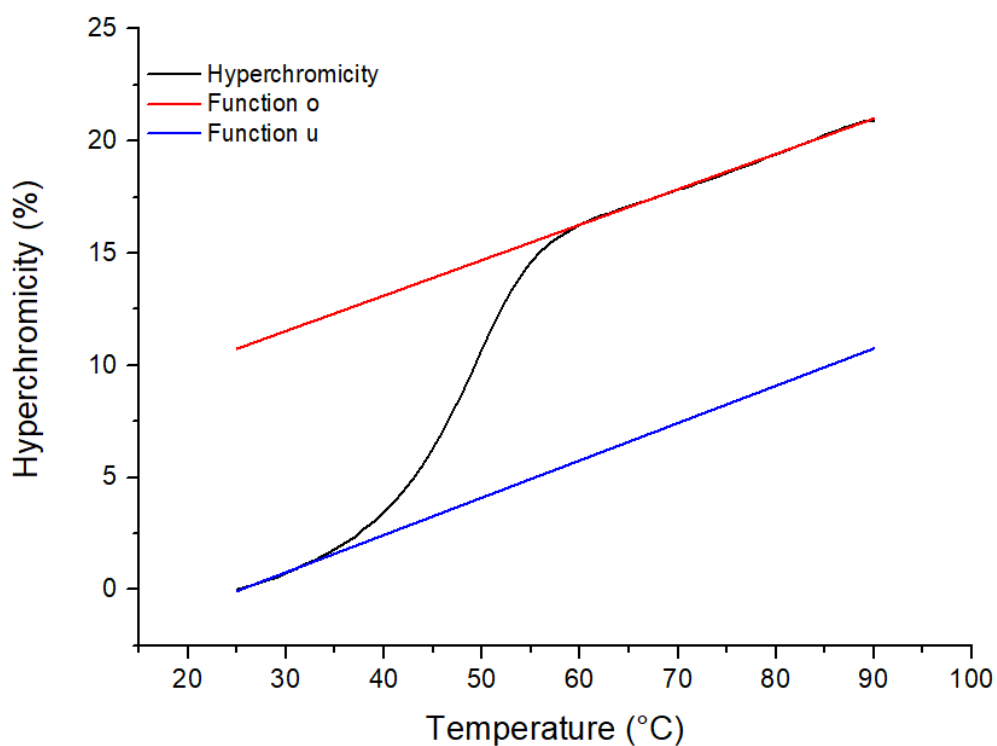


Figure S5. Depiction of function $o(y_o)$ in red and function $u(y_u)$ in blue.

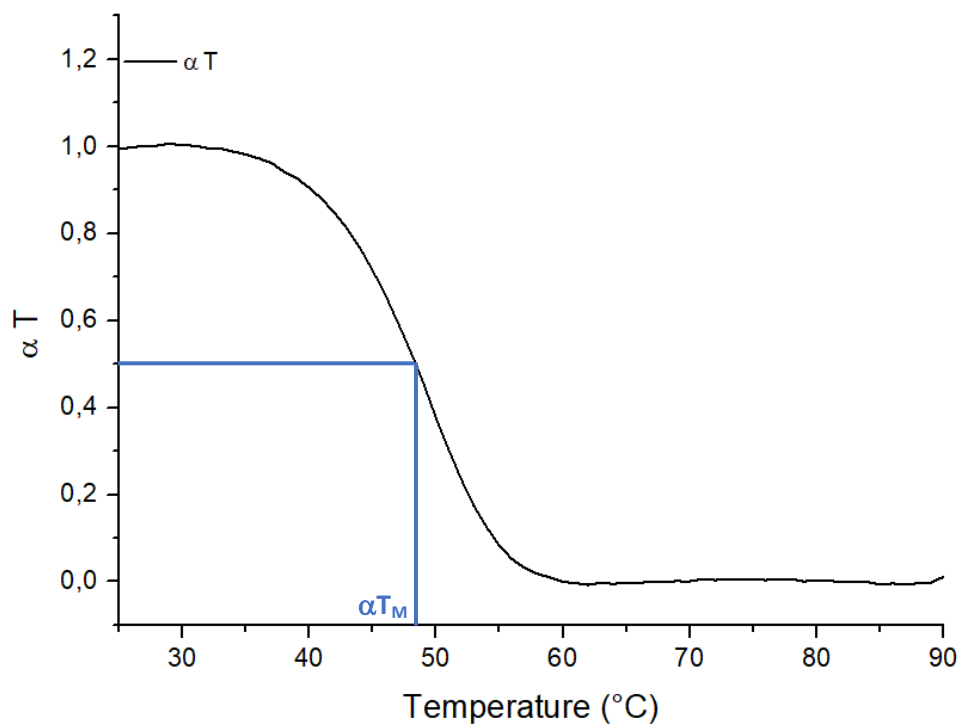


Figure S6. Determination of αT_m values using the αT curve with αT_m for $\alpha T = 0.5$.

Mismatch melting temperature experiments with gapmers 1 and 2

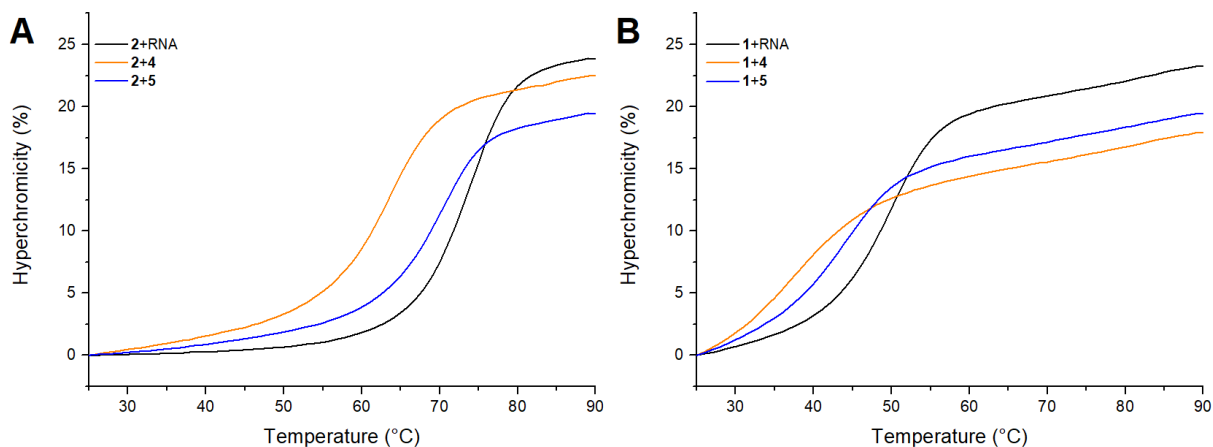


Figure S7. A. Melting curves of DNA/LNA-gapmer **2** in complex with native RNA, mismatch RNA **X** ('2+4'), and mismatch RNA **Y** ('2+5'). **B.** Melting curves of NAA/LNA-gapmer **1** in complex with native RNA, mismatch RNA **X** ('2+4'), and mismatch RNA **Y** ('2+5'). All depicted curves are the average of technical triplicates.

References

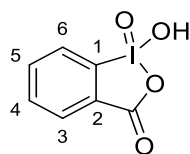
[S1] B. Schmidtgal, A. P. Spork, F. Wachowius, C. Höbartner, C. Ducho, *Chem. Commun.* **2014**, *50*, 13742-13745.

[S2] B. Schmidtgal, C. Höbartner, C. Ducho, *Beilstein J. Org. Chem.* **2015**, *11*, 50-60.

6.3 Syntheses Appending to Manuscript C

The following synthetic procedures are based on already established and published routes^[143,145,175–178] and were not developed in the frame of this thesis. However, in order to provide a complete overview of the syntheses performed during this work, the following reactions as well as the analysis of the resulting products are listed.

6.3.1 Synthesis of 2-Iodoxybenzoic Acid 4



2-Iodobenzoic acid (25.0 g, 101 mmol, 1.0 eq.) was added to a solution of oxone (2 $\text{KHSO}_5 \cdot \text{KHSO}_4 \cdot \text{K}_2\text{SO}_4$, 186.5 g, 303 mmol, 3.0 eq.) in water (1.0 L) and stirred at 70 °C for 2 h. The suspension was cooled to 0 °C, filtered and the remaining solid was washed with water (6 x 200 mL) and acetone (2 x 200 mL) at 0 °C, respectively. The product was dried under reduced pressure for several days. Further purification was not required.

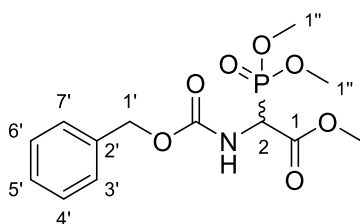
Yield: 28.3 g (101 mmol, 68%) of a white solid.

¹H-NMR (500 MHz, DMSO- d_6): δ [ppm] = 7.84 (dt, $J = 7.4$ Hz, $J = 1.0$ Hz, 1 H, 3-H), 7.97-8.05 (m, 2 H, 6-H, 4-H), 8.14 (d, $J = 7.5$ Hz, 1 H, 5-H).

¹³C-NMR (126 MHz, DMSO- d_6): δ [ppm] = 125.08 (C-3), 130.20 (C-6), 131.51 (C-1), 133.02 (C-5), 133.51 (C-4), 146.61 (C-2), 167.59 (C=O).

6.3.2 Synthesis of *tert*-Butyl Ester Phosphonate 6

Methyl ester phosphonate 5



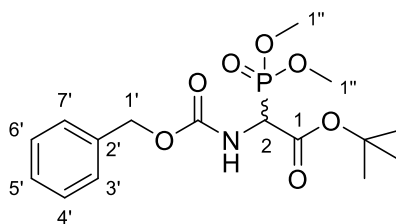
Methyl-2-methoxy-*N*-benzyloxycarbonylglycinate (12.0 g, 47.4 mmol, 1.0 eq.) was dissolved in anhydrous toluene (50 mL) and subsequently, phosphorus trichloride (4.64 mL, 53.0 mmol, 1.12 eq.) was added dropwise. The mixture was heated under reflux and stirred for 4 h. Then, trimethyl phosphite (6.33 mL, 53.5 mmol, 1.13 eq.) was added, the reaction was stirred under reflux for further 2 h and the solvent was removed under reduced pressure. The remaining yellow substance was dissolved in ethyl acetate (300 mL). The organic layer was washed using sat. aqueous sodium bicarbonate solution (3 x 100 mL), dried over sodium sulfate, filtered and the solvent was removed *in vacuo*. To the resultant colorless liquid, *n*-hexane (50 mL) was added and the suspension was stirred for 30 min at room temperature. The suspension was filtered, washed with cold *n*-hexane (0 °C, 3 x 20 mL) and the remaining solid was dried for several days under reduced pressure to afford the title compound without further purification.

Yield: 13.2 g (39.7 mmol, 84%) of a white solid.

¹H-NMR (500 MHz, CDCl₃): δ = 3.78 (s, 3 H, 1''-H), 3.82 (s, 3 H, 1''-H), 3.84 (s, 3 H, COOCH₃), 4.92 (dd, ²J_{PH} = 22.5 Hz, J = 8.4 Hz, 1 H, 2-H), 5.12 (d, J = 2.0 Hz, 2 H, 1'-H_a, 1'-H_b), 5.66 (d, J = 8.6 Hz, 1 H, NH), 7.25-7.40 (m, 5 H, ArH).

¹³C-NMR (126 MHz, CDCl₃): δ = 51.91 (d, ¹J_{CP} = 148.5 Hz, C-2), 53.48 (COOCH₃), 53.51 (d, ²J_{CP} = 6.9 Hz, C_a-1''), 53.97 (d, ²J_{CP} = 6.6 Hz, C_b-1''), 67.43 (C-1'), 128.03 (C-5'), 128.19 (C-3', C-7'), 128.38 (C-4', C-6'), 135.78 (C-2'), 155.1 (d, ³J_{CP} = 8.0 Hz, C(O)ONH), 167.9 (d, ²J_{CP} = 2.9 Hz, C-1).

³¹P-NMR (203 MHz, CDCl₃): δ = 19.73.

tert-Butyl ester phosphonate 6

The first step of the following reaction sequence was not performed under inert gas conditions. *N*-(Benzyloxycarbonyl)-2-(dimethylphosphinyl)-glycine methyl ester **5** (10.0 g, 30.2 mmol, 1.0 eq.) was dissolved in dioxane (9 mL) and cooled to 15 °C. An aqueous solution of sodium hydroxide (15.7 mL, 31.3 mmol, 2 M, 1.04 eq.) was added dropwise and the resulting mixture was stirred for 30 min at 15 °C. The reaction was cooled to 0 °C, hydrochloric acid was added until a pH of 2 was reached and water (45 mL) and ethyl acetate (100 mL) were added. The aqueous layer was extracted with ethyl acetate (4 x 50 mL), the organic layer was dried over Na₂SO₄ and the solvent was removed under reduced pressure.

For the second step, inert gas conditions were applied. The remaining colorless liquid was dissolved in dry dichloromethane (100 mL) and dry *tert*-butanol (400 mL) and the mixture was stirred for 4 h at room temperature under the addition of activated molecular sieve (3 Å, 4 Å). *N*-ethoxycarbonyl-2-ethoxy-1,2-dihydroquinoline (8.96 g, 36.2 mmol, 1.2 eq.) was added and the reaction was stirred for 16 h at room temperature. The mixture was filtered over Celite[®], the Celite[®] was washed with ethyl acetate (4 x 200 mL) and the solvent was removed *in vacuo*. The resulting light-yellow liquid was dissolved in ethyl acetate (500 mL), cooled to 0 °C and washed using hydrochloric acid (3 x 100 mL, 0 °C) and sat. aqueous sodium bicarbonate solution (2 x 100 mL, 0 °C). The organic layer was dried over sodium sulfate, filtered and the remaining solvent was removed under reduced pressure. The crude product was purified by column chromatography (PE/EtOAc, 1:1) yielding the title compound.

Yield: 8.97 g (22.7 mmol, 75%) of a white solid.

TLC: R_f (PE/EtOAc 3:7) = 0.23.

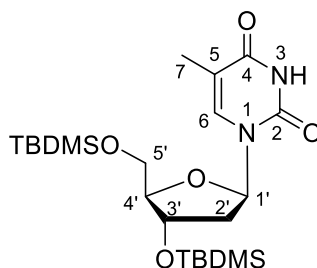
¹H-NMR (500 MHz, CDCl₃): δ = 1.44 (s, 9 H, C(CH₃)₃), 3.72 (d, *J* = 10.7 Hz, 3 H, 1''-H_a), 3.78 (d, *J* = 9.6 Hz, 3 H, 1''-H_b), 4.80 (d, *J* = 22.0 Hz, 1 H, 2-H), 5.09 (d, ³*J*_{PH} = 12.0 Hz, 1 H, 1'-H_a), 5.14 (d, *J* = 12.0 Hz, 1 H, 1'-H_b), 5.68 (d, *J* = 8.5 Hz, 1 H, NH), 7.21-7.35 (m, 5 H, ArH).

¹³C-NMR (126 MHz, CDCl₃): δ = 27.79 (C(CH₃)₃), 52.70 (d, ¹*J*_{CP} = 148.3 Hz, C-2), 53.80 (d, ²*J*_{CP} = 6.7 Hz, C_a-1''), 53.82 (d, ²*J*_{CP} = 6.5 Hz, C_b-1''), 67.60 (C-1'), 83.69 (C(CH₃)₃), 128.00 (C-3', C-7'), 128.18 (C-5'), 128.38 (C-4', C-6'), 135.88 (C-2'), 155.49 (d, ³*J*_{CP} = 7.2 Hz, C(O)ONH), 165.40 (C-1).

³¹P-NMR (203 MHz, CDCl₃): δ = 19.34.

6.3.3 Synthesis of the T-Building Block

3',5'-*O*-Bis-(*tert*-butyldimethylsilyl)-thymidine 7



Thymidine (4.05 g, 16.7 mmol, 1.0 eq.) was dried under reduced pressure for 3 h to remove residual water and then dissolved in dry pyridine (40 mL). Imidazole (3.42 g, 50.2 mmol, 3.0 eq.) and *tert*-butyldimethylsilyl chloride (7.57 g, 50.2 mmol, 3.0 eq.) were added and the mixture was stirred for 24 h at room temperature. After cooling to 0 °C, water (20 mL) was added to quench the reaction and the solvent was removed *in vacuo*. The remaining crude product was dissolved in ethyl acetate (40 mL), the organic layer was washed with sat. sodium bicarbonate and sodium chloride solution, dried over sodium sulfate, filtered and the solvent was removed under reduced pressure. The title compound was obtained after purification by column chromatography (PE/EtOAc, 4:1).

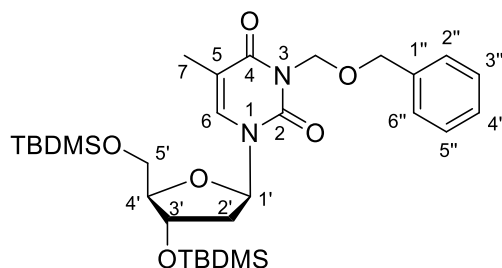
Yield: 7.93 g (16.3 mmol, 98%) of a white solid.

TLC: R_f (PE/EtOAc 1:1) = 0.55.

¹H-NMR (500 MHz, CDCl₃): δ = 0.07 (s, 3 H, SiCH₃), 0.08 (s, 3 H, SiCH₃), 0.10 (s, 3 H, SiCH₃), 0.11 (s, 3 H, SiCH₃), 0.89 (s, 9 H, SiC(CH₃)₃), 0.92 (s, 9 H, SiC(CH₃)₃), 1.91 (d, J = 1.2 Hz, 3 H, 7-H), 2.00 (ddd, J = 13.2 Hz, J = 11.0 Hz, J = 7.0 Hz, 1 H, 2'-H_a), 2.24 (ddd, J = 13.1 Hz, J = 5.8 Hz, J = 2.6 Hz, 1 H, 2'-H_b), 3.76 (dd, J = 11.4 Hz, J = 2.4 Hz, 1 H, 5'-H_a), 3.86 (dd, J = 11.4 Hz, J = 2.6 Hz, 1 H, 5'-H_b), 3.93 (q, J = 2.5 Hz, J = 2.5 Hz, 1 H, 4'-H), 4.38-4.41 (m, 1 H, 3'-H), 6.33 (dd, J = 8.0 Hz, J = 5.8 Hz, 1 H, 1'-H), 7.47 (d, J = 1.2 Hz, 1 H, 6-H), 8.63 (brs, 1 H, NH).

¹³C-NMR (126 MHz, CDCl₃): δ = -5.31 (SiCH₃), -5.22 (SiCH₃), -4.69 (SiCH₃), -4.50 (SiCH₃), 12.68 (C-7), 18.16 (SiC(CH₃)₃), 18.55 (SiC(CH₃)₃), 25.89 (SiC(CH₃)₃), 26.08 (SiC(CH₃)₃), 41.52 (C-2'), 63.14 (C-5'), 72.43 (C-3'), 84.98 (C-1'), 87.99 (C-4'), 110.95 (C-5), 135.63 (C-6), 150.28 (C-2), 163.69 (C-4).

MS (ESI⁺): calc. for C₂₂H₄₂N₂O₅Si₂: m/z = 471.72 [M+H⁺], found: m/z = 471.73 [M+H⁺]

3',5'-O-Bis-TBDMS-3-N-(benzyloxymethyl)-thymidine 8

A suspension of sodium hydride (710 mg, 29.7 mmol, 2.0 eq., 60% suspension in mineral oil) in DMF (20 mL) was cooled to $-10\text{ }^{\circ}\text{C}$ and a solution of 3',5'-O-bis-(*tert*-butyldimethylsilyl)-thymidine **7** (7.00 g, 14.9 mmol, 1.0 eq.) in DMF (45 mL) was slowly added dropwise and stirred for 30 min at $5\text{ }^{\circ}\text{C}$. Benzyl chloromethyl ether (3.49 g, 22.3 mmol, 1.5 eq.) was slowly added and the reaction was stirred at $0\text{ }^{\circ}\text{C}$ for another 3 h. The mixture was diluted with ethyl acetate (250 mL) and water was added (80 mL). Then, the organic layer was washed with sat. sodium bicarbonate and sodium chloride solution, dried over sodium sulfate, filtered and the solvent was removed *in vacuo*. The title compound was purified by column chromatography (PE/EtOAc, 9:1).

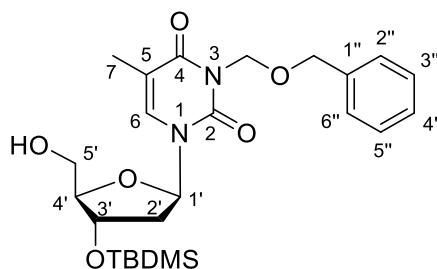
Yield: 7.62 g (12.9 mmol, 87%) of a colorless oil.

TLC: R_f (PE/EtOAc 4:1) = 0.32.

$^1\text{H-NMR}$ (500 MHz, CDCl_3): δ = 0.00 (s, 3 H, SiCH_3), 0.01 (s, 3 H, SiCH_3), 0.04 (s, 3 H, SiCH_3), 0.04 (s, 3 H, SiCH_3), 0.82 (s, 9 H, $\text{SiC}(\text{CH}_3)_3$), 0.86 (s, 9 H, $\text{SiC}(\text{CH}_3)_3$), 1.85 (d, $J = 1.2\text{ Hz}$, 3 H, 7-H), 1.87-1.92 (m, 1 H, 2'- H_a), 2.19 (ddd, $J = 13.1\text{ Hz}$, $J = 5.8\text{ Hz}$, $J = 2.6\text{ Hz}$, 1 H, 2'- H_b), 3.69 (dd, $J = 11.4\text{ Hz}$, $J = 2.4\text{ Hz}$, 1 H, 5'- H_a), 3.79 (dd, $J = 11.4\text{ Hz}$, $J = 2.6\text{ Hz}$, 1 H, 5'- H_b), 3.87 (dd, $J = 2.5\text{ Hz}$, $J = 2.5\text{ Hz}$, 1 H, 4'-H), 4.30-4.34 (m, 1 H, 3'-H), 4.63 (s, 2 H, NCH_2OCH_2), 5.43 (s, 2 H, NCH_2O), 6.28 (dd, $J = 7.9\text{ Hz}$, $J = 5.8\text{ Hz}$, 1 H, 1'-H), 7.16-7.20 (m, 1 H, ArH), 7.22-7.26 (m, 2 H, ArH), 7.29-7.32 (m, 2 H, ArH), 7.38 (d, $J = 1.2\text{ Hz}$, 1 H, 6-H).

$^{13}\text{C-NMR}$ (126 MHz, CDCl_3): δ = -5.31 (SiCH_3), -5.23 (SiCH_3), -4.70 (SiCH_3), -4.49 (SiCH_3), 13.38 (C-7), 18.13 ($\text{SiC}(\text{CH}_3)_3$), 18.53 ($\text{SiC}(\text{CH}_3)_3$), 25.88 ($\text{SiC}(\text{CH}_3)_3$), 26.07 ($\text{SiC}(\text{CH}_3)_3$), 41.57 (C-2'), 63.11 (C-5'), 70.67 (NCH_2O), 72.32 (C-3'), 72.39 (NCH_2OCH_2), 85.65 (C-1'), 87.96 (C-4'), 110.23 (C-5''), 127.72 (C-4''), 127.81 (C-3'', C-5''), 128.40 (C-2'', C-6''), 134.33 (C-6), 138.20 (C-1''), 151.12 (C-2), 163.67 (C-4).

MS (ESI+): calc. for $\text{C}_{30}\text{H}_{50}\text{N}_2\text{O}_6\text{Si}_2$: $m/z = 591.33$ [$\text{M}+\text{H}^+$], found: $m/z = 591.35$ [$\text{M}+\text{H}^+$]

3'-O-TBDMS-3-N-(benzyloxymethyl)-thymidine 9

3',5'-*O*-Bis-(*tert*-butyldimethylsilyl)-3-*N*-(benzyloxymethyl)-thymidine **8** (3.80 g, 6.43 mmol, 1.0 eq.) was dissolved in abs. methanol (200 mL) and cooled to -10 °C. Acetyl chloride (92 μ L, 1.3 mmol, 0.2 eq.) was slowly added and the reaction was stirred for 3.5 h at 0 °C under TLC control (PE/EtOAc, 1:1). After 2 h more acetyl chloride was added (83 μ L, 1.0 mmol, 0.16 eq.) to achieve better conversion. The reaction was quenched through addition of sat. sodium bicarbonate solution (10 mL) and stirring for 15 min at room temperature. The mixture was then diluted with ethyl acetate (300 mL), the organic layer was washed with sat. sodium bicarbonate solution, water and sodium chloride solution, respectively. It was then dried over sodium sulfate, filtered and the solvent was removed under reduced pressure. The title compound was obtained through column chromatography (PE/EtOAc, 3:2), in which 342 mg of **8** could be recovered.

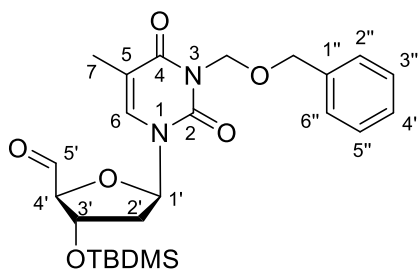
Yield: 2.26 g (4.74 mmol, 74%, 81% brsm) of a colorless oil.

TLC: R_f (PE/EtOAc 4:1) = 0.32.

$^1\text{H-NMR}$ (500 MHz, CDCl_3): δ = 0.10 (s, 6 H, SiCH_3), 0.92 (s, 9 H, $\text{SiC}(\text{CH}_3)_3$), 1.94 (s, 3 H, 7-H), 2.22-2.35 (m, 2 H, 2'- H_a , 2'- H_b), 3.77 (dd, J = 12.5 Hz, J = 3.6 Hz, 1 H, 5'- H_a), 3.89-3.97 (m, 2 H, 4'-H, 5'- H_b), 4.46-4.53 (m, 1 H, 3'-H), 4.72 (s, 2 H, NCH_2OCH_2), 5.51 (s, 2 H, NCH_2O), 6.16 (t, J = 6.7 Hz, J = 6.7 Hz, 1 H, 1'-H), 7.24-7.42 (m, 6 H, 6-H, ArH).

$^{13}\text{C-NMR}$ (126 MHz, CDCl_3): δ = -4.71 (SiCH_3), -4.54 (SiCH_3), 13.40 (C-7), 18.09 ($\text{SiC}(\text{CH}_3)_3$), 25.85 ($\text{SiC}(\text{CH}_3)_3$), 40.69 (C-2'), 62.26 (C-5'), 70.68 (NCH_2O), 71.71 (C-3'), 72.38 (NCH_2OCH_2), 87.61 (C-1', C-4'), 110.49 (C-5), 127.76 (C-4''), 127.81 (C-3'', C-5''), 128.42 (C-2'', C-6''), 135.70 (C-6), 138.13 (C-1''), 151.15 (C-2), 163.54 (C-4).

MS (ESI+): calc. for $\text{C}_{24}\text{H}_{36}\text{N}_2\text{O}_6\text{Si}$: m/z = 477.24 [$\text{M}+\text{H}^+$], found: m/z = 477.24 [$\text{M}+\text{H}^+$]

3'-O-TBDMS-3-N-(benzyloxymethyl)-thymidine-5'-aldehyde 10

To a suspension of 3'-O-TBDMS-3-N-(benzyloxymethyl)-thymidine **9** (2.20 g, 4.61 mmol, 1.0 eq.) in dry acetonitrile (40 mL), 2-iodoxybenzoic acid **4** (3.23 g, 11.5 mmol, 2.5 eq.) was added. The reaction was stirred under reflux conditions (80 °C) for 1 h under TLC control. The mixture was then cooled to 0 °C and stirred for another 30 min. The resulting suspension was filtered through silica and washed with cold ethyl acetate (160 mL, 0 °C). The solvent was removed under reduced pressure to yield title compound **10** without further purification.

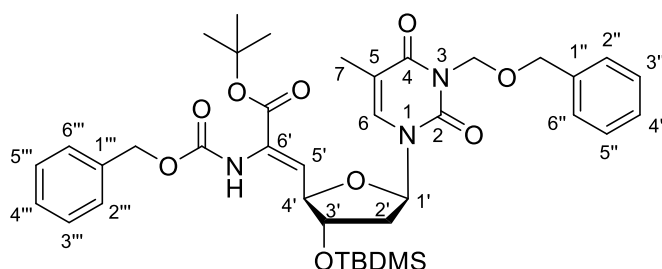
Due to the limited stability of aldehyde **10**, its identity was only confirmed by ¹H-NMR spectroscopy, after which it was immediately used in the next reaction.

Yield: 2.00 g (4.21 mmol, 91%) of a white foam.

TLC: R_f (PE/EtOAc 1:1) = 0.34.

¹H-NMR (500 MHz, C₆D₆): δ = 0.01 (s, 3 H, SiCH₃), 0.02 (s, 3 H, SiCH₃), 0.91 (s, 9 H, SiC(CH₃)₃), 1.68-1.75 (m, 1 H, 2'-H_a), 1.77 (d, J = 1.2 Hz, 3 H, 7-H) 1.85-1.90 (m, 1 H, 2'-H_b), 4.44-4.46 (m, 1 H, 3'-H), 4.68 (s, 2 H, NCH₂OCH₂), 5.44 (d, J = 2.8 Hz, 2 H, NCH₂O), 5.86 (dd, J = 6.7 Hz, J = 6.7 Hz, 1 H, 1'-H), 6.69 (d, J = 1.2 Hz, 1 H, 6-H), 7.01-7.06 (m, 1 H, 4''-H), 7.10-7.13 (m, 2 H, 3''-H, 5''-H), 7.33-7.36 (m, 2 H, 2''-H, 6''-H), 9.31 (s, 1 H, 5'-H).

MS (ESI⁺): calc. for C₂₄H₃₄N₂O₆Si: m/z = 475.23 [M+H⁺], found: m/z = 475.23 [M+H⁺]

(Z)-3-N-BOM-6'-N-Cbz-O-*t*-Bu-5',6'-didehydro-3'-O-TBDMS-thymidinyl amino acid 11

Potassium *tert*-butoxide (50.0 mg, 4.42 mmol, 1.05 eq.) was dissolved in dry tetrahydrofuran (40 mL) and the resulting solution was cooled to $-78\text{ }^{\circ}\text{C}$. Then, a cold solution of *tert*-butyl ester phosphonate **6** (1.76 g, 4.72 mmol, 1.1 eq., $-78\text{ }^{\circ}\text{C}$) in dry tetrahydrofuran (35 mL) was added dropwise and the reaction was stirred for 10 min at $-78\text{ }^{\circ}\text{C}$. A cold solution of 3'-O-TBDMS-3-*N*-(benzyloxymethyl)-thymidine-5'-aldehyde **10** (2.00 g, 4.21 mmol, 1.0 eq., $-78\text{ }^{\circ}\text{C}$) in dry tetrahydrofuran (15 mL) was slowly added over a period of 60 min and the resultant mixture was stirred for 17 h during which it was allowed to warm to room temperature. After cooling the reaction to $0\text{ }^{\circ}\text{C}$, methanol (4 mL) was added to quench the reaction and ethyl acetate (150 mL) was added. The organic layer was washed with brine (150 mL) and water (150 mL) and then dried using sodium sulfate. Removal of the organic solvent under reduced pressure gave crude title compound **11**, which was purified by column chromatography (PE/EtOAc 4:1).

Yield: 2.36 g (3.27 mmol, 78%) of a white foam.

TLC: R_f (PE/EtOAc 1:1) = 0.57.

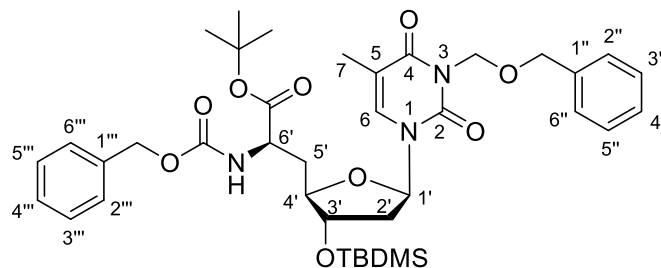
$^1\text{H-NMR}$ (500 MHz, CDCl_3): δ = 0.01 (s, 3 H, SiCH_3), 0.01 (s, 3 H, SiCH_3), 0.80 (s, 9 H, $\text{SiC}(\text{CH}_3)_3$), 1.39 (s, 9 H, *t*-Bu CH_3), 1.84 (d, J = 1.0 Hz, 3 H, 7-H), 1.98-2.05 (m, 1 H, 2'-H_a), 2.29 (ddd, J = 13.5 Hz, J = 6.5 Hz, J = 4.3 Hz, 1 H, 2'-H_b), 4.26 (dd, J = 10.0 Hz, J = 4.2 Hz, 1 H, 3'-H), 4.61 (s, 2 H, NCH_2OCH_2), 4.70-4.73 (m, 1 H, 4'-H), 5.05 (d, J = 3.5 Hz, 2 H, CbzCH_2), 5.39 (s, 2 H, NCH_2O), 6.05 (d, J = 7.7 Hz, 1 H, 5'-H), 6.21 (dd, J = 6.5 Hz, J = 6.5 Hz, 1 H, 1'-H), 6.70 (brs, 1 H, NH), 7.02 (s, 1 H, 6-H), 7.14-7.19 (m, 2 H, ArH), 7.20-7.25 (m, 4 H, ArH), 7.26-7.30 (m, 4 H, ArH).

$^{13}\text{C-NMR}$ (126 MHz, CDCl_3): δ = -4.75 (SiCH_3), -4.62 (SiCH_3), 13.51 (C-7), 18.04 ($\text{SiC}(\text{CH}_3)_3$), 25.81 ($\text{SiC}(\text{CH}_3)_3$), 28.02 ($\text{OC}(\text{CH}_3)_3$), 40.71 (C-2'), 67.75 (CbzCH_2), 70.68 (NCH_2O), 72.39 (NCH_2OCH_2), 76.13 (C-3'), 77.16 ($\text{OC}(\text{CH}_3)_3$), 82.85 (C-4'), 87.01 (C-1'), 110.48 (C-5), 124.88

(C-5'), 127.77 (C-4''), 127.81 (C-3'', C-5''), 128.40 (C-2'', C-6''), 128.41 (C-4'''), 128.51 (C-3''', C-5'''), 128.69 (C-2''', C-6'''), 129.90 (C-6'), 134.19 (C-6), 135.83 (C-1''), 138.13 (C-1'''), 150.88 (C-2), 153.68 (Cbz-C=O), 162.90 (C-4), 163.47 (ester-C=O).

MS (ESI+): calc. for $C_{38}H_{51}N_3O_9Si$: $m/z = 722.35$ [$M+H^+$], found: $m/z = 722.44$ [$M+H^+$]

6'-N-Cbz-O-*t*-Bu-3-N-BOM-3'-O-TBDMS-(*R*)-thymidinyl amino acid **12**



The following reaction was performed under strict exclusion of oxygen. (*Z*)-3-*N*-BOM-6'-*N*-Cbz-*O*-*t*-Bu-5',6'-didehydro-3'-*O*-TBDMS-TAA **11** (1.13 g, 1.57 mmol, 1.0 eq) was dissolved in dry methanol (10 mL), coevaporated, again dissolved in dry methanol (40 mL) and degassed with argon for 10 min. Then, (*R,R*)-Me-DUPHOS-Rh catalyst (approx. 20 mg, approx. 28 μ mol) was added and the reaction was again degassed with argon for 10 min. The resulting orange mixture was flushed with hydrogen quality (6.0, 1 bar) and stirred for 21 days at room temperature during which the hydrogen atmosphere was renewed on a daily basis. Reaction control using 1H -NMR spectroscopy indicated completion of the reaction. The solvent was then removed *in vacuo* and the resulting orange foam was purified by column chromatography (PE/EtOAc 3:2) to yield title compound **12**.

Yield: 1.08 g (1.49 mmol, 95%) of a yellowish foam.

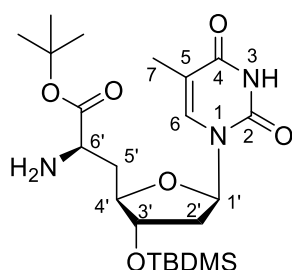
TLC: R_f (PE/EtOAc 3:2) = 0.35.

1H -NMR (500 MHz, $CDCl_3$): $\delta = 0.01$ (s, 3 H, $SiCH_3$), 0.02 (s, 3 H, $SiCH_3$), 0.82 (s, 9 H, $SiC(CH_3)_3$), 1.40 (s, 9 H, *t*- $BuCH_3$), 1.82 (s, 3 H, 7-H), 1.91-1.97 (m, 1 H, 5'-H'), 1.99-2.03 (m, 1 H, 5'-H_b), 2.12-2.21 (m, 2 H, 2'-H), 3.72-3.77 (m, 1 H, 4'-H), 3.97-4.02 (m, 1 H, 3'-H), 4.37-4.44 (m, 1 H, 6'-H), 4.63 (s, 2 H, NCH_2OCH_2), 5.03 (s, 2 H, $CbzCH_2$), 5.41 (s, 2 H, NCH_2O), 5.53 (d, $J = 8.6$ Hz, 1 H, NH), 6.08 (t, $J = 6.3$ Hz, $J = 6.3$ Hz, 1 H, 1'-H), 7.00 (s, 1 H, 6-H), 7.18-7.32 (m, 10 H, ArH).

¹³C-NMR (126 MHz, CDCl₃): δ = -4.77 (SiCH₃), -4.55 (SiCH₃), 13.31 (C-7), 17.92 (SiC(CH₃)₃), 25.71 (SiC(CH₃)₃), 28.00 (OC(CH₃)₃), 35.17 (C-5'), 40.27 (C-2'), 52.73 (C-6'), 66.92 (CbzCH₂), 70.55 (NCH₂O), 72.24 (NCH₂OCH₂), 74.92 (C-3'), 82.44 (OC(CH₃)₃), 83.42 (C-4'), 86.10 (C-1'), 110.40 (C-5), 124.61 (C-5'), 127.64 (C-4''), 127.68 (C-3'', C-5''), 128.08 (C-2'', C-6''), 128.20 (C-4'''), 128.28 (C-3''', C-5'''), 128.51 (C-2''', C-6'''), 133.91 (C-6'), 134.02 (C-6), 136.27 (C-1''), 138.05 (C-1'''), 150.68 (C-2), 156.02 (Cbz-C=O), 163.33 (C-4), 170.60 (ester-C=O).

MS (ESI+): calc. for C₃₈H₅₃N₃O₉Si: m/z = 724.36 [M+H⁺], found: m/z = 724.43 [M+H⁺]

O*-*t*-Bu-3'-*O*-TBDMS-(*R*)-thymidinyl amino acid **13*



n-Butylamine (205 mg, 277 μL, 2.80 mmol, 20 eq.) and palladium on activated charcoal (10%, 1 spatula tip) were added to a solution of 6'-*N*-Cbz-*O*-*t*-Bu-3'-*N*-BOM-3'-*O*-TBDMS-(*R*)-thymidinyl amino acid **12** (100 mg, 138 nmol, 1.0 eq.) in dry methanol (4 mL) and the reaction was stirred for 24 h under hydrogen atmosphere (1 bar). After complete conversion was confirmed by TLC, the catalyst was filtered off through a syringe filter and washed three times with dry methanol (3 x 5 mL, 40 °C). The combined fractions were dried under reduced pressure. The resulting crude product was then purified by column chromatography (CH₂Cl₂/MeOH 96:4) to yield **13**.

Yield: 63.7 mg (136 nmol, 98%) of a yellowish foam.

TLC: R_f (CH₂Cl₂/MeOH 15:1) = 0.38.

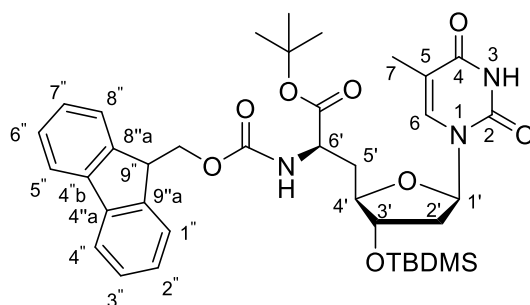
¹H-NMR (500 MHz, CDCl₃): δ = 0.05 (s, 3 H, SiCH₃), 0.06 (s, 3 H, SiCH₃), 0.87 (s, 9 H, SiC(CH₃)₃), 1.45 (s, 9 H, *t*-BuCH₃), 1.85-1.95 (m, 5 H, 2'-H, 7-H), 2.01-2.09 (m, 1 H, 5'-H_a), 2.20-2.27 (m, 1 H, 5'-H_b), 3.49-3.55 (m, 1 H, 6'-H), 3.95-3.98 (m, 1 H, 4'-H), 4.05-4.12 (m, 1 H, 3'-H), 6.19 (t, *J* = 6.5 Hz, *J* = 6.5 Hz, 1 H, 1'-H), 7.21 (s, 1 H, 6-H).

¹³C-NMR (126 MHz, CDCl₃): δ = -4.68 (SiCH₃), -4.51 (SiCH₃), 12.69 (C-7), 18.03 (SiC(CH₃)₃), 25.81 (SiC(CH₃)₃), 28.13 (OC(CH₃)₃), 37.76 (C-5'), 40.47 (C-2'), 52.93 (C-6'), 75.25 (C-3'),

81.51 (OC(CH₃)₃), 83.76 (C-4'), 85.05 (C-1'), 111.17 (C-5), 135.50 (C-6), 150.39 (C-2), 164.04 (C-4), 174.92 (ester-C=O).

MS (ESI⁺): calc. for C₂₂H₃₉N₃O₆Si: m/z = 470.27 [M+H⁺], found: m/z = 470.16 [M+H⁺]

6'-N-Fmoc-O-*t*-Bu-3'-O-TBDMS-(*R*)-thymidinyl amino acid **14**



To a solution of *O-t*-Bu-3'-O-TBDMS-(*R*)-thymidinyl amino acid **13** (800 mg, 1.70 mmol, 1.0 eq.) in dry tetrahydrofuran (16 mL), triethylamine (570 μL, 4.09 mmol, 2.4 eq.) and 9-fluorenylmethoxycarbonyl chloride (573 mg, 2.21 mmol, 1.3 eq.) were added. The resulting mixture was stirred at 0 °C for 60 min. After complete conversion has been confirmed by TLC control (CH₂Cl₂/MeOH 15:1), the reaction was quenched by addition of water (9 mL) and diluted with ethyl acetate (25 mL). The organic layer was separated, washed with water (35 mL) and brine (35 mL) and dried over sodium sulfate. The solvent was removed under reduced pressure and title compound **14** could be obtained after purification by column chromatography (PE/EtOAc 7:3).

Yield: 1.15 g (1.66 mmol, 98%) of a white foam.

TLC: R_f (CH₂Cl₂/MeOH 15:1) = 0.41.

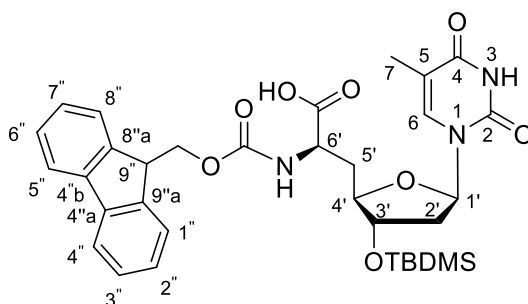
¹H-NMR (500 MHz, C₆D₆): δ = 0.01 (s, 3 H, SiCH₃), 0.03 (s, 3 H, SiCH₃), 0.93 (s, 9 H, SiC(CH₃)₃), 1.36 (s, 9 H, *t*-BuCH₃), 1.65 (s, 3 H, 7-H), 1.84 (dd, *J* = 13.6 Hz, *J* = 6.2 Hz, 1 H, 2'-H_a), 1.94-1.98 (m, 1 H, 2'-H_b), 2.09-2.17 (m, 2 H, 5'-H), 3.87-3.92 (m, 1 H, 4'-H), 4.06-4.11 (m, 2 H, 3'-H, 9''-H), 4.29 (dd, *J* = 10.6 Hz, *J* = 7.5 Hz, 1 H, FmocCHH_a), 4.38 (dd, *J* = 10.6 Hz, *J* = 6.9 Hz, 1 H, FmocCHH_b), 4.65 (brs, 1 H, FmocNH), 5.57 (dd, *J* = 6.2 Hz, *J* = 6.2 Hz, 1 H, 6'-H), 5.81-5.86 (m, 1 H, 1'-H), 6.39 (s, 1 H, 6-H), 7.19-7.26 (m, 4 H, 1''-H, 4''-H, 5''-H, 8''-H), 7.41 (d, *J* = 7.3 Hz, 1 H, 2''-H), 7.52 (d, *J* = 7.5 Hz, 1 H, 7''-H), 7.55-7.58 (m, 2 H, 3''-H, 6''-H), 9.39 (brs, 1 H, 3-NH).

¹³C-NMR (126 MHz, C₆D₆): δ = -4.60 (SiCH₃), -4.45 (SiCH₃), 12.46 (C-7), 18.13 (SiC(CH₃)₃), 25.99 (SiC(CH₃)₃), 28.09 (SiC(CH₃)₃), OC(CH₃)₃, 35.47 (C-5'), 40.09 (C-2'), 47.93 (C-9''), 53.53

(C-6'), 67.39 (FmocCH₂), 75.73 (C-3'), 81.92 (OC(CH₃)₃), 84.03 (C-4'), 87.26 (C-1'), 110.95 (C-5'), 120.27 (C-4'', C-5''), 125.42 (C-1''), 125.54 (C-8''), 127.36 (C-6''), 127.96 (C-3''), 128.16 (C-7''), 128.35 (C-2''), 136.11 (C-6), 141.90 (C-4''_a, C-4''_b), 144.59 (C-8''), 144.68 (C-9''), 150.37 (C-2), 156.24 (Fmoc-C=O), 163.44 (C-4), 171.17 (ester-C=O).

MS (ESI⁺): calc. for C₃₇H₄₉N₃O₈Si: m/z = 692.34 [M+H⁺], found: m/z = 692.37 [M+H⁺]

6'-N-Fmoc-3'-O-TBDMS-(R)-thymidinyl amino acid **15**



The following reaction was not performed under inert gas conditions. 6'-N-Fmoc-*O*-*t*-Bu-3'-O-TBDMS-(*R*)-thymidinyl amino acid **14** (1.12 g, 1.62 mmol, 1.0 eq.) was dissolved in dry toluene (48 mL) and silica gel (2.90 g) was added. The resulting suspension was stirred under reflux (111 °C) for 24 h. The solvent was then removed *in vacuo* and the remaining crude product was purified by column chromatography (CH₂Cl₂/MeOH 10:1 + 0.1% formic acid).

Yield: 827 mg (1.30 mmol, 80%) of a white foam.

TLC: R_f (CH₂Cl₂/MeOH 15:1) = 0.41.

¹H-NMR (500 MHz, CD₃OD): δ = 0.11 (s, 6 H, SiCH₃), 0.91 (s, 9 H, SiC(CH₃)₃), 1.85 (s, 3 H, 7-H), 2.07-2.16 (m, 2 H, 5'-H), 2.18-2.24 (m, 2 H, 2'-H), 3.92 (ddd, *J* = 10.4 Hz, *J* = 2.9 Hz, *J* = 2.9 Hz, 1 H, 4'-H), 4.21 (t, *J* = 7.1 Hz, *J* = 7.1 Hz, 1 H, 9''-H), 4.29-4.40 (m, 4 H, 3'-H, 6'-H, FmocCH₂), 6.24 (dd, *J* = 6.9 Hz, *J* = 6.9 Hz, 1 H, 1'-H), 7.29 (dd, *J* = 7.3 Hz, *J* = 7.3 Hz, 2 H, 3''-H, 6''-H), 7.38 (m, 2 H, 2''-H, 7''-H), 7.44 (s, 1 H, 6-H), 7.65 (m, 2 H, 4''-H, 5''-H), 7.78 (d, *J* = 7.5 Hz, 2 H, 1''-H, 8''-H).

¹³C-NMR (126 MHz, CD₃OD): δ = -4.66 (SiCH₃), -4.59 (SiCH₃), 12.40 (C-7), 18.80 (SiC(CH₃)₃), 26.26 (SiC(CH₃)₃), 36.31 (C-5'), 40.55 (C-2'), 49.28 (C-9''), 52.69 (C-6'), 68.08 (FmocCH₂), 76.74 (C-3'), 84.97 (C-4'), 86.73 (C-1'), 112.01 (C-5), 120.91 (C-1'', C-8''), 126.24 (C-5'', C-4''),

128.17, (C-3''), 128.78 (C-6''), 129.21 (C-2'', C-7''), 137.70 (C-6), 142.56 (C-4''_a, C-4''_b), 145.18 (C-8''), 145.29 (C-9''_a), 152.27 (C-2), 158.61 (Fmoc-C=O), 166.28 (C-4), 175.56 (COOH).

MS (ESI+): calc. for **C₃₃H₄₁N₃O₈Si**: $m/z = 636.27$ [M+H⁺], found: $m/z = 636.36$ [M+H⁺]

7. Curriculum Vitae

Persönliche Angaben

Geburtsdatum/-ort	06.11.1990, Neunkirchen (Saar)
Staatsangehörigkeit	Deutsch

Ausbildung

seit 11/2015 Promotion	Universität des Saarlandes, Deutschland Promotionsstudentin im Fachbereich Pharmazeutische und Medizinische Chemie (Leitung: Prof. Christian Ducho) Thema der Arbeit: Properties of Nucleosyl Amino Acid-Modified Oligonucleotides
09/2016 Approbation	Universität des Saarlandes, Deutschland Approbation als Apothekerin, drittes Staatsexamen im Fachbereich Pharmazie
05/2015-11/2015	Landmann Apotheke, Saarbrücken Zweiter Teil des praktischen Jahres
10/2014-05/2015 Diplom	Harvard Medical School, Boston, USA Universität des Saarlandes, Deutschland Diplomarbeit im Fachbereich Immunologie und Virologie der Harvard Medical School (Leitung: Prof. Michaela Gack), erster Teil des praktischen Jahres Thema der Arbeit: Immune evasion of the antiviral interferon response by human papillomaviruses
08/2014	Universität des Saarlandes, Deutschland Zweites Staatsexamen im Fachbereich Pharmazie
08/2012	Universität des Saarlandes, Deutschland Erstes Staatsexamen im Fachbereich Pharmazie
04/2009	Steinwaldgymnasium, Neunkirchen Abitur

Professionelle Erfahrung

Arbeitserfahrung

- seit 04/2020 **Sanofi-Aventis Deutschland GmbH**
Trainee Industrial Affairs im Bereich SFD QA Internal Operations
- seit 11/2015 **Universität des Saarlandes, Deutschland**
Promotion im Fachbereich Pharmazeutische und Medizinische Chemie mit Schwerpunkt auf den Gebieten:
- Organische Chemie (Synthese, Automated DNA Synthesis)
 - Instrumentelle Analytik (HPLC-MS, NMR-/IR-/UV-Vis-, CD- und Fluoreszenzspektroskopie)
 - Biologische Testung (Assay-Entwicklung und -Etablierung, PAGE, Zellkultur, Umgang mit radioaktiven Substanzen)
- 10/2014-05/2015 **Harvard Medical School, Boston, USA**
Universität des Saarlandes, Deutschland
Diplomarbeit im Fachbereich Immunologie und Virologie mit Schwerpunkt auf dem Gebiet:
- Biologische Testung (Zellkultur, Immunoblotting, Protein- und DNA-Aufreinigung)
- 07/2013-10/2013 **ElexoPharm GmbH, Saarbrücken**
Wissenschaftliche Hilfskraft, Durchführung von:
- High-Throughput Inhibitor Screenings
 - Zytotoxizitäts-Screenings
 - Zellkultur
- 04/2013-06/2013 **University of Otago, Neuseeland**
Wissenschaftliche Hilfskraft im Fachbereich Pharmakologie und Toxikologie, Durchführung von:
- Zellviabilitäts-Assays
- 10/2012-04/2013 **Universität des Saarlandes, Deutschland**
Wissenschaftliche Hilfskraft im Fachbereich Pharmazeutische und Medizinische Chemie, Durchführung von:
- Zellkultur
 - LC-MS-Analysen und -Methodenentwicklung

Besuchte Konferenzen

- 09/2019 **Universität des Saarlandes, Deutschland**
Treffen der Deutschen Nucleinsäurechemie-Gemeinschaft (*geladene Rednerin*)
- 06/2019 **Newport, USA**
Gordon Research Conference on Nucleosides, Nucleotides and Oligonucleotides (*Posterpräsentation*)

03/2019	Merck, Darmstadt, Deutschland Internationales Doktoranden/Postdoc Meeting 2019 der Deutschen Pharmazeutischen Gesellschaft (DPhG) (<i>geladene Rednerin</i>)
09/2018	Bad Herrenalb, Deutschland Doktorandenseminar der Deutschen Nucleinsäurechemie-Gemeinschaft (<i>geladene Rednerin</i>)
08/2018	San Diego, USA International Roundtable on Nucleosides, Nucleotides and Nucleic Acids (<i>Posterpräsentation</i>)
09/2017	Mainz, Deutschland Treffen der Deutschen Nucleinsäurechemie-Gemeinschaft (<i>Posterpräsentation</i>)
09/2017	Universität des Saarlandes, Deutschland Jahrestagung der deutschen pharmazeutischen Gesellschaft (DPhG) (<i>Posterpräsentation</i>)
09/2016	Bad Herrenalb, Deutschland Doktorandenseminar der Deutschen Nucleinsäurechemie-Gemeinschaft (<i>Posterpräsentation</i>)

Publikationen

C. Chiang, E. K. Pauli, J. Biryukov, K. F. Feister, M. Meng, E. A. White, K. Münger, P. M. Howley, C. Meyers, M. U. Gack: The human papillomavirus E6 oncoprotein targets USP15 and TRIM25 to suppress RIG-I-mediated innate immune signaling, *J. Virol.* **2018**, 92, 1717-37.

B. Schmidtgall, A. Kuepper, M. Meng, T. N. Grossmann, C. Ducho: Oligonucleotides with cationic backbone and their hybridization with DNA: Interplay of base pairing and electrostatic attraction, *Chem. Eur. J.* **2018**, 24, 1544-1553.

M. Meng, C. Ducho: Oligonucleotide analogues with cationic backbone linkages, *Beilstein J. Org. Chem.* **2018**, 14, 1293-1308. (Review)

M. Meng, B. Schmidtgall, C. Ducho: Enhanced stability of DNA oligonucleotides with partially zwitterionic backbone structures in biological media, *Molecules* **2018**, 23, 2941-2952.

A. Saady, V. Böttner, M. Meng, E. Varon, Y. Shav-Tal, C. Ducho, B. Fischer: An oligonucleotide probe incorporating the chromophore of green fluorescent protein is useful for the detection of HER-2 mRNA breast cancer marker, *Eur. J. Med. Chem.* **2019**, 173, 99-106.

A. Saady, M. Wojtyniak, C. Ducho, B. Fischer: Synthesis of 2'-deoxyuridine modified with 3,5-difluoro-4-methoxybenzylidene imidazolinone derivative for incorporation into oligonucleotide probes for detection of HER2 breast cancer marker, *Curr. Protoc. Nucleic Acid Chem.* **2020**, *80*, e104.

A. Saady, M. Wojtyniak, E. Varon, V. Böttner, N. Kinor, Y. Shav-Tal, C. Ducho, B. Fischer: Specific, sensitive, and quantitative detection of HER-2 mRNA breast cancer marker by fluorescent light-up hybridization probes, *Bioconjug Chem.* **2020**, *31*, 1188-1198.

M. Wojtyniak, B. Schmidtgall, P. E. Kirsch, C. Ducho: Towards Zwitterionic Oligonucleotides with Improved Properties: the NAA/LNA-Gapmer Approach, *ChemBioChem.* **2020**, *21*, 3234-3243.

Weitere Fähigkeiten und Kenntnisse

Fremdsprachen

Englisch	Verhandlungssicher in Wort und Schrift
Französisch	Erweiterte Grundkenntnisse
Russisch	Basiswissen

Stipendien

08/2018	Universität des Saarlandes, Deutschland GradUs Global Stipendium
09/2014	Universität des Saarlandes, Deutschland UdS-Mobil Stipendium (zur Unterstützung studentischer Auslandsaufenthalte)